The assessment of potential impacts of open cast gold mining on the regional groundwater flow system in hard rock environments: with special reference to Ghana

By

Frederick Sam

A dissertation submitted to the School of Geography, Earth and Environmental Sciences and the Committee on the Board of Graduate Studies of University of Birmingham UK in partial fulfillment of the requirements for the Degree of

Doctor of Philosophy

in

Water Sciences (Hydrogeology)

May, 2013

Abstract

The aim of this research has been to determine under what circumstances gold mines in Ghana are likely to have adverse effect on water levels and volumes in surrounding villages/farms and in particular to try and come up with heuristic rules that would indicate under what circumstances there may be derogation problems in the regional groundwater flow system. In the absence of adequate data, a simple semi-empirical scoping calculation has been suggested to estimate radius of impact (R_i, defined here as the radius to a point of 1m drawdown). This approach involves: assessment of local mine geometries (G); collation and examination of hydraulic conductivity (K) data on hard rock aquifers from around the world; assessment of recharge (R) using unsaturated zone flow model to account for infiltration rejection; use of simple mathematical models with G, K and R data to undertake scoping calculations; and use of the outcome to determine what conditions would result in significant derogation issues.

Due to the sensitivity of simple models to K, the entire K dataset (Group A) was regrouped to include Group B (all data except those from radioactive waste studies where very low K terrains were targeted) and C (all data except those from radioactive waste and grouting projects where very high K was encountered). Most of the simple models used in conjunction with Group A mine geometries, recharge rates, and range of relevance predicted very close radius of impacts to the mine, less than few 100m with a median distance of 400m from the mine's edge. Although it is expected that 25% of cases could reach up to 2km, and further if the system was anisotropic. Derogation of water level and volume is more of a problem for Group B and C aquifer systems of higher K. For these two systems, model results show that 50% of cases could reach up to 3.6km with a range of 2.7km to 5.1km, and 3km with a range of 2km to 4.6km from mine centre respectively. However, in extreme cases the radius of impact could reach at least 7.6 km and further if the system was anisotropic. With regards to Ghana, by constraining K using water volumes produced by mines in Ghana, and comparing with the model output, it is tentatively suggested that the most likely R_i values are those calculated with the Group B dataset.

It should, however, be noted that this results are very sensitive to K, and therefore there is the need in Ghana to publish K and volume data that will enable suggestions from this work to be confirmed. Thus, the use of simple models has proved adequate for determining the qualitative risk for derogation around mines in Ghana. More sophisticated models would have been useful but would have meant estimating even more variable values. The technique is applicable elsewhere. Calculations show that where recharge is much more limited, the radius of influence for mines of similar geometry to those in Ghana could have much more extensive radii of impact.

Dedication

I dedicate this PhD thesis to my loving father Benjamin K Sam and mother Mary B Sam for their immense contribution towards my education up to this level.

Acknowledgment

First, I would like to express my profound appreciation to my supervisors; Prof. J. H Tellam and Prof. Rae Mackay, especially my lead supervisor Prof. J. H. Tellam for his invaluable contribution through his supervision of this PhD research. He had a paramount input into this research, through his guidance from initial proposition to its completion and brought out the best of me. In fact, it would not have been possible to accomplish this without his full support, interest and help. More important for me is his extraordinary spirit of free communication and friendliness. Thank you Prof.

I wish to give special thanks to The Commonwealth Scholarship Commission for awarding me the PhD Scholarship and also, The University of Cape Coast Ghana for granting me study leave and financial support.

I am very much grateful to The Environmental Simulation International Group (ESI) UK, for making available to me the computer software package, Ground Water Vistas and the MODFLOW suit of codes for groundwater flow modelling. Also not forgetting, is Dr Damian Lawler of School of Geography, Earth and Environmental Sciences, University of Birmingham for providing me with SEEP/2007 computer software package for the unsaturated zone flow modelling.

Finally, I would like to affectionately thank the many friends I met at The University of Birmingham among which I always found encouragement, concern and help with special attention to Dr Baah Sefa-Ntri and my Hydrogeology Research Group members, both students and staff: Mahmoud Jaweesh; Norsyafina Roslan; Ban To; Abdulkhaliq AlJuhani; Bryony Anderson; Timothy Batty; Omar Al Azzo; Lindsay McMillan; Simiao Sun; Prof. John Tellam; Dr Michael rivett; Dr Michael Riley; Dr Joanna Renshaw; Dr Alan Herbert; Dr Stefan Krause; Dr Mark Cuthbert and Dr Stephanie Handley-Sidhu.

And last but not the least; I am indebted to my dear wife, Eunice and son, Bjorn who gave me confidence and motivation with their patience and understanding whiles with me here in the United Kingdom.

Table of Contents

List of Figures

List of Tables

CHAPTER 1

GENERAL INTRODUCTION

1.1 Background

It has long been established that surface mining operations can potentially have adverse effects on the quality, levels and flow characteristics of both groundwater and surface waters, and on associated sensitive receptors such as wetland habitats, public water supply boreholes and others (Heath, 1993; Canter, 1996; Veiga, and Beinhoff, 1997; Warhurst, 1999; Morris et al, 2003; Singh, 2006; and Kuma and Younger, 2004). But major concerns are the effects from groundwater levels and composition. According to Siegel (1997) in developing a mine plan of operations, operational procedures, hydrological control structures and other best management practices to prevent environmental impacts require accurate knowledge of the variables associated with hydrological conditions at a mine. The most important is proper characterization of baseline hydrogeological conditions so that the extent of impacts to hydrologic and other related resources can be minimized or avoided.

The extraction of base and precious metals from hard rock mines by surface and underground mining can create environmental problems and safety hazards. Owing primarily to their size, open pit mines are typically thought to create more significant impacts, where as underground mining is generally viewed as resulting in less damage to the environment. According to Hartma (1987) approximately 75 to 85% of all minerals extraction worldwide is carried out using open pit methods with much of the underground mining reserve for coal, using either room-and-pillar or full-face mining. With the advent of modern technology, surface mining operations have increased both in physical size and efficiency. The availability of new improved methods and machinery has led to a vast increase in the economic depth of extraction possible. This has resulted in surface mine workings extending well below the water table, consequently making groundwater and occasionally, surface water derogation becoming a major concern. Lerner et al., (2009), mentioned three major roles that groundwater plays in the environment as; providing base flow to rivers keeping them flowing all the year round, maintaining the quality of our rivers by diluting effluents, and serving as an excellent source of water supply providing over 75

per cent of the potable supply in some regions. Groundwater has a strong influence on the health and diversity of plant and animal species in riparian areas, lakes, wetlands, forests, grasslands, and cave systems. It is intimately connected with the landscape and land use that it underlies, and is therefore vulnerable to the anthropogenic activities on the land surface above.

Mining operations conducted below the potentiometric surface in confined aquifers or below the groundwater table in an unconfined aquifer require a drawdown of the water table through dewatering operations (Figure 1.1). The lowering of the water table creates a ''cone of depression'' which extends radially outward from the mine workings and depends on: depth of dewatering (i.e. the amount by which the water table has been lowered); the rate and distribution of rainfall and other forms of recharge (e.g. stream leakage), hydraulic conductivity and homogeneity of the aquifer which determines the zone of dewatering influence (Barfield et al., 1981; Warhurst, 1999). Conceptually, a dewatered mine acts as a large diameter well; consequently the water table in an aquifer can be drawn down for a relatively large radial distance creating a region around the mine, known as the radius of influence within which potential mining impacts may occur. The drawdown of the water table can potentially cause a disruption of groundwater systems, including its flow pattern. In this regards the direction of groundwater flow can be affected by shifting gradients and lines of flow toward the mine field and as a result, groundwater levels may be permanently or temporary lowered. Shallow aquifers may be drained or physically removed and existing drainage systems such as lakes, springs, wells, small streams and rivers may become ephemeral or completely dry (Curtis, 1971). Consequently, water yields from local wells can be reduced or wells may need to be drilled deeper to account for the decreased elevation of the water table or potentiometric surface. The effects can impact wetlands associated with springs and riparian zones associated with streams. A reduction in stream flows can also affect aquatic habitats and fish populations and moreover, a regional lowering of the water table can impact neighbouring water supply and irrigation wells. In areas where ground and surface waters interact due to varying influent and effluent conditions, mining impacts to ground water quality can result in impacts to surface water quality. Furthermore, the excavation of large tonnages of overburden from the open cut mine may also impact upon the local fracture systems in the hard rock aquifers. This unloading can cause fracture

systems to open up, and as a results increasing permeability and continuity which in turn, increase groundwater flows and impacts upon the surface water systems. All such impacts could extend for a number of kilometres outward from the mine working centre and therefore can potentially threaten the socio-economic activities and development of the inhabitants of the communities in and around where surface mining operations take place. From the preceding paragraphs, the radius of influence R_e within which all the derogatory risks are experienced therefore becomes the most important parameter of this research. Although, mine dewatering in general affects the quality of water discharged from mines to surface reservoirs, however, groundwater quality is not a subject of the present research.

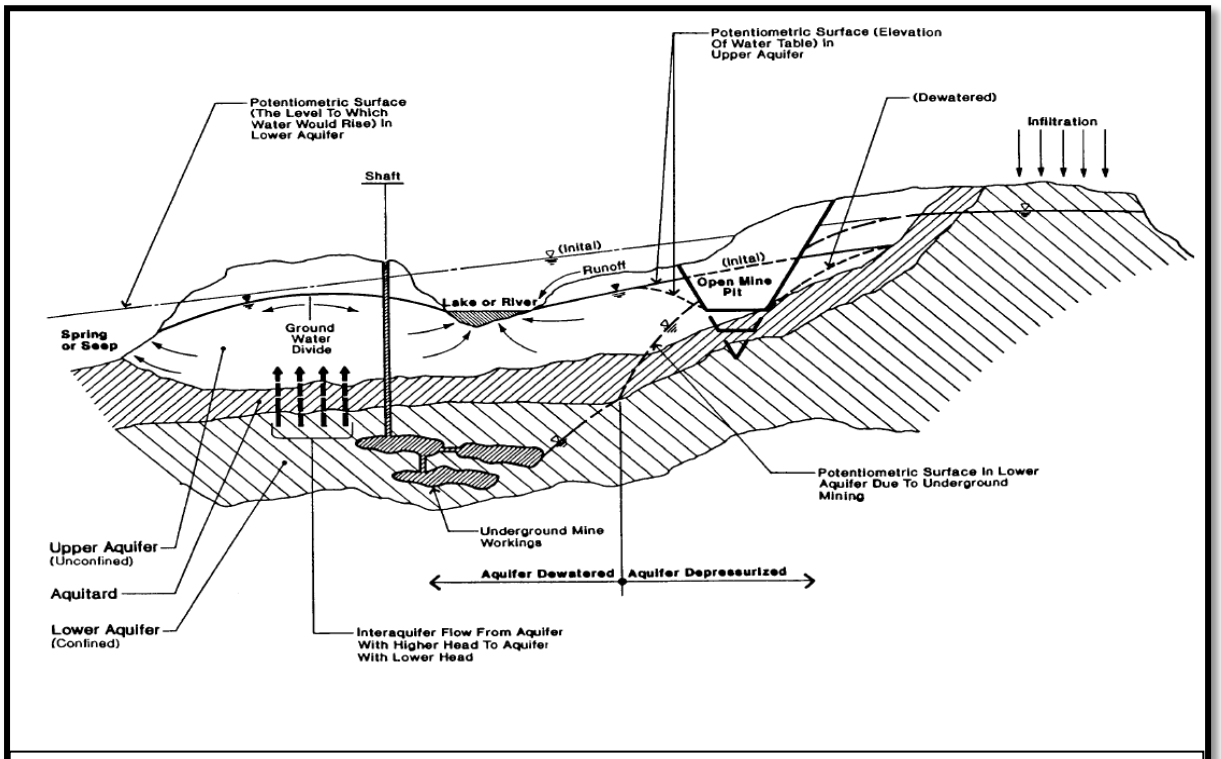

Figure 1.1 Dynamics of mining impacts on the groundwater flow systems (modified from Siegel, 1997)

According to Akabzaa and Darimani (2001) mining is of considerable importance in the economic development of Ghana. The country's colonial name – the Gold Coast - reflects how important mining has long been to the country. Ghana is the second most important producer of gold in Africa after the Republic of South Africa, and the third largest, of Mn and Al, and a significant producer of diamonds and recently, oil (Coakley, 1999; Appiah, 1993;

Akabzaa and Darimani, 2001). Gold dominates the mining sector in Ghana with prospective gold deposits localized in the three regions: Western, Ashanti and Brong Ahafo and cover eight municipalities/districts specifically, Wassa west, Obuasi, Amansie Central, Mpohor Wassa East, Amenfi East, Asutifi, Tano North and Ahafo Ano North. Gold mining companies with concessions in these areas include AngloGold Ashanti Iduapriem Mine, Obuasi Mine; Newmont Ahafo mine, AngloGold Ashanti (AGA), Golden Star Resources and Goldfields Ghana Limited. The Western and Ashanti regions of Ghana have varying years and experiences of mining whilst communities in the Brong Ahafo region are yet to experience the full scale effects of surface mining. In fact, the Tarkwa area in the Wassa West District of South Western Ghana is said to have the single largest concentration of mines and mining companies on the African continent (Akabzaa and Darimani, 2001) where about one-third of the total land area is under concession to mining companies.

Despite this potential, decades of mining and the recent method of surface mining continue to cause destruction to the quantity and quality of surface and groundwater bodies in Ghana. The mine and its owners have been criticised in the past for the loss of community livelihood and the environment, pollution and drying up of local rivers and water sources, and the lack of action to combat these issues. The current high gold price has generated a vibrant economy in Ghana and especially, Tarkwa and its environs and has increased population and water use. Consequently, the water resources of the mining environments in Ghana are getting under pressure. For example according to Kuma and Younger (2004) mining activities in the Tarkwa District draw a huge amount of water from the Bonsa River, the main source of portable water supply to Tarkwa Township and this has resulted in lower water flow levels in the Bonsa River and the lower reaches of the Angonabeng River and has lengthened patches of dryness during the dry season. These researchers further estimated that about 40% of the groundwater resources in the Tarkwa area have been destroyed by increasing mining operations, whilst the remaining 60% is at some distance from the population centres. Mining is therefore considered to be one of the major industries in the region which consumes a large quantity of groundwater through its operations. For instance the annual volume of groundwater usage of some of the leading mining companies in Ghana from 2005 to 2008 is shown in Table 1.1. Kuma and Ewusi (2009), affirm that data on annual ratio of water produced by Ghana Water Company Limited at the Bonsa Treatment Plant to

population growth of Tarkwa from 1987 to 2008 revealed an amount of 76litres/person/day in 1987 decreasing to 40litres/person/day in 2008. These Figures demonstrate that the amount of water produced over the years has not kept pace with population growth in Tarkwa and its environs. More evidence of surface mining impacts on the environment is discussed in Chapter 2.

Table 1.1 Annual volumes of freshwater usage for major mining operations in Ghana (Source: Anglogold Ashanti Obuasi, Tarkwa goldfields and Iduaprem Country report 2008)

Gold mining company in Ghana	Volume of water (m^3)/Year			
	2005	2006	2007	2008
Goldfields Limited (TGL) Tarkwa	5,200,000	3,529,537	5,596,000	7,941,690
Goldfields Limited (TGL) Tarkwa Damang	800,000	673,439	594,376	547,910
Ghana Australia gold-fields Limited (GAG) Iduaprem Tarkwa	977,466	98,000	100000	100000
Ashanti Goldfields Limited (AGC) Obuasi	9,005,564	10, 356,870	10,621,257	9,419,952

1.2 The rationale of the Research

Over the last several decades, improved mining methods and practices have been proposed in order that cuttings, excavations and dewatering at high risk for impacts on the groundwater flow system in hard rock mining environments are identified early enough and preventive measures effectively prioritized (Hartma, 1987; Warhurst, 1994; Soni, 2006; 2008; Kuma, Younger and Bowell, 2002). Anticipation and control of groundwater-related problems are therefore, critically important for the optimum performance of surface mining operation and the satisfaction of set production targets. Thus, an assessment of mining impacts needs to become an integral part of mine planning at the early stages of a mining operation, when there are few data, on which to base estimates and still more time to consider favorable planning and design alternatives.

Kuma (2007) reported that in Ghana, the many debates which have taken place relating to the environmental impacts of mining include the following; de-forestation, loss of farmlands, surface and groundwater pollution, resettlement, community livelihood and the

environment, and violent conflicts and human rights violations. Although water contamination has been the main concern, other aspects of groundwater management have received little recognition, for example, mine dewatering and its effects on aquifers, possible changes of groundwater flow directions, reductions in stream-flow, potential loss of groundwater-dependent ecosystems, land subsidence, and groundwater recharge. Kuma (2007) contended that the importance of the mining industry to the growth of the Ghanaian economy necessitates a wider approach to the solution of issues relating to surface and groundwater.

In the present context, the general desire has been to determine under what conditions mines derogate local villages significantly. Initially it was intended to investigate a particular mine in Tarkwa area of Ghana and develop a detailed model of it and thereby investigate how the mine affects surrounding areas. However after two visits to Ghana and discussions with mine companies regulators and researchers, only very limited amount of data could be obtained. Hence the project aim changed to attempting to determine in general if mine derogation impacts are likely to be significant in Ghana and other areas and if so under what conditions, and also could the derogation be assessed using the limited data that was likely to be available ahead of mine development.

1.3 Research Aim

The fundamental aim of this research is therefore to determine under what circumstances gold mines in Ghana are likely to have an adverse effect on water levels in surrounding villages/farms and in particular to try and come up with heuristic rules that would indicate under what circumstances there may be derogation problems to the regional groundwater flow system. Although, the study places emphasis on gold mining in Ghana, but with the intention that the concluding results could be used elsewhere with similar hydrogeological environments. Additionally, the research objectives are as follows:

1. To determine how important the effect of surface mining on the regional groundwater flow system can be
2. To investigate the circumstances under which the effect is greatest

1.4 Research Application

In view of the above mentioned objectives, it is hoped that the research will have the following application:

1. providing a general evaluation of the importance of groundwater impact for African mining communities in general, and for Ghana in particular

2. providing a first-hand quantitative information and guidelines for hydrogeologists and engineers for gold mining design purposes

3. providing an indication of what are the most important data to collect for early assessment of derogation impacts

4. providing means of informing decision-making and regulatory bodies on environmental implications when allocating mining concessions or giving out permits for mining operations.

1.5 Research Approach

In this study, the research approach/methodology is based on the application of scoping calculations using very simple numerical models. Data on hydraulic conductivity K, recharge R, and mine geometry G have been used as input data into the numerical models to explore the effect of open pit mines on the regional groundwater flow system in hard rock environments with specific reference to Ghana. Because the data apart from the mine geometry data were quite uncertain, the intention was to use as simple a model representation as possible. Sophisticated models would include the estimation of even more parameter values and would not necessarily increase the reliability of the predictions. This approach of course can be reviewed after the modelling results are obtained from the simple models.

In detail, the approach adopted involves first of all, a comprehensive international literature search of hydraulic conductivity estimates as insufficient could be obtained from Ghana, and mine geometry ranges of hard rock areas in mining environments. Standard statistics have been employed to characterize hydraulic conductivity and to provide a statistical range of estimates for use in subsequent groundwater modelling activities. The HYDRUS-1D

Computer Code has been used to simulate direct rainfall infiltration (i.e. potential direct recharge) of the top soil of hard rock areas. Simple computer models have been developed using the MODFLOW and SEEP computer codes to enable scoping estimates to be made of derogatory risk. In Figure 1.4, a step-by-step process of the development of the semi-quantitative method is summarized in a flow chart whilst, in Figure 1.5 a block diagram of input-output parameters for modelling simulations is shown.

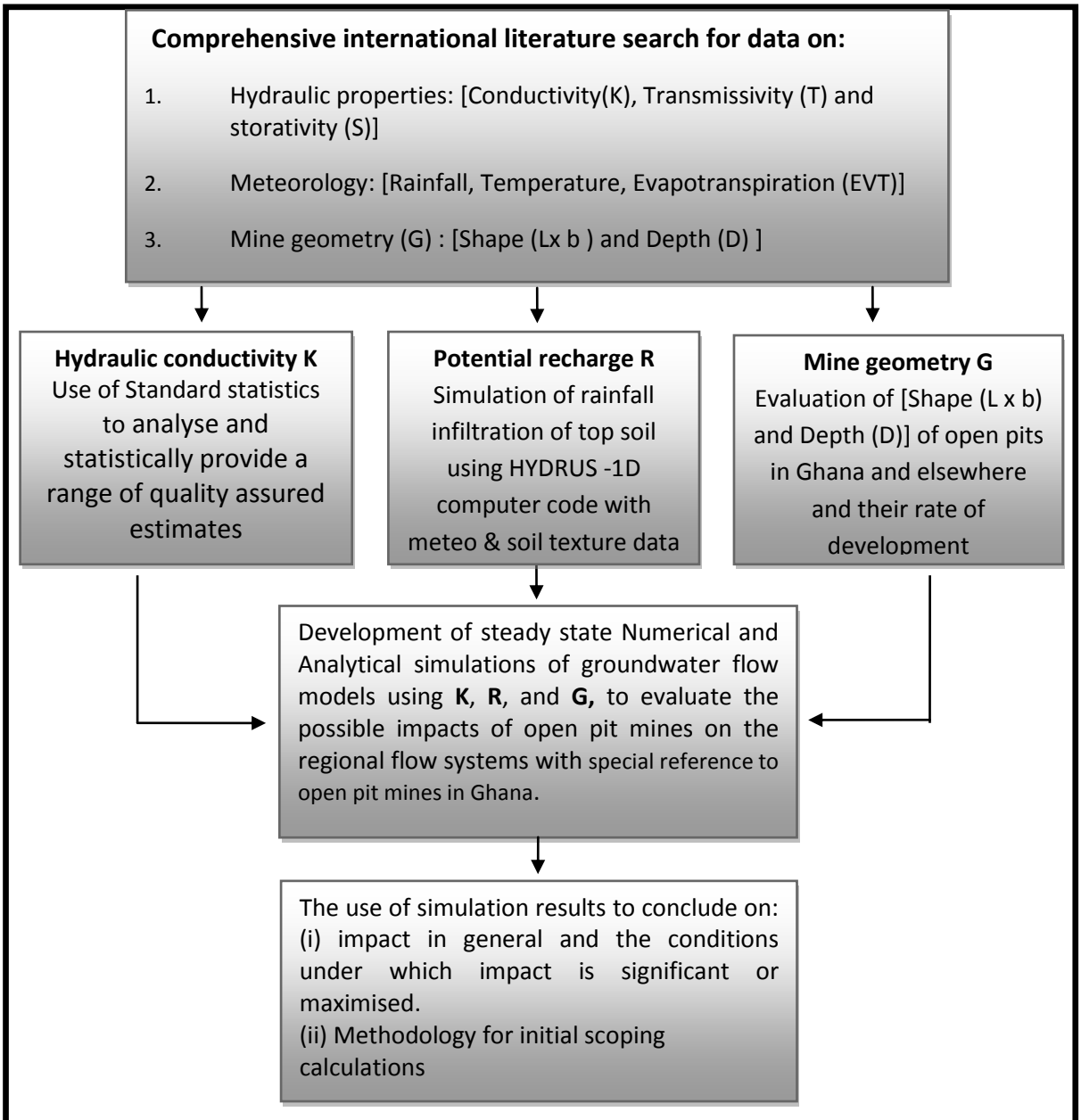

Figure 1.4 A flow chart of proposed method and approach to research

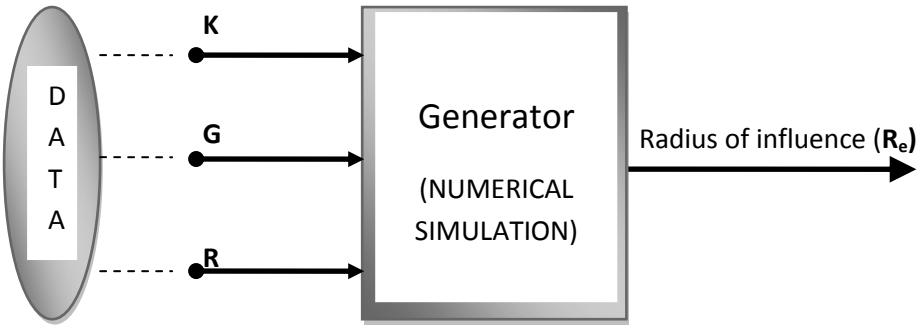

Figure 1.5 A block diagram for input-output parameters for model simulations

1.6 Structure of the thesis

The whole thesis is divided into seven chapters as outlined below:

1. **Chapter 1** presents an introduction to the research, highlighting the background, the aim and objectives, application, methodology and approach, and briefly outlines the structure of the thesis.
2. **Chapter 2** describes the dynamics of open pit mines in general with emphasis on mines in Ghana. The geometry [size (length x width x depth)], time of existence and rate of development of the mines and evidence of derogation is also discussed.
3. **Chapter 3** details the characterization of hydraulic conductivity of hard rocks in the mining environment. Issues relating to difficulty in estimating appropriate K values from field testing and factors affecting the choice of appropriate K for modelling at regional scale are discussed. The approach adopted and a summary of the findings are also presented.
4. **In Chapter 4** the characterization of Potential Direct Recharge of hard rock areas in the mining environments is presented. The method and approach followed and the use and application of the HYDRUS-1D Computer Code in the characterization process is discussed. The results and conclusions drawn are also presented.
5. **Chapter 5** presents the approach and methodology adopted in the risk assessment of the potential surface mining impacts through the use of steady-state numerical modelling. Issues relating to the representation of open pit mine as conceptualized in chapter three are discussed.

6. **Chapter 6** presents the results of the modelling work based on the models from Chapter five and using data on mine geometry, hydraulic conductivity and groundwater recharge which were obtained from Chapters two, three and four respectively. Chapter six then discusses the implication of the results.
7. **Chapter 7** concludes the research effort by summarizing and drawing general conclusions from the present study and provides recommendations for future research.

CHAPTER 2

DYNAMICS OF GHANA OPEN PIT GOLD MINES: DEROGATION AND GEOMETRY

2.1 Introduction

Historically, the majority of gold in Ghana was mined from "placer deposits", a process whereby gold is obtained from accumulation of unconsolidated minerals, form by gravity separation at the downstream of an existing water course from its source (Hirdes and Nunoo, 1994). Most modern mines in Ghana are hard rock mines that directly mine the source, or "lode" of gold, from where it has originally been deposited by geochemical processes or tectonic activities. In Ghana, the majority of hard rock mines operate surface mining with very few of them reaching underground and are usually more environmentally destructive than the ancient placer mining. In the following sections, the development of gold mining in Ghana and its derogation effects have been discussed. Detailed description of geographical characteristics and the rate of development of surface mining in Ghana have also been discussed with specific consideration to geometry (shape and size) of open-pit mines.

2.2 Brief history of gold mining in Ghana

West Africa has been a key source of gold for almost two thousand years (Griffis, et al., 2002). In fact, nearly all the known gold deposits in Ghana, Burkina Faso and Cote d'Ivore are hosted by the Proterozoic Birimian rock belt in West Africa (see Figure 2.1). It is also worth to note that Ghana's economic geology (Figure 2.2) is centered on the Birimian and Tarkwaian rock systems (Grubaugh, 2002). Beginning from West Africa, gold reached the Mediterranean by camel caravan across the Sahara desert. As at 1460, the Portuguese navigators were shipping African gold directly back to Europe, and later the English and the Dutch ships also brought gold to London and Amsterdam (Griffis, et al., 2002). Formal gold exploration and mining in Ghana began in the 19th century when Ghana was colonized by the Europeans. The first European gold concession in Ghana was issued in Tarkwa area in 1877, and in 1897 Ashanti Goldfields Corporation Limited was founded. This is followed by The Ghana Chamber of Mines which is Africa's second oldest. Other major mines that were

started about the same time include: Abosso (1896); Bibiani (1901); Prestea (1903); and Tarkwa (1909) all in the South Western part of Ghana except Bibiani. Ghana is the second most important producer of gold after the Republic of South Africa, and the third largest producer of manganese and aluminium, and a significant producer of bauxite diamonds and recently, oil (Coakley, 1999 and Appiah, 1993). Gold dominates the mining sector in Ghana with prospective gold deposits localized in the western part of the country where about one-third of the total land area is under concession to mining companies. In fact, as put it by (Akabzaa and Darimani, 2001) the Tarkwa area in the Wassa West District of South Western part of Ghana is said to have the single largest concentration of mines and mining companies on the African continent.

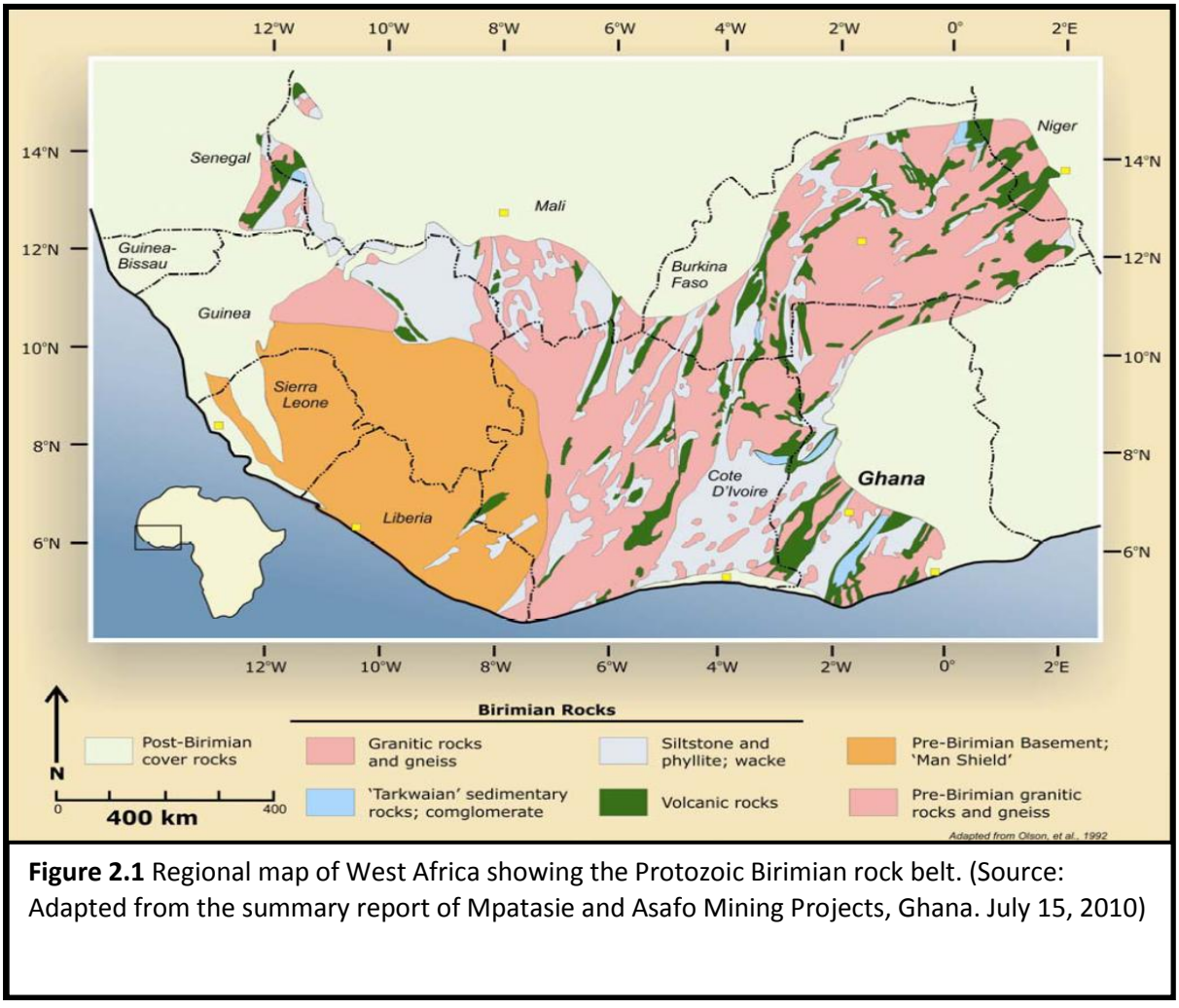

Figure 2.1 Regional map of West Africa showing the Protozoic Birimian rock belt. (Source: Adapted from the summary report of Mpatasie and Asafo Mining Projects, Ghana. July 15, 2010)

2.3 Structure of the mining industry in Ghana

As presented by Akabzaa and Darimani (2001), the ownership structure of the mining industry in Ghana is made up of some few large companies from Canada, Australia, and South Africa and recently the United States. There are however, lesser investors from China, United Kingdom and Norway. In terms of nationality of ownership, 85% of the industry is owned by foreign nationals and the rest by Ghana Government and several small scale Ghanaian operators. According to Kwesi and Kwesi (2011) there are eleven large scale mining companies operating in the country currently of which eight are gold mines. The rest are, bauxite, diamond and Mn mines. Excepting the Anglo Gold Ashanti mine at Obuasi which still operates underground mining, all the other mines operate surface mining. And out of the eleven large-scale mines in Ghana, seven of them are located in Tarkwa District in the Western region (W/R) producing a significant proportion of the country's gold output. The only manganese mine in the country is also located in the Tarkwa area. Table 2.1 shows the location, date mining commenced and mining/processing method of large scale mining companies operating in the Western region (W/R), Ashanti region (A/R) and Brong Ahafo region (B/A).

Table 2.1 Leading gold mines in Ghana after 1986 (Source: Ghana Chamber of Mines annual reports; Akabzaa, 2001)

Mining Company	Mine Location	Starting Date	Mining / Processing Method
Goldfields Ghana Ltd.	Tarkwa (W/R)	1993	Open-Pit/Heap leach
Of South Africa	Damang (W/R)	1997	Open-Pit/CIL
	Abosso (W/R)	1997	Open-Pit /CIL
Anglo Gold Ashanti of	Obuasi (A/R)	2004	Open-Pit/Underground
South Africa	Iduapriem (W/R)	1992	Open-Pit /Heap leach
(Central Africa Gold)	Bibiani (W/R)	1997	Open-Pit/CIL
Golden Star Resources	Bogosu (W/R)	1990	Open-Pit/CIL
Ltd. Of Canada	Akyempim (W/R)	2005	Open-Pit /CIL
	Preastea (W/R)	1995	Open-Pit/Underground
Red Back Mining Inc. Of	Chirano (W/R)	2005	Open-Pit/Heap leach
Canada			
Newmont Ghana Gold	Ahafo (B/A)	2006	Open-Pit /CIL
Ltd. Of Denver USA.	Akyem (B/A)	2011	Open-Pit /CIL

2.4 Mining methods used in Ghana

The process of gold mining from prospecting to exploration to development to extraction and finally to reclamation consists of several distinct steps. Currently, there are several different methods used for mining gold deposits and extracting the valuable metal from the ground. The method used varies and depends on: the geology and topography of the area; location, type, size and orientation of the mineral resource (Hartman, 1987; Hoek and Bray, 1974). In Ghana, targets of gold deposits are of two general categories; placer and ore-body deposits. Placer deposits are made up of minerals contained within river gravels, and beach sands mostly found in the Ankobra, Birim and Offin rivers and other unconsolidated materials. Ore-body deposits are valuable minerals found in veins, stratified layers or mineral grains which are generally distributed throughout the Birimian and the Tarkwaian rock system of the Ashanti belt (Agyapong et al., 1992). Both surface and underground mining methods are used in Ghana to mine both types of ore deposits. Typical surface mining methods include: strip and open pit mining; dredge, placer and hydraulic mining in riverbeds, beaches and terraces. Most of the large scale companies in Ghana operate hard-rock open pit mining where the ore-body or lode of gold is directly mined from the source where it has originally been deposited by geochemical processes or tectonic activities. Despite its negative impacts, surface mining has been promoted in Ghana and many mining countries worldwide in recent years due to the following reasons:

1. **Location of the ore-bodies**- The location of ore-bodies in most part of the country are close to the surface which makes it easier to be mined by surface mining (Agyapong et al., 1992). For instance the approximately horizontally stratified reserves with a thin covering of overburden in Tarkwa and Ahafo area. Similarly, the Obuasi deposits occur along a zone of faulting within Precambrian greenstones (Eisenlohr, 1989). According to Agyapong et al. (1992) and Eisenlohr (1989), two main types of minerals are found in the mining environments in Ghana namely; quartz veins containing high-grade native gold and the main sulphide ore where narrow veins contain gold within arsenopyrite. Both surface and underground mining are operated in the Obuasi area.

2. **Low grade ore which requires processing huge quantities**- Most of the ore grade in Ghana, particular Tarkwa and Bibiani in the western region, are very low and therefore require large volumes of ore to be mined and processed for a small yield. Hence, the only option left for a successful and profitable mining is surface mining which is relatively cheaper.

3. **Cost considerations**- The operating cost of mining has gone up drastically in the last two decades. The price of fuel, power, chemicals and other consumables have all increased sharply during the last decade or two. Comparatively, surface mining is relatively cheaper, safer and mechanically easier to operate than underground mining. Also the demand for power, especially in developing countries and Ghana in particular, far outweighs supply. Therefore, there is always inadequate supply of power for mining resulting in increased cost for energy alternative. In the face of high cost of mining inputs and inadequate supply of power, surface mining therefore becomes the favourable, cost effective and preferred option in Ghana and most countries worldwide.

4. **Safety considerations**- Comparatively, there are also low number of accidents and fatalities in surface mining than underground mining, there is no risk of cave in or toxic gas. For example the Lost Day Injury Frequency Rate (LDIFR) of mining companies in Ghana indicate higher rate in underground mines than in surface mines. (Goldfields Ltd, Annual Report, 2007). Also, there are high numbers of fatal accidents in underground mines than in surface mines.

5. **Competition among gold producing countries for investors**- Ghana has been the only most important gold producing country in west Africa for the past three decades until recently joined by Burkina Faso, Mali and Guinea. This situation has created competition among these countries as an investor destination with investors easily attracted to countries whose laws allow surface mining.

2.5 Geographical Characteristics of Tarkwa District: The hub of gold mining in Ghana

The Tarkwa District in South Western Ghana is located at (Lat 5^0 18 N, Long 2^0 W) with Tarkwa as it administrative capital (Figure 2.2). The area lies along the main gold belt of Ghana, the Ashanti belt that stretches north-eastwards from Axim in the southwest to Agogo in the northeast making the area one of the main gold mining Districts of Ghana.

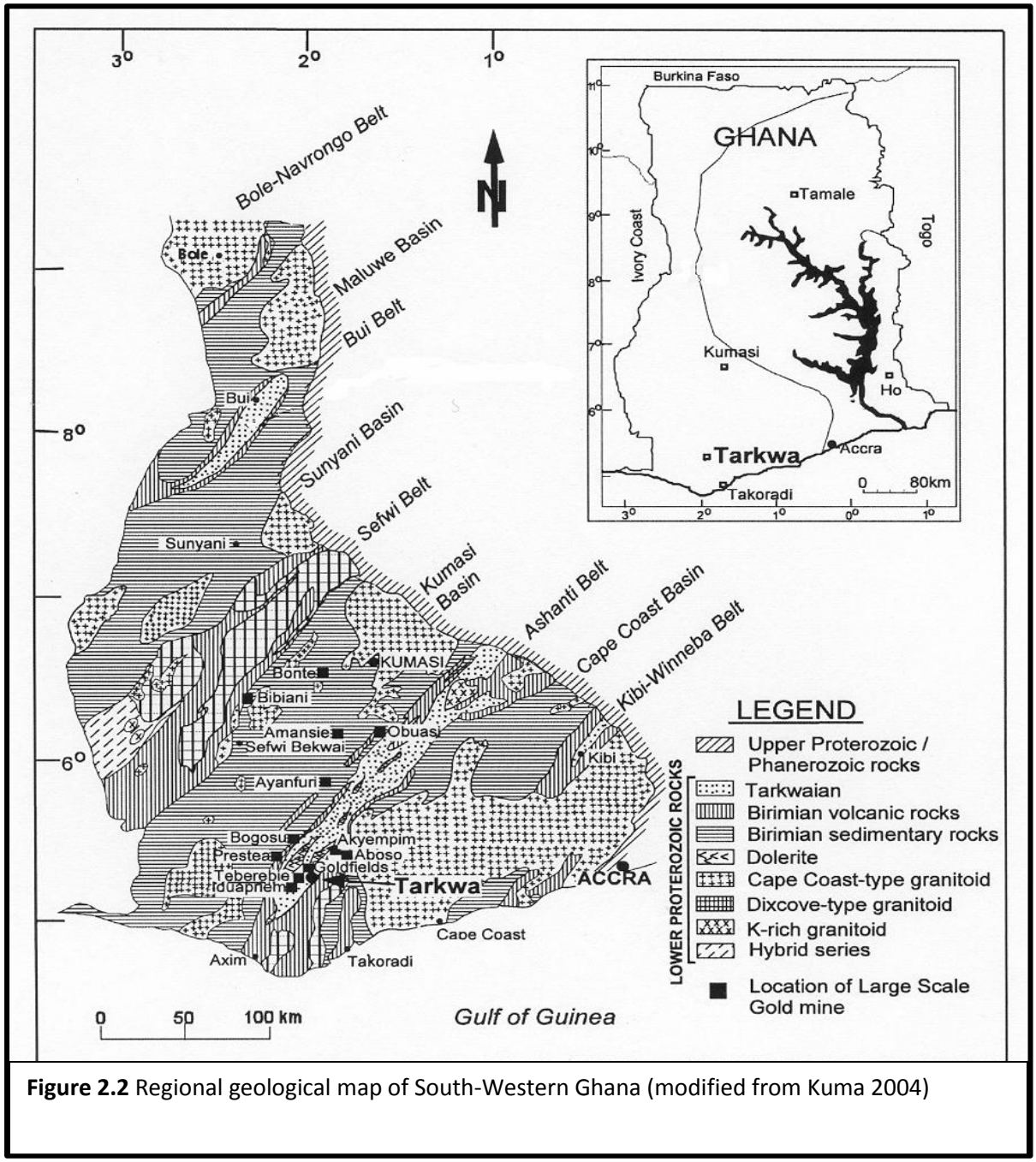

Figure 2.2 Regional geological map of South-Western Ghana (modified from Kuma 2004)

In general, Ghana is characterized by low physical relief with the Precambrian rock system underlying most part of the country and worn down by erosion almost to a plain. The relief of Tarkwa District is moderate and decreases to the south from an altitude of 300m to 150m above sea level. The population of the district is approximately 236,000 and is mainly composed of the indigenous Wassa tribe but with representation of all tribal entities in Ghana (Acquah, 1992 and Agyapong *et al.,* 1992). Industries of the district are mining (gold, manganese) with gold mining being the main industrial activity in the area and subsistence farming. The principal crops grown are; cocoa, plantain, pineapple, maize, cassava, yam and some oil palm, coffee and rubber (Avotri et al. 2002; Asklund, Eldvall and Björn 2005).

The rainfall pattern in Ghana generally decreases from the south to the north with the south-western part being the wettest and where annual rainfall is over 2,000 mm. In the extreme north, the annual rainfall is less than 1,100 mm (Dickson and Benneh, 1988). The south-eastern coastal edge is the driest area where the rainfall is about 750 mm per annum. Much of the rain falls in intense storms of short duration, which normally occur at the beginning of the season resulting in heavy runoff and erosion (Dickson and Benneh, 1988; Benneh and others 1990).

The main vegetation formation of Ghana (Figure 2.3) as described by Benneh *et al*. (1990) are the Coastal Mangrove and Strand, the Coastal Savannah, the Closed Rain Forest and the Moist Semi-deciduous Forest, the Derived Savannah and the Interior Savannah. South western Ghana has about 75 percent of its vegetation within the high forest zone, with Tarkwa District located within the transition zone between the rain forest and the moist semi-deciduous forest (Dickson and Benneh 1988).

Tarkwa Distrct in South Western Ghana has a tropical and humid climate with mean annual rainfall between 1500mm and 2000mm. The region is characterized by two main rainfall periods within each year; from May to July with a peak in June, and September to November with a peak in October (Dickson and Benneh 1988). Intermittent minor rains occur also throughout the year. Figure2.4 shows the average rainfall distribution pattern from 1940 to 2001. During the dry season the dry North-East Trade winds (Harmattan) blow from the North to the South. The mining District of Tarkwa is very humid and warm with

mean annual rate of pan evaporation of 1500mm and the average air temperature ranges from 28 and 33°C. The high rainfall regime creates much moisture culminating in high relative humidity and ranges between 70 to 90 per cent in most parts of the region (Dickson and Benneh 1988).

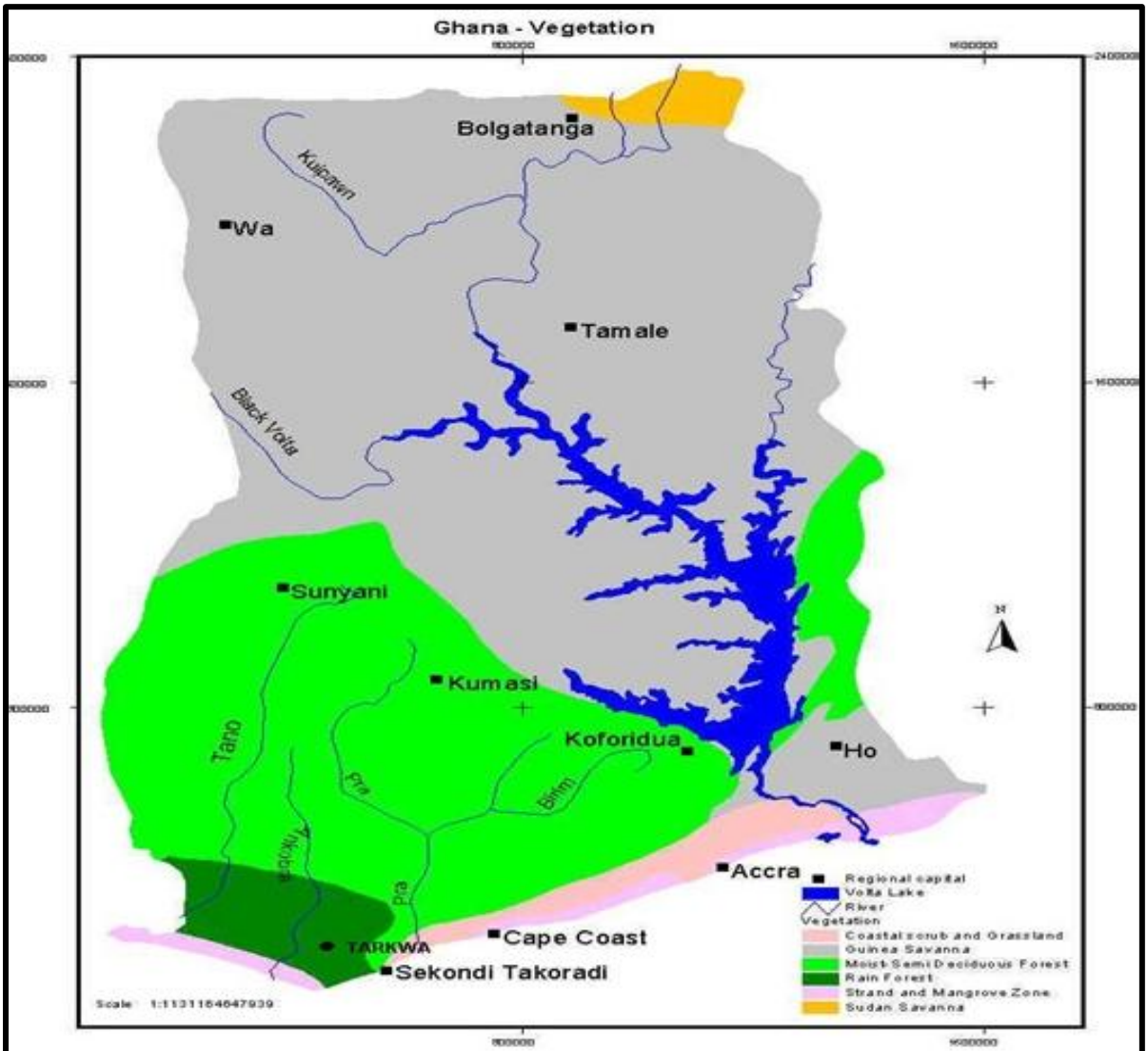

Figure 2.3 Vegetation map of Ghana showing the rain forest of Tarkwa District in South Western Ghana (Dickson and Benneh, 1988)

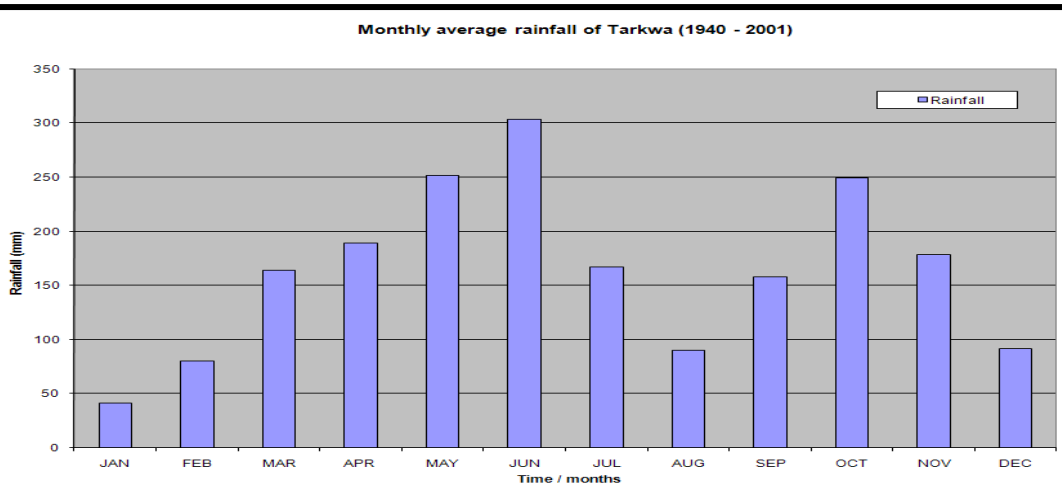

Figure 2.4 Average monthly rainfall pattern in the mining district of Tarkwa in South Western Ghana (From 1940 – 2001)

2.6 Local Geology

The Tarkwa orebodies are located within the Tarkwaian System (Figure 2.5) which forms a significant portion of the stratigraphy of the Ashanti Belt (Figure 2.2) in southwest Ghana (Kesse, 1985; Leube and Hirdes, 1986). The Ashanti Belt strikes in a north-easterly direction and it is broadly synclinal in structure (Kesse, 1985). According to Leube and Hirdes (1986), the belt is made up of the Lower Proterozoic sediments and volcanics, and underlain by the metamorphosed volcanics and sediments of the Birimian System. These researchers argue that the contact between the Tarkwaian and the Birimian is intensely sheared with significant associated gold deposits, including in the mining areas of Prestea, Bogoso and Obuasi. The Tarkwaian unconformably overlies the Birimian and is characterized by lower intensity metamorphism and the predominance of coarse grained, immature sedimentary units (Table 2.2.)

Table 2.2 Division of the Tarkwaian rock system (modified from Kuma and Younger2001)

Series	Thickness (m)	Composite lithology
Kawere Group	250-700	Quartzites, grits, phyllites and conglomerates.
Banket Series	120-160	Tarkwa phyllite transitional beds and sandstones, quartzites, grits breccias and conglomerates.
Tarkwa Phyllite	120-400	Huni sandstone transitional beds, and greenish-grey phyllites and schists.
Huni Sandstone	1370	Sandstones, grits and quartizes with bands of phyllite.

Whitelaw (1929) and Hirst (1938) describe the boundary between the Banket Series and the overlying Tarkwa Phyllite as marked by a deep valley which follows a sill with the Tarkwa Phyllite highly fractured at shallow depth. These researchers further described the Huni Sandstone as a fine grained quartzite with low relief. Sedimentological studies and modelling of the detailed stratigraphy within individual reef units have resulted in the recognition of a cycle of events from initial channel formation and rapid downcutting of the central channel (basin downwarp time units T_1 and T_2) through a period of uplift and reworking (T_3) and finally a period of meandering channel bars and flow reduction leading to the development of low grade silty interbeds (Whitelaw, 1929). This sequence has been recognised in each of the main reef units with the T_3 sequence recognised as the principal episode of gold deposition and concentration.

The local geology in the Tarkwa area (Figure 2.5) is dominated by the Banket Series which forms the highest topographic features and is generally resistant to weathering. The beds are divided into three zones on the basis of their texture and mineralisation into the following categories (Whitelaw 1929);

1. "The beds above the gold-bearing conglomerate zone consist of fine to medium grained, siliceous quartzites with coarse grits and bands of breccia, which are normally dense and hard and are almost exclusively responsible for the ridges.

2. The gold-bearing conglomerate zone comprises alternating bands of quartzites, grits and conglomerate. This zone is dense and compact when fresh but weathers generally to coarse and loose material.

3. The beds below the conglomerate zone also consist of quartzites, grits and conglomerates but these rocks are mostly soft and easily weathered and therefore, poorly exposed at the surface."

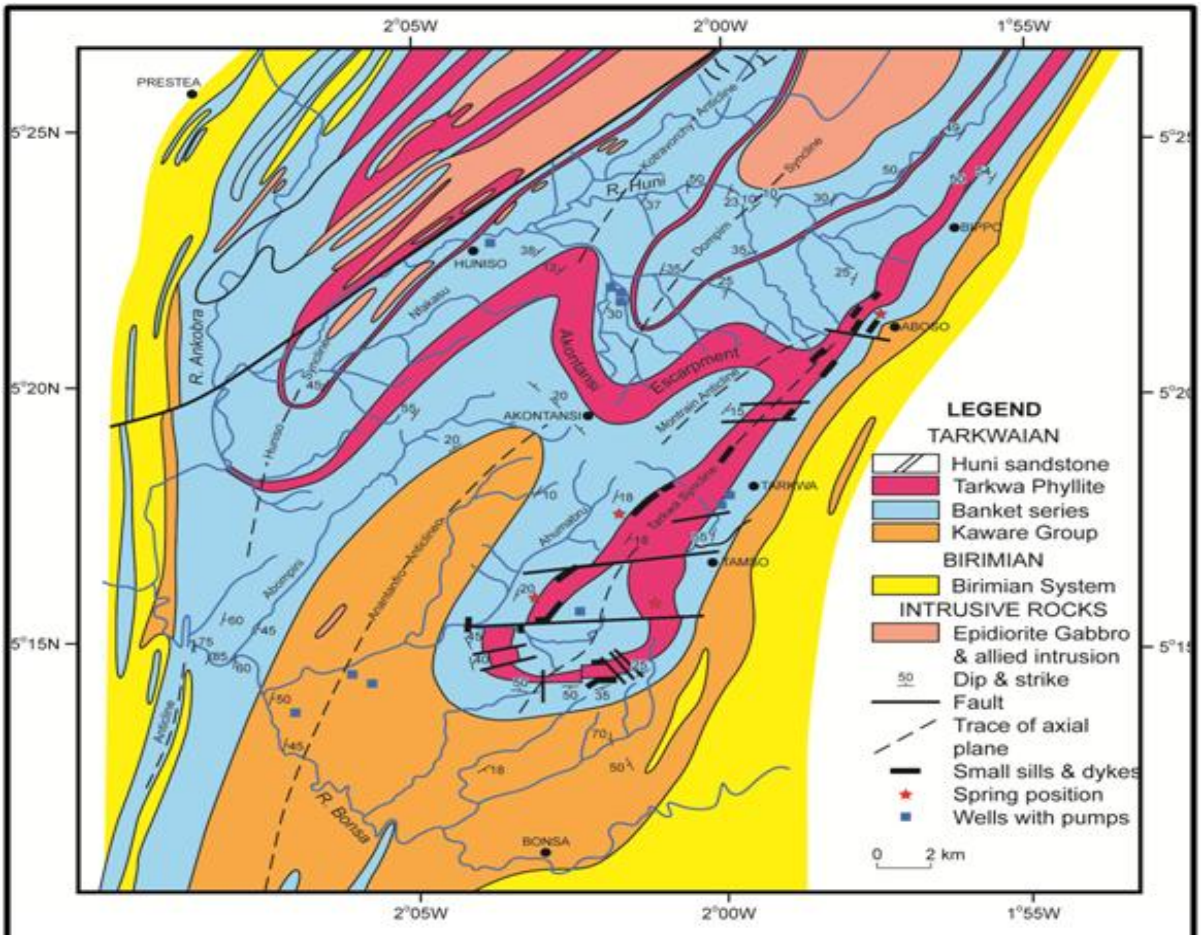

Figure 2.5 Local geological map of Tarkwa District in Wassa West, South Western Ghana

2.7 Evidence of mine derogation in Ghana

The environmental and health impact of mining activities in Ghana is well documented by researchers such as; Akosa et al., 2002; Ntibery et al., 2003; Dzigbodi-Adzimah, 1996; Smedley et al., 1996; Kortatsi, 2004; and Kuma, & Younger, 2004, among others. The principal environmental problems caused by both mining companies and artisanal miners are; dewatering effects and the free use of water for mining operations, chemical pollution of ground water and streams, siltation, increased faecal matter, deforestation, loss of farmlands and resettlement (Kortatsi, 2004 and Kuma, 2007).

The introduction of surface mining in the 1980s had a lot of implications for fresh water protection in Ghana. Many writers such as; Amonoo-Neiser & Busari, 1980; Jetuah, 1997; Carbo and Sarfo-Armah, 1997 and Clement et al., 1997 anticipated that the development of

extensive mining operations in ecologically sensitive areas such as Obuasi in the Ashanti region and Tarkwa in the Western region with undulating topography would certainly give rise to environmental problems. They argued that the government's intention to permit large scale surface mining in the country had overwhelming impact on water bodies in the mining environments and that mining has destroyed many communities' sources of water with it accompanied untold hardships.

It is a statutory requirement for EPA to demand from the mining companies, when leasing concession, a Baseline Environmental Study on: Climatic Conditions; Flora and Fauna; Hydrological Resources; Settlements; Socioeconomic and Cultural Elements; and Social Services, so that future damage to the environment could be assessed. In most cases these baseline studies indicates pristine mining environments which later become adversely affected by surface mining (e.g., CGML, 2010).

Today, through the adoption and adaptation of modern technology, such as the heap leach (HL) and carbon in leach (CIL) methods in surface mining, agriculture which employs 80% of Ghana's population, have suffered from mining activities (WACAM, 2011). This method of mining has led to the mining of fertile lands, a situation which has often initiated conflict over land use between farmers and mining companies. Moreover, most mining concessions lie within the few forest reserves left, for example about 60% of the concession of Chirano Gold Mines Limited (CGML) in the Western region, lies within the productive Tano Suraw and Tano Suraw Extension forest reserves (Brammer, 1956).

Research work conducted by Akabzaa and Darimani (2001) on Tarkwa in the Wassa West District reveals that extensive areas of land have been cleared in preparation for surface mining activities. They opined that over 70% of the total land area of Tarkwa has been given out as mining concessions. The researchers further estimated that about 40-60% of a given concession would have been used at the close of mining for activities such as siting of mines, open pits, mine camps, roads, heap leach facilities, tailings dump and resettlement for displaced communities. Table 2.3 shows progress of reclamation work of various mines on disturbed landmass in 2003. This has significant adverse impact on the land, vegetation and water resources which are the main sources of livelihood of the people. Although,

efforts are made by the mining companies to reclaim the land by reforestation, they end up modifying the natural ecosystem thereby destroying the biodiversity. The Wassa West District Assembly Medium Term Development Plan (2002-2004) also noted that this condition is worsened by the activities of the small scale miners who clear the forest and dig trenches, thereby exposing the soil to erosion and also serving as breeding grounds for mosquitoes.

Table 2.3 Progress of reclamation work on various mines in Ghana in 2003 (Source: Peprah and Pappoe (2008). Environmental Statistics of Ghana)

Mine	Area disturbed (Ha)	Area reclaimed (Ha)
Goldfields Ghana Ltd. (Tarkwa)	1654.00	260.00
Anglo Gold Ashanti (Oboasi)	2241.00	60.17
Anglo Gold Ashanti (Bibiani)	298.00	90.00
Anglo Gold Ashanti (Iduapriem)	1360.00	180.00
Aboso Goldfields Damang	645.00	257.00
Bonte Gold Mine	698.17	424.69
Ghana Manganese (Nsuta-Tarkwa)	2137.00	308.60
Resolute Amansie (Sunyani)	348.00	209.50

In the work of Kusimi (2007), to determine land use/cover change resulting from mining and other anthropogenic activities such as; farming, settlements, lumbering animal grazing and forest reserves in the Wassa West District from the period 1980 to 2002, he concluded that natural land cover has been diminishing and human-induced land use increasing (Figures 2.6 and 2.7). He opined that the most significant force for this change had been the rapid growth in the mining industry attracting a lot of people leading to the expansion of major mining towns in and around Tarkwa and increase use of water by mining companies and the growing population.

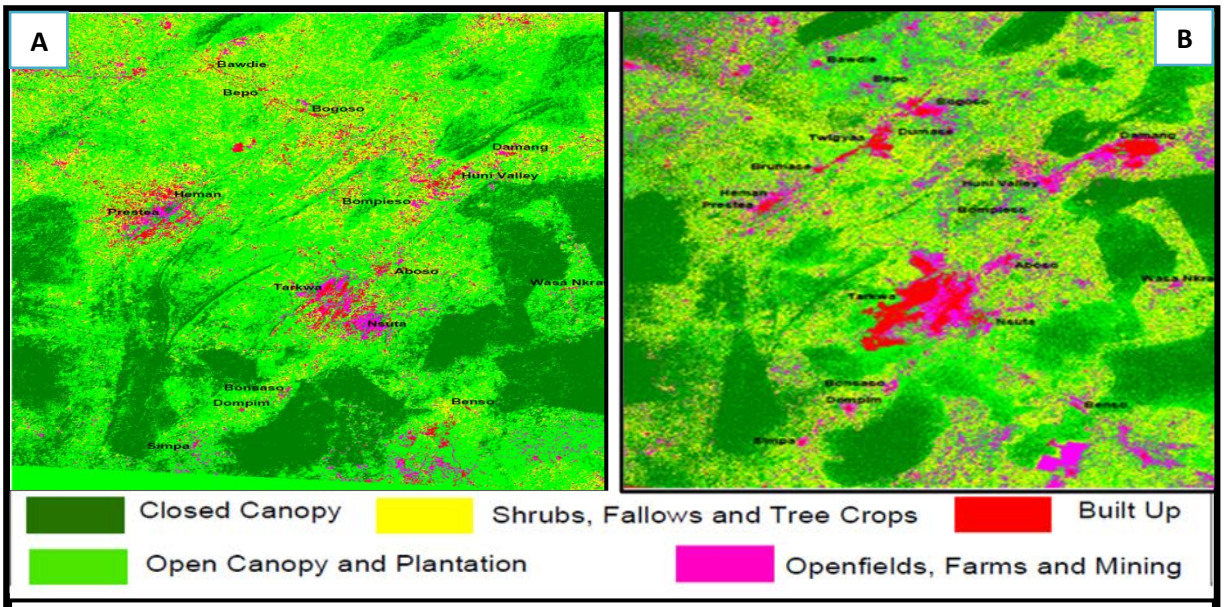

Figure 2.6 Classified landuse/cover distribution in Wassa West District as seen on (a) the TM imagery 1986 and (b) the TM imagery 2002. (Source: Classified Landsat TM imagery of 1986 and 2002, Kusimi (2007))

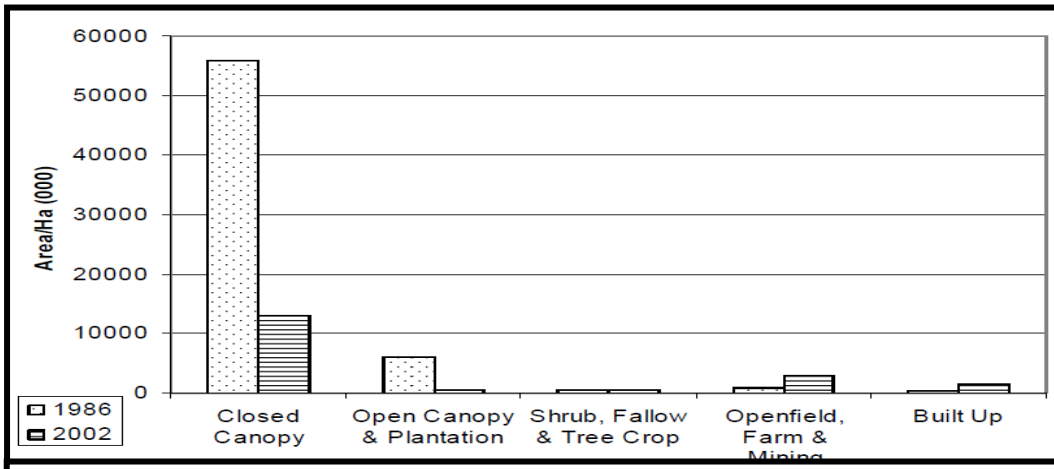

Figure 2.7 Comparison of the major landuse/lancover types in the Wassa West District based on TM imageries of 1986 and 2002 (modified from Kusimi, 2007)

The concentration of mining operations in Ghana has been a major source for the quality and availability of surface and groundwater. According to Mining watch (2000) and the Cyanide Investigative Committee (2002), in June 1996 a spill at Teberebie Goldfields sent thirty six million litres of cyanide solution into the Angonaben stream, a tributary of the Bonsa River in the western region of Ghana. The spillage destroyed Cocoa trees and fishponds while the local people complained of skin rashes. Since 1989 to 2002, Ghana recorded eight accidental cyanide spillages by mining companies and four of these which

occurred in Tarkwa in the Wassa West District affected major water bodies. According to the Cyanide Investigative Committee (2002), investigations conducted indicated that the number of officially reported cyanide spillages had increased from eight between 1989 and 2002 to about 13 cyanide spillages as at 2006.

According to Kuma and Younger (2000), surface mining operations consume a large amount of water which is obtained from the groundwater. Moreover, extensive excavation of large tracts of land and the heaping of large mounds of soil along watercourses results in the reduction of groundwater recharge sources and ultimately the reversal of the direction of groundwater flow. It is therefore not a surprise as reported by Kortatsi (2004) that a number of boreholes, hand-dug wells and streams in the area have become unproductive and provide less water.

A survey carried out by a non-governmental organisation, Wassa Association of Communities Affected by Mining (WACAM, 2008), to investigate about how water bodies are affected in communities affected by mining operations as well as communities with the potential of being affected by mining operations had the following results. The study targeted mining communities in three regions of Ghana namely Western, Ashanti and Brong Ahafo and covered eight municipalities/districts in Ghana specifically Wassa west, Obuasi, Amansie Central, Mpohor Wassa East, Amenfi East, Asutifi, Tano North and Ahafo Ano North. Mining companies with concessions in these areas include AngloGold Ashanti (AGA), Obuasi Mine; Newmont Ahafo mine, AngloGold Ashanti Iduapriem Mine, Golden Star Resources and Goldfields Ghana Limited. The areas selected for the survey have varying years and experiences of mining whilst others especially the communities in the Brong Ahafo region are yet to experience the full effects of surface mining. Whilst the Wassa West and Obuasi Municipalities had long history of mining, the Asutifi and Mpohor Wassa East areas have less than ten years of mining experience. In all about 127 communities were covered under the survey by the use of questionnaire and responses from community members under the following: List of water bodies in communities and their uses; Community perception of the conditions of water bodies; Alternative sources of water provided by mining companies and how communities perceived the alternative sources of water. The following are the results of their findings.

1. List of water bodies in communities and their uses

From the 127 communities within the three mining environments, 622 respondents from the study area listed 468 water bodies in the survey. According to them, these water bodies run through 852 communities as shown in Table 2.4. Of the 302 respondents from Oboasi in the Ashanti region, 34% regarded their stream to be used for both domestic and spiritual functions whiles 64% were of the view that the water bodies are used for only domestic purposes. All the 320 respondents from communities in Kenyase (195) in the Brong/Ahafo region and Tarkwa (125) in the Western region regarded water bodies to be used for spiritual, domestic, recreational and income generating purposes.

Table 2.4 Breakdown of communities in study area, number of water bodies and downstream communities (WACAM, 2008)

Code	Area	Number of communities	Number of respondents	Number of Water bodied listed	Down-Stream Communities listed
Obuasi Area	Obuasi Municipality and Amansie Central District	58	302	160	254
Tarkwa Area	Wassa West District, Amenfi and Mpohor Wassa East	30	125	117	179
Kenyase Area	Tano North, Asutifi and Ahafo Ano North Districts	39	195	191	419
Total		**127**	**622**	**468**	**852**

2. Community perception of the conditions of water bodies and causes of pollution

Whilst communities in both Tarkwa and Obuasi area had many of the water bodies perceived to be polluted by respondents (Table 2.5), the respondents in Kenyase area showed very little pollution of their rivers. Out of 160 rivers listed in Obuasi area, respondents' said 145 were polluted with only 15 perceived as not polluted. Respondents from Tarkwa area perceived all the 117 listed rivers as polluted. In the case of Kenyase however, Respondents said only 10 out of the 191 listed rivers were polluted. The results from the field study expressed in Table 2.5 could be explained that Kenyase has very short history of surface mining hence the small number of rivers perceived by respondents as polluted. It is important to note that though the study did not cover all the communities in the Kenyase area, the area had the highest number of listed rivers with minimal number of

rivers perceived by communities as polluted. On causes of pollution of water bodies, the study established that greater percentage of these water bodies in both Obuasi and Amansie area in the Ashanti region were polluted as a result of mining activities. All the 125 respondents in Tarkwa area believed that the 117 rivers listed were polluted by mining. However, 10 out the 125 respondents in Tarkwa area believed that both small and large scale mining destroyed rivers. In Figure 2.8 respondent's perception of causes on causes of pollution of the water bodies is expressed in percentages for easy interpretation.

Table 2.5 respondent's perception of condition of listed water bodies (WACAM, 2008)

Area	Number of rivers listed	Condition of river	
		Polluted	Not polluted
Obuasi	160	145	15
Tarkwa	117	117	0
Kenyase	191	10	181
Total	468	272	196

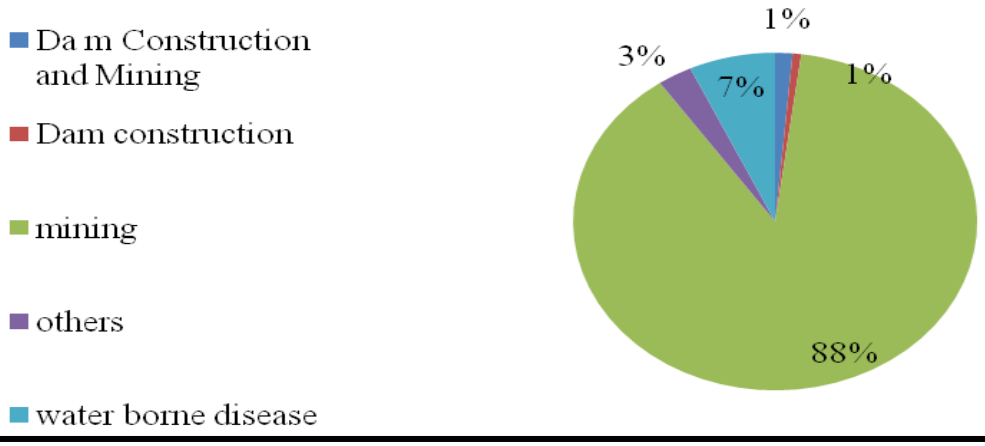

Figure 2.8 respondents perception on the causes of pollution of water bodies (WACAM, 2008)

3. Alternative sources of water provided by mining companies

Although, Ghana government and the mining companies have provide some communities with potable water as a result of polluted water bodies but the study indicated that majority of the communities do not have access to adequate potable water. As indicated in Figure 2.9, 84% of the 117 respondents' in Tarkwa area, continue to use polluted water bodies

because of the lack of potable water. Other communities in Tarkwa area had experiences with wells getting dried up during dry seasons and others getting muddy when it rains. They complain that the wells do not yield enough water for the whole population as the numbers of wells are not enough and easily get broken down. In Tarkwa and Obuasi areas some communities are provided with water in tanks which are not cleaned for many years.

In conclusion, the study confirmed that many mining communities are facing water problems and moreover, the alternative water provided is inadequate, thus making the provision of sustainable water to water-stressed mining communities in Ghana an urgent one. Figure 2.10 presents in pictures some of the derogation of surface mining in the mining communities.

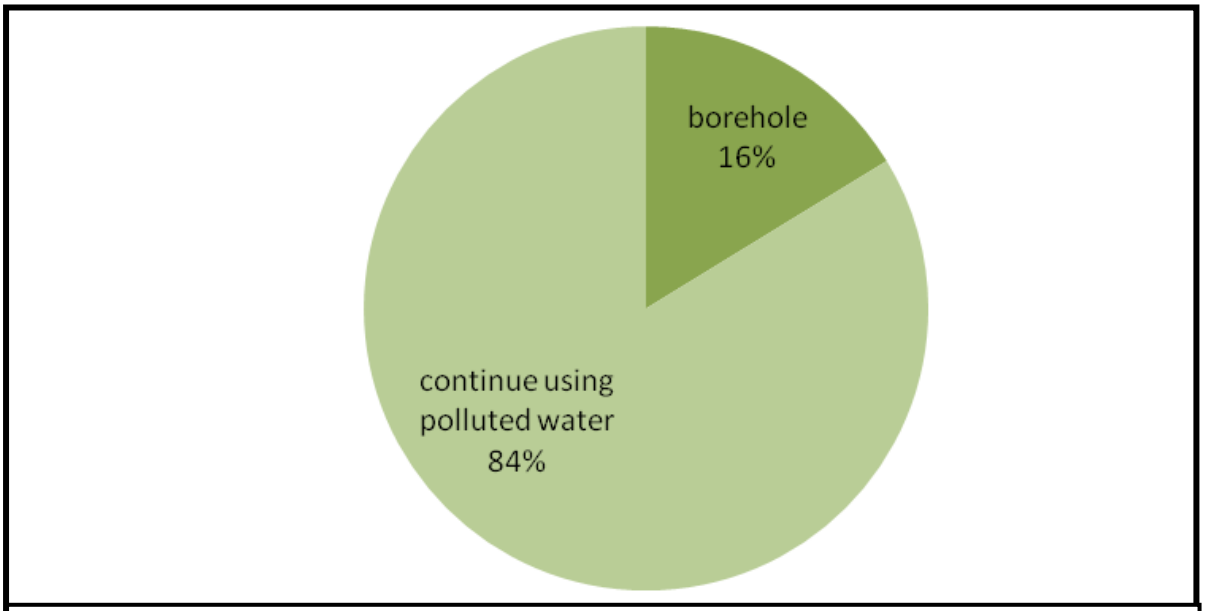

Figure 2.9 Alternative water sources available for the community in Tarkwa area (WACAM, 2008)

Figure 2.10 (A) Cyanide contaminated stream (B) Flooded open pit mine at Iduaprem near Tarkwa (c) Dead stream due to mine dewatering (D) Deforestation of farmlands to give way to surface mining (E) Illegal small scale miners panning for gold in cyanide contaminated tailing dam (F) dry water well due to mine dewatering (G) resettlement of a mining community (Atoabo) in the Western region (H) Water shortage in one of the mining communities in Ghana

2.8 Hard-rock open pit mining in Ghana

According to Lyon et al. (1993), open pit surface mining is the main type of mining method for major-scale hard-rock gold mining in Ghana and the world all over, especially when the shape of the ore body is in the form of a pipe, vein, irregular or steeply dipping stratified. They further affirm, it is the preferred method because the characteristics of the ore deposit (e.g. grade, size, location) make it the most cost-effective way of mining the low-grade ores that are located close to the surface over a wide area.

The process involves the removal of the overburden after which the pits are excavated of the exposed ore in ever-expanding terraces to increasing depths (Figure 2.11). Depending on the thickness, the ore-body may be mined in a single vertical pass or in multiple benches. According to Hartman (1987), when the ore-body is large as in the case of gold mining the ore-body is mined in benches. Vertical holes are drilled from the top of the bench and then the ore is blasted onto the adjacent lower level.

In case of less resistant materials, the ore-body is excavated with digging/scraping machinery without the use of explosives. Figure 2.12 shows a cross-sectional view of a typical open pit and the terminology used in pit design. Benches are normally excavated from about 2-15m in height in stacks of 3-4, in between which is a crest on which the haul road is positioned. The road gradient increases with increasing number of benches in the stack with benches having a steep face angle whilst the slope angles of the stack and overall slope are flatter, thereby helping to prevent slope failures (Hoek & Brown, 1980).

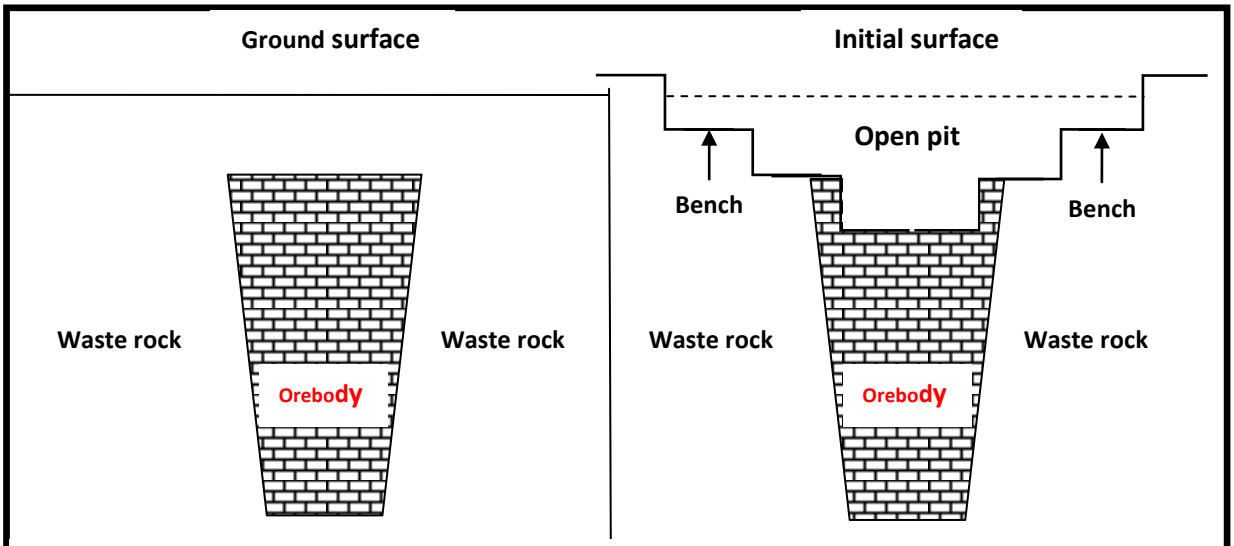

A. Section through an ore-body before open pit commences

B. Section through an ore-body as waste stripping and ore production commences

Figure 2.11 Open pit mining sequence for a pipe-like ore-body

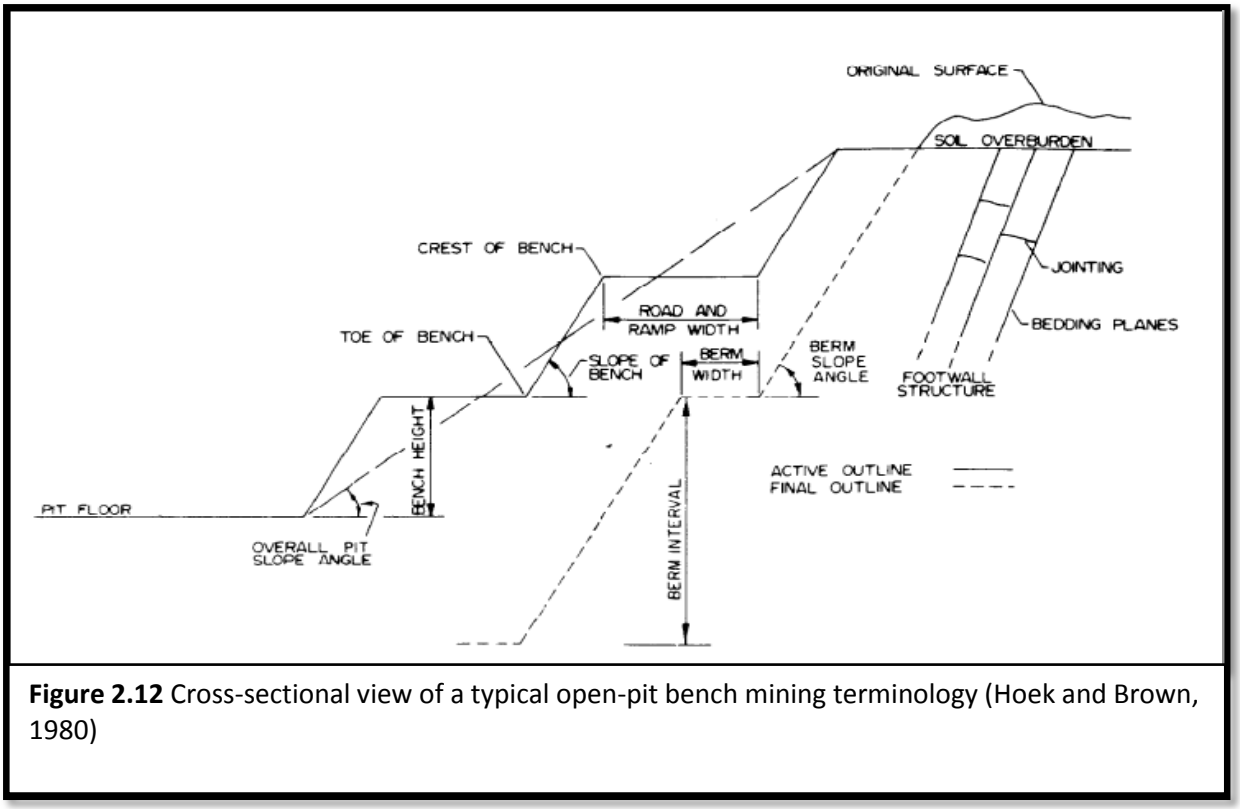

Figure 2.12 Cross-sectional view of a typical open-pit bench mining terminology (Hoek and Brown, 1980)

2.8.1 Geometry of open pit mines: Shape and size

Open pit mining is suitable for geometry of almost any ore-body especially when the ore-body is typically vein-type, pipe-shaped, steeply dipping stratified or irregular and closer to the surface (Hartman, 1987; Hoek and Bray, 1974). Although it can be of any shape but in most cases the shape and size of the pit is designed to fit the geometry properties (shape, size and depth) of the deposit. These researchers further mentioned that the pit design is guided by taking into consideration results from pit optimization programs which take into account historical and predicted operational costs. For example, the Chirano gold deposits which occur in long thin dyke-like granite, at the eastern edge of the Sefwi Belt, immediately adjacent to the Tarkwaian wedge. According to Allibone et al. (2004), the deposits occur like a string of beads along a lode horizon several kilometres long and the geometry of the deposits ranges from tabular (Obra site), to pipe like (Tano site), to several parallel lodes (Paboase site). Allibone et al. (2004) assert that lode thickness ranges from a few metres to 70 metres and most deposits dip very steeply towards the west or southwest, and also plunge very steeply. Figure 2.13 shows an open pit mine design of a typical pipe-shaped hydrothermal gold mineralisation of the Damang and Wassa mine in the Tarkwa district of South Western Ghana.

Taking into consideration the geometry properties of ore reserves in Ghana, most open pits are oval and rectangular in shape reaching an average depth of approximately 300m (Tarkwa and Damang Gold mine Technical Short Form Report, 2010). In Figure 2.14 and 2.15 the aerial view of the various configurations of the Damang, Tarkwa and Iduapriem open pits are shown with most of the pits having either oval or rectangular shape at varying depths. Currently, narrow, tabular auriferous conglomerates ore-body is being exploited by Tarkwa gold mines from six open pits namely; Pepe, Atuabo, Mantraim, Teberebie, Akontansi and Kottraverchy (Tarkwa Gold Mine Technical Short Form Report, 2010).

Sedimentological studies of detailed stratigraphy of the footwall reef units of ore-bodies of Damang and Tarkwa reserves reveal both the lateral and vertical facies variations of the area (Table 2.6) (Damang and Tarkwa Gold Mine Technical Short Form Report, 2010). Similaly, the Ahafo South Project of Newmont Gold Ghana Limited (NGGL) in the Brong Ahafo region operates four open pit mines namely; Amama, Subika, Awonsu, and Apensu, of various configurations and depth ranges shown in Table 2.6 (CGML, 2010).

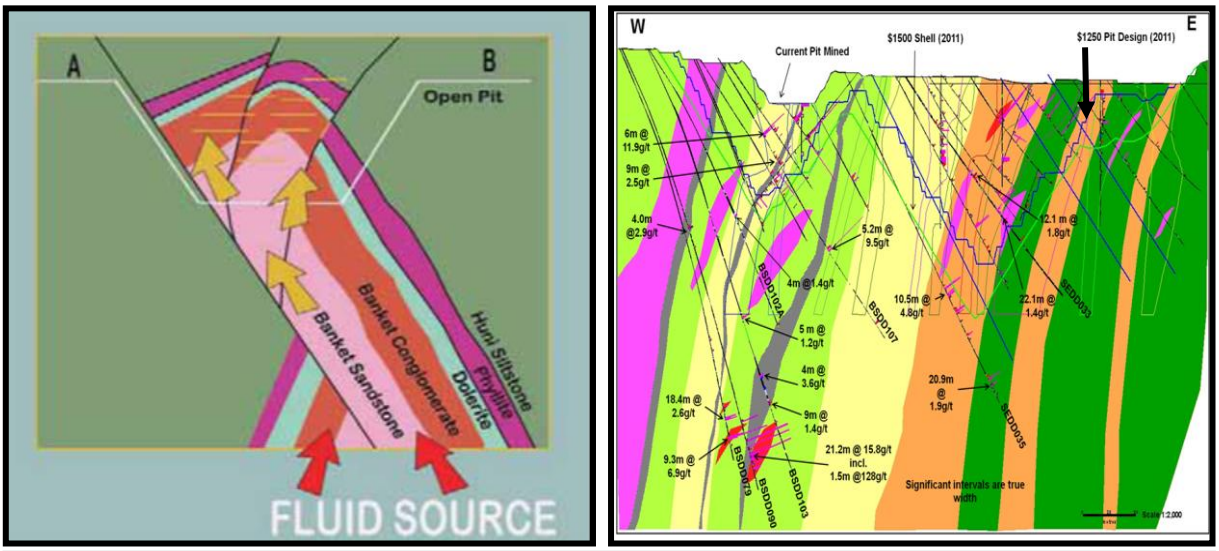

Figure 2.13 cross-sectional views of sections of gold mineralisation pit design of the Damang open-pit (left) and The Wassa Mine open-pit (right) (source: Goldfields Ltd. Damang and Wassa Mine Technical report 2010)

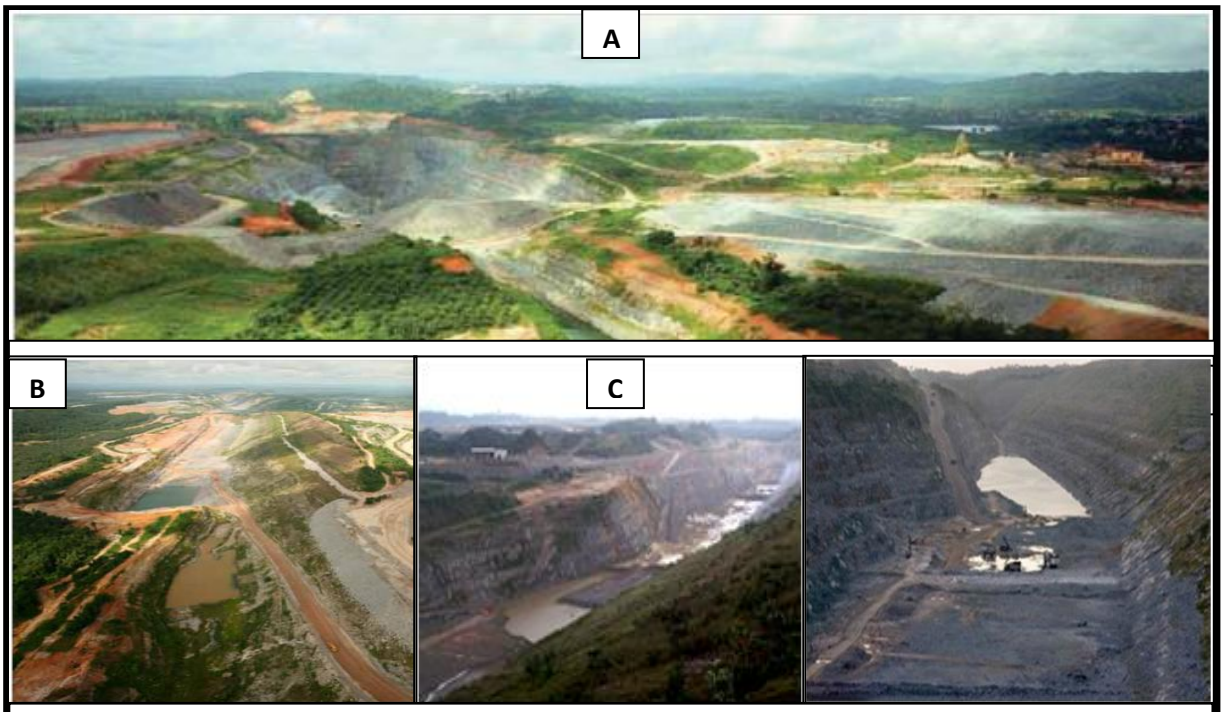

Figure 2.14 Photographs of some of the major open pit gold mines in Ghana: (A) Goldfields Ghana Ltd. Damang (B) Tebrebe Goldfields Ltd. Tarkwa (C) Anglogold Ashanti, Iduaprem (D) Goldfields Ghana Ltd. Tarkwa

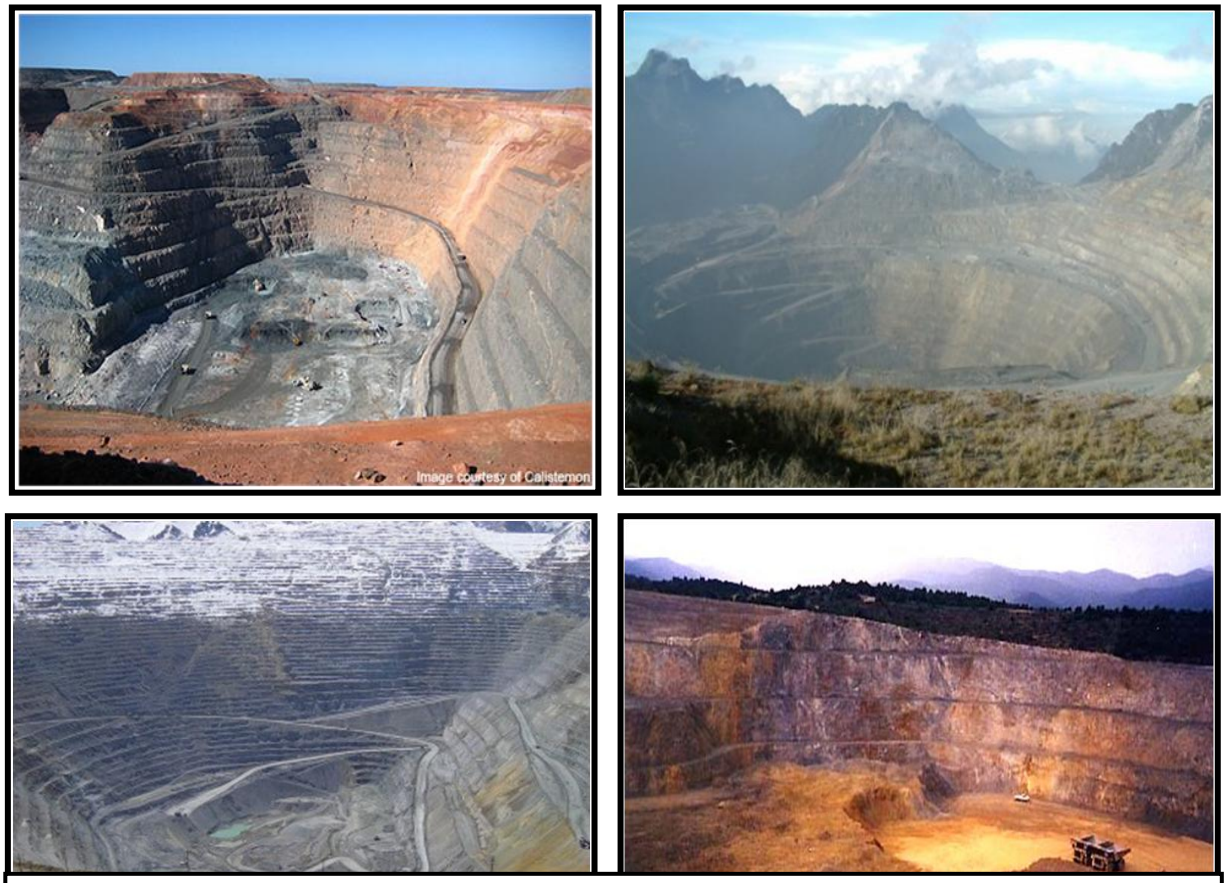

Figure 2.15 Photographs of some of the world's largest open-pit mines. Clockwise from top left are: (a)The Super Pit Gold Mine of Western Australia (b) The Grasgberg Gold Mine of Indonesia (c) Ruby Hill Open Pit Mine, Nevada USA and (d) The Bingham Canyon Mine of Utah USA

Table 2.6 Geometry (Shape and size) of some leading open pit gold mines in Ghana and outside Ghana

Mining Company	Mine Location	Start Date	Type of mine	Geometry		
				Length (m)	Width (m)	Depth (m)
Goldfields Ghana Ltd. Of South Africa	Tarkwa (W/R) Damang (W/R) Abosso (W/R)	1993 1997 1997	Open-Pit Open-Pit Open-Pit			200-300 70 200
Anglo Gold Ashanti of South Africa (Central Africa Gold)	Obuasi (A/R) Iduapriem(W/R) Bibiani (W/R)	2004 1992 1997	Open-Pit Open-Pit Open-Pit	690	20-40	200 177
Golden Star Resources Ltd. Of Canada	Bogosu (W/R) Akyempim(W/R) Preastea (W/R)	1990 2005 1995	Open-Pit Open-Pit Open pit			200 150-200
Red Back Mining Inc. Of Canada	Chirano (W/R)	2005	Open-Pit . Obra . Tano . Paboase			20-70
Newmont Gold Ltd. Of Denver USA.	Ahafo South project in Brong-Ahafo Region (B/A)	2006	Open-Pit . Amama . Subika . Awonsu . Apensu	36 ha. of land 52 ha. of land 74 ha. of land 88 ha. of land		144 140 285 270
Super pit Goldfield Limited, Australia	Kalgoorlie in Western Aust.		Open- pit	3600	1600	512
The Bingham Canyon Mine	Utah, USA		Open-pit	4000		1200

W/R=Western region A/R=Ashanti region B/A=Brong-Ahafo region

2.9 Summary and discussion

Assessment of mine geometries shows that generally, the layout of surface mines depends on the geometry (shape, size and depth) of the mineral deposit. In most cases, the shape and size of the pit is designed to fit the geometry of the deposit as well as the characteristics of the host rock, especially when the ore-body is typically of vein-type, pipe-shaped, steeply dipping stratified or irregular and closer to the surface. Considering the geometry properties of ore reserves in Ghana and elsewhere, the layout of most open pits mines are characterised by rectangular and oval shape with benches and spiral roads. In plan-view, the dimensions of the pits on the average range from 500m to 2000m and reach a maximum economic depth of approximately 300m. These average values have been used by the MODFLOW computer code in the design, simulation and assessment of mine derogation on domestic wells and surface water systems in Ghana (Chapters 5 and 6).

CHAPTER 3

CHARACTERISATION OF HYDRAULIC PROPERTIES OF CRYSTALLINE ROCKS

3.1 Introduction

In this chapter a database of hydraulic property information on crystalline rocks has been developed, analysed and statistically evaluated. Hence, the results produced have provided estimates that have been used in selecting modelling parameters for use in groundwater flow modelling activities in hard rock mining environments, and in particular, in the calculations on mine radius of influence of impacted area.

The rest of the chapter is arranged as following: **section 3.2** is devoted to a general summary of previous work by other authors; **section 3.3** gives the specific aim and objectives for the characterisation process; in **section 3.4**, the methods adopted to characterise the hydraulic properties of crystalline rocks are discussed; also in **section 3.5**, the issues relating to the difficulty of estimating appropriate K values for regional scale modelling are enumerated; in **section 3.6**, the factors affecting K values in a given mining environment have been discussed; the data analysis of the entire characterisation process have been presented in **section 3.7**, and finally, the summary and discussions of the characterisation process are devoted to **section 3.8**.

3.2 Summary of previous work by different authors on hydraulic conductivity of crystalline rocks

3.2.1 Introduction

In general, crystalline rocks are characterised by very low primary porosity and permeability. These can be significantly increased by weathering and fracturing; therefore, the climate, topography and rock structure may be important in accounting for differences in well yield. In particular, thick areally extensive weathered layers can form reliable aquifers which can be an important source of groundwater. While in arid and semi-arid regions the weathered layer is usually thin (less than 1m), in humid tropical regions the thickness may reach 100m (Singhal & Gupta, 1999). According to these authors, coarse-grained, quartz-rich rocks such as granite and quartzite are more brittle than slate and schist, and have a coarse-grained

weathering product. Therefore, they tend to develop and preserve open joint systems and develop higher permeability weathered zones. Weathering products of phyllite, schist and slate include clay minerals that tend to fill the fractures and have lower permeability. In section 3.2.3, studies on the properties of weathered zone have been described separately. In particular, however, in the present research study, the hydraulic properties of the whole sequence of bedrock starting from the ground surface have been considered.

3.2.2 Previous major research studies on hydraulic conductivity of crystalline rocks

In Table 3.1 a summary of major research studies of in-situ hydraulic conductivity tests conducted by various research groups have been presented. Hydraulic conductivity values derived from in-situ well tests at various scales ranging from 10^{-11} to 10^{-4} m/s have been tabulated. The most typical values are centred on log K = −8±1 m/s at up to 4 km depth.

Apart from the above, several studies have compared published values for hydraulic conductivity at laboratory, borehole and regional scales (Brace, 1980, 1984; Clauser, 1992). These workers compiled data on hydraulic conductivity of crystalline rocks measured at a variety of spatial scales (see Figure 3.1). An increase in average permeability of about 3 orders of magnitude from the laboratory scale to the borehole scale is observed. Core material for laboratory measurements is usually derived from non-fractured samples, and may be biased towards the lower end of a rock's permeability range. Hydraulic conductivities measured at the borehole scale generally range between 10^{-7} and 10^{-2} m day^{-1} (permeability of 10^{-19}–10^{-14} m^2). They also found out that the porosity of unweathered crystalline rock usually varies from 0.1% and 1%.

Table 3.1 Summary of site characterisation of hydraulic conductivity of previous studies

Study Area	Rock Type	Depth (m)	Hydraulic conductivity K (m/s)	Author Reference
Äspö, Sweden	Granitic rocks	<450 +1,680	$3x10^{-10}$–$1x10^{-8}$, no depth dependence (ndp)	Stanfors et al. 1999; Walker et al. 1997; Mazurek et al. 2003
Olkiluoto, Finland	Mica-rich gneisses, minor granite	<1,000	$1x10^{-9}$–$1x10^{-8}$ ndp up to $1x10^{-5}$	Pitkänen et al. 1992; Palmén et al. 2004
Stripa, Sweden	Granite	<1,232	$1x10^{-11}$ – $1x10^{-8}$ representative value (rep) $1x\ 10^{-9}$, K decreases with depth	Gale et al. 1982, 1987; Nordstrom et al. 1989a,b
Carnmenellis, Cornwall, UK	Granite	<2,200	$1x10^{-9}$–$1x10^{-5}$ ndp to 700 m rep $1x10^{-8}$–$1x\ 10^{-7}$ K lower values at depth >700 m	Pine and Ledingham 1984; Watkins 2003
Canadian Shield, -NW Territories	Granitic rocks	<550	$8x10^{-9}$–$4x10^{-7}$, rep $2x\ 10^{-7}$, K possibly decreases with depth	Kuchling et al. 2000;
Canadian Shield, -Manitoba	Granitic rocks	<1,000	$1x10^{-13}$–$1x10^{-4}$ rep $1x\ 10^{-7}$	Stevenson et al. 1996; Gascoyne 2004
NIAGRA, deep wells Northern Switzerland	Granite, gneiss	<2,500	$1x10^{-13}$–$4x10^{-4}$ ndp, rep $1x10^{-9}$	Leech et al. 1984; Ostrowski and Kloska 1989; Pearson et al. 1989
Unrach3, S. Germany	Gneisses	<4,444	$1x10^{-9}$	Stober and Bucher 2000
KTB, Germany	Amphibolite	<4,000	$4x10^{-8}$	Stober 1995, 1996
Soultz-sous-Forêts, France	Granites	<5,000	3,600–3,800m: $7x10^{-8}$–$2x10^{-6}$	Aquilina et al., 2004
Cajon Pass in California, U.S.A	Gneisses	<2,077	$3.8x10^{-12}$–$1.4x10^{-9}$ rep $1x10^{-11}$, K increases with depth	Coyle and Zoback 1988

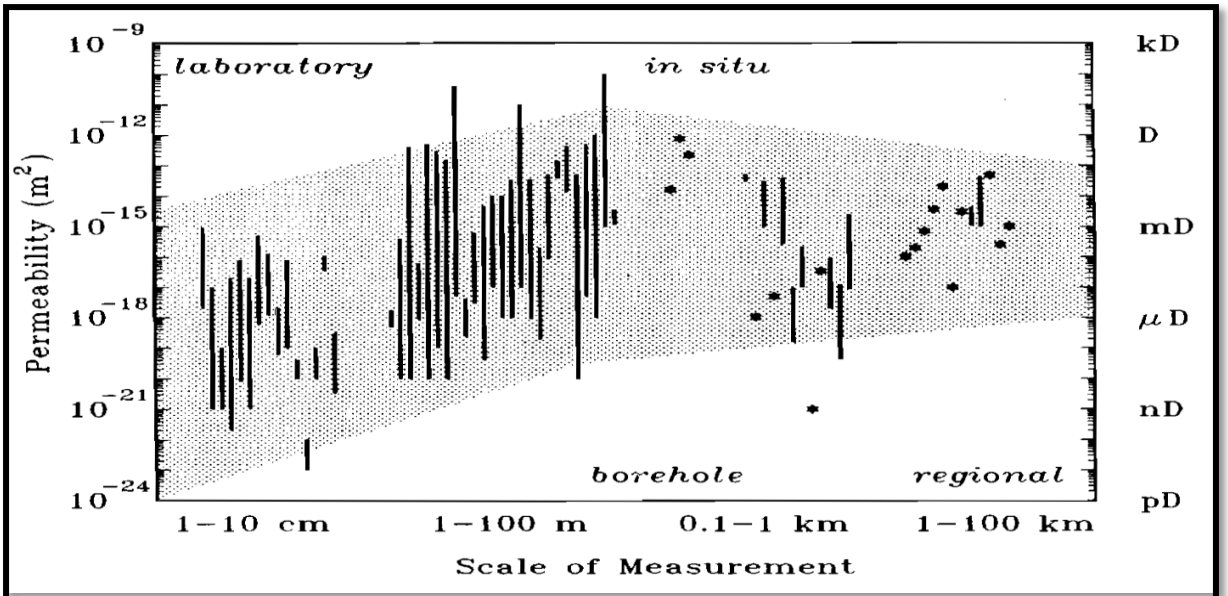

Figure 3.1 The work of Clauser (1992) on permeabilities of crystalline rocks measured at different scales. Bars mark the permeability range when several individual values are reported; circles represent individual values. Hydraulic conductivity (m day^{-1}) at 20 ^{o}C is very approximately equal to intrinsic permeability (m^2) x 10^{12}.

3.2.3 Weathered zone properties

The geological structure, normally encountered in hard-rock environment is characterized by the existence of a hard rock basement overlain by a weathered overburden of variable thickness. Hydro-geologically, the weathered material which constitutes the overburden has high porosity and contains a significant amount of water, and at the same time, it presents low permeability due to its relatively high clay content Barker (2001). Many research studies on weathered zone have been conducted by various authors; and in this section their works have been enumerated. A weathered zone can be defined as a near surface zone in which the upper exposed rock has either been chemically or physically changed due to the action of rain, water, and etc (Acworth, 1987). Some studies in terrains have concentrated on shallow depths – the top 10 to tens of metres. In many areas these shallow systems are largely within the weathered zone. It is generally known that a very shallow zone has much greater permeability than the deeper parts of hard rock systems. In Table 3.2, a summary of estimated permeability ranges of weathered zones from studies around the world conducted by Gilson (2010) is presented.

Table 3.2 Summary of estimated permeability ranges of weathered zones from studies around the world (Gilson 2010)		
Country	**K (md^{-1})**	**Reference**
Malawi/Zimbabwe	0.08 – 0.7	Chilton and Foster (1993)
Zimbabwe	0.02 – 4.9	Wright (1992)
Australia	0.01 – 1	Wilkes et al. (2004)
Uganda	0.04 – 0.2	Taylor and Howard (2000)
Ghana	0.22 – 2.2	Martin (2005)
Burkina Faso	0.216 – 1.152	Ouattara et al. (2007)

Various conceptual models have also been suggested for shallow weathered systems, including those of Jones (1985); Acworth (1987); Gupta (2001); Chilton and Foster (1995). Figure 3.2 shows the conceptualization of weathered-fractured rock by Chilton and Foster (1995). In the work of Wright and Burgess (1992), the conceptualisation of the weathered zone involves the division of the geology up into a weathering series, based on their degree of weathering, without considering the geology of the individual series (See Table 3.3). Their division consist of the following; from bottom to the top, the ''Fresh bedrock" is referred to as zone I, the ''Saprock" zone II-III, then the ''Regolith" which is further divided into ''saprolite" zone IV-V, and finally the ''residual soil" zone VI, where the Roman numerals I-V indicate the weathering grades and as defined in Table 3.3.

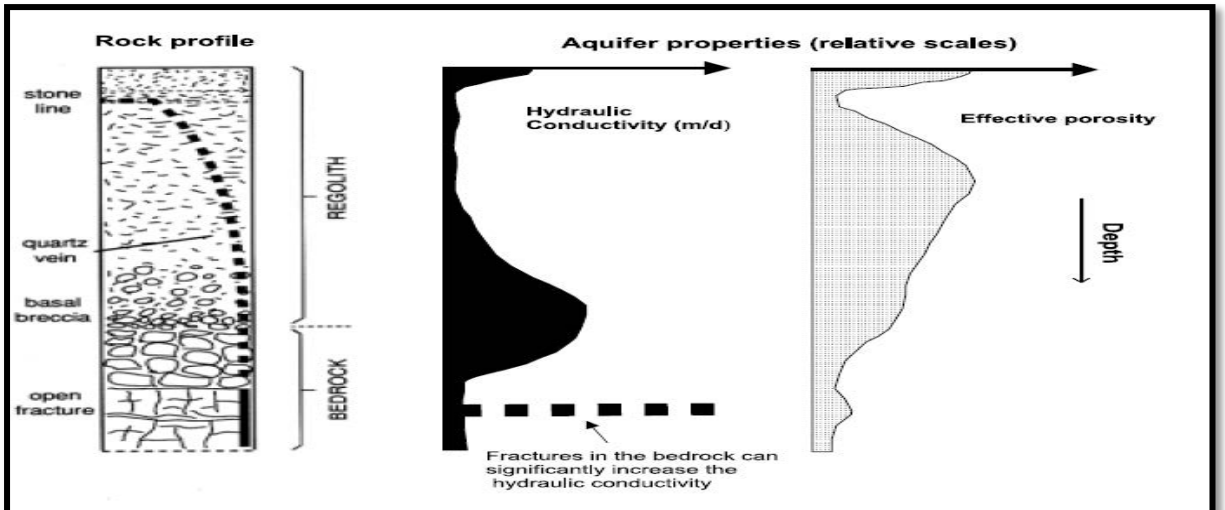

Figure 3.2 A weathering profile developed upon crystalline basement rocks vs. depth (Chilton and Foster, 1995)

Table 3.3 Description of weathering profile based on the degree of weathering (modified from Wright and Burgess 1992)

Weathering series		Zone	Name	Description
Regolith	Residual soil	VI	Residual Soil	All rocks converted into soil
	Saprolite	V	Completely weathered	Soil, but the fabric is still intact largely
		IV	Highly weathered	Some soil and fresh rock is only present as a discontinuous framework
Bedrock	Saprock	III	Moderately weathered	Discoloured and weakened rock material
		II	Slightly weathered	Discoloured but not noticeably weak
	Fresh bedrock	I	Fresh rock	No visible sign of weathering rock material

The depth of weathering in the gold-mining areas of Ghana especially in the Tarkwa rock system is usually in the order of 20m (Kortatsi 2004), and as such is small in comparison with the depth of the mines (~300m). Thus, most of the exposed mine walls are in fractured bedrock rather than heavily weathered material. However, this does not mean that the weathered zone is unimportant since most water supply wells are found in the weathered zone, and indeed its impact is explored in Chapter 4 of this thesis. Figure 3.3 shows a typical weathered profile in Ghana. Hence, in this study it is necessary to take note of weathered zone properties as well as of hydraulic properties of deeper parts of the system. It should be noted that the studies described in the previous subsections have included data from rocks of various degrees of weathering, and that the database assembled and described in the following subsections include data from both shallow and deep depths

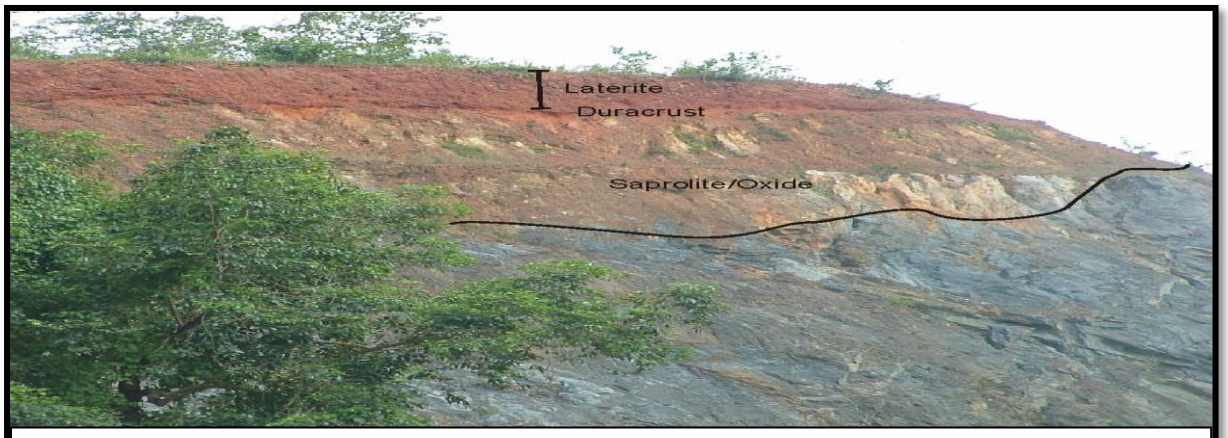

Figure 3.3 A profile of a typical crystalline basement rock in South Western Ghana (Source: Technical Short Form Report on Damang Gold Mine, Ghana December 2010)

3.3 Specific Aim and Objectives

Under the present scenario, the specific aim is to extract from the literature a reasonable range of possible permeability values for use in investigating the impacts of hard rock mines in Ghana. More specifically, the objectives are:

1. to develop a conceptual model for hydraulic conductivity (K) distribution (e.g., depth dependence; anisotropy; fracture connectivity)
2. to provide K distribution type and distribution parameter values (e.g., central tendency and spread) applicable for generic calculations of groundwater flow near mines

In order to constrain the ranges for hydraulic conductivity, it is necessary to determine if it is affected by depth, rock type/class, climate and tectonic history. By determining the dependency of hydraulic conductivity on these factors, better estimates for the likely range for Ghana may possibly be made.

3.4 Methods of characterisation

3.4.1 Introduction

In this research, in order to achieve the specific aim and objectives, the methodology adopted included: (1) international literature search of hydraulic-property estimates (i.e., hydraulic conductivity, transmissivity and storativity), concentrating on data from depths appropriate for large open cast mines; (2) evaluation and presentation of data; (3) the use of Data Thief and a Scanning Pen for the extraction of data points from graphs; and (4) application of statistical methods. Each of these aspects is described in the following subsections.

3.4.2 International Literature Review

3.4.2.1 Introduction

Literature searches have been conducted for both published and unpublished data from various geosciences databases, technical reports and memoranda from different hydro-geological institutions in the mining environment worldwide, using computer world wide web (www.), relying on formal technical literature search through the University of

Birmingham's Library Services and literature search engines such as Google. These typically provided extensive regulatory (i.e. federal, provincial and state agencies) industry publications and less frequently conference proceedings. In all, about 150 papers were found to be relevant to the current project yielding information on hydraulic-property estimates (such as; hydraulic conductivity, transmissivity, specific capacity and fracture characteristics). The type of information found has been divided into the following categories:

1. Refereed scientific publications or research papers specifically related to metal ore extraction, hard-rock geology and hydrogeology.
2. Research publications and reports including government agencies such as the US Geological Survey, State of Minnesota Department of Natural Resources, and Environment Canada.
3. Scientific publications not directly related to ore extraction and source water protection, but containing technical information relevant to the types of impacts that could occur through ore extraction.
4. Information of interest found in references that aid in understanding issues related to ore extraction and source water protection; these including case histories, unpublished reports and legal or environmental assessments.

3.4.2.2 Data Sources and Compilation

Hard rock aquifer property data were collected from a variety of sources requiring varying degrees of pre-processing. Apart from collating existing hydraulic conductivity, transmissivity, and storativity data obtained from field tests, transmissivity values that had been obtained from specific capacity data were also collated.

Though hydraulic property data are scarce in Ghana as already mentioned in Chapter 1, hence, there was the need for the current work on international literature to obtain hydraulic property values. Despite the lack of data in Ghana, an attempt was made to obtain some information from the following institutions and organisations;

1. Water Research Institute (WRI) at the Centre for Scientific and Industrial Research (CSIR) - Accra, Ghana

2. World Vision International (WVI), Ghana

3. Ghanaian Australian Goldfields (GAG) Limited (Teberebie Mine) at Tarkwa, Ghana

4. Ashanti Gold Fields Limited at Obuasi, Ghana

5. Gold Star Resources Limited (Wassa Mine) Tarkwa, Ghana

The following paragraphs expand on the nature and the type of data collected from these various institutions and organizations.

3.4.2.3 The use of Data Thief / Scanning pen

Data Thief is a Java based software application that is used to extract data points from a graph. Typically, a graph is scanned from a publication or a journal, and the scanned information is loaded into the Data Thief. The saved resulting coordinates, are used in calculations or graphs that include one's own data. The coordinates of the data points are then exported as text file.

A sizable amount of conductivity data used in this study was extracted from graphs using data thief purchased purposely for this study. The method help in acquiring data from hydraulic conductivity depth relationships of works conducted by researchers including the following: Gale (1982) – Hydrogeological Characterisation of the Stripa Site; Zhao (1998) - Rock mass hydraulic conductivity of the Bukit Timah granite, Singapore; and Nastev (2008) - Developing conceptual hydrogeological model for post dam sandstones in southwestern Quebec, Canada and others.

3.4.2.4 Depth limit for data acquisition

According to Ugorets and Howell (2008), hydrogeological investigations must have a much larger area of influence than those considered in mining and geotechnical investigations. Mining investigations focus on the identification of ore and waste, and the radius or scale of the investigation is limited by the size and form of the ore body. Geotechnical investigations include a small distance from the boundary of the open pit or underground mine. Ugorets

and Howell (2008) assert that depending on the projects hydrogeological condition and vulnerabilities, hydrogeological investigations can include areas of up to 100s of meters outside of the ore body boundary in order to have reasonable estimates of inflow to the mine, impacts of the operation on the groundwater levels and quality, and groundwater discharge to the surface water bodies during the mining and post-mining conditions. These researchers assert that, because groundwater flow in the vicinity of an open pit or underground mine is three-dimensional, they recommended that vertical field characterisation is to be conducted to a depth, sufficient to characterise inflow to the mine base. Regulatory agencies in some countries recommend doing this to a depth of at least 50m below the proposed ultimate bottom of the open pit or underground mine.

3.4.3. Evaluating and presenting the data

In the data compilation process, every effort was made to exclude duplicate site locations and hydraulic property measurements from the dataset. Tests that were reported by the published source with insufficient location or aquifer assignment information needed for analysis were also excluded. Data compiled came from a variety of sources, resulting in the aquifer transmissivity (T) or hydraulic conductivity (K) data being reported in several different types of unit of measurement needed to be calculated from the information provided by the source. To create a consistent basis for evaluating and presenting the data, the aquifer (T) or K-data was converted to consistent units of metres for length, and seconds for time. Ideally, random locations would have been sampled but many of the data were from either dam and tunnel regions (with higher K values than average K expected) or from radioactive waste region with lower K values than the average K expected.

Several different methods were used by various researchers to analyze the data acquired from tests of constant-rate pumping; specific capacity, slug (injection and bailing), packer and drill stem tests. For example, constant-rate pumping and injection tests were analyzed by using curve-fitting methods. In rare cases, original data were available so it was assumed in this thesis that reported hydraulic property values have been correctly calculated. In addition, methods used were not of the same reliability or scale. For example as in the works of Theis (1963) and Brown (1963), estimated transmissivity and hydraulic conductivity

values derived from specific capacity and step drawdown data were generally not as accurate as estimates obtained from time-drawdown data. Many of these dataset compiled were based on specific capacity test data. Most transmissivity data reported in this study were data which have been estimated from specific capacity test data by researchers from various analytical and empirical methods based on the Theis (1963) non-equilibrium approach (for example, Thomasson and others, 1960; Theis, 1963; Brown, 1963; Logan, 1964; Razack and Huntley, 1991; Huntley and others, 1992; El-Naqa, 1994; Mace, 1997).

Further discussion on reliability and validity of methods is given in Section 3.5.2.1. A compilation of hydraulic conductivity estimates from all data collected is combined into one dataset in excel format under the headings; Data source (study), Rock type (Lithology), Regional climate/location, Project type, Test type, Well depth, and corresponding hydraulic conductivity estimates.

3.4.5 Statistical methods for data analysis

3.4.5.1 Introduction

The main goal of the statistical analyses was to determine if there was a significant difference between hydraulic conductivity values determined from various data sources and test methods and also to determine the nature of distributions (similarities and differences) existing among dataset. Due to the wide variation in K values over short distances and uneven distribution of data, a statistically based approach has been used to describe frequency distributions of hydraulic conductivity and to determine the likely effective regional values for crystalline fractured rocks. Standard statistics used include descriptive statistics, regression correlation analysis and comparative statistical analysis. The three main statistical methods used are described in the following subsections. In section 3.4.5.2 descriptive statistics is presented; analysis of variance (ANOVA) is devoted to section 3.4.5.3; and section 3.4.5.4 describes the Kolmogorov-Smirnov (K-S) significance test.

3.4.5.2 Descriptive statistics

Descriptive statistics including the geometric and arithmetic means, median, range and variance of the hydraulic conductivity are reported for each data sources obtained. Hess et al. (1992), for example, suggest that use of box plots (also known as box-and-whiskers plot) is a convenient way of graphically describing data by representing the following values: minimum, lower quartile (Q1), median (Q2), upper quartile (Q3), and maximum (Figure 3.4). A box plot may also indicate which observations, if any, might be considered outliers. Bjerg et al. (1992) reported that differences between populations are displayed without making any assumptions of the underlying statistical distribution, hence they are non-parametric.

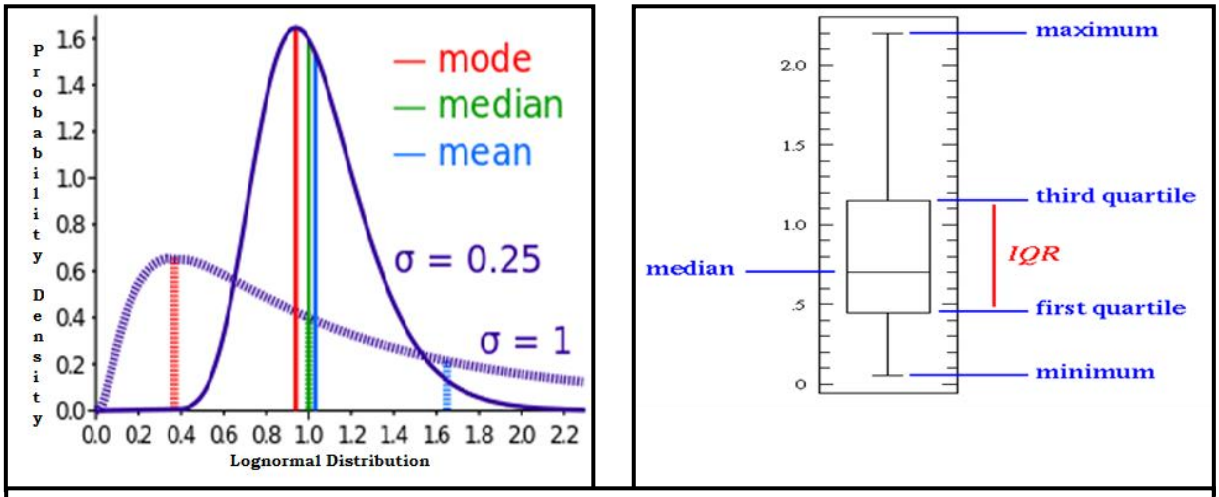

Figure 3.4 (Left): Probability density function of a lognormal distribution comparing the mean, median and mode of two log-normal distributions with different skewness. (Right): Box–and–whisker diagram showing the six data summary where IQR is the interquartile range

In fact, hydraulic conductivity of aquifer materials is most often found to be log-normally distributed (e.g., Freeze 1975; Bjerg et al. 1992; Hess et al. 1992; Sudicky 1986; Woodbury and Sudicky 1991; Rehfeldt et al. 1992 and Neuman et al 1980). The mean, geometric mean (the mean value of log-transformed values of the estimates) and standard deviation of the values assuming a log normal distribution (see Figure 3.4) have been calculated using the following equations. These are:

$$\text{Mean} = 10^{(\mu+\sigma^2/2)} \qquad (3.1)$$

$$\text{Standard deviation} = \left\{\left[\left(10^{(\sigma^2)}-1\right)\right]\left[10^{(2\mu+\sigma^2)}\right]\right\}^{0.5} \qquad (3.2)$$

where μ and σ are the mean and standard deviation of the log-transformed K values. However, the log K values are not perfectly normally distributed, and other measures that rely less on the assumption of normality should also be applied. A common measure of central tendency is the geometric mean, identical in value to the median K value if the values are log-normally distributed:

$$\text{Geometric mean} = 10^{\mu} \qquad (3.3)$$

In addition, the median, interquartile range and Median Absolute Deviation (MAD) of the untransformed data have been calculated. MAD is defined as the median of the absolute differences between the untransformed K data and their median value:

$$\text{MAD} = \text{median IdI} \qquad (3.4)$$

where IdI = absolute value of (measurement – median) (e.g. Helsel and Hirsch, 1992). This measure of spread is resistant, i.e. insensitive to outliers. A measure of skew that implies nothing about the parent distribution is the quartile skew coefficient (qs) as described by Helsel and Hirsch (1992) is written as:

$$\text{qs} = \frac{[(\text{P75}-\text{P50})-(\text{P50}-\text{P25})]}{(\text{P75}-\text{P25})} \qquad (3.5)$$

where, for example P75 is the 75 percentile. This measure of skewness is resistant, i.e. insensitive to outliers.

Finally, Swanson's method for estimating the mean of skewed distributions has also been calculated (e.g. Hurst et al., 2000 as quoted in: http://www.mhnederlof.nl/lognormal.html):

$$\text{Estimate of mean} = 0.3\text{P10} + 0.4\text{P50} + 0.3\text{P90} \qquad (3.6)$$

The estimate is good if

$$\frac{(P10-P50)}{(P50-P90)} < 2.5 \qquad (3.7)$$

3.4.5.3 Analysis of Variance (ANOVA)

ANOVA is a parametric test software package in Microsoft Excel which assumes a normal distribution and uses the mean, variance and a table of critical values for ''F'' distributions to

calculate an ''F'' value (F-test) and the probability ''P''. The acceptance or rejection of the statistical significance of the differences in two or more means is based on a standard that no more than 5% (0.5 Level) of the difference is due to chance or sample error and that the same difference will occur at 95% of the time should the test be repeated.

For an analysis of data, F and P are the variables of concern. The F value obtains from the programme, tests for variance of the data set and also should be used as a comparison of standard deviation. The F value tests whether two standard deviations differ significantly and is a ratio of the two sample variances: ($F = S_1^2/S_2^2$). If the ratio between standard deviations is close to one, then the null hypothesis (no difference between the hydraulic conductivity values) should be accepted (Miller and Miller, 1993). The P value allows the significance of the test to be determined. If the P value is less than 0.05 then at 95% confidence level, there is a statistical difference between the data sets, but if the P value is greater than 0.05, then there is no statistical difference between data sets. It is important to note that P values do not provide a yes/no answer, but rather how strong the case is against the null hypothesis. Therefore, the lower the P-value the stronger the case that there is a difference between data sets (http://www.texasoft.com/pvalue.html). The P-value is the probability of making a Type 1 error, which means, rejecting the null hypothesis when it is true. Analysis of variance can be used for several types of analysis including: One Way Analysis of Variance, N way Analysis of Variance, Multiple Regression and Analysis of Covariance.

3.4.5.4 The Kolmogorov-Smirnov (K-S) Significance and Normality Tests

In the work of Helsel and Hirsch (1992), the Kolmogorov-Smirnov significance and normality tests is described as follows. The Kolmogorov-Smirnov (K-S) test attempts to determine if two sets of data differ significantly or to decide if a sample comes from a population with a specific statistical distribution. A useful property of the K-S test is that it makes no assumption about the distribution of the data, i.e. it is non-parametric / distribution free.

Helsel and Hirsch (1992) define the K-S test as follows: If H_0 (the data follow a specified distribution) and H_a (the data do not follow the specified distribution) then, the Kolmogorov-Smirnov test statistic (D statistics) is defined as:

$$D = \max_{1 \le i \le N} \left(F(Y_i) - \frac{i-1}{N}, \frac{i}{N} - F(Y_i) \right) \qquad (3.8)$$

where F is the theoretical cumulative distribution of the distribution being tested. This distribution must be continuous, and it must be completely specified. The hypothesis regarding the distributional form is rejected if the test statistics ''D'' is greater than the critical value ''P'' obtained; where the critical value allows the significance of the test to be determined.

For normally distributed data, it is expected that about 68.3% of the data will be within 1 standard deviation of the mean (i.e., in the range $X_{avg} \pm \sigma$) and 95% of the data to be within 1.96 standard deviations of the mean (i.e., in the range $X_{avg} \pm 1.96$) (e.g. Helsel and Hirsch (1992)). Hurst et al. (2000) call the latter a 95% confidence interval for the sample.

In the present study, the K–S test has been applied at 0.05 significance level (α) to test for significant differences and spread of K-distributions between different studies (i.e. from different data source), rock types and depth intervals. Furthermore the K-S test has been used to determine whether a set of measurements comes from a normal distribution population or not.

3.5 Difficulty of estimating appropriate K values for regional scale modelling: Anticipated related issues

3.5.1 Introduction

The K-value is subject to variation in space which means a representative value must be adequately assessed. In the estimation of appropriate K-values for modelling at the regional scale in this study, two main issues or difficulties were encountered: (1) the process of transforming or linking the apparent conductivity (K_{app}) values obtained from field testing to the representative conductivity (K_{reg}) values appropriate for modelling at regional scale, and (2) the possible bias in field data resulting from the purpose for which the field measurements were made. In the following sections brief explanations of the above difficulties have been presented.

3.5.2 The mechanics of linking apparent field testing conductivity values to conductivity values appropriate for regional scale modelling

The compiled field testing conductivity values for this study were obtained from different field testing methodologies and hydrogeological environments. In general, it is always appropriate to process all field estimates of hydraulic conductivity into conductivity values appropriate for regional scale modelling (Neuman, 1982). Hence some of the encountered possible factors that gave rise to the difficulty in transforming field testing conductivity values into appropriate values for regional scale modelling include the following:

1. the validity of different types of test methods
2. scales of measurement of different types of test where the mean value of hydraulic conductivity changes with measurement scale
3. possible effect of local vs. regional connectivity of fractures
4. the assumption that tests were properly interpreted whereas there might be some flaws in the methodology used
5. use of equivalent porous medium models to interpret data from fractured aquifers
6. the purpose of studies from which data extracted lead to bias. All these setbacks are explained in detail in the sections below

3.5.2.1 The validity of different types of test methods

3.5.2.1.1 Introduction

A number of methods are available for estimating the hydraulic conductivity of hard rock aquifers. In the current study, four categories of aquifer property data were encountered and each data type varies in its reliability, validity and level of supporting documentation based on the method of collection by the authors. In the order of validity and reliability, the data collection methods used include data derived from hydraulic field tests which involve (i) single well and multiple well pumping tests, (ii) specific capacity tests, (iii) slug or pulse test, and (iv) packer/constant head injection tests and drill stem tests (DSTs). In the following, the general reliability and validity of the different types of test methods in order of the categories mentioned above are explained.

3.5.2.1.2 Single well and multiple well pumping tests

Although, single-well pumping tests enable an estimation of the average aquifer hydraulic conductivity in the vicinity of the borehole, they do not provide any information on its spatial variability (Cook, 2003). Various studies have shown that single-well pumping tests conducted on nested piezometers or on intervals of uncased boreholes that are isolated using Packers give information on the vertical variation of hydraulic conductivity.

Multiple-well pumping tests on the other hand, can provide information on fracture connectivity and aquifer anisotropy, but are much more difficult and expensive to conduct (Cook, 2003). Meanwhile, with these two tests methods, if the scales of heterogeneity are greater than the scale of the pumping test, then very irregular drawdown can occur, which can be difficult to interpret quantitatively. In general, pumping tests either inject or remove fluid from a borehole and measure the response (i.e. change in pressure) of the aquifer in the same or in nearby observation boreholes. In this regard, the pumping period may be on the order of hours to several days, resulting in a high resolution data set which may consist of hundreds of data points measured with automated high-precision equipment (Kruseman, 1990). Here, it is worthy to note that the longer a well pumps, the more far-reaching its radius of influence, hence the greater the volume of aquifer tested and more representative of the bulk aquifer conditions. Consequently, potential bias due to well-bore storage diminishes with time.

Moreover, multiple borehole tests offer a number of advantages over single borehole tests. In the former, fluid is pumped from (or into) one well and drawdown is observed in the pumped well and in one or more nearby observation wells. If the test is conducted over a sufficiently large scale, then it may be able to treat the rock mass as a porous medium, and so determine both vertical and radial anisotropy (Sahimi, 1995). In other cases, multiple borehole pumping tests allow the interconnection between fractures to be investigated. In heterogeneous systems, it is frequently observed that nearby observation wells show little or no drawdown, while more distant wells may show large drawdown. Yet still, in some cases, this may occur even though the bores lie in the same direction from the pumping well. Accordingly, it can be demonstrated that the system is behaving as an equivalent porous media; hence estimation of model parameters from multiple borehole pumping

tests may be difficult. According to NRC (1996), it may be tempting to analyse the response in each observation well separately, using methods developed for isotropic porous media. This approach leads to a range of hydraulic properties being estimated, which might be interpreted as representing the range of hydraulic properties of the rock mass. However, NRC (1996) suggests that the approach can be very misleading. The alternative as according to Hsieh (2000) is to use a numerical model to attempt to simulate pumping test results. Hsieh (2000) posited that this will usually require the use of geophysical and other fracture mapping techniques to help constrain the location of high conductivity zones in the model, or otherwise issues of non-uniqueness are likely to arise.

Nevertheless, despite the difficulty of quantifying hydraulic parameters from multiple well pumping tests, such tests often provide valuable information on aquifer behaviour, and help constrain conceptual models than in single well and other testing methods (e.g., slug test, drill stem test) Belcher et al., (2001).

So far, it can be conjectured that data quantity, collection and analysis methods of multiple pumping tests provide the highest level of certainty relative to the other types of tests methods. Freeze and Cherry (1979) have observed that on the whole, single well pumping tests are less reliable than multiple well pumping tests due to well losses and issues to do with well storage and seepage faces.

3.5.2.1.3 Specific capacity tests

This type of test is generally conducted after a well is completed to determine the pumping rate a well can sustain or it used to measure the productivity of a well; mathematically, it consists of the pumping rate divided by the drawdown in the pumped well (Freeze and Cherry, 1979). During a specific capacity test, water level measurements are generally collected only at the beginning and at the end of a generally shorter-duration test. Due to the generally shorter test duration (often 1-4 hours) the volume of aquifer tested is typically less than a longer-term aquifer pumping test. Specific capacity tests of longer duration provide data representative of the surrounding aquifer rather than of the well bore and/or filter pack and provide water levels which are more representative of equilibrium

conditions. Generally, the specific capacity is reflective of aquifer transmissivity as the well efficiency approaches 100 percent (Heath, 1983). In this regard, well efficiency is considerably less than 100 percent in screened wells and approaches 100 percent in some open-hole wells. In other words, specific-capacity estimates in open-hole wells is considered closer to actual aquifer transmissivity, and those derived from screened wells may be of lower or minimum transmissivity.

For a porous media the relation between specific capacity of a well and the local transmissivity is described by the Theis nonequilibrium equation (Theis, 1935). In accordance to the work of Walton (1970), the Theis equation has an advantage if the pumping start time and the drawdown are known, but has a disadvantage if restrictive assumptions such as; a fully penetrating well in a homogeneous, isotropic porous medium; negligible well loss; and an effective radius equal to the radius of the production well. For these assumptions, modified measures of specific capacity have been suggested over the years for; adjusting head loss to account for the theoretical effects in porous media of partial penetration of the saturated thickness of the aquifer, well loss due to turbulent flow and well depth. In fractured media, the Theis equation often may be a poor representation of the relation between specific capacity and the other variables including transmissivity (Huntley et al, 1992). Other investigators (Siddiqui and Parizek, 1971; Yin and Brook, 1992) have shown that there are vital structural factors such as local fault zones, dip of the rock, fracture size and concentration, and folding patterns that affect transmissivity in fractured rock. These workers claim that a generalised deterministic model linking these features to specific capacity or transmissivity does not exist.

3.5.2.1.4 Slug or Pulse tests

Schwartz (1975) described slug test as an aquifer testing method used to determine hydraulic conductivity using a single well and that the method involves rapid addition or removal of a measured quantity of water from a borehole and monitoring its recovery. In this test, water level rise (or fall) is monitored as it returns to quasi equilibrium conditions, and it produces data on the basis of which numerous researchers have developed methods to determine hydraulic conductivity and transmissivity (Kruseman and de Ridder, 1991). The water level-time recovery curve has been used by numerous researchers, for example, in

the works of Hvorslev (1951), Bower and Rice (1976) and Cooper et al. (1967) they have used an analytical model that describes how the water level changes over time as a function of well and formation geometry, and hydraulic conductivity. A document by ASTM (1996), shows that by substituting recovery curve data and well geometry parameters, the hydraulic conductivity can be calculated. Research shows that various slug tests methods have been developed and each test method was made to accommodate certain features that previous methods overlooked or ignored (for example, Hvorslev, 1951; Cooper et al., 1967; Ferris and Knowles, 1963; Theis (modified), 1935; Bureau of reclamation, 1960; Nguyen-Pinder, 1984; and Bower and Rice, 1976). For example, the method of Cooper and others (1967) is for analyzing slug tests in confined aquifers, which was later extended by Bredehoeft and Papadopulos (1980) to very low permeability sequences. In the solution of Cooper and others (1967), ratios of the water-level drawdown or rise to the static water level (H/H_0) are plotted as a function of log-time since the test was initiated. The data curve is then matched to a dimensionless type curve to obtain values of hydraulic properties.

As with other testing methods slug tests also have their unique advantages and disadvantages. Cooper et al. (1967) enumerated some of the advantages of slug tests to include the following: relatively cost effective; requires little time to conduct; the amount of water extracted or added is insignificant. Cooper et al. (1967) also observed that transmissivity and hydraulic conductivity values obtained are not particularly sensitive to the technique used for analysis. Also, Faust and Mercer (1984) have mentioned that the reliability of the calculated storage coefficient may be limited. Furthermore, these researchers contend that in certain geologic formations data obtained from slug tests may be sometimes difficult to interpret especially when there is reduced permeability in the zone around the borehole (a 'skin' effect). To this end, Faust and Mercer, (1984) suggested the use of proper well installation techniques and development in order to reduce drilling effects. Because slug tests are of short duration a small portion of the aquifer adjacent to the well bore is evaluated, however, this does not provide an evaluation of portions of the aquifer not screened by the well being tested. Therefore, slug test is both less valid and less reliable as a test method compared to single and multiple pumping tests methods.

3.5.2.1.5 Packer/constant head injection tests

Bliss and Rushton (1984) describe a packer as an expanding plug which can be used to seal off sections of the open or cased well to isolate them for testing. They also define packer tests as consisting of isolating specific sections (usually around 3m) of a bedrock borehole, as it intersects various hydrogeological units, with inflatable packers so that aquifer tests can be conducted. A series of such tests allows characterization of the vertical distribution of hydraulic conductivity to be determined. However, Rushston (1984) contended that open-hole pumping tests can give misleading results in such environments.

According to Bliss and Rushton (1984) one of the major drawbacks of packer test is that the test is affected by only a limited volume of rock around the well bore. For instance they estimated that a packer test interval of length 3m will affect approximately a radius of 10m around the borehole although this could go further in sparsely fractured aquifers with a very low permeability.

3.5.2.1.6 The drill-stem test

The drill-stem test is yet another standard method of estimating hydraulic properties of potential oil and gas reservoirs in the petroleum industry (Bredehoeft, 1965). The test involves the measurement of pressure behaviour at the drill stem and is a valuable way to obtain important sampling information on the formation fluid and conductivity to establish the probability of commercial production. Research has shown that the drill-stem tests have similar drawbacks as packer test methods.

Optimally, drill-stem tests, packer tests and slug tests determine hydraulic properties in the near-borehole environment, but the accuracy can be decreased by convergence of flow lines and related head losses as water flows into or out of sections of perforated casing, and between the test-interval depth and the pump-intake depth. As with the analysis of any aquifer test data, the accuracy of the results depends upon the validity of the assumptions invoked in the model and the relative importance of extraneous effects in the field data.

3.5.2.2 Scales of measurement of different test types

It has been observed that hydraulic conductivity has an apparent dependency on the scale of the measurement (e.g., laboratory, field and regional). The usual pattern is for the mean value of hydraulic conductivity to get larger with scale of measurement up to the scale defined by the minimum representative volume (MRV). At greater scales of measurement the hydraulic conductivity often becomes approximately constant for several orders of magnitude or more (Dagan, 1986; Neuman, 1990; Clauser, 1992; Rovey, 1998). A few authors (for example, Butler and Healey, 1998) have considered this scale dependence to be linked to artefacts and bias in field measurements. Interestingly, Clauser (1992), Neuman (1994) and Sanchez-Villa et al. (1996) have linked this scale dependence to heterogeneity.

According to Neuman (1994), this scale dependence is attributable to the fact that large scale hydraulic tests are more likely to intercept preferential groundwater flow zones. Small scale measurements could measure higher conductivity values, but it would be unlikely for the test to be located in a high permeability zone. This condition holds so as far as the volume of the higher permeability zones within the aquifer is much smaller than that of lower permeability zones. In other way round it is likely that small scale hydraulic tests will result in higher conductivity values. Thus, given a similar number of tests of small and large size, it would be expected that the large scale test would have the higher average, but that the small scale test would have the higher maximum. The scale of the test is extremely important when assessing the quality and quantity of the data for the intended purpose, especially for fractured hydrogeological units (HGUs) Clauser (1992).

Belcher et al. (2001, 2002) grouped the following test types according to their scales from largest to smallest: Multiple-well constant-rate pumping tests, Single-well constant-rate pumping tests, Specific-capacity and Drill stem tests (DST's), Slug, Packer, and Step-drawdown tests, and Permeameter tests. In other words, the scale-effect can be regarded as a result of the aquifer heterogeneity, of the scale and of the spatial distribution of the field measurements. Belcher et al. (2002) have indicated that hydraulic-conductivity and transmissivity estimates are functions of test scale and as the volume of the testing media increases, the more aquifer heterogeneity is encountered and influences the test results.

Consequently, because of this 'scale effect' values of hydraulic parameters are typically influenced by methods used in their determination. For example, the possibility exists to involve a larger network of fractures in the aquifer response to the imposed stress. In fact, in laboratory permeameter tests of core samples for determining rock matrix properties, the core samples needed for successful results must be unfractured. Laboratory analyses of core samples are limited by (1) very small sample size relative to field conditions, and (2) bias toward more competent rock samples because core from fractured, solution-riddled, and friable rocks typically are only partially recovered or not recovered at all. Because of these limitations, core data may not be comparable to field tests, and results of core analyses may be biased toward the lower values that reflect matrix permeability rather than secondary permeability features. Thus, only matrix rock properties are determined from permeameter tests, and the estimates generally are not useful for regional-scale ground-water flow models of fractured-rock aquifer systems. Hence, results for permeameter tests of core samples are not utilized in the descriptive statistical calculations of the hydraulic parameters in the current study.

Constant-head injection tests, and drill stem tests, with a radius of influence of only several metres, examine very restrained aquifer volumes around the vertical interval delimited by the packers. Similarly, slug or pulse tests, with a radius of influence of only tens or hundreds of centimetres examine a relatively small amount of aquifer material adjacent to the borehole and its vicinity. Because of this, hydraulic-property estimates from slug and pulse tests might not be representative of an entire aquifer unit although they manifest the influence of field-scale features but in a smaller amount. Due to the relatively low duration of the specific capacity tests and the single-well aquifer tests (including the pumping or injection well in multiple-well tests), the corresponding radius of influence is most probably several tens to hundreds of metres. As such, for the same set of wells transmissivity estimates derived from single-well tests tend to be less than those of multiple-well tests. Although, this depends on the correction methods used. Similarly, estimates of storage coefficients from single-hole tests are less reliable than those from multiple-well tests.

Kruseman and de Ridder (1991) have explained that, depending on the rate of extraction and the duration of pumping, multi-well pumping tests may have radii of influences of

several hundreds of metres or more and therefore multiple-well pumping tests record the highest hydraulic conductivity values. These researchers therefore suggest that results from these tests could be biased towards larger values. Furthermore, these researchers argue that multiple-well pumping tests tend to be more reliable because they manifest the influence of field-scale features, such as fractures and faults, as well as the water-transmitting properties of the rock matrix. Because of the inherent nature of variability, typical longer-term aquifer tests will produce more representative hydraulic-property estimates than shorter-term aquifer tests or tests with shorter screened intervals such as packer tests. Thus, while the different testing methods may complement each other, inherent biases such as this one must be considered when comparing and integrating data measured at different scales for regional modelling activities. Hydraulic property estimates presented in this study are based on the results of mostly field-scale tests involving wells but majority of these tests include only a small amount of the volume of aquifer material within the hydrogeological unit (HGU) and thus test only a very small part.

3.5.2.3 Possible effects of local vs. regional connectivity

The degree of interconnection of a network of fractures greatly affects its hydraulic conductivity and the ability of fractures to act as conduits for groundwater flow (e.g. Long and Witherspoon (1995)). Fracture connectivity can affect the results of an aquifer test. In this study most of the tests researchers used are packer and drill-stem tests of short radius of influence. Connectivity of fracture sets are such that if connection extends only a little way beyond the radius of influence, one can interpret a value for K that is larger than the regional value. One way in which this might happen is if the aquifer has a number of large fractures, largely unconnected, and a network of smaller fractures (or matrix permeability). The major fractures, being unconnected, may not be very important for the regional permeability. However, if a borehole passes through one of these fractures, it may act as an efficient collector of water, thus, indicating a locally much higher apparent permeability.

Again, with longer pumping tests, there may be a point when the lower, regional permeability is 'seen', but this may not be the case with packer tests. One could also have a system where despite very low background 'matrix' or 'micro-fracture' K; fractures could collect enough water from the matrix such that the radius of influence never reaches the end of the fracture. In such systems, the fractures may not connect regionally and the regional K would be approximately the matrix value. Thus, the fracture system exhibited by the entire dataset could be represented conceptually using two models of fractured aquifer systems, namely; locally connected fracture aquifer system or a regionally connected fracture aquifer system as shown in Figures 3.5a and 3.5b, respectively. At this juncture, it can be inferred that if this model is correct, then measured K values may be in excess of those that are appropriate for use in regional flow studies.

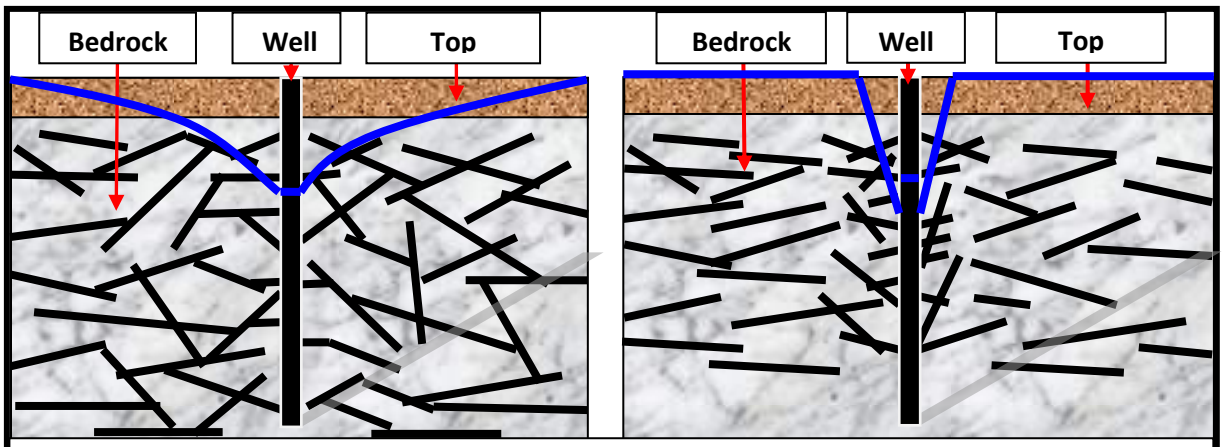

Figure 3.5 (a) Regionally connected fracture network, and (b) Locally connected fracture network

3.5.2.4 Assumption that tests were properly interpreted – an account

There are a number of reasons why field tests are unlikely to provide useful continuum estimates of hydraulic conductivity for regional groundwater flow modelling. The main reasons identified in the course of this study are human error in measurement resolution of field instrumentation, well conditions and construction, and analysis of aquifer property values, and the ignoring of possible conditions that violate the assumptions of the method of analysis (e.g. Hoek and Bray (1974). But however, an assumption was made here that in most cases various aquifer tests were properly conducted and interpreted by the respective researchers.

Further to the above, it is important to mention that most models for interpreting pumping tests represent the aquifer as a homogeneous, isotropic porous medium, and adopt one of the three basic geometries (spherical, radial and linear flow models) as shown in Figure 3.6. First, spherical flow models describe fluid flow toward a spherical cavity in a homogeneous porous medium of infinite extent in all directions (Figure 3.6a). Flow is three-dimensional, and equipotential surfaces are concentric spheres around the spherical cavity. This geometry might be used where the length of the test interval is not very different from the well radius. Second, radial flow geometry (Figure 3.6b) describes flow toward a well that pumps from a homogeneous layer of infinite lateral extent (bounded above and below by impervious materials). In this, flow is two-dimensional and equipotential surfaces are cylinders centred about the well axis. This geometry might also represent a horizontal

fracture zone or a single horizontal fracture bounded by impermeable rock. Third, linear flow geometry describes flow that is unidirectional, such as linear flow towards a highly transmissive vertical fracture that intersects a well (Figure 3.6c). According to NRC (1996), combinations of these three basic geometries are also possible. Methods for interpreting single well pumping tests using these various models are described in a number of texts.

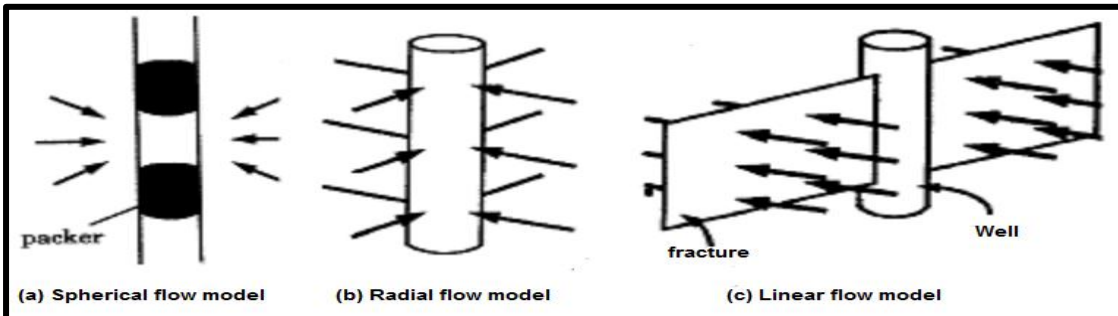

Figure 3.6 Contrasting models of groundwater flow to wells use for interpreting single well hydraulic tests. (a) Flow to a short test interval in a borehole that approximates spherical geometry. (b) Radial flow to a cylinder. (c) Linear flow to a well that intersects a highly transmissive vertical fracture. (Modified from NRC, 1996)

In order for pumping tests to provide useful continuum estimates of aquifer hydraulic conductivity in fractured rocks, the estimate of hydraulic conductivity should be highly sensitive to the model chosen to analyse the data. Most often none of the simplistic models represented in Figure 3.6 are appropriate, yet this may not be obvious from test results. Observed hydraulic head data may still superficially resemble one of these models but because hydraulic conductivity is highly spatially variable in fractured rock systems, the hydraulic conductivity of the test interval is likely to change during a hydraulic test as the area of influence of the test increases. It is also common for the model that most closely approximates the test data to change throughout the test (e.g., from radial flow at short time to spherical flow at later time). The above deliberations are taken care of in the concept of flow dimension in hydraulic testing which reflects the fact that flow to a borehole during pumping may change from one to three dimensional with time, i.e. that the flow system may assume various values, including non-integer values, of flow system geometry. This idea has been quantified in Barker's (1988) paper on generalised pumping test analysis.

Furthermore, most techniques commonly used in the interpretation of aquifer test, disregard anisotropy of the tested formation. Although, the pioneering work by Hvorslev

(1951) considered anisotropic hydraulic conductivity, anisotropy was not included in more general treatment by Bouwer and Rice (1976) and Dagan (1978). Many researchers use the Bouwer-Rice method and ignore anisotropy. Chirlin (1990) concludes that anisotropy is not easily addressed in aquifer test interpretation and Dawson and Istok (1991) recommended Bouwer and Rice's method (1976) only for isotropic conditions. Several numerical methods used by (eg., Braester and Thunvik, 1984; Widdowson et al., 1990; and Melville et al., 1991) account for anisotropy, but there exist no analytical techniques for interpreting slug test and packer test data in general case of fully or partially penetrating wells in a confined or unconfined anisotropic aquifer. For the above reasons, Sidle and Lee (1995) have indicated that hydraulic conductivity values determined using different methods may sometimes differ substantially in terms of validity and reliability.

3.5.2.5 Using equivalent porous medium models to interpret data from fractured aquifers

Most of the analytical methods used in the processing of the aquifer tests results assume that an aquifer is a porous medium. Though, the influence of fractures is fundamental to the flow of water in fractured crystalline rocks. In order to apply these aquifer test methods to fractured rocks it is necessary to assume that the rocks are sufficiently homogeneously fractured and interconnected such that the rock being tested can be considered "an equivalent porous medium". This is because the aquifer test can be affected by the spacing of fractures, as well as their interconnectivity. In areas where fractures are closely spaced and interconnected, values of transmissivities are generally higher than in areas where the fractures are widely spaced and not interconnected. Although some workers (e.g., Shapiro and Hsieh, 1998) have conducted studies on transmissivity in crystalline rock using either porous or fractured media methods and provided estimates of transmissivity within an order of magnitude of each other. Moreover, fractured rock has a "dual-permeability" response that comes from the immediate de-watering of fractures (being the most permeable), and then followed by the delayed response of de-watering from the smaller fractures.

In fractured hydrogeologic media, the contribution of fluid to the system can be either from fractures or the smaller fractures. This "dual-permeability" concept involves the exchange of

water between the fractures and the smaller fractures and therefore can also be another source of variation of conductivity values. Sampling variability can also arise in fractured rocks as a result of a borehole failing to penetrate rock fractures especially for vertical boreholes penetrating rocks with steeply dipping (sub-vertical) fractures. Because of the inherent nature of variability, it is expected that typical longer-term aquifer tests will produce more representative hydraulic-property estimates than shorter-term aquifer tests or tests with shorter screened intervals such as Packer tests.

3.5.3 Purpose of studies from which data extracted lead to bias

In the present study, two main purposes which are the choice of very low conductivity site for nuclear waste disposal and much high K data from dam and tunnel sites for grouting purposes have been identified.

On the basis of the above, spatial bias could be significant for the hydraulic property estimates compiled in this thesis. For example, some workers drilled wells and boreholes to meet the original goals of their respective studies, but not to collect data to determine statistically representative regional-scale hydraulic properties. Also, many workers installed wells in relatively shallow formations because of the difficulties and cost associated with drilling deep wells. In this work, data obtained from the studies of Gale and Witherspoon (1979) and Miguel et al. (2009) account for more than half (about 416 of the K values) of the total data collected have the lowest conductivity values. This is simply because they conducted their studies with the main aim of identifying a very low conductivity geological formation for nuclear waste repository. This represents the low modal distribution of the data set. About 178 conductivity measurements of the rest of the data most of which have high K values were obtained from studies conducted by Snow (1979). Snow (1979) conducted his studies in drilled holes in fractured rocks at dam and tunnel sites for grouting purposes at near surface depth and therefore recorded high K values representing the higher modal point of the distribution. These measurements would not have been done except in the highest K parts of the systems investigated. The rest of the data are for water supply purposes

3.6 Factors affecting K values in a given mining area

3.6.1 Introduction

In this section, four local conditions have been considered to affect the estimation of appropriate representative hydraulic conductivity values for regional groundwater flow modelling in mining areas. Notably of these conditions are; **d**epth, **r**ock type, **c**limate, and **t**ectonic history. The basic question is: do these factors have a sufficiently large effect that they have to be taken into account in choice of hydraulic properties when using the full, international data set, covering many rock types, climates, tectonic settings, and depths, to obtain estimates for these properties at a given location, e.g. Ghana? In the following sections, the background and previous work on each of these four factors is reviewed.

3.6.2 Effect of depth in the estimation of hydraulic conductivity for regional groundwater flow modelling around mines

Ignoring any upper layer dominated by weathering, many published studies have indicated a decrease in permeability with depth for both porous media (e.g., Neuzil 1986; Whittemore et al. 1993; Hart and Hammon 2002; Wang et al. 2009) and fractured media (e.g., Davis and Turk, 1964; Snow 1968a; Louis 1974; Carlsson et al. 1983; Zhao 1998; Jiang et al. 2009), but a considerable scatter is generally detected for the rock mass. On the other hand, some investigators argue that it is not reasonable to expect any regular trend below an upper layer of the bedrock (e.g. Voss and Andersson, 1993). However Wei et al. (1995) have observed that in order to effectively model subsurface flow a quantitative description of the permeability-depth relationship is indispensable. And as observed by Louis (1974), conventionally, empirical equations which are based on statistical analysis of permeability measurements are used to ascertain the permeability-depth relationship. In particular, he noted that the most frequently model used is the log (permeability)-depth relationship, which assumes permeability to decrease exponentially with depth. Louis (1974) advocated the use of exponential relationships and later this was accepted by most researchers.

Several authors have discussed the observed decrease in conductivity with depth in relation to a measured rock stress increase with depth. For example, Carlsson and Olsson (1977) compared in-situ measured conductivity within the upper five hundred metres of crystalline

bedrock in Sweden with theoretical stress-conductivity relationships and suggested a power function of the type given below to describe the depth dependence.

$$K = K_0 Z^{-b} \qquad (3.9)$$

where K is the hydraulic conductivity, K_0 is a reference value of conductivity at the surface, Z is the vertical depth below ground surface and b is a constant. As an alternative approach, Gustafson *et al*. (1989), when evaluating data from the Aspo area in Sweden also assumed a logarithmic function of the form;

$$K = K_0 10^{-z/c} \qquad (3.10)$$

where c is a constant. The above two equations have been used by many other investigators as well for curve fitting. Although it is well known that there is a strong relationship between effective rock stress and fracture conductivity, it is likely that other mechanisms and processes such the tectonic regime also affect the variation of hydraulic conductivity over a depth range of hundreds of metres (Raven and Gale, 1985; Dershowitz *et al*., 1991).

More complex models of permeability variation with depth than the above two equations have been proposed by Oda *et al*. (1989) and Wei *et al*. (1995). These two models are similar and they are based on the assumption that the magnitude of permeability to a great extent is governed by the rock stress magnitude, but also influenced by the fracture properties. The underlying assumption is that fracture apertures in bedrocks decrease with increasing depth and stress in accordance with a hyperbolic relationship as suggested by Bandis et al. (1983) on the basis of laboratory tests on rock joints. The model by Oda et al. (1989) is expressed as;

$$K_{ij} = \lambda \frac{\langle {t_0}^3 \rangle (\frac{N^q}{h})}{\langle |n.q| \rangle} \left(1 - \frac{z}{z + \frac{h}{c.\acute{y}}}\right)^3 \left(\delta_{ij} - N_{ij}\right) \qquad (3.11)$$

where λ is the connectivity, t_o is the fracture aperture at the surface (z=0), h is the fracture stiffness, c is an aspect ratio (a measure of the fracture shape) and ý is the effective unit weight of the rock. (N^q/h) is the number of fractures crossed by a unit length of a scanline with a direction parallel to **q**, and $\langle |\boldsymbol{n}.\boldsymbol{q}| \rangle$ is a correction factor with respect to the selected

direction **q** and **n** a normal vector perpendicular to the direction of **q**. δ_{ij} is the Kronecker delta and N_{ij} the crack tensor describing the geometry of joints.

In an attempt to provide empirical equations to describe rock mass permeability with depth Cheng-Yu et al. (2009) noted that the following researchers; Snow (1970); Louis (1974); Burgess (1977); Carlsson & Olsson (1977); Black (1987); and Wei et al. (1995) all provided empirical equations that attempted to describe rock mass hydraulic conductivity variation with depth as indicated in Table 3.4. Ceng-Yu et al. (2009) further observed that although the equations provided give a quicker means of characterizing hydraulic properties of rock mass, the applicability however is limited since depth is not the only important factor. For instance rock mass hydraulic properties may as well vary with geostatic stress, rock type and fracture characteristics. These fracture properties have been extensively dealt with by the following authors; Lee & Farmer (1993); Sahimi (1995); Foyo et al. (2005); Hamm et al. (2007). It is therefore suggested that a more applicable empirical equation for estimating hydraulic conductivity of rock mass possibly must include the aforementioned factors. From the above discussion, depth is seen as a very important factor to be considered when estimating K values appropriate for regional groundwater flow modelling around mines. A depth dependent analysis has been carried out using empirical relationships of Snow (1970); Carlsson & Olsson (1977); and Wei et al. (1995) to compare with the current studies. The results are presented in subsection 3.7.5.2.2.

In many cases a weathered zone will occur above the relatively unweathered deeper rock. In general, the permeability of this layer will be greater than that of the deeper fractured rock (Section 3.2.3). Within this layer, permeability will change with depth, reflecting for example in a granitic terrain the progression of weathering from deeper weakly weathered zones through the initial stages of weathering that produce granular material through to almost completely weathered clayey material (Acworth, 1987). The thickness of the weathering zone will vary from location to location, thus influencing the groundwater flow to varying extents. In the data set considered, K data are available from ground surface, and consideration is given to K variation from zero depth.

Table 3.4 Diverse approximations for estimating rock mass hydraulic conductivity (source: Cheng-Yu (2009)

Equation	Reference
$k = \mathrm{az}^{-\mathrm{b}}$	Black (1987) a and b are constants. z is the vertical depth below the groundwater surface.
$LogK = -8.9 - 1.671Logz$	Snow (1970) K (ft^2) is the permeability. z (ft) is the depth.
$K = 10^{-(1.6logz+4)}$	Carlson and Olsson (1977) K (m/s) is the hydraulic conductivity. z (m) is the depth.
$K = K_s e^{-(Ah)}$	Louis (1974) K (m/s) is the hydraulic conductivity. *Ks* is the hydraulic conductivity near ground surface. H (m) is the depth. A is the hydraulic gradient.
$Log\ K = 5.57 + 0.352Logz - 0.978(Logz)^2 + 0.167Logz)^3$	Burgess (1977) K (m/s) is the hydraulic conductivity. Z (m) is the depth.
$K = K_{\mathrm{i}}[1 - \mathrm{Z}/[58.0 + 1.02\mathrm{z}]^3$	Wei et al. (1995) Z is the depth. K is the hydraulic conductivity. K_i (m/s) is the hydraulic conductivity near ground surface.

3.6.3 Effect of climate in the estimation of hydraulic conductivity for regional groundwater flow modelling around mines

Climate affects rocks and soil exposed to these elements. The amount of daily temperature, precipitation, and the variation in temperatures over a period of time affect the rate of weathering of rocks. Weathering processes cause important changes in rock porosity and the distribution of pore sizes and it is influenced by so many factors that it is difficult to make a meaningful generalization concerning the weathering of specific rock types. Limestone, for example, may weather and erode into a soil-covered valley in a humid climate, whereas the same formation forms a cliff in an arid climate. Similarly, well-cemented quartz sandstone may be extremely resistant to weathering, whereas sandstone with high clay content is likely to be soft and weak and weather rapidly.

Climate affects both chemical and mechanical weathering rates and it is therefore clear that the processes of weathering cause a substantial increase in the porosity and hydraulic conductivity of the source rock (Ollier, 1975). Despite these complications, there may be a general relationship between the permeability of hard rock sequences and climate, both in terms of the shallow weathering zone and also the deeper fracture network. In this study, therefore, the hydraulic conductivity data set obtained from the literature has been examined to determine if there is any observable relationship between permeability and climate zone (Semi-Arid, Tropical, Mediterranean, Temperate, and Sub-Arctic).

3.6.4 Effect of tectonic history in the estimation of hydraulic conductivity for regional groundwater flow modelling around mines

The tectonic history of the study area may have an effect on the hydraulic properties. Fracture permeability in crystalline rocks is the result of the cooling and deformation of igneous and metamorphic rocks, faulting, jointing and weathering. Also, the sedimentary facies and architecture, the tectonic settings, and the genesis of the aquifer have a greater influence on the distribution and estimation of hydraulic properties. Many groundwater pathways through rocks are related to tectonic features. Fractures, fissures, and joints determine hydrogeological properties and enable or limit the groundwater flow. Studies have shown that virtually all movement of water in crystalline rocks is through fractures or joints in the rocks.

In this study, most of the study areas where hydraulic property data have been obtained from have active geologic history, including large-scale plutonism, volcanism, compressive deformation, and extensional tectonics. Most of the mining environments in Ghana especially Tarkwa in Western region have experienced tectonic activities in the late Proterozoic, and combinations of strike-slip faulting, normal, reverse, and and folding episodes which have resulted in a complex distribution of rocks (Leube and Hirdes, 1986). Consequently, various rock types, ages, and deformational structures of most of the areas under study are often juxtaposed and subsurface conditions are variable and complex.

3.6.5 Effect of rock type/rock class in the estimation of hydraulic conductivity for regional groundwater flow modelling around mines

Crystalline rocks include intrusive igneous rocks (e.g., granite, diorite, granodiorite, gabbro, dolerite, and pegmatite) and metamorphic rocks (e.g., gneiss, quartzite, marble, schist, slate, phyllite and meta-sandstone). Many of the intrusive igneous rocks (e.g., granite, diorite, granodiorite, gabbro) form large intrusive bodies (plutons) while others (e.g., dolerite, pegmatite) tend to occur as linear features of restricted extent, such as dykes and sills. The fundamental characteristic of crystalline rock aquifers is extreme spatial variability in hydraulic conductivity, and hence groundwater flow rate. Hydraulic properties can also be highly anisotropic, so that hydraulic properties must be defined in conjunction with directional information. Water velocities through individual fractures can be extremely high, but the fractures usually occupy only a very small fraction of the aquifer. Thus, even when water velocities through individual fractures may be high, average volumetric flow rates through the aquifer can be quite low. In volcanic rocks, a characteristic change from lava flows to welded tuffs and then ultimately, non-welded and bedded tuffs with increasing distance from eruptive centres can cause hydraulic properties of the stratigraphic unit to exhibit great spatial variability (Chilton and Foster, 1984)

Particular attention in the present study has been paid to the characterization of the hydraulic properties of the fractured aquifers composed of fifteen main lithologic rock types namely: granite ; mica-schist/phyllite; quartzite; sandstone/meta sandstone; porphyry; tuff-breccia, tuff-siltstone; diabase; greenstone; meta-andesite/meta-rhyollite; metavolcanics, amphibolite; sandstone and shale; sandstone/ tuff and conglomerate; quartz, porphyry / granodiorite; slate/talc schist/serpentinite; and gneiss. For the purpose of analysis, these rock types have further been grouped into igneous, metamorphic and sedimentary as follows:

Igneous - granite; diabase; porphyry; quartz porphyry/ granodiorite: **Metamorphic** - gneiss; sandstone/meta-sandstone; mica schist/ phyllite; slate/ talc schist/ serpentine; greenstone; meta-andesite/rhyolite; metavolcanic amphibolite; primary/secondary/tertiary quartzite; **Sedimentary** - sandstone and shale; tuff-breccia/siltstone; sandstone/ conglomerate/ tuff

3.7 Data Analysis

3.7.1 Introduction

Section 3.7 is divided into five main subsections. Subsection 3.7.2 provides the presentation and overview of the data and data sources. Subsection 3.7.3 statistically discusses the data as one dataset irrespective of source, geological, or climatic context. Subsection 3.7.4 describes the general characteristics of dataset of individual study. Subsection 3.7.5 considers the four possible factors influencing K values introduced in Subsections 3.7.2 to 3.7.5 namely: depth below ground surface; rock type; climate; and tectonic regime. Subsection 3.7.6 concludes.

3.7.2 Presentation and overview of data and data sources

The entire database includes 768 hydraulic property estimates (hydraulic conductivity (K), transmissivity (T) and specific capacity (Sc)) collected from 17 different studies and about 20 published reports worldwide. Of the total number of estimates, 27 were compiled from pumping tests, 13 from specific capacity tests, 90 from slug/pulse tests, and 645 from packer/injection and drill stem tests. Published reports used in the data compilation include: Snow (1979); Merecel et al. (2004); Akaha et al. (2008); Ali-El Naqa (1994); Walker (1962); Muguel *et al*. (2009); Stober and Bucher (2004, 2005); Gale and Witherspoon (1979); Zhao (1998); Nastev (2008), and others. A summary of the entire dataset is presented in Table 3.5. The table entry shows aquifer property data points of the entire dataset by data source, project type and test type. Analyses of aquifer property were performed after combining all data derived from aquifer pumping tests, specific capacity tests, slug or pulse tests, packer/injection and drill stem tests into one dataset, though the types of data are recorded and taken into consideration when discussing the dataset. Standard statistics and graphical plots are used to summarize hydraulic conductivity data of different studies, different lithological groupings (rock type/rock class), climate zones and depth intervals. Standard statistics used include descriptive statistics and regression correlation analysis. Descriptive statistics, including the geometric and arithmetic means, median, range, variance of the hydraulic conductivity values are reported for each study. Statistical significance tests have also been conducted to determine the nature of distributions (similarities and differences) existing among dataset. Comparative statistical analyses tests (e.g. Kolmogorov-Smirnov test (KS-test) and Analysis of variance (ANOVA)) are performed to determine if there is a

significant difference between hydraulic conductivity values of different data sources, depth intervals, rock types and climate zones.

Table 3.5 Aquifer property data points by data source, rock type, project type/country and test type (see table 3.8 for further relevant factors)

Data Source (Study)	Rock type	Project Type/Country	Test type					Total
			Aquifer Pumping Test		Specific Capacity test	Slug/ Pulse Test	Packer/ Drill stem test	
			K	Sc	T	K	K	
WRI, CSIR Accra Ghana (Anglogold Obuasi Mines)	Metamorphic/igneous	Mine inflow Studies, Ghana		9				9
Ghana- Australia Goldfield (GAG) Tarkwa, Ghana	Metamorphic/igneous	Mine inflow Studies, Ghana					16	16
World Vision International. Ghana	Metamorphic	Water supply, Ghana			13			13
Snow (1979) and other published reports.	Igneous/metamorphic/sedimentary	Grouting at dam & tunnel sites, USA, Australia and South Korea					178	178
Merecel et al., (2004)	igneous	Water resources, India				31		31
Akaha et al., (2008)	igneous	Water resources, Nigeria	12					12
Ali-El Naqa (1994)	sedimentary	Water resources, Jordan					26	26
Larry Cook and Associates (2008)	igneous	Mine inflow quarry project , Australia				7		7
Cheng-Yu Ku et al, (2009)	sedimentary	Water resources, Taiwan					27	27
Moore (1962, p. 31-34)	Igneous/sedimentary	Water resources, USA				1		1
Hood (1961) USGS file	Igneous/sedimentary	Water resources, USA				3		3
Plume (1996)	Igneous/sedimentary	Water resources, USA				4		4
Walker (1962)	Igneous/sedimentary	Water resources, USA				3		3
Price(1960); Houser & Poole(1959)	Igneous/sedimentary	Water resources, USA				1		1
Ken kuchling *et al*.,	Igneous	Hydraulic testing, Canada					5	5
Muguel *et al*., (2009)	Igneous	Hydraulic testing, Spain				40		40
Gale and Witherspoon (1979); Stober and Bucher (2004, 2005)	Igneous	Radioactive waste disposal site, Stripa in Sweden					392	392
Total			12	9	13	90	645	**768**

3.7.3 Descriptive statistics of the combined dataset

Descriptive statistics is used to describe the dataset irrespective of source, geological, or climatic context. Because quantities of hydraulic parameters in fractured and heterogeneous crystalline rocks do not usually follow a normal distribution, but instead are often strongly skewed to the right, the arithmetic mean is hardly a useful parameter to describe the hydraulic characteristics of crystalline rock formation. As shown in Table 3.6 the arithmetic mean is much larger than the corresponding median and therefore cannot be considered a good representative measure of hydraulic conductivity for the combined data. Instead, the median in combination with the inter-quartile range (IQR) data in the boundaries of the 25th and 75th percentile provides a much better representation of hydraulic conductivity for the combined dataset.

Also, by definition, 50% of all K values observed fall within the inter-quartile range represented by the dimensions of the ''box''. Figures 3.7, 3.8 and Table 3.6 show a histogram, box-and-whisker plot and a summary statistics of the combined dataset respectively. On a very close examination, the overall distribution appears asymmetric, spread and skewed to lower conductivity values on the natural scale (Figure 3.7b). The skewing of the distribution to lower conductivity values is probably in part due to the scales of measurements of the different types of tests and the collection methods used. However, the log-transformed frequency distribution appears more normally distributed but exhibits a bi-modal character consisting of two apparently approximately log-normal distributions (Figure 3.7a). The bi-modality of the distribution is also probably due to differences in weathering of the shallow rock system as well as studies from which the data have been extracted (e.g., choice of very low conductivity sites for nuclear waste disposal and much high conductivity data from water supply, dam and tunnel sites). The effect of low conductivity data of radioactive waste and high conductivity data of grouting at dam and tunnel sites on the entire database has been dealt with in chapter six by regrouping the data for further analysis. The box-and-whisker plot of Figure 3.8 shows the median and the characteristic percentiles for the combined dataset. By definition, 50% of all K values observed fall within the inter-quartile range in the boundaries of **9.94E-07 and 1.10E-10** m/s represented by the dimensions of the ''box''. At 95% confidence interval for actual mean, most of the data are estimated to lie within the range of **$7.71x10^{-06}$** to **$2.18x10^{-05}$** m/s.

Summary statistics of K-parameter values (Table 3.6 in Appendix A-1) ranges from the lowest value of **1.40x10^{-13}** m/s to the highest value of **1.45x10^{-03}** m/s with an overall mean, median and standard deviation of **1.48x10^{-05}** m/s, **3.80x10^{-09}** m/s, and **9.74x10^{-05}** m/s respectively. The geometric mean of **1.57x10^{-08}** m/s is three orders lower than the arithmetic mean. The difference between the mean and median reflects the non-normal nature of the distribution. In section 3.2, previous work conducted by various researchers on crystalline rocks indicated in-situ hydraulic conductivity values to range from **10^{-11} to 10^{-4}** ms^{-1} with the most typical values centre on a geometric mean of **(−8±1)** ms^{-1}. Similar studies conducted by Brace (1980, 1984) and Clauser (1992) and measured at the borehole scale generally range between **10^{-7}** and **10^{-2}** m day^{-1} (**10^{-12}** and **10^{-7}** m/s). Thus from statistical point of view, the geometric mean of **1.57x10^{-08}** m/s obtained for current study appear to agree with the results of previous work on the characterisation of hard rocks.

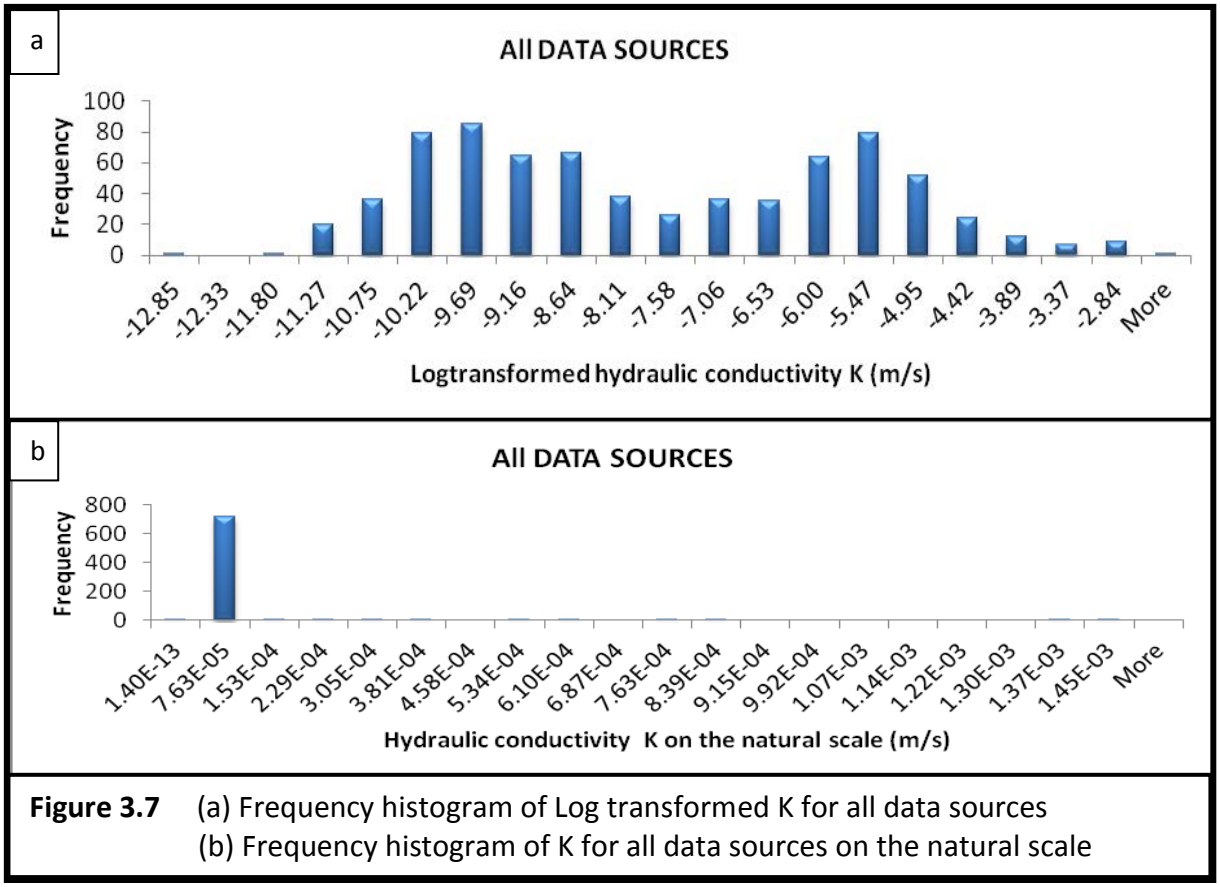

Figure 3.7 (a) Frequency histogram of Log transformed K for all data sources
(b) Frequency histogram of K for all data sources on the natural scale

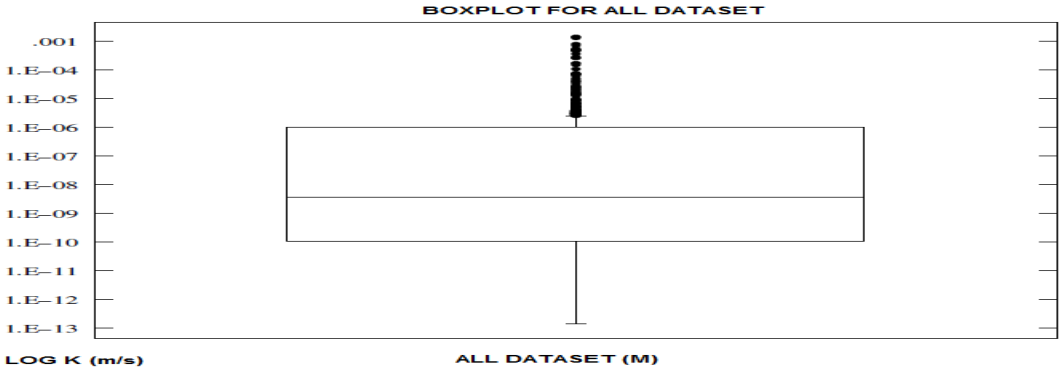

Figure 3.8 Box-and-whisker plot summary statistics of Log K for all dataset

3.7.4 Descriptive statistics of individual study

The general characteristics of the individual datasets have been described. Figures 3.9a, 3.9b, 3.9c and Table 3.7 (in Appendix A-2) show a histogram, box-and-whisker plot and a summary statistics of K parameter values of each study respectively. It is generally observed, on the natural scale, that the frequency distributions are mostly skewed to lower conductivity values (Figure 3.9b). However, the log-transformed frequency distributions appear normally distributed especially in the cases where a significant number of measurements are available (Figure 3.9a).

By definition, 50% of all K values of individual study observed fall within the boundaries of the 25th and 75th percentile represented by the dimensions of the ''box'' (Figure 3.9c). Plots of central tendency measures against spread measures of conductivity values (Figure 3.10) show a change in the averages with variance as you move from the surface to deeper depths. The change depicts the gradual decrease in K (z) from the surface to deeper depths. Also the non-normal nature of the distributions indicates that the application of Analysis of variance (ANOVA) is less appropriate to use since ANOVA assumes normal distribution of the dataset.

On a very close examination it is observed that sufficient number of values (i.e. population size) for statistical analysis is available for the studies of Witherspoon and Gale (1979) and Snow (1979) and to a lesser extent for the studies of Merecel et al. (2004) and Miguel *et al*. (2009) and the rest. Hydraulic conductivity values from studies of Witherspoon and Gale

(1979), Miguel *et al*. (2009), Ghana Australia Goldfields (GAG) and Cheng-Yu Ku et al, (2009) appear to be comparable (with median < 10^{-7}m/s). Similarly the rest of the studies including the few data from Ghana (with median > 10^{-7}m/s) show similar hydraulic characteristics and therefore associated with each other. Thus for the sake of an improved statistical analysis, two main **aquifer groups** are said to be formed by combining studies with median < 10^{-7}m/s as "basement rock formations" on the one hand and studies with median > 10^{-7}m/s on the other hand. The datasets are mainly distributed with the following observations:

1. A total of 376 K values of granite were recorded from studies of Gale and Witherspoon (1979). This forms the largest number of data points and the highest concentration of data available for any of the studies. Statistically, hydraulic conductivity ranges from **1.40E-13** m/s to **6.80E-06** m/s, and the data are very heterogeneous and spread, asymmetric about a mean value of **4.50E-08** m/s and with a standard deviation of **4.36E-07** m/s. The geometric mean of **2.05E-10** m/s is two orders of magnitude below the arithmetic mean.
2. From the studies of Snow (1979), a total of 178 K values of various rock types were collected. This collection forms the second largest number of data points. Hydraulic conductivity ranges from **4.65E-09** m/s to **1.45E-03** m/s with high variability and asymmetric about the mean value of **3.79E-05** m/s. It has a standard deviation of **4.36E-07** m/s and a geometric mean of **1.52E-06** m/s which is 20 times smaller than the arithmetic mean.
3. A total of 40 K values of granite were recorded from the studies of Miguel *et al*. (2009), the third largest number of data points. Hydraulic conductivity ranges from **2.80E-12** m/s to **3.20E-07** m/s, with a mean value of **1.22E-08** m/s and a standard deviation of **5.22E-08** m/s. Again the geometric mean of **5.33E-10** m/s is much lower than the arithmetic mean by two orders of magnitude.
4. A total of 31 K values of granite were recorded from studies of Merecel et al. (2004), the fourth largest number of data points. Hydraulic conductivity ranges from **2.00E-08** m/s to **5.10E-04** m/s, with respect to a mean value of **3.15E-05** m/s. It has a standard deviation of **9.14E-05** m/s and a geometric mean of **4.58E-06** m/s which is again lower than the arithmetic mean by two orders of magnitude.

5. The remaining datasets were fewer in comparison to those described above, and they add up to 111 K values and altogether the K values range from **2.86E-10** m/s to **5.60E-04** m/s.

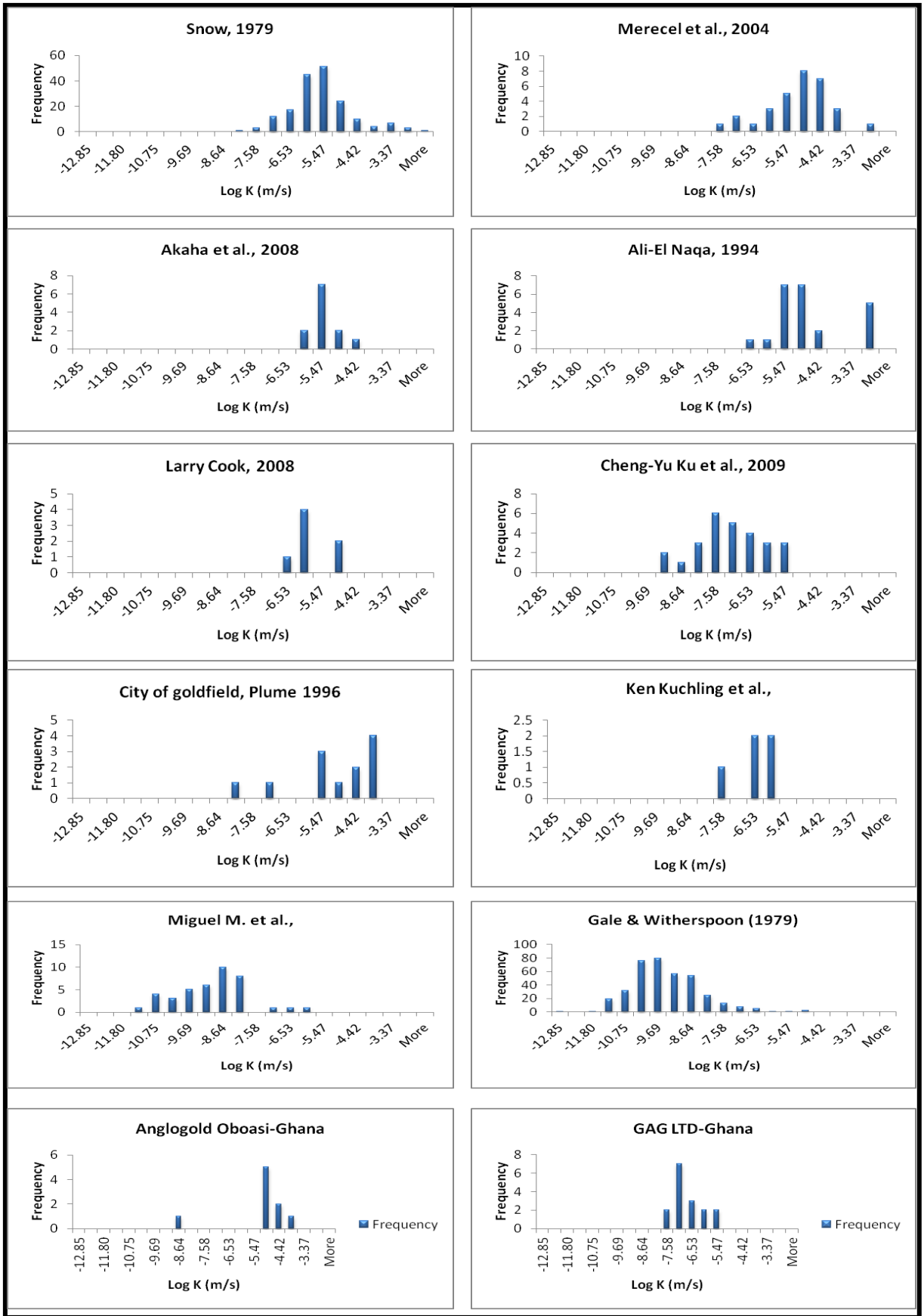

Figure 3.9a Histogram of log-transformed hydraulic conductivity for each study

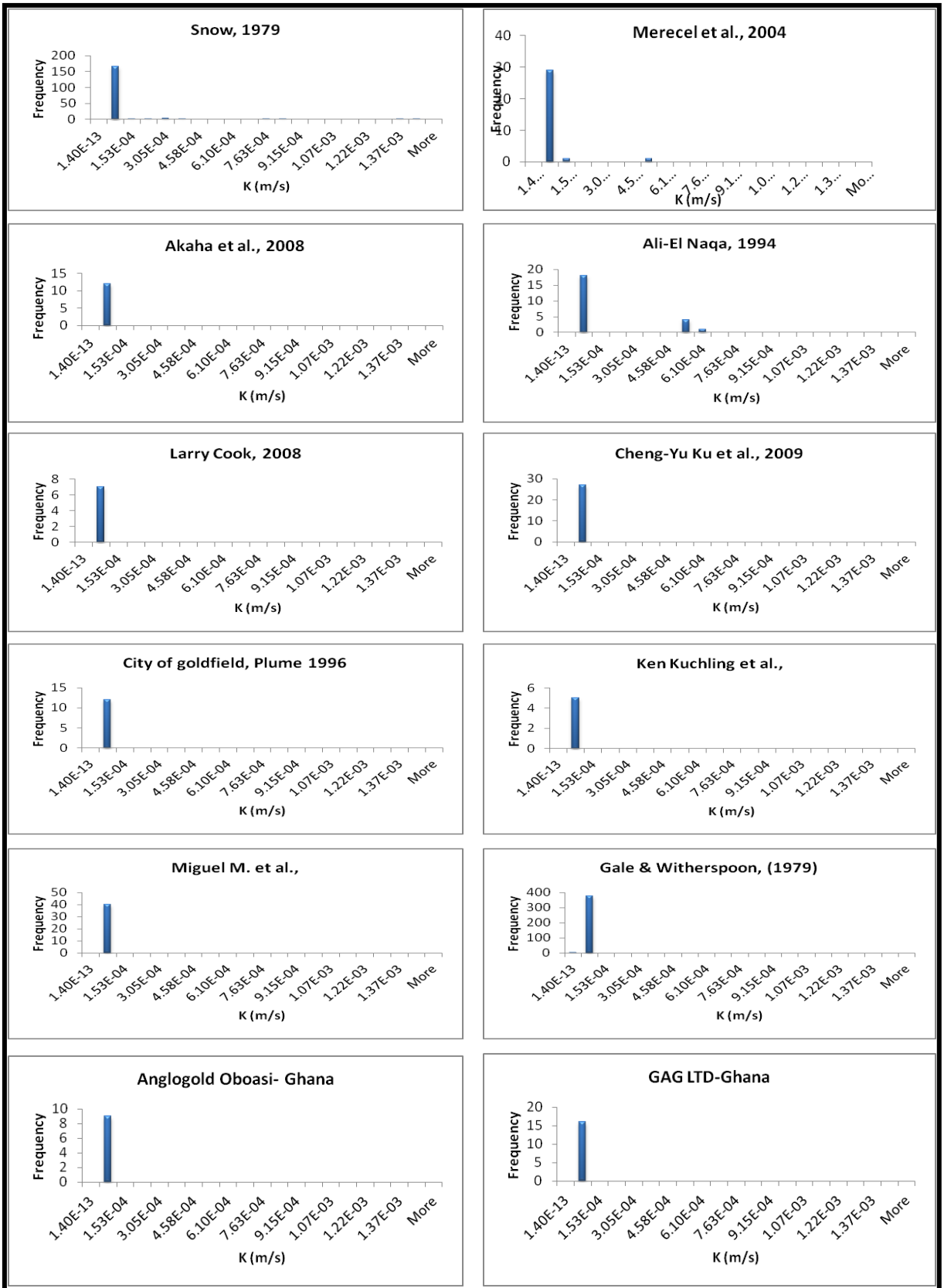

Figure 3.9b Histogram of hydraulic conductivity for each study on the natural scale. (Note that there are a small number of values even for the largest bin.)

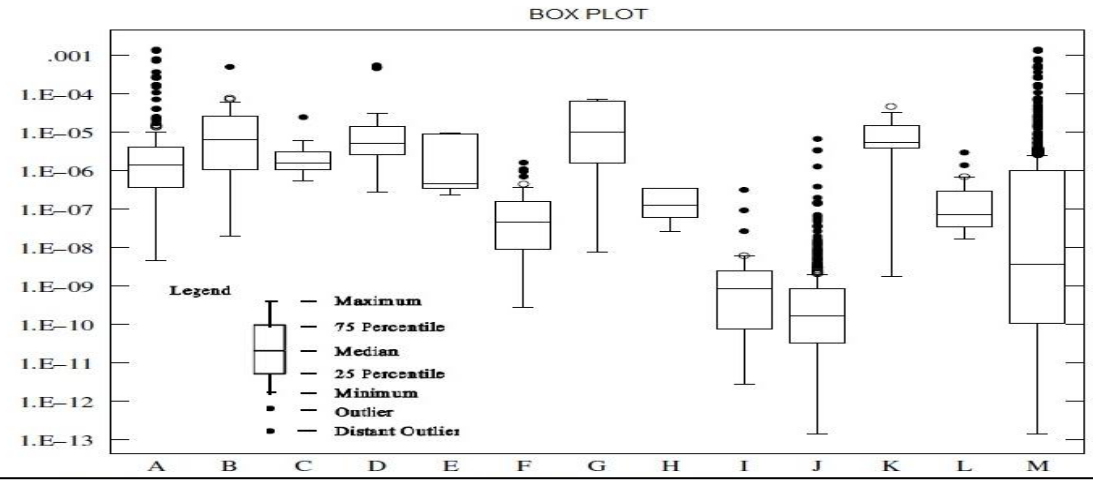

A- Snow, (1979)	*E- Larry Cook & Associates (2008)*	*I- Miguel M et al,(2009)*
B- Merecel et al., (2004)	*F- Cheng-Yu Ku et al, (2009)*	*J- Witherspoon and Gale (1979)*
C- Akaha et al., (2008)	*G- City of Goldfield; Plume (1996)*	*K- Anglogold Obuasi Ghana (AGC)*
D- Ali-El Naqa, (1994)	*H- Ken Kuchling et al, (2009)*	*L- Ghana Australia Goldfields (GAG)*

Figure 3.9c Box-and-whisker plot summary statistics of log-transformed hydraulic conductivity for each study, M is all dataset together.

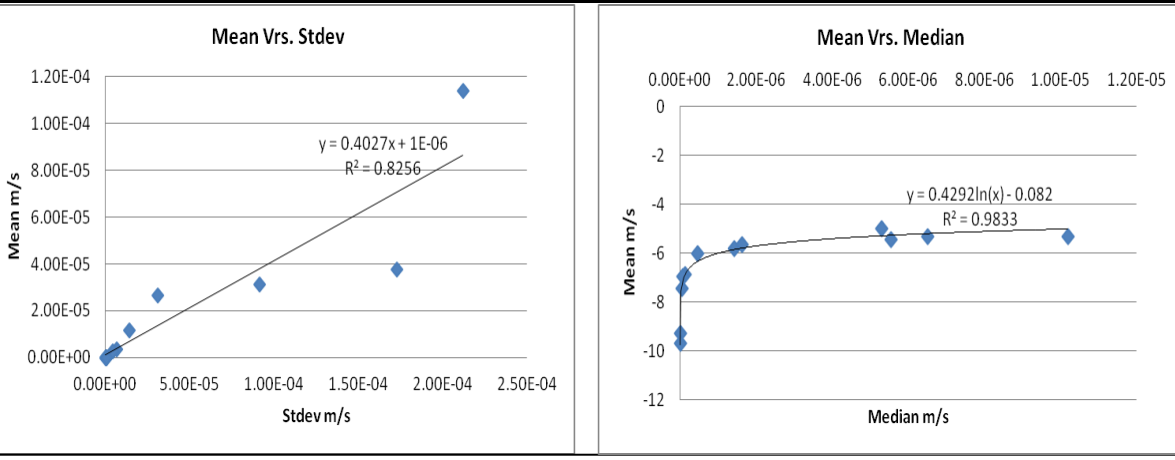

Figure 3.10 Plots of central tendency measures against spread measures

3.7.5 The sensitivity of K values to depth, rock type, rock class and climate

3.7.5.1 Introduction

The estimation of appropriate representative hydraulic conductivity values for regional groundwater flow modelling in mining areas is considered to be affected by local factors including: depth, rock types/class, climate, test type and tectonic history. Statistically, these factors have been used to constrain the estimation of site specific parameters (K parameters) in the mining environments, to try and determine the importance of these factors. If these factors come out to be important, then application of global ''average'' values (combined dataset, Section 3.7.3) may not be appropriate, or at least most useful, for a given location. Table 3.8 shows how the dataset obtained maps out in terms of three of these factors: depth, rock type/class and climate. Because, there are too few datasets to separate out the effects of each factor statistically one-by-one, a step-wise approach has been adopted. Each factor has been assessed as far as possible using all the data, and then, where possible, by limiting the data used to within a certain range of parameter values for the other variables (Table 3.9). The investigation is carried out keeping in mind that many of these combinations are not possible because there are very few data to look at. The results of investigation are discussed in subsections 3.7.5.2 to 3.7.5.5 for each of the factors (depth, rock type, rock class and climate) respectively.

Table 3.8 Factors relevant to individual datasets

Study	Factors				
	Purpose for K Studies	**Test type**	**Rock type**	**Depth interval (m)**	**Climate**
WRI, CSIR Accra Ghana (Anglogold Obuasi Mines)	Mine inflow studies	Pumping Test	Phyllite	41 - 62	Tropical
Ghana- Australia Goldfield (GAG) Tarkwa, Ghana	Mine inflow studies	Packer/Drill stem test	Quartzite	21 - 165	Tropical
World Vision International. Ghana	Water supply	Specific Capacity test	Quartz diorite	14 - 50	Tropical
Snow (1979)	Grouting at dam and tunnel sites	Packer/Drill stem test	Granite, gneis, schist, amphibolites etc	2 - 168	Semiarid
Merecel et al., (2004)	Water resources	Slug/Pulse test	Granite	27 - 60	Semiarid
Akaha et al., (2008)	Water resources	Pumping Test	Granite	42 - 88	Tropical
Ali-El Naqa (1994)	Water resources	Packer/Drill stem test	Sandstone	4 - 38	Semiarid
Larry Cook and Associates (2008)	Mine inflow quarry project	Slug/Pulse test	porphyry	11 - 28	Semiarid
Cheng-Yu Ku et al, (2009)	Water resources	Packer/Drill stem test	Sandstone	26 - 250	Tropical
Moore (1962, p. 31-34)	Water resources	Slug/Pulse test	Basalt and tuff	0 - 406	Semiarid
Hood (1961) USGS file	Water resources	Slug/Pulse test	Sandstone, conglomerate, and tuff	0 - 549	Semiarid
Plume (1996)	Water resources	Slug/Pulse test	Sandstone with interbedded claystone	0 - 126	Semiarid
Walker (1962)	Water resources	Slug/Pulse test	Quartz porphyry & granodiorite	246 - 549	Semiarid
Price(1960); Houser & Poole(1959)	Water resources	Slug/Pulse test	Argillized, and chloritized granodiorite	0 - 366	Semiarid
Ken kuchling *et al*., (2009)	Hydraulic testing	Packer/Drill stem test	Granite	45 - 300	Subarctic
Muguel *et al*., (2009)	Hydraulic testing	Slug/Pulse test	Granite	32 - 200	Mediterranean
Gale and Witherspoon (1979	Radioactive waste disposal site	Packer/Drill stem test	Granite	3 - 382	Temperate

Table 3.9 The order of investigation and sections showing where investigation is either possible, not possible or lacks data.					
Investigate	**Fix:**				
	Nothing	**Depth**	**Rock type**	**Rock class**	**Climate zone**
Depth	Done	Not possible	Done	Done	Done
Rock type	Done	Lacks data	Not possible	Not possible	Lacks data
Rock class	Done	Lacks data	Not possible	Not possible	Lacks data
Climate zone	Done	Lacks data	Lacks data	Lacks data	Not possible

3.7.5.2 The dependence on depth of K

3.7.5.2.1 Introduction

In this section, the spatial variability of all datasets with respect to depth and also for a couple of sites for which good depth data with similar geology and climate exist has been analysed. Conclusions are then drawn as to the importance of K(z) relationship in general and to what conceptual model can be derived from the K(z) analysis (e.g., the trend of constant K with depth, exponentially decreasing K with depth or high K upper layer with K approaching zero at the lower layer). Implications for looking at other factors, if we should compare only data from tests at certain depth ranges are also considered. Detailed analysis of spatial variability of depth dependence of K distribution of datasets is given in sub-sections 3.7.5.2.2 - 3.7.5.2.4.

3.7.5.2.2 The variation of K with depth: for whole dataset

Intuitively, hydraulic conductivity is expected to decrease with depth as confining pressures seal fractures and faults, and compress sedimentary units. A plot of log-transformed hydraulic conductivity values and the mid-point depth of the tested interval starting from the top of the rock surface for all the different data sources are shown in Figure 3.11. Visual examination of these plots shows an apparent K-depth relationship, but with high data scatter due to the fact that most of the data are obtained from small scale test measurements (section 3.5.2.2.).

A moving average and exponential relationship are fitted to determine the true changes of slope from the scattered data (Figure 3.12). Although data shown suggest a relatively large scatter, the moving average and exponential fits suggest a decreasing K with depth with the exponential fit significant at greater than 99% confidence. Model fitting curves with the

dataset compiled in the present study is carried out using empirical relationships in literature from studies conducted by Snow (1970), Carlsson & Olsson (1977) and Wei et al. (1995) to see how much K is expected to vary down to and beyond the base of mines.

Depending on the variability of the study area (geostatic stress, lithology, and fracture properties), the plots show different ranges of conductivity values for different studies (Figures 3.13). The three relationships show variation of K with depth for the sites investigated in the original studies: the relationship of Wei et al. (1995) shows the least variation of K with depth about two orders of magnitude from the surface to 600m depth. Both relationship of Olsson and Carlson (1997) and Snow (1970) show a wider range of K variation with depth, about four orders of magnitude. In these two latter studies, K decreases rapidly to about a depth of 100-200m where it more gently decreases to a depth of 600m.

Although, mean values of all three relationships are less than that of the current dataset (-8+-1) m/s, they could be used to analyse the current dataset with the relation of Wei et al. (1995) which seems to yield the best result. These relationships have therefore been adopted for future interpretations of conductivity-depth relationship of database in mining environments.

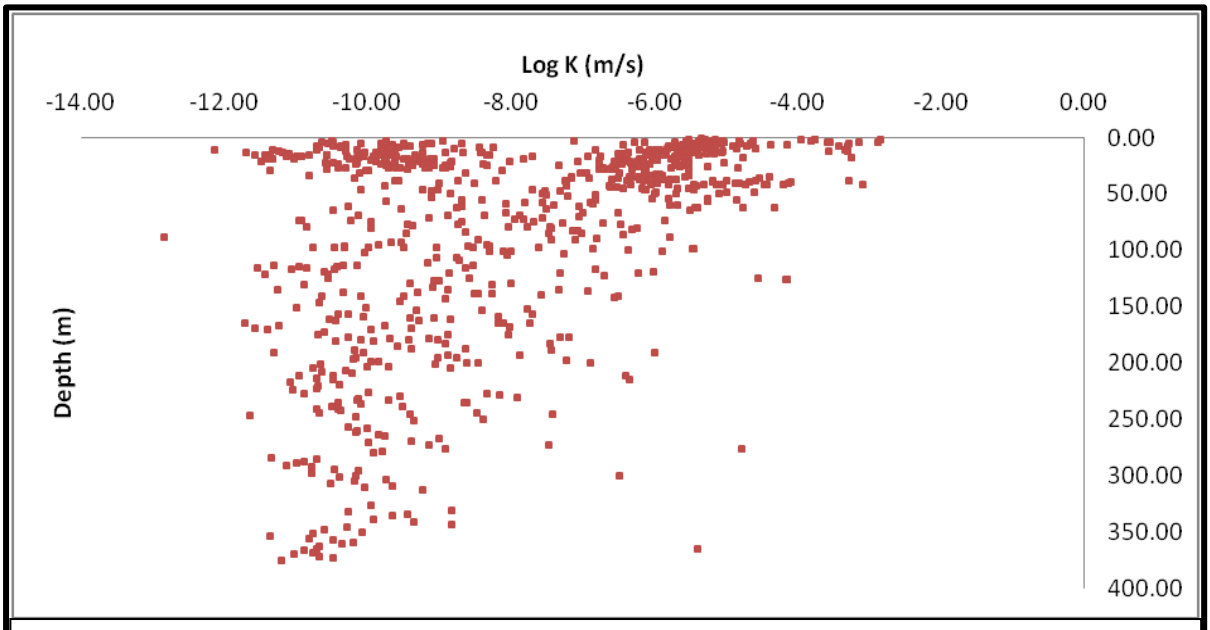

Figure 3.11 Variation of hydraulic conductivity with depth for the whole dataset

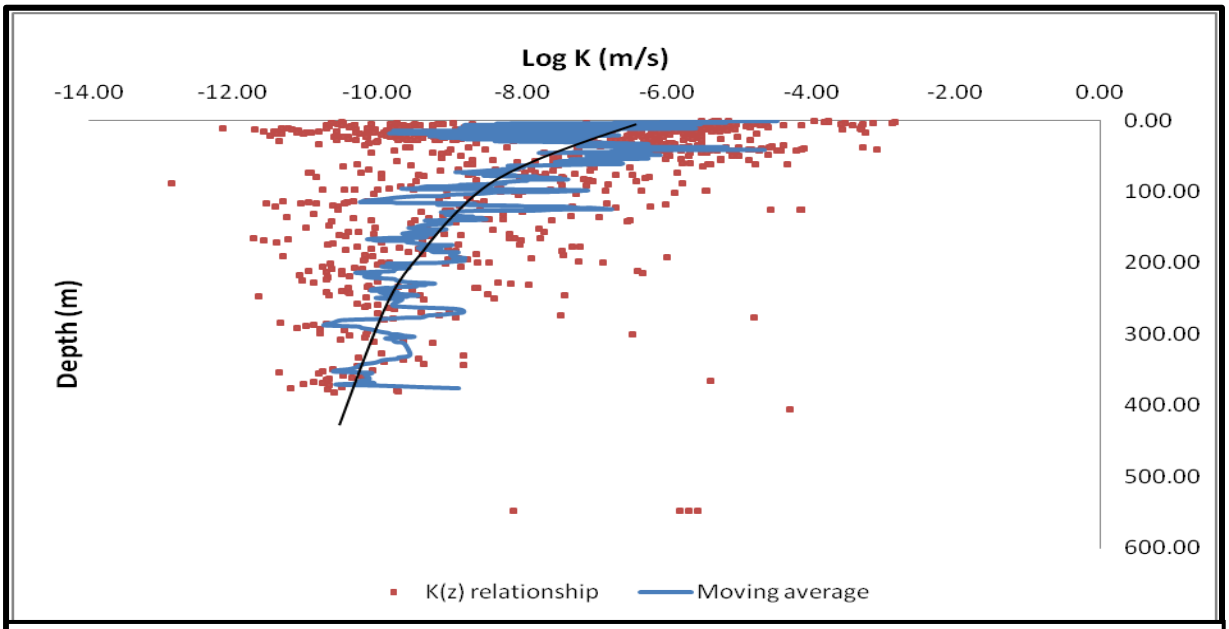

Figure 3.12 Log-transformed hydraulic conductivity distributions with depth for whole dataset. Thicker blue line is a 2-point moving average of the values; thinner black line is a least squares fit of the exponential relationship indicated

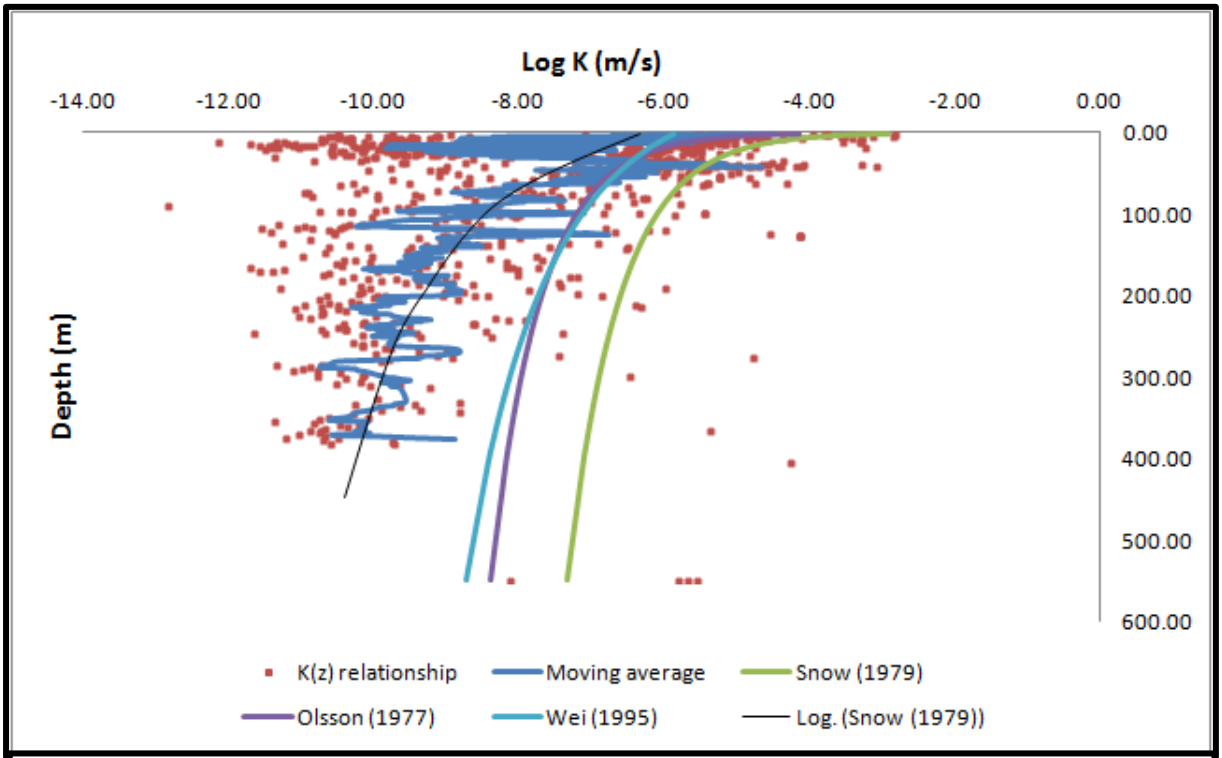

Figure 3.13 Comparison of empirical K(z) relations of various studies (Snow, Olsson and Wei) with K database

Because hydraulic conductivity values and depth from different studies are determined to be significant factors for change of conductivity values, the depth data are combined into depth intervals of 100m to investigate further whether there are any detectable differences in K distribution. Investigations are conducted first for the first 0-100m at 20m depth intervals, followed by the entire 0-500m depth range by applying the Kolmogorov-Smirnov (K-S) statistical test (Sheskin, 2007) at 95% significance level. The statistical summary of the results in the form of tables, histogram and box-and-whisker plots are presented in Tables 3.10 and 3.11 and Figures 3.14 and Figure 3.15 respectively.

Results from K-S test show that at 95% confidence level there is a significant difference in depth intervals between the first 100m depth and between the first and second 200m depth range as indicated in Table 3.11 and 3.12 respectively. The spread (inter-quartile ranges) of Figure 3.14 and frequency distribution plots of Figure 3.15 of K distribution, decreases with depth from the surface. In Figure 3.14, a plot of log K against depth interval shows a decrease in K with depth to about 300m over a scale of three orders of magnitude after which there seems to be no significant difference in K distribution up to the 400m depth. This indicates that by ignoring different study sites permeable fractures are present at shallow depths but reduce in frequency with depth as expected.

Table 3.10 K-S Test results for the first 100m depth range at 20m depth intervals

Depth intervals (m)	D statistics	P value	Significant at the 95% confidence level
(0-20) and (20-40)	0.26	0.00	Yes
(20-40) and (40-60)	0.30	0.00	Yes
(40-60) and (60-80)	0.35	0.00	Yes
(60-80) and (80-100)	0.43	0.00	Yes

Table 3.11 K-S Test results for the entire 500m depth range at 100m depth intervals

Depth intervals (m)	D statistics	P value	Significant at the 95% confidence level
(0-100) and (100-200)	0.42	0.00	Yes
(100-200) and (200-300)	0.30	0.00	Yes
(200-300) and (300-400)	0.14	0.67	No
(300-400) and (400-500)	0.28	0.56	No

Table 3.12 Summary statistics of log K (m/s) distribution within 100m depth intervals of the entire 0-500m depth range

Sections of depth intervals (m)		Count	Descriptive statistics for different test sections (log K)					Significant at the 95% confidence level
			Min	Max	Mean	Median	St dev.	
A	**0 – 100**	**500**	-12.85	-2.840	-7.39	-6.85	2.14	Yes
B	**100 – 200**	**123**	-11.72	-4.140	-8.99	-9.09	1.64	Yes
C	**200 – 300**	**73**	-11.66	-4.790	-9.73	-10.14	1.30	No
D	**300 – 400**	**39**	-11.38	-4.290	-9.86	-10.27	1.46	No
E	**Total Depth**	**736**	-12.85	-2.840	-8.02	-8.42	2.18	-

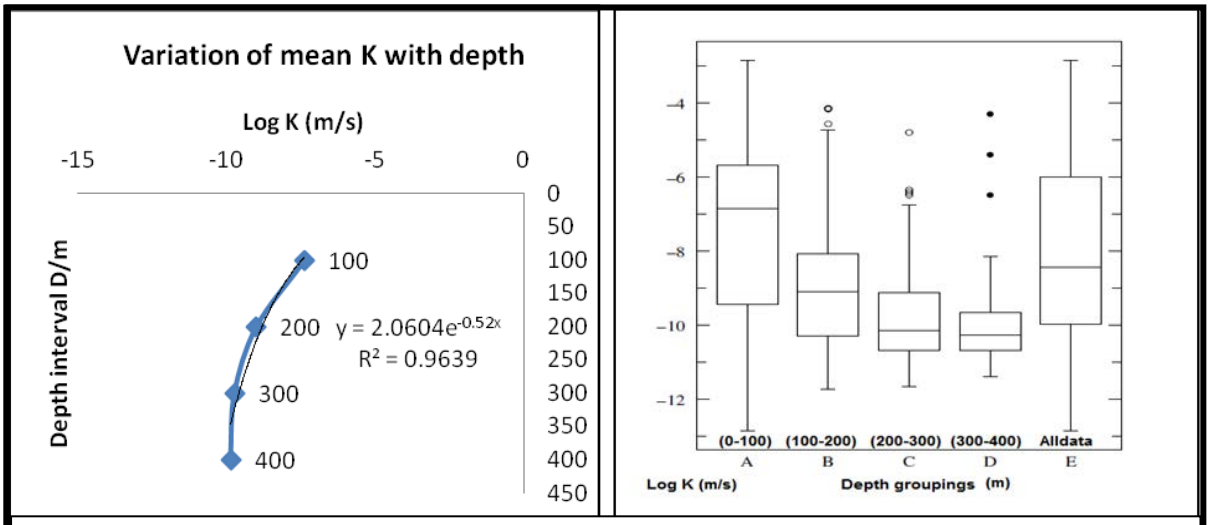

Figure 3.14 Variation of Log of mean K with depth intervals (left) and corresponding box-and-whisker plot of log K distribution at constant depth interval of 100m from A-E

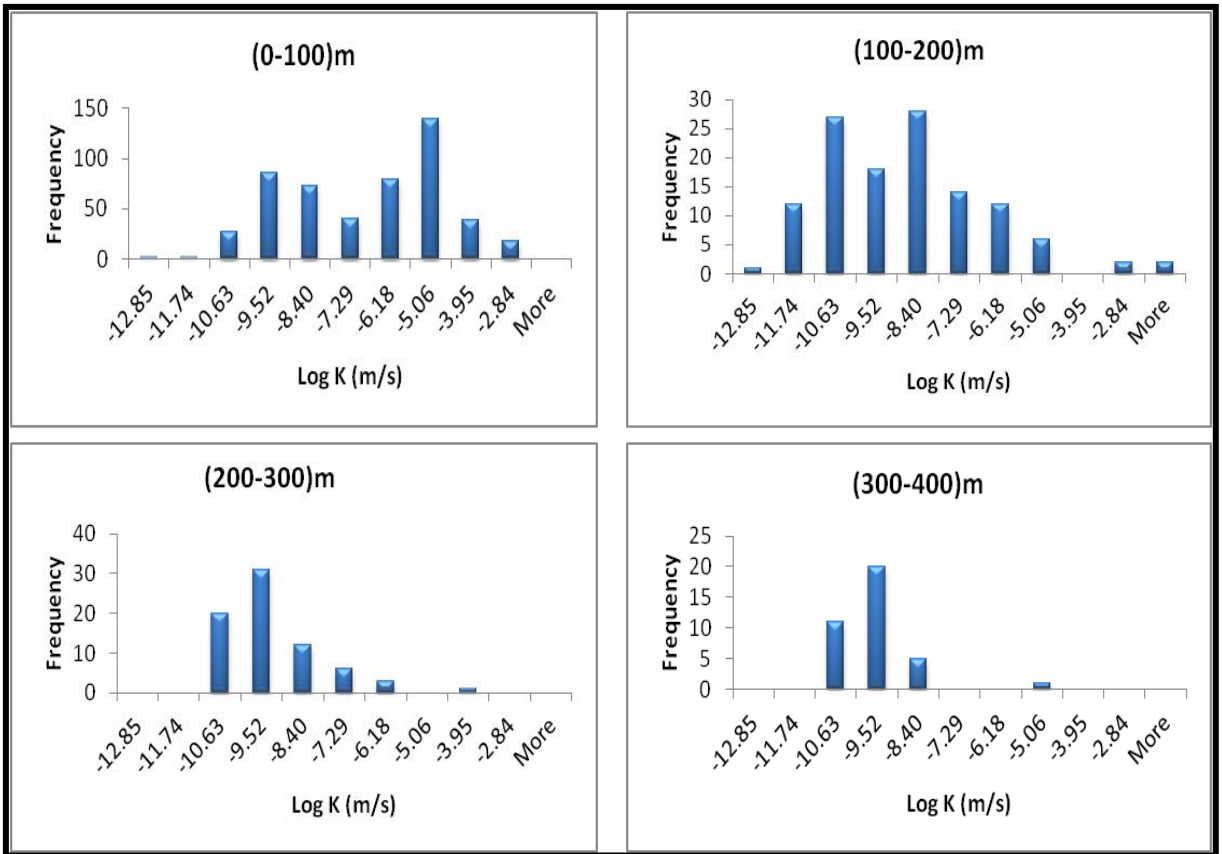

Figure 3.15 Log of hydraulic conductivity frequency distribution with depth for test interval of 100m from 0-400 m for all dataset

3.7.5.2.3 The variation of K with depth: for sites with similar geology, climate and other variables

The variations of conductivity and log (conductivity) values with depth have been examined for sites with similar geology, climate and other variables of studies for which most data are available (Figures 3.16 and 3.17). The results show a general decrease in hydraulic conductivity with depth for all the different studies with an apparent great deal of scatter. It is observed that depth variation is poorly developed at any specific site but with higher K at shallow depths. The high data scatter may be due to the fact that most of the data are obtained from small scale test measurements. The main factors likely to affect K, including rock type, climate and tectonic regime, are likely to be constant at each site. Thus, the relationship between depth and K should be strongest for individual sites.

In general the Pearson correlation coefficients (r^2) for power relationships of the form Log K=m (e) ^{CZ} are low for individual studies. This may be attributed to small depth range of sample numbers in some cases and also for the fact that most of the sites are of similar

climate and geology. Data from studies conducted by Cook (2008) and Anglogold Obuasi (2010) in Ghana have the maximum and the minimum (r^2) values of 0.47 and 0.002 respectively for depth / K relationships. Although K-S tests conducted on the top 100m depth interval show some significant differences in K distribution at shallow depths, in general by limiting K (z) relationship to sites of similar geology and climate resulted in a poor variation in K distribution.

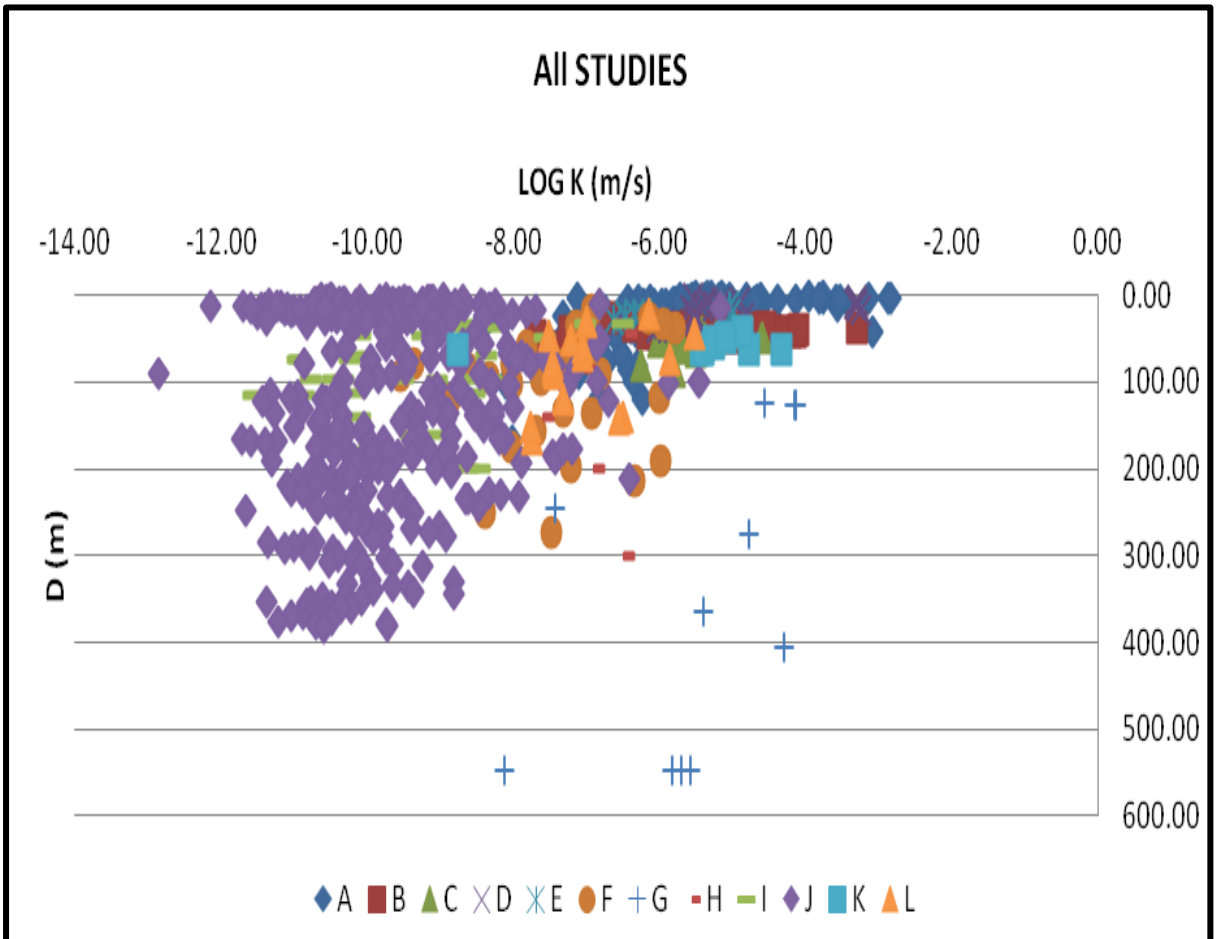

A- Snow, (1979)	*E- Larry Cook & Associates (2008)*	*I- Muguel M et al, (2009)*
B- Merecel et al., (2004)	*F- Cheng-Yu Ku et al, (2009)*	*J- Witherspoon and Gale (1979)*
C- Akaha et al., (2008)	*G- City of Goldfield; Plume (1996)*	*K- Anglogold Obuasi Ghana (AGC)(2010)*
D- Ali-El Naqa, (1994)	*H- Ken Kuchling et al, (2009)*	*L- Ghana Australia Goldfields (GAG)(2010)*

Figure 3.16 Variation of hydraulic conductivity with depth for all studies yet in a section that is dealing with studies from sites with similar geology, climate and other variables

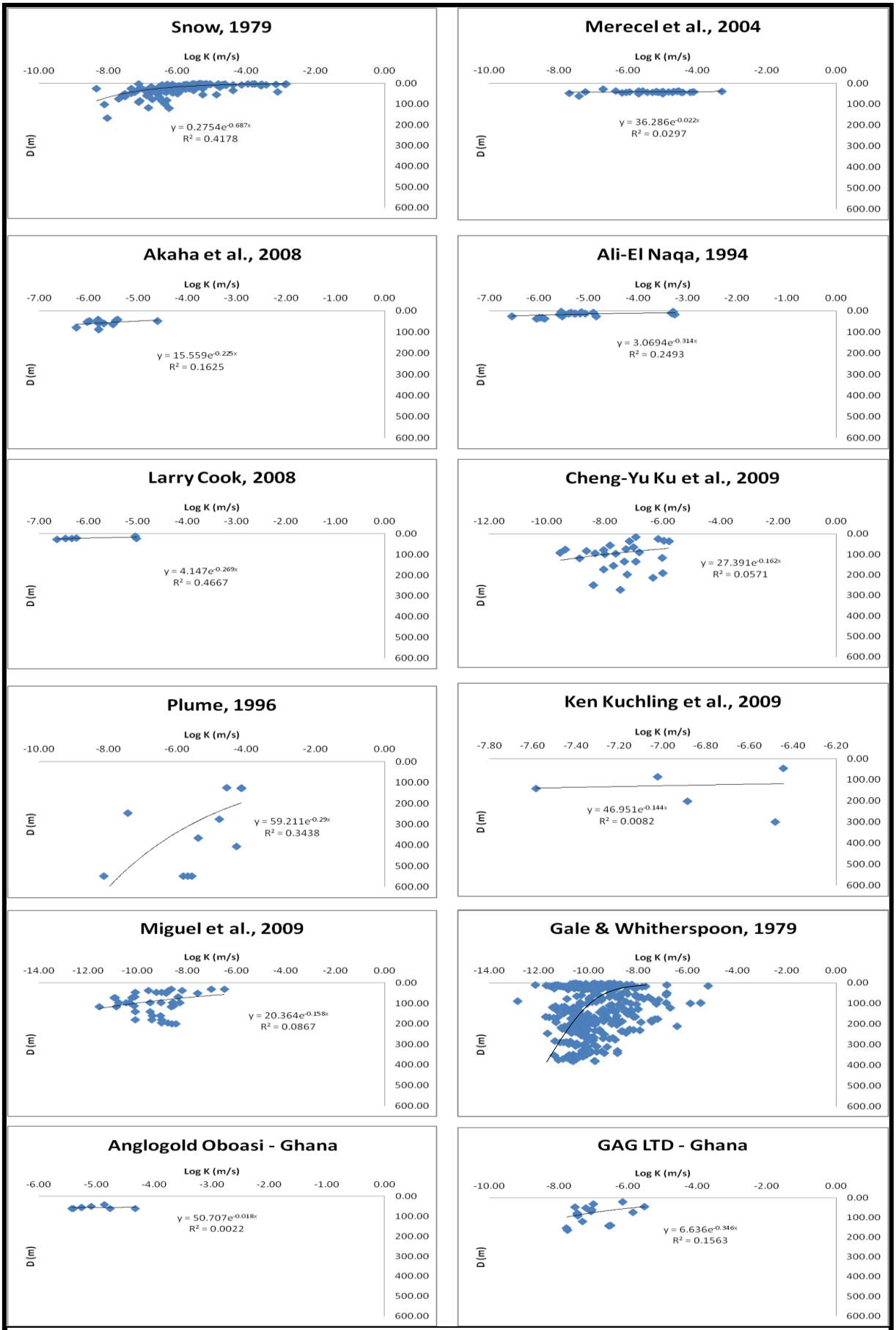

Figure 3.17a Variation of log-transformed hydraulic conductivity with depth for each study

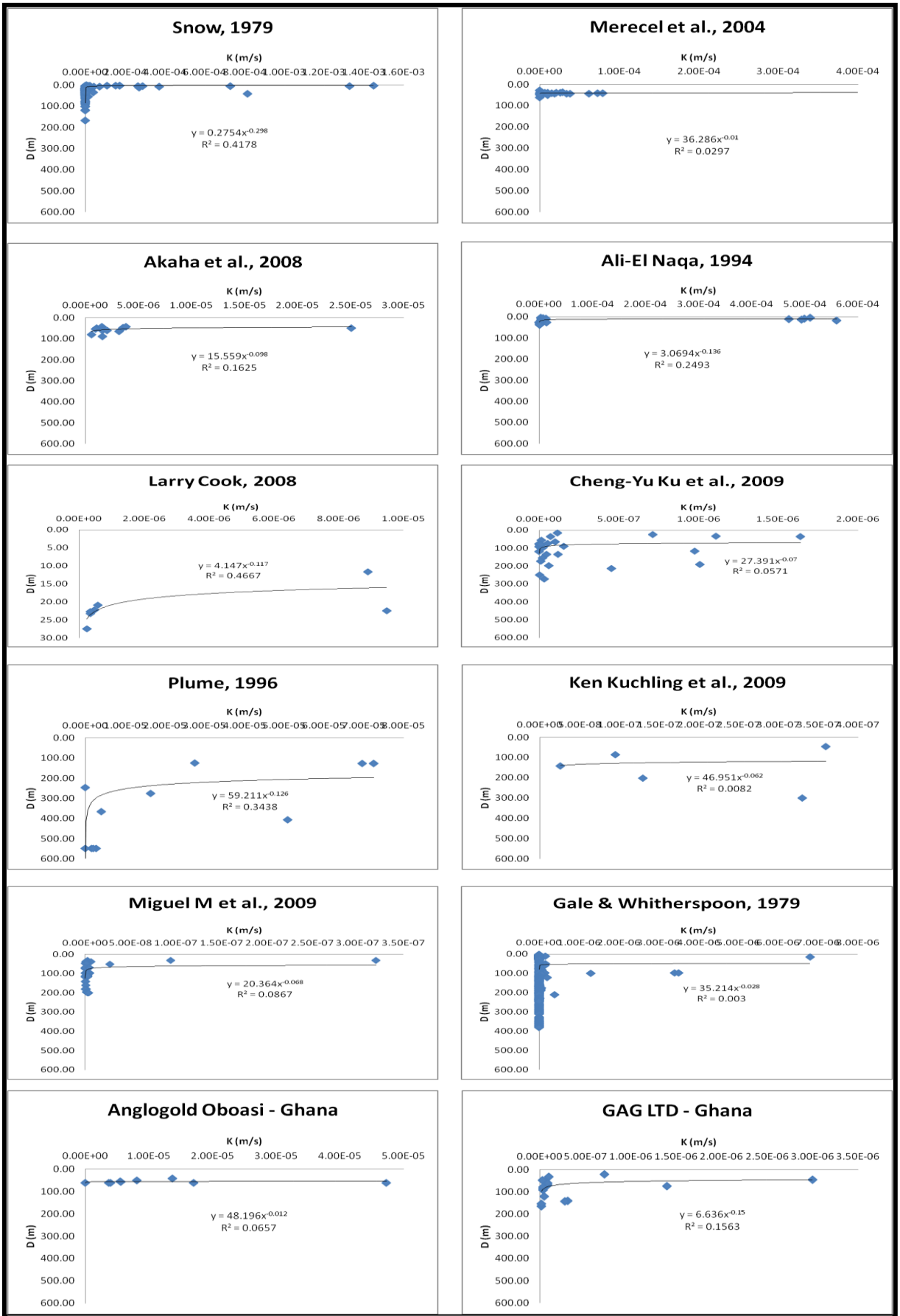

Figure 3.17b Variation of hydraulic conductivity with depth for each study on the natural scale

3.7.5.2.4 Conclusion on the dependence on depth of K

As expected in a fractured aquifer system, visual examination of a plot of log K against depth (Figure 3.11) for combined dataset shows an apparent K-depth relationship, but relatively high data scatter. A moving average analysis (Figure 3.12 and 13) provides a reasonable visualization of the variability of K with depth, with the rate of decrease in K with depth decreases with depth.

The application of K-S tests at 95% confidence level on depth intervals show that there is significant difference in K distribution with depth between the top 100m and the first and second 200m depth intervals (Table 10, and 11).

Also, a plot of mean log K values against depth (Figure 3.14) shows a decrease in K with depth to about 300m over a scale of three orders of magnitude after which there seems to be no significant difference in K distribution up to 400m depth. Such a decrease of K values with depth may be used as an indication that the extent of variation and interconnection of fractures in these crystalline rocks is most abundant in the upper 200-300 metres. From the above investigations conclusions can be drawn that generally, by ignoring different study sites K decreases approximately exponentially with depth in hard rock aquifer systems with permeable fractures present at shallow depths but reduce in frequency with depth as expected.

However, it must be emphasized that locally, by limiting the investigation to sites of similar geology and climate, the relationship with depth may be very different, and that the dataset is characterized by a great deal of scatter. It is observed that depth variation is poorly developed at any specific site but with higher K at shallow depths. The high data scatter may be due to the fact that most of the data are obtained from small scale test measurements and also due to weathering differences of rock types. The main factors likely to affect K, including rock type, climate and tectonic regime, are likely to be constant at each site. Thus, the relationship between depth and K should be strongest for individual sites. Although K-S tests conducted on the top 100m depth interval show differences in K distribution at shallow depths, in general results doesn't show any good variations by limiting the dataset to sites of similar geology and climate.

3.7.5.3 The dependence on rock type of K

3.7.5.3.1 Introduction

In this section, the dependence on rock type of K has been analysed by first of all considering variation of K values for all rock types and then limiting the analysis to rock types at sites with the same depth and climate.

3.7.5.3.2 The variation of K with rock type: for whole dataset

Before conducting statistical evaluation on the general characteristics of the rock types, variations existing between studies of different and the same rock types are investigated. Most of the rocks for which data are available are granites. Out of the 736 measurements collated, 489 are from granites of Gale and Witherspoon (1979), Muguel (2009), Merecel (2004) and Snow (1979). Results of Kolmogorov–Smirnov significance tests conducted at 95% confidence level on the 489 conductivity values of the granitic rocks from different studies and different rock types show that at 0.05 significance level the population mean is significantly different among the different studies and the different rock types (Table 3.13 and 3.14).

Statistically, the relative frequency distribution of K and log K parameters of rock type(s) in the entire dataset is illustrated in Figure 3.18a. The box-and-whisker plots of Figure 3.18b and the descriptive statistics of Table 3.15 (in Appendix A-3) summarize and compare statistics obtained for each rock type(s) in terms of their central tendencies and spread. The following observations can be accounted to indicate the variation in K trend among the various rock types:

1. A total of 489 conductivity values of **granitic rocks** were recorded from six different studies from different climates. This is the largest number of data points and the highest concentration of data available for any of the rock types. K values for granites ranges from **1.40E-13**m/s to **6.80E-06**m/s and show a bi-modal distribution. The distribution is spread but asymmetric with respect to geometric mean value of **3.92E-09** m/s and standard deviation of **4.71E-05** m/s. K-S test conducted on the

granitic rocks from different studies show that K values are all different from each study (see Table 3.15).

2. 56 conductivity values of **sandstone/meta-sandstone** were recorded, and this is the second largest number of data points. Distribution of K values ranges from **2.86E-10** to **5.60E-04** m/s. The distribution varies and it is asymmetric to the geometric mean value of **5.91E-07** m/s and has a standard deviation of **1.48E-04**m/s.
3. **Quartzite** with 35 K values, were recorded and has the third largest number of data points. Hydraulic conductivity ranges from **1.70E-08** to **6.73E-06**m/s, being spread but asymmetric with respect to the mean value of **9.16E-07** m/s and has a standard deviation of **1.7E-06**m/s.
4. A total of 32 K values of gneiss were recorded and has the fourth largest number of data points. Hydraulic conductivity ranges from **4.65E-09** to **1.74E-04**m/s, and asymmetric with respect to the mean value of **9.05E-06**m/s and has a standard deviation of **9.14E-05**m/s.
5. The rest of the data sets show low data points, and their distribution characteristics are as shown in Figures 3.18a, 3.18b and Table 3.15.

In general with the K parameter values the standard deviation (stdev) values are very large in comparison with the means – in most cases the stdev is greater than the mean and in the case of granites about 10 times. Given that negative values cannot occur, this is a strong indicator of the non-normal nature of the distributions. Similarly with Log K parameters, with the exception of the median and the spread (inter quartile ranges) measures which appear to show very little variations (r^2~1), plots of central tendency measures against spread measures (Figure 3.19) show changes in the averages with variance. The change in the averages with variance depicts the non-normal nature of the distributions and therefore application of Analysis of variance (ANOVA) is less appropriate as a test method to use to distinguish between differences and similarities of rock types since ANOVA assumes normal distribution of the dataset. It can be concluded that differences among K distribution of different rock types of different studies are influenced not only by differences in the weathering processes of rock formation but also differences in the methods used to measure K in the different studies examined, and the purposes for which the studies were conducted. In general rock type is not a major factor influencing variation in K distribution.

Table 3.13 K-S Test for differences in granitic rocks for different studies			
Studies	**D statistics**	**P values**	**Significance at 95% confidence level**
(Gale and Witherspoon, 1979) and (Miguel et al., 2009)	1.0000	0.000	Yes
(Gale and Witherspoon, 1979) and (Snow, 1979)	1.0000	0.000	Yes
(Gale and Witherspoon, 1979) and (Merecel et al.,2004)	1.0000	0.000	Yes

Table 3.14 K-S Test for differences in granitic rocks and different rock types			
Studies	**D statistics**	**P values**	**Significance at 95% confidence level**
Granites and (sandstone/meta sandstone)	0.6822	0.000	Yes
Granites and quartzite	0.8078	0.000	Yes
Granites and gneiss	0.7908	0.000	Yes
Granite and greenstone	0.8315	0.000	Yes
Granite and mica schist and phyllite	0.8031	0.000	Yes

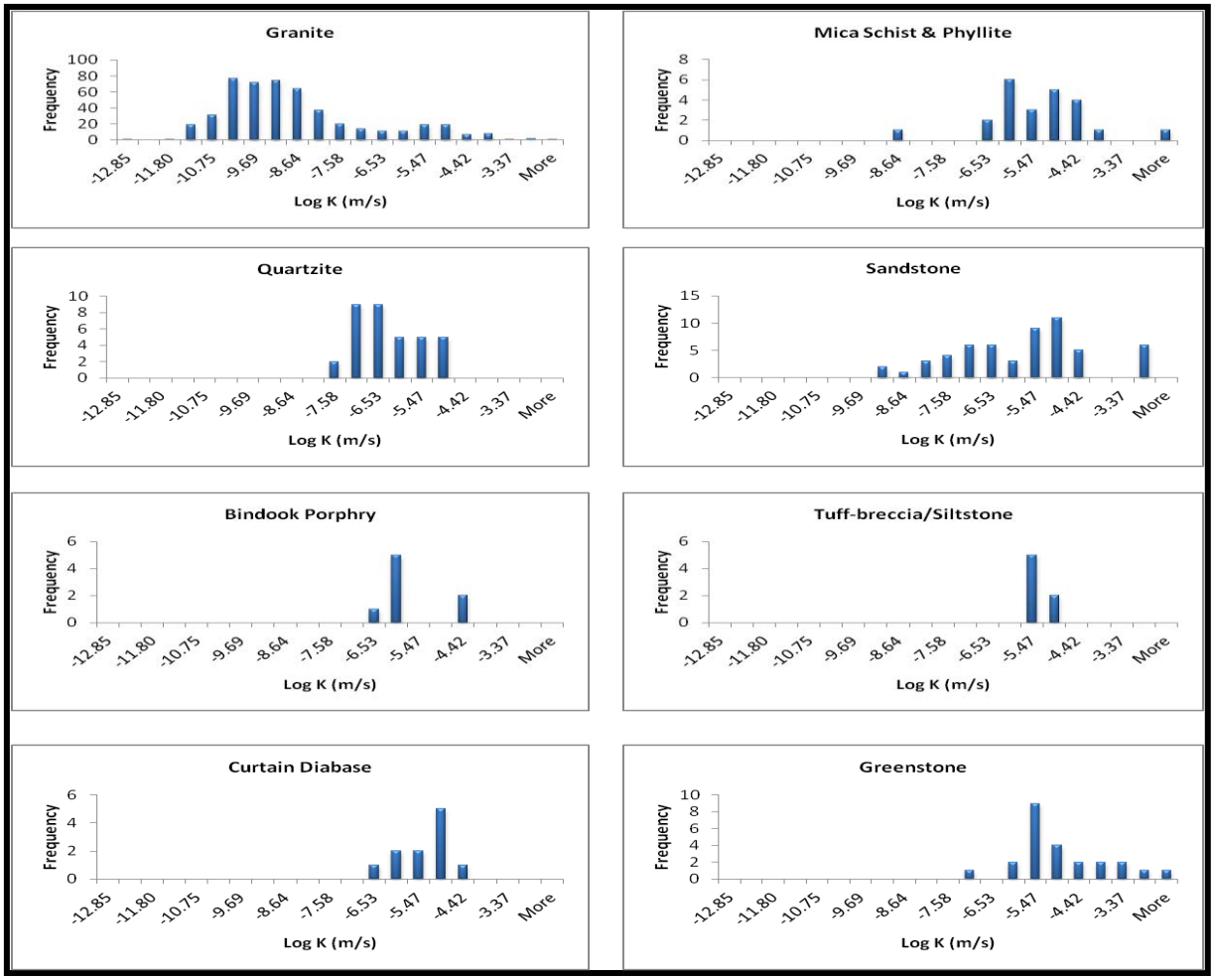

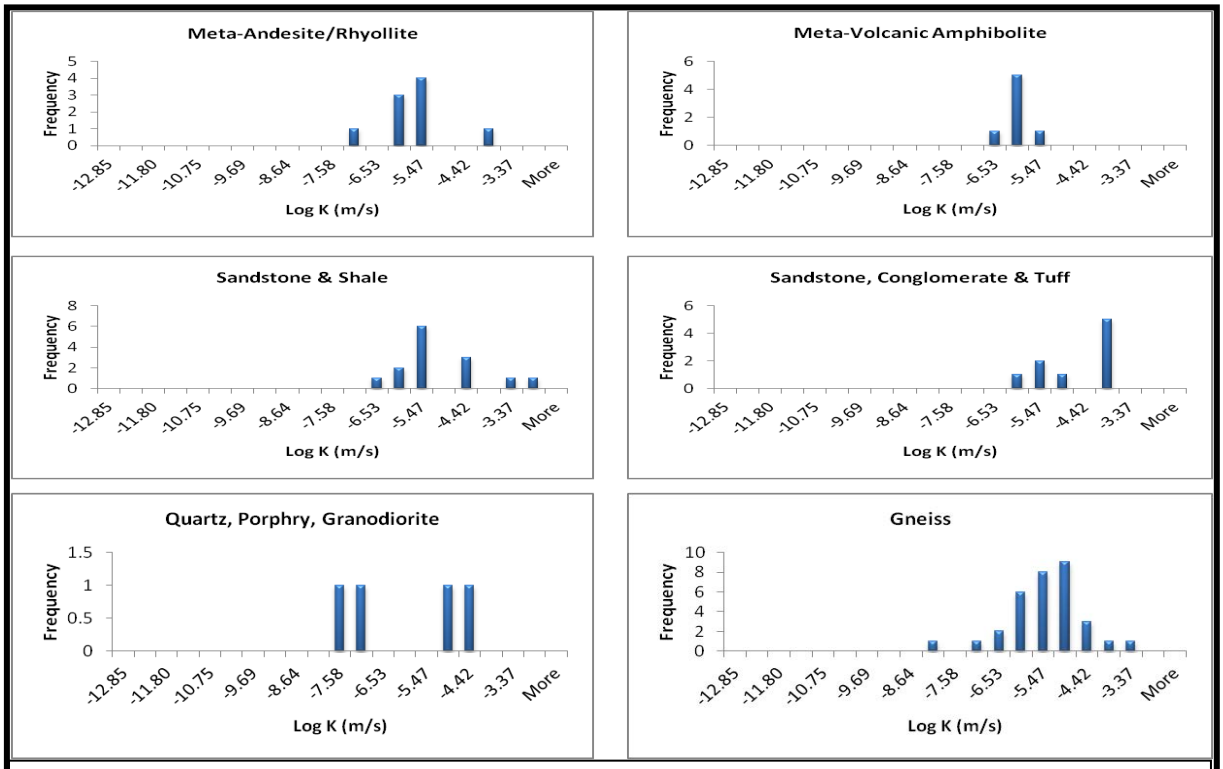

Figure 3.18a Histogram of log of hydraulic conductivity (K) for each rock type

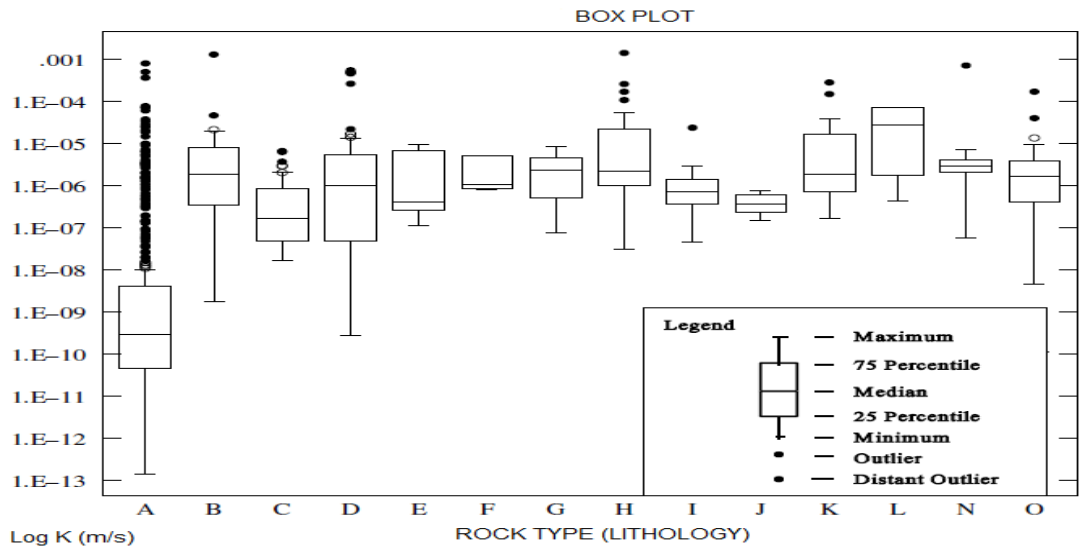

A = *Granite*	**B** = *Mica schist & phyllite*	**C** = *Quartzite*
D = *Sandstone , meta sandstone*	**E** = *Porphyry*	**F** = *Tuff-breccia, tuff-siltstone*
G = *diabase*	**H** = *Greenstone*	**I** = *Meta andesite, meta-rhyollite*
J = Metavolcanic amphibolite	**K** = *Sandstone and shale*	**L** = *Sandstone, tuff & conglomerate,*
M = *Quartz porphyry & granodiorite*	**N** = *Slate, talc- schist, talc- Serpentine*	**O** = *Gneiss*

Figure 3.18b Box plot summary statistics of hydraulic conductivity (K) for each rock type (lithology)

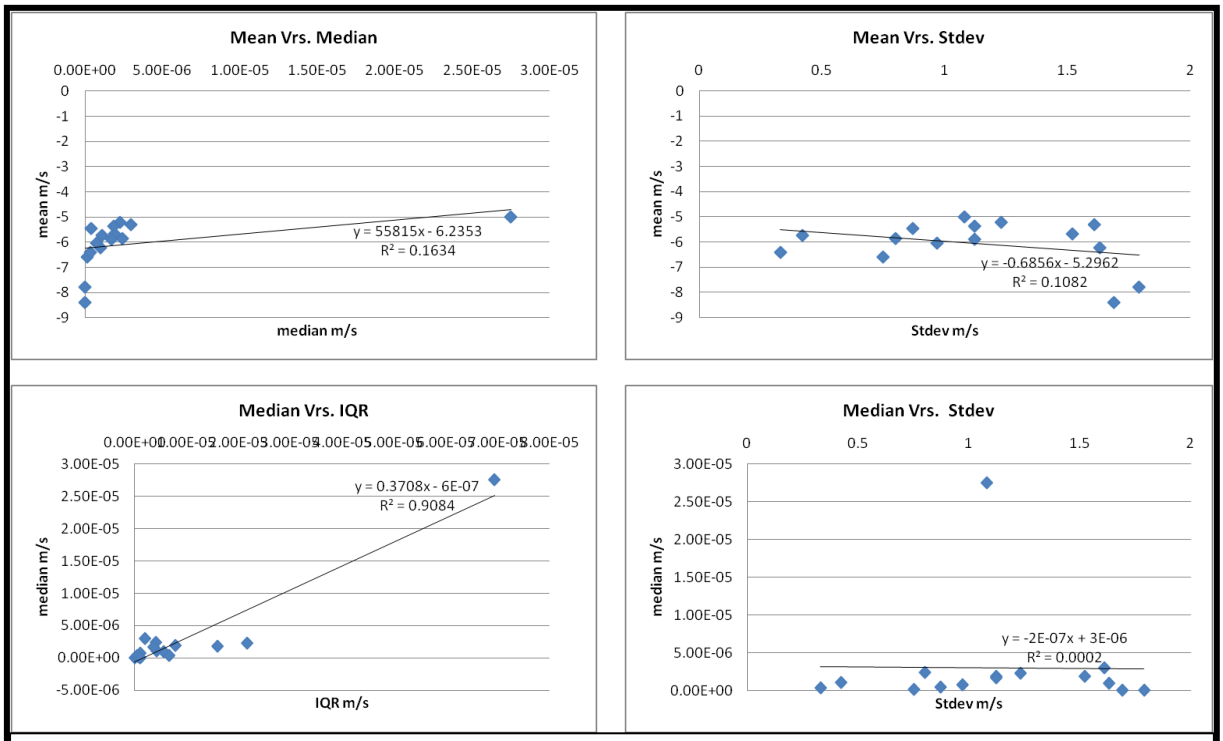

Figure 3.19 Plots of Log N-parameters showing the relationship between central tendency measures and spread measures

3.7.5.3.3 The variation of K with rock type: depth limited

Regression analysis of conductivity values with depth on both the natural and logarithm scale for each of the 15 different rock types have been conducted and presented in Figures 3.20a, 3.20b and 3.20c. The results show a general decrease in hydraulic conductivity with depth for all the different rock types. Analysis of exponential change in Log K with depth (z) (Log K=m e^{cz}) conducted on (tuff-breccia/siltstone) and (sandstone, conglomerate and tuff) gave the maximum and minimum coefficient of determination (r^2) of 0.80 and 0.006, respectively. In most cases the correlation coefficients are low, and the lines fitted are not very good guides to the change in measured K values with depth. It is observed that depth variation is poorly developed at any specific site but with higher K at shallow depths. The high data scatter may be due to the fact that most of the data are obtained from small scale test measurements. The results show that in general the correlation between hydraulic conductivity and rock type is not improved by limiting the investigation to depth.

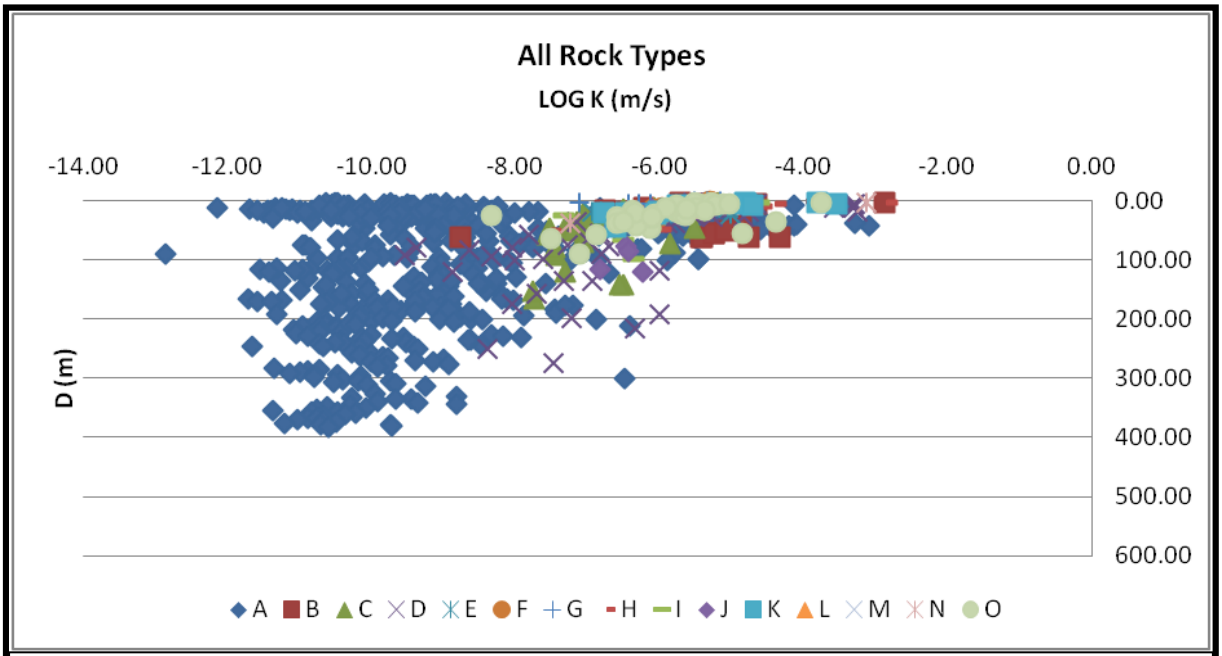

A = *Granite*	**B** = *Mica schist & phyllite*	**C** = *Quartzite*
D = *Sandstone , meta sandstone*	**E** = *Porphyry*	**F** = *Tuff-breccia, tuff-siltstone*
G = *diabase*	**H** = *Greenstone*	**I** = *Meta andesite, meta-rhyollite*
J = Metavolcanic amphibolite	**K** = *Sandstone and shale*	**L** = *Sandstone, tuff & conglomerate,*
M = *Quartz porphyry & granodiorite*	**N** = *Slate, talc- schist, talc- Serpentine*	**O** = *Gneiss*

Figure 3.20a Log-transformed hydraulic conductivity distributions with depth for all rock types yet in a section that is dealing with studies from sites with similar depth intervals

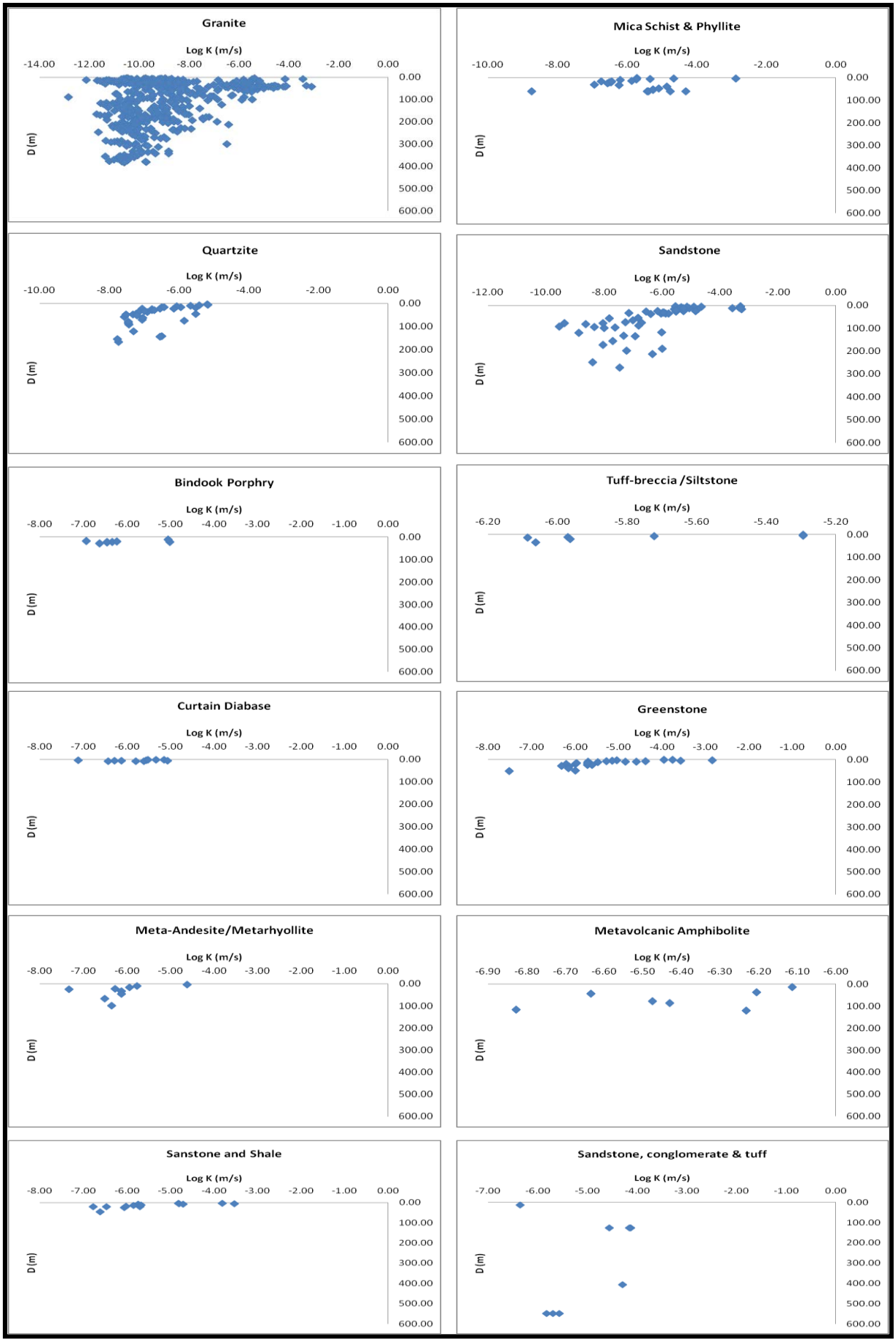
Granite
Log K (m/s)
-14.00 -12.00 -10.00 -8.00 -6.00 -4.00 -2.00 0.00
D (m)
0.00 100.00 200.00 300.00 400.00 500.00 600.00
Mica Schist & Phyllite
Log K (m/s)
-10.00 -8.00 -6.00 -4.00 -2.00 0.00
D (m)
0.00 100.00 200.00 300.00 400.00 500.00 600.00
Quartzite
Log K (m/s)
-10.00 -8.00 -6.00 -4.00 -2.00 0.00
D (m)
0.00 100.00 200.00 300.00 400.00 500.00 600.00
Sandstone
Log K (m/s)
-12.00 -10.00 -8.00 -6.00 -4.00 -2.00 0.00
D (m)
0.00 100.00 200.00 300.00 400.00 500.00 600.00
Bindook Porphry
Log K (m/s)
-8.00 -7.00 -6.00 -5.00 -4.00 -3.00 -2.00 -1.00 0.00
D (m)
0.00 100.00 200.00 300.00 400.00 500.00 600.00
Tuff-breccia /Siltstone
Log K (m/s)
-6.20 -6.00 -5.80 -5.60 -5.40 -5.20
D (m)
0.00 100.00 200.00 300.00 400.00 500.00 600.00
Curtain Diabase
Log K (m/s)
-8.00 -7.00 -6.00 -5.00 -4.00 -3.00 -2.00 -1.00 0.00
D (m)
0.00 100.00 200.00 300.00 400.00 500.00 600.00
Greenstone
Log K (m/s)
-8.00 -7.00 -6.00 -5.00 -4.00 -3.00 -2.00 -1.00 0.00
D (m)
0.00 100.00 200.00 300.00 400.00 500.00 600.00
Meta-Andesite/Metarhyollite
Log K (m/s)
-8.00 -7.00 -6.00 -5.00 -4.00 -3.00 -2.00 -1.00 0.00
D (m)
0.00 100.00 200.00 300.00 400.00 500.00 600.00
Metavolcanic Amphibolite
Log K (m/s)
-6.90 -6.80 -6.70 -6.60 -6.50 -6.40 -6.30 -6.20 -6.10 -6.00
D (m)
0.00 100.00 200.00 300.00 400.00 500.00 600.00
Sanstone and Shale
Log K (m/s)
-8.00 -7.00 -6.00 -5.00 -4.00 -3.00 -2.00 -1.00 0.00
D (m)
0.00 100.00 200.00 300.00 400.00 500.00 600.00
Sandstone, conglomerate & tuff
Log K (m/s)
-7.00 -6.00 -5.00 -4.00 -3.00 -2.00 -1.00 0.00
D (m)
0.00 100.00 200.00 300.00 400.00 500.00 600.00

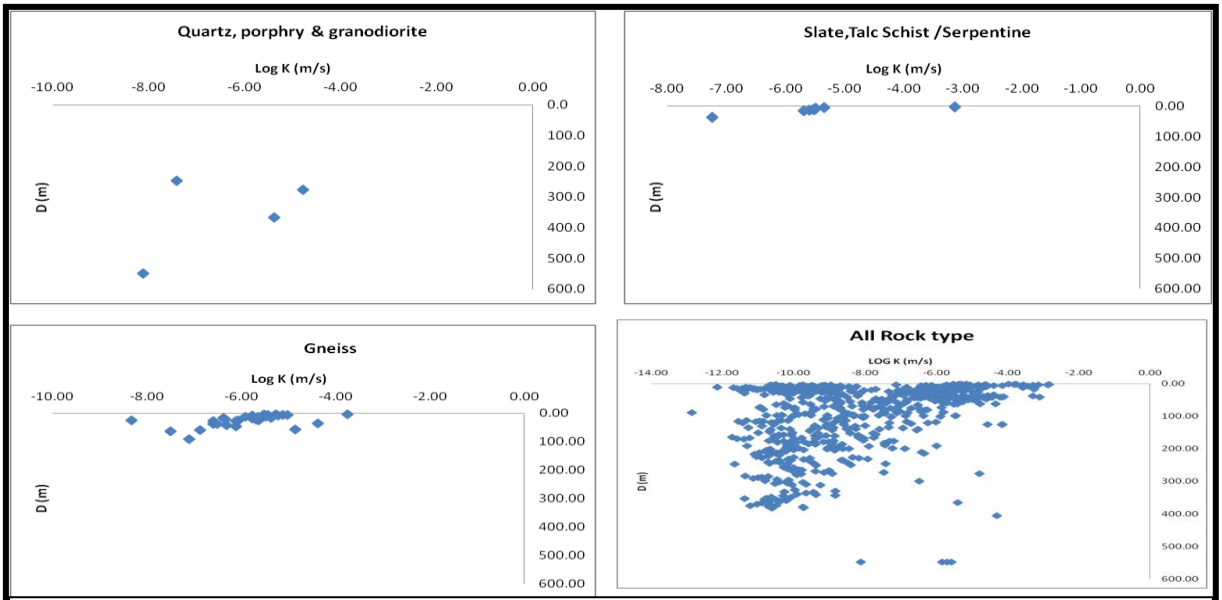

Figure 3.20b Variation of Log transformed of K distribution with depth for each rock type

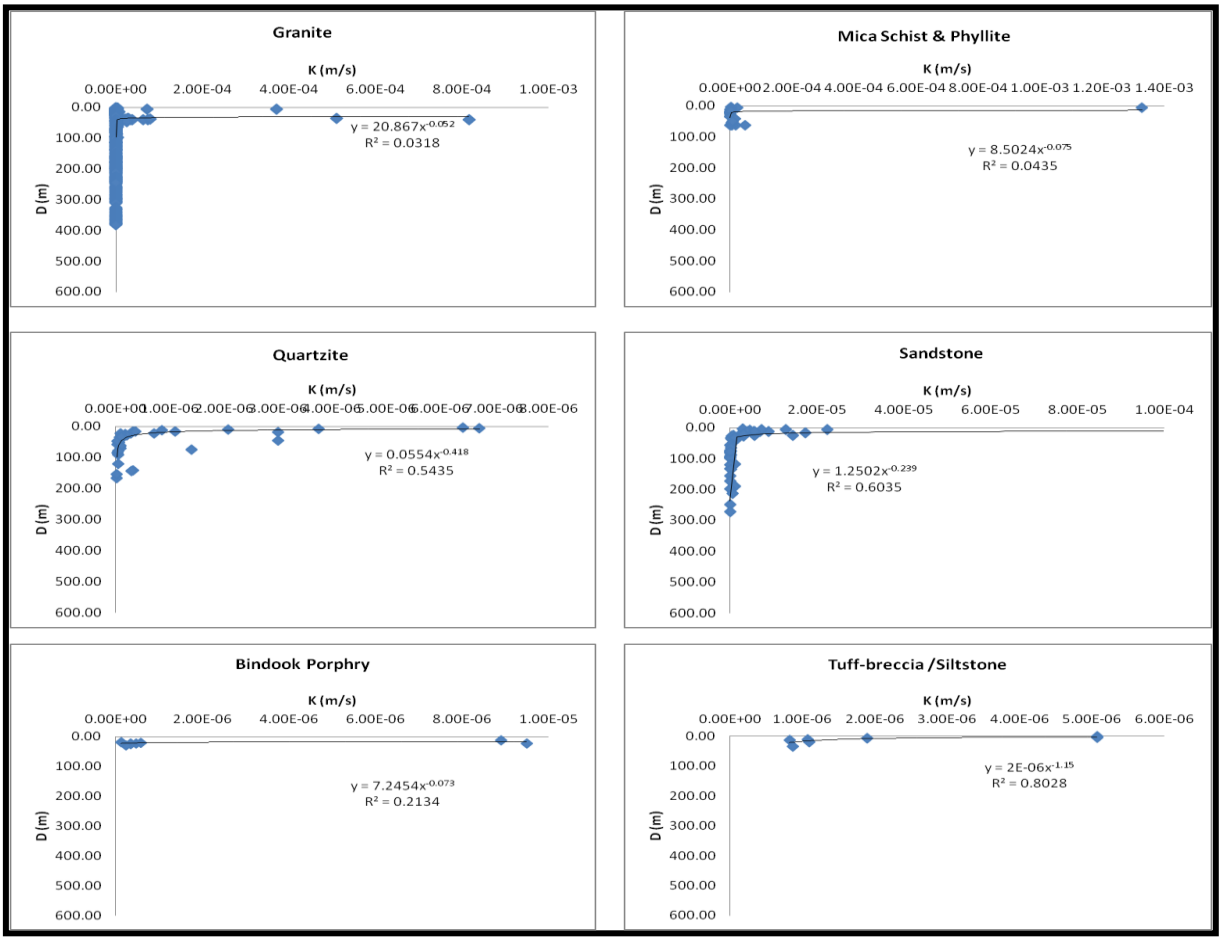

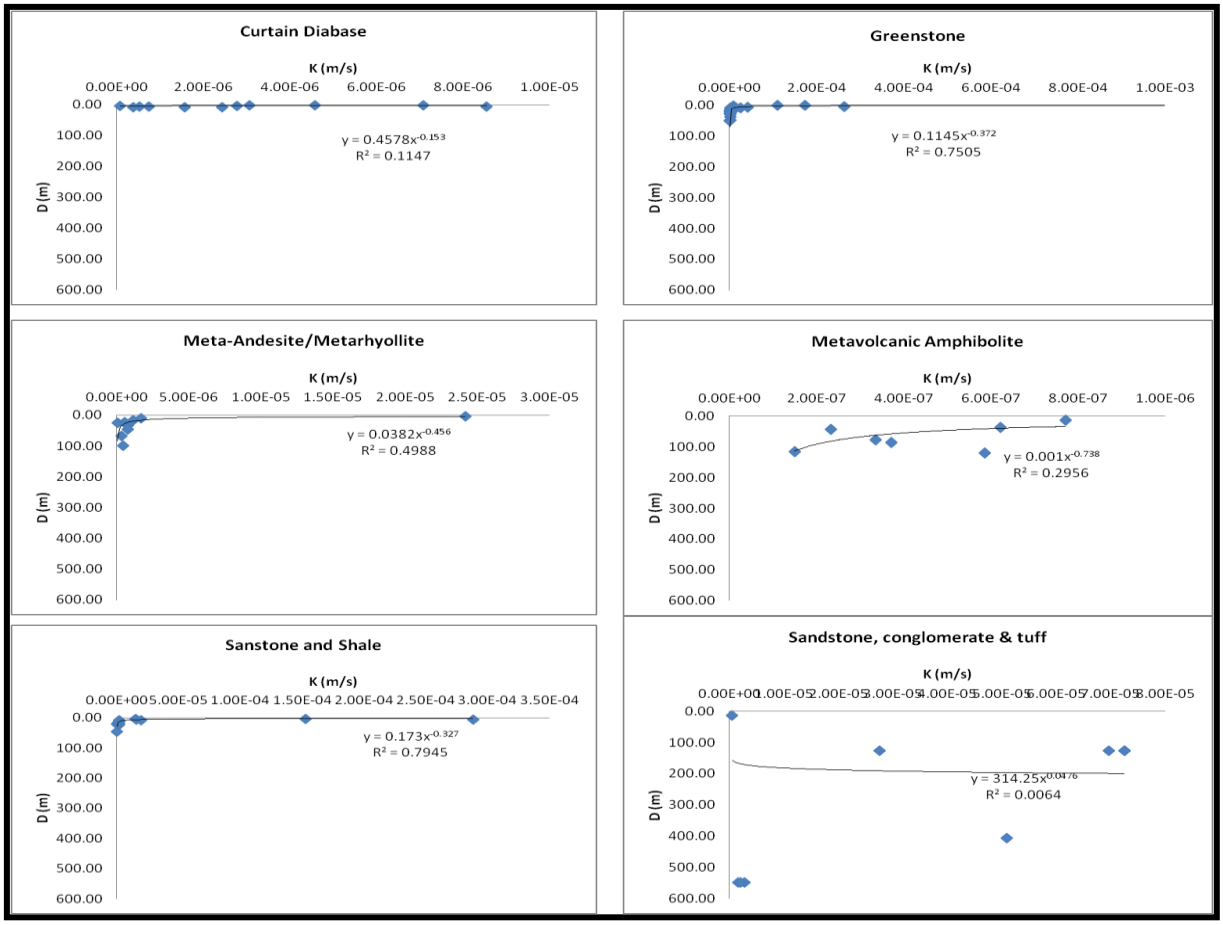

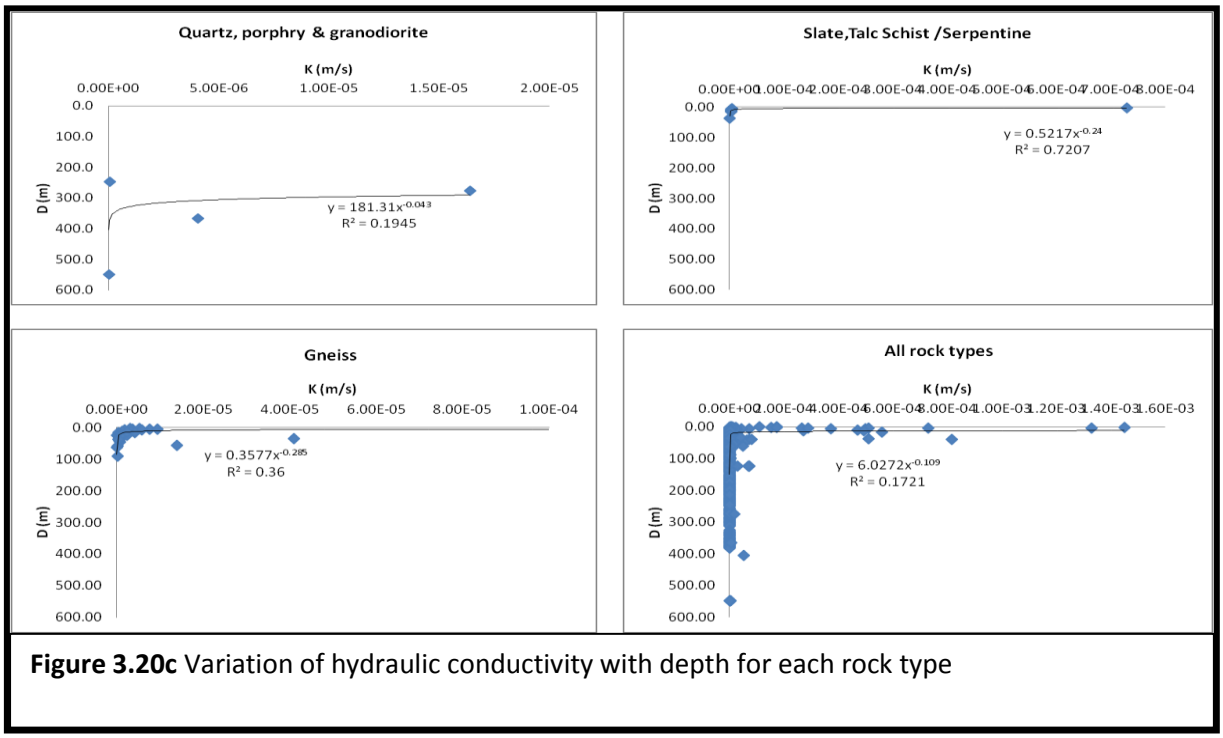

Figure 3.20c Variation of hydraulic conductivity with depth for each rock type

3.7.5.4 The dependence on rock class of K

3.7.5.4.1 Introduction

In this section, the dependence on rock class of conductivity values has been analysed by first of all considering the variation of K values for all rock classes and then limiting the investigation to same depth and climate.

3.7.5.4.2 The variation of K with rock class: for whole dataset

The various rock types are grouped under the three major rock groups or classes; igneous, metamorphic and meta-sedimentary. Figure3.21a presents the relative frequency histogram of K values for each rock class on the logarithmic scale and Table 3.17 and Figure 3.21b summarize and compare statistics obtained for each rock group. Table 3.16 indicates factors relevant to individual rock classes whiles Table 3.18 (in Appendix A-4) show results of summary statistics conducted on the rock classes. Evaluation of plots and Figures indicate variations in K values on the logarithmic scale between the rock groups with the following observations made:

1. The K distribution of igneous rocks has the highest range of values from **1.40E-13** to **8.16E-04** m/s. The distribution is asymmetric with respect to the geometric mean value of **4.55E-09** m/s. The distributions appear to be of bi-modal character and this might due to the fact that the rock formations come from sources of different hydrogeological environments. For instance, some were from sites particularly investigated for deep radioactive waste disposal and other factors which have already been explained in previous sections of this chapter. From Table 3.16 igneous is obtained from different sources and dominated by granite and granite by radioactive waste sites. K-S test conducted on the granitic rocks indicated differences between granites from different studies.
2. Estimates from metamorphic rocks have the least range of K values, from **1.74E-09** to **1.45E-03** m/s; the log K distribution appears almost normally distributed and symmetric with respect to a geometric mean value of **1.49E-06** m/s**.**
3. The Meta-Sedimentary rocks provide data ranging from **2.86E-10** to **5.60E-04** m/s; they are spread and almost symmetric with respect to a geometirc mean value of **8.69E-07** m/s.

In Table 3.17, results of K-S tests conducted on the rock classes show that at 95% confidence level there is a significant differences between Igneous and Metamorphic, and Igneous and meta-sedimentary rocks whereas there is not much significant difference between Meta-sedimentary and Metamorphic rocks. It should be noted that differences among K distribution of different rock classes of different studies are influence not only by differences in the weathering processes but also differences in the methods used to measure K in the different studies examined, and the purposes for which the studies were conducted. Also there is not much change in the measurements of spread and central tendencies indicating weak relationship between rock classes. Thus from above analysis we can conclude that rock classes are seen not to be a major factor influencing variation in K distribution.

Table 3.16 Factors relevant to individual rock classes

Rock class	Factors			
	Purpose for K Studies	Test type	Depth interval (m)	Climate
Igneous	Water resources, Mine inflow Studies, Grouting at dam and tunnel sites, Hydrauli testing, Rad waste	Pumping test, Specific Capacity test, packer/drill stem test, slug/pulse test,	1 -549	Temperate, Mediterranean, Tropical and Semi arid
Metamorphic	Mine inflow, Water resources studies	Specific Capacity, slug/pulse Packer/Drill stem test	2 - 165	Semiarid, Tropical and Temperate
Meta-Sedimentary	Water supply, Water resources studies	packer/drillstem, slug/pulse, Specific capacity test	2 - 549	Semiarid and Tropical

Table 3.17 K-S Test for differences in rock classes

Rock Classes	D statistics	P values	Significance at 95% confidence level
Igneous and Metamorphic	0.76	0.00	Yes
Igneous and Meta-Sedimentary	0.68	0.00	Yes
Meta-Sedimentary and Metamorphic	0.14	0.23	No

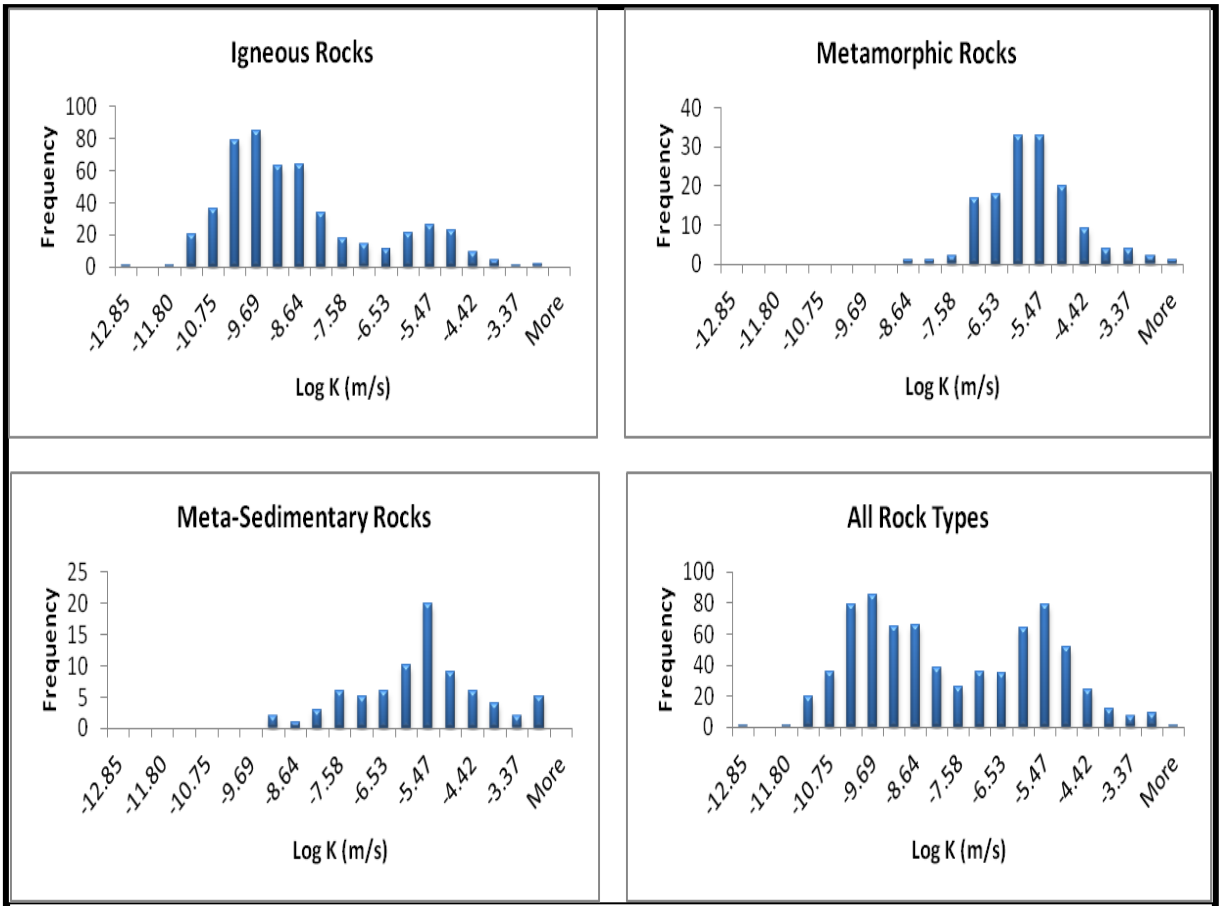

Figure 3.21a Histogram of log of hydraulic conductivity (K) for each rock class (I M & S)

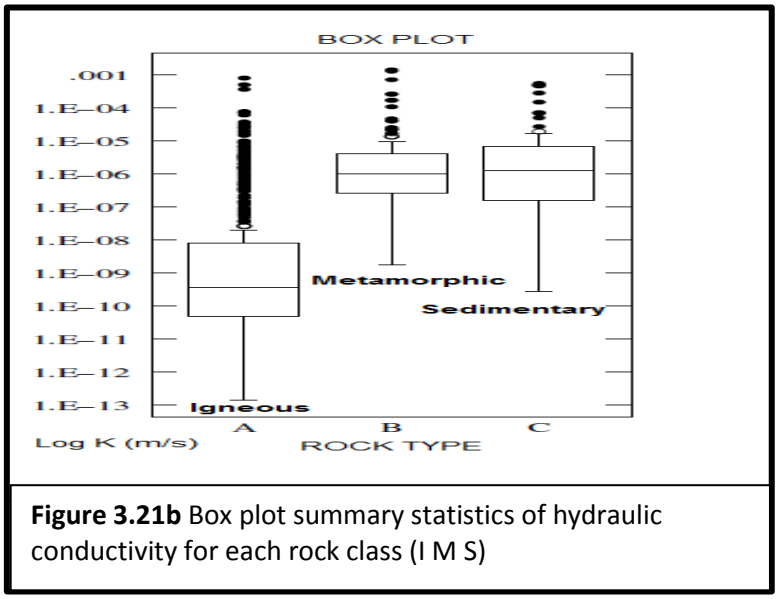

Figure 3.21b Box plot summary statistics of hydraulic conductivity for each rock class (I M S)

3.7.5.4.3 The variation of K with rock class: depth limited

K-S Test results of rock classes (Igneous, metamorphic and meta-sedimentary) for the top 100m depth range at 20m depth intervals is shown in Table 3.19. Although, at 95% confidence level almost all the different rock classes are different in the top 100m depth interval, very close examination of the D-statistics (0.30-0.82) reveals that there isn't much variations in K distribution with the rock classes. Thus the observed variations in rock classes might have come from weathering differences between different classes of rocks.

Regression analysis of conductivity values with depth for all rock classes, and on both the natural and logarithm scale for each of the three different rock classes have been conducted and presented in Figures 3.22a, 3.22b and 3.22c respectively. Analysis of exponential change in Log K with depth (z) in the form $\text{Log } K = m\, e^{C z}$ conducted on metamorphic/depth and igneous/depth relationships gave the maximum and minimum coefficient of determination (r^2) of 0.44 and 0.06, respectively. In most cases the correlation coefficients are low, and the lines fitted are not very good guides to the change in measured K values with depth. It is observed that depth variation is poorly developed at any specific site but with higher K at shallow depths. The high data scatter may be due to the fact that most of the data are obtained from small scale test measurements and weathering difference between rock classes. The results show that in general the correlation between hydraulic conductivity and rock type is not improved by limiting the investigation to depth.

Table 3.19 K-S Test results of the rock classes (Igneous vs. metamorphic vs. meta-sedimentary) for the top 100m depth range at 20m depth intervals

Rock classes	Depth intervals (m)	D statistics	P value	Significant at the 95% confidence level
Igneous vs. metamorphic	(0-20)	0.81	0.00	Yes
Igneous vs. meta-sedim		0.82	0.00	Yes
Metamorphic vs. meta-sedim		0.17	0.52	No
Igneous vs. metamorphic	(0-20) and (20-40)	0.65	0.00	Yes
Igneous vs. meta-sedim		0.68	0.00	Yes
Metamorphic vs. meta-sedim		0.64	0.00	Yes
Igneous vs. metamorphic	(20-40) and (40-60)	0.31	0.12	Yes
Igneous vs. meta-sedim		0.40	0.1	Yes
Metamorphic vs. meta-sedim		0.33	0.28	Yes
Igneous vs. metamorphic	(40-60) and (60-80)	0.74	0.00	Yes
Igneous vs. meta-sedim		0.49	0.03	Yes
Metamorphic vs. meta-sedim		0.31	0.57	No

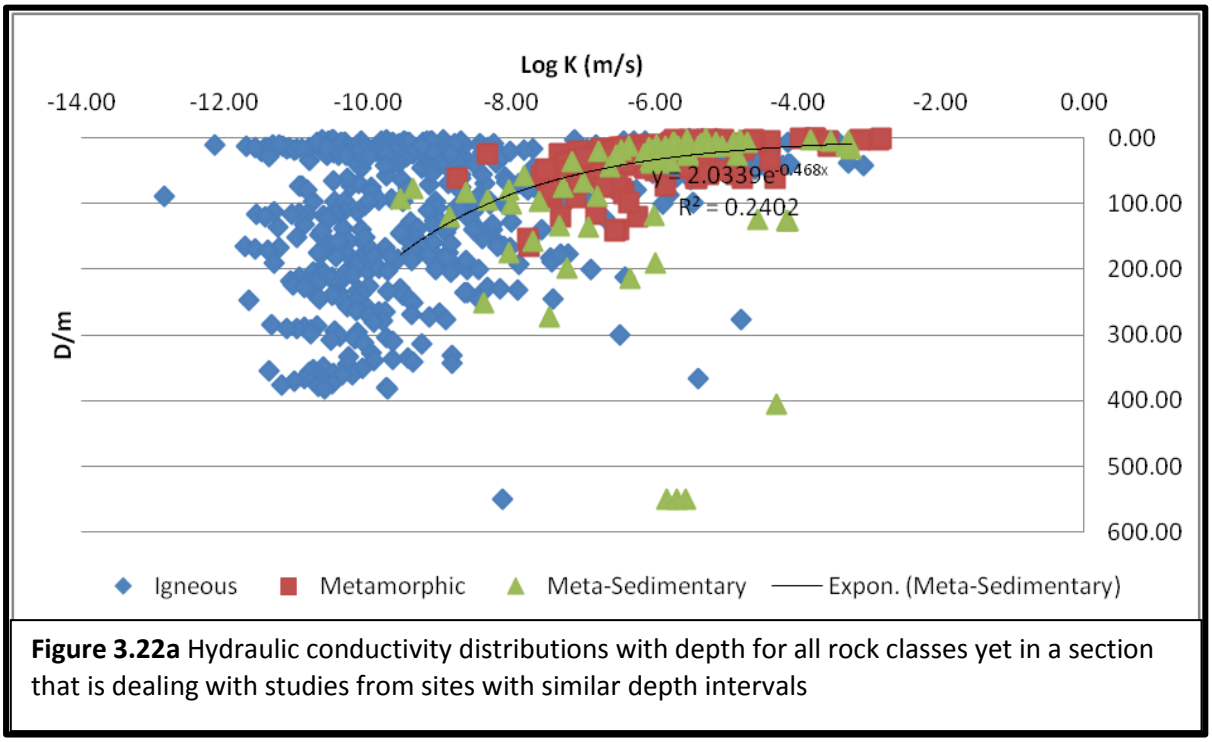

Figure 3.22a Hydraulic conductivity distributions with depth for all rock classes yet in a section that is dealing with studies from sites with similar depth intervals

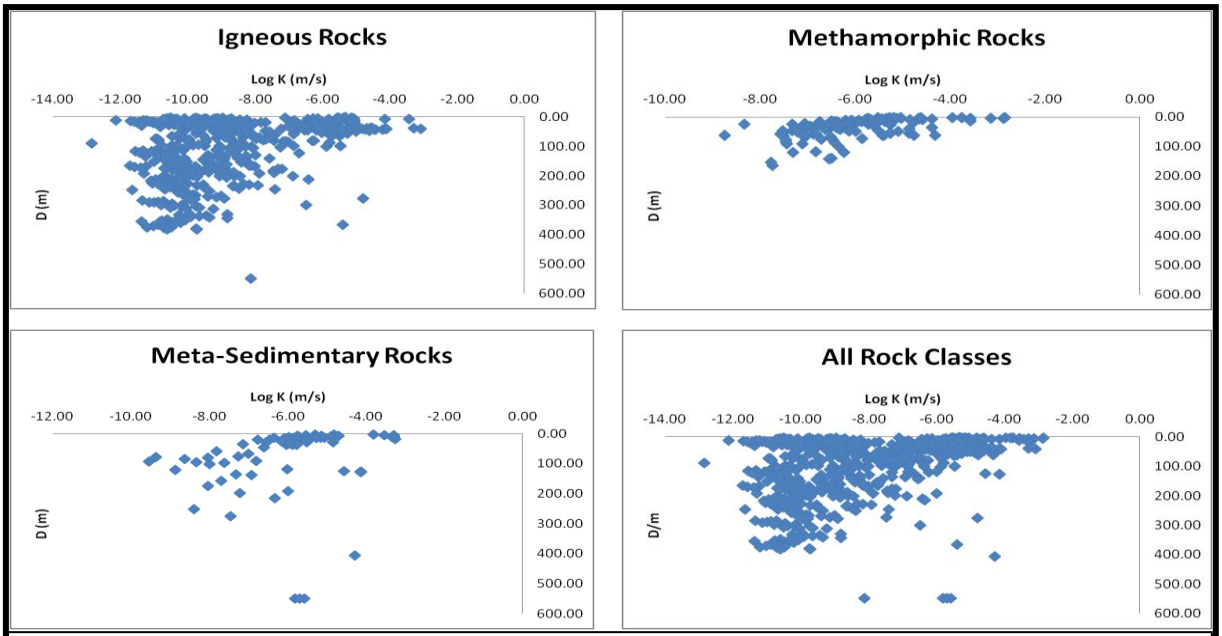

Figure 3.22b Variation of Log of hydraulic conductivity with depth for each rock class

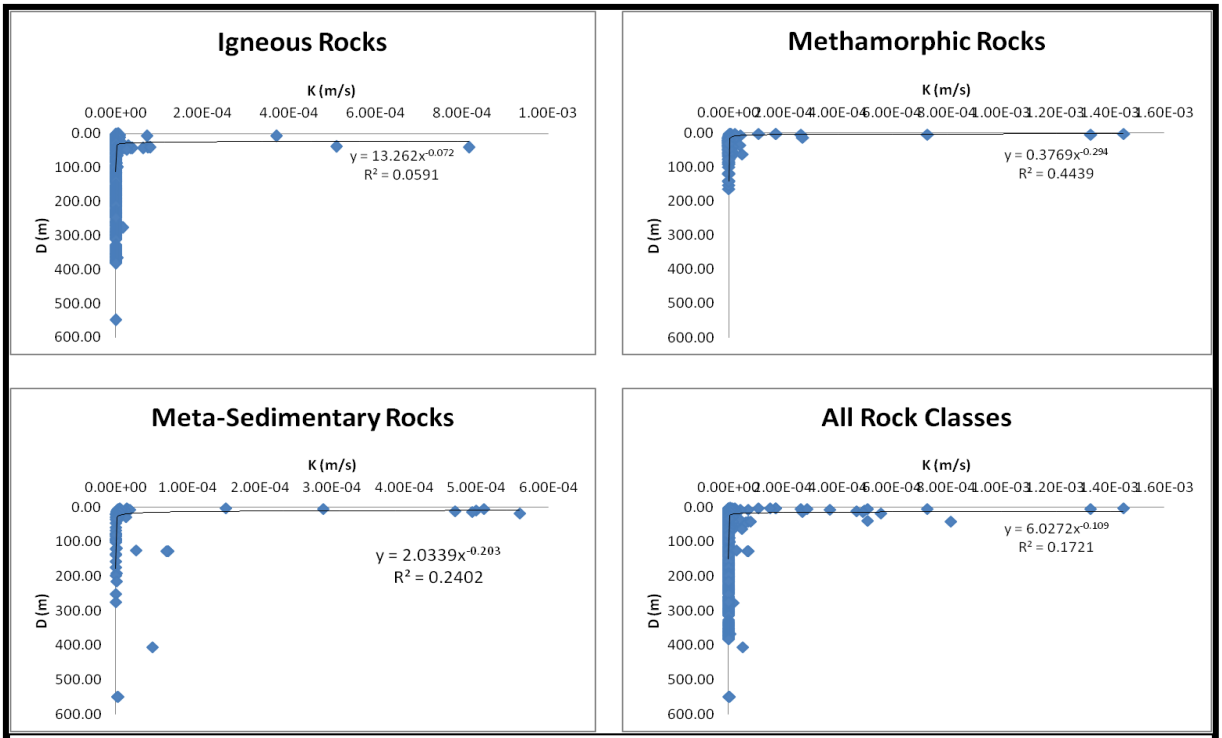

Figure 3.22c Variation of hydraulic conductivity with depth for each rock class

3.7.5.5 The dependence on climate of K

3.7.5.5.1 Introduction

In this section we have analysed spatial variability of K (central tendency and spread) in different climatic conditions (Tropical, Temperate, Mediterranean, Semi-arid and Sub-arctic). The analyses have been conducted by first of all considering the variation in K values of all dataset and then limiting to depth, rock type and, rock type and climate where possible.

3.7.5.5.2 The dependence on climate of K: for whole dataset

The variability of hydraulic conductivity in five climatic regions of the world has been analysed. Evaluation of plots and Figures of hydraulic conductivity values indicate variation in K trend among the different climates. Figure 3.23a reports the relative frequency histogram of K values for each climate on the logarithmic scale. Figure 3.23b and Table 3.20 (in Appendix A-5) summarize and compare statistics of K values obtained for each climate. The following are some general observations made from the tables and Figures as mentioned above:

1. The Semi-arid climatic region has distribution of K values which ranges from **4.65E-09** to **1.45E-03** m/s. The distribution is symmetric with respect to a geometric mean value of **2.56E-06** m/s
2. The K distribution of the Tropical climate ranges from **2.86E-10** to **4.73E-05** m/s. It is spread and symmetric with respect to the geo-mean of **1.66E-07** m/s)
3. The K distribution of the temperate climate ranges from **1.40E-13** to **6.80E-06** m/s. It is asymmetric and skewed to higher conductivity values with respect to the geo-mean value of **5.54E-10** m/s
4. The distribution from Sub-Arctic climatic region ranges from **2.60E-08** to **3.60E-07** m/s. It is asymmetric with respect to the geo-mean value of **1.27E-07** m/s and it has the least sample values.
5. The Mediterranean climatic region has distribution of K values, ranging from **4.65E-09** to **1.45E-03** m/s. The distribution is symmetric with respect to geo-mean value of **6.12E-10** m/s

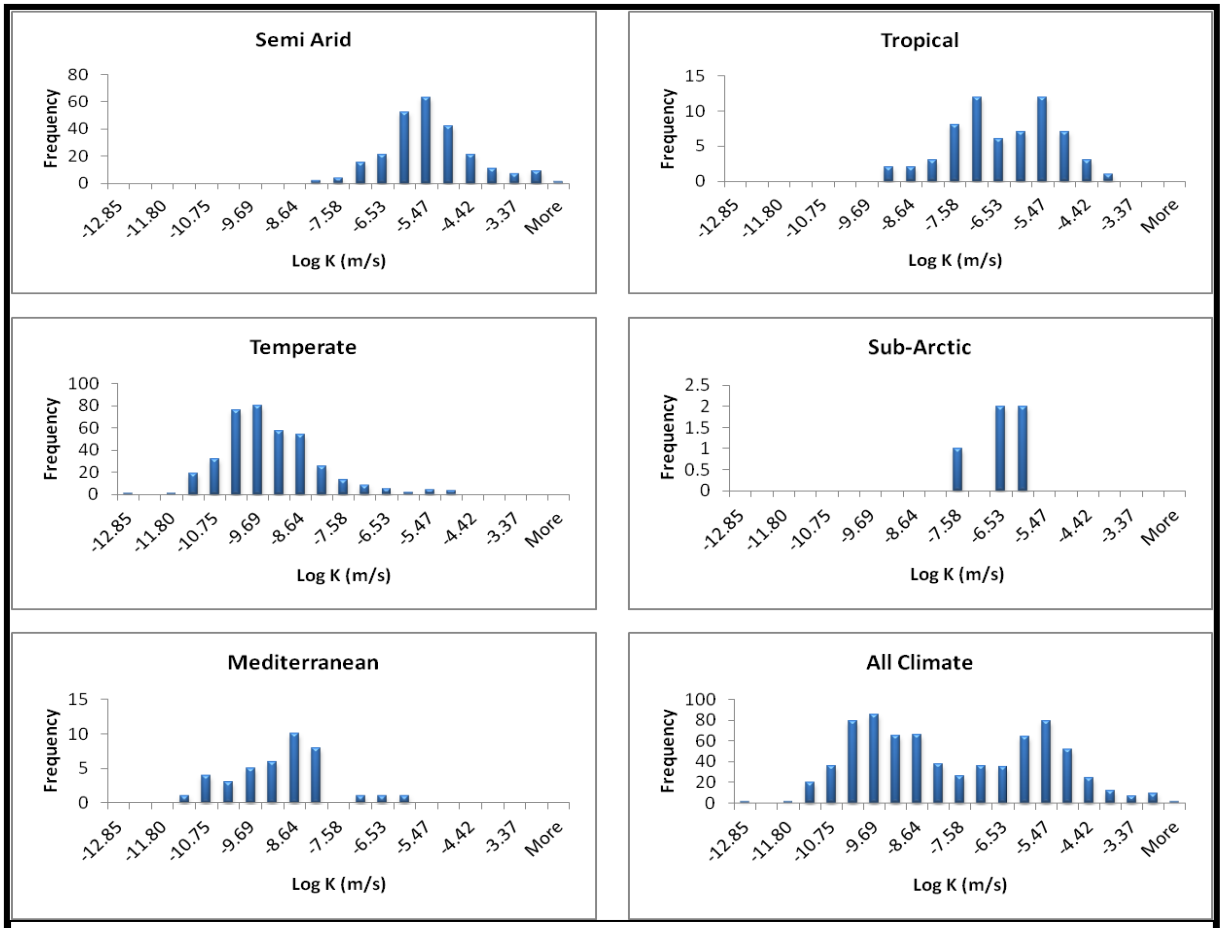

Figure 3.23a Histogram of log of hydraulic conductivity (K) for each climate

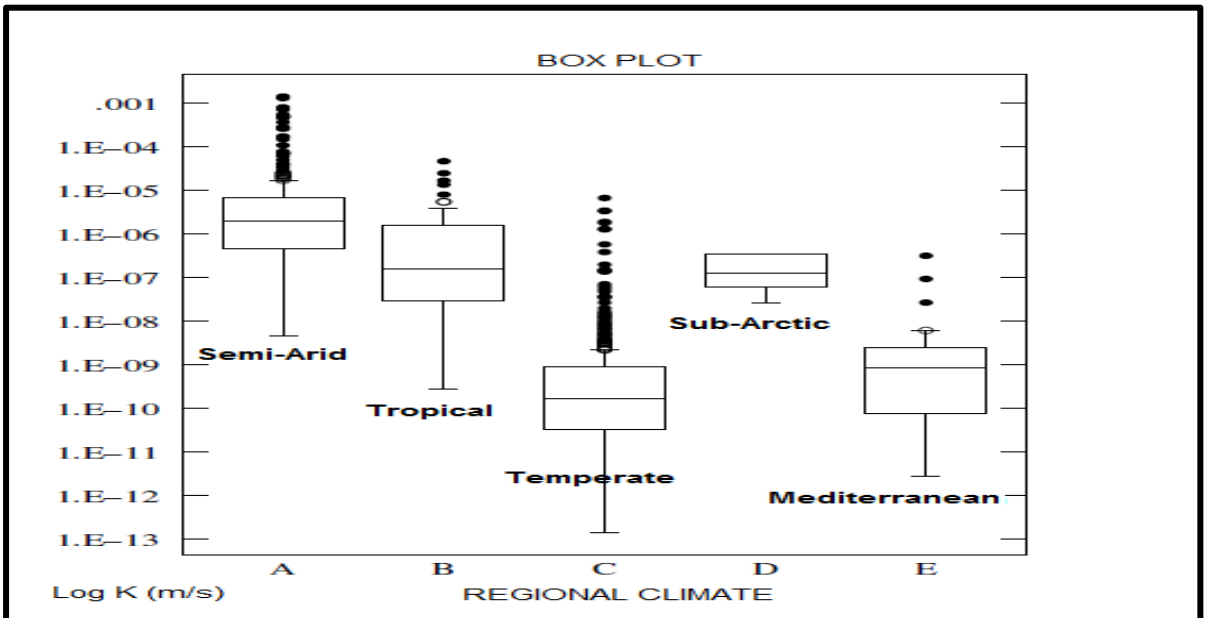

Figure 3.23b Box-and-whisker plots of summary statistics of log hydraulic conductivity (K) for each climate

3.7.5.5.3 The variation of K with climate: depth limited

In this study, regression analysis of conductivity values with depth for all climates zones and each of the five climate zones on both the natural and logarithm scale are presented in Figures 3.24a, 3.24b and 3.24c. The results show a general decrease in hydraulic conductivity with depth for all the different climates with a great deal of scatter. However, it must be emphasized that by limiting the investigation to local sites of similar climate and geology, the relationship with depth appear different, and that the dataset is characterized by a great deal of scatter (Figures 3.24b and 3.24c). Pearson regression analysis for power relationships of the form Log K=m (e) ^{CZ} conducted in the Tropics and in the Temperate climates gave a maximum and the minimum coefficient of determination (r^2) of 0.44 and 0.06, respectively. It is observed that depth variation is poorly developed at any specific site but with higher K at shallow depths. The high data scatter may be due to the fact that most of the data are obtained from small scale test measurements and also weathering differences of the different climates zones. The main factors likely to affects K, including geology and tectonic regime, are likely to be constant at each site. Thus, the relationship between depth and K should be strongest for individual sites. However, in general by limiting K (z) relationship to sites of similar geology and depth did not improve variation in K distribution.

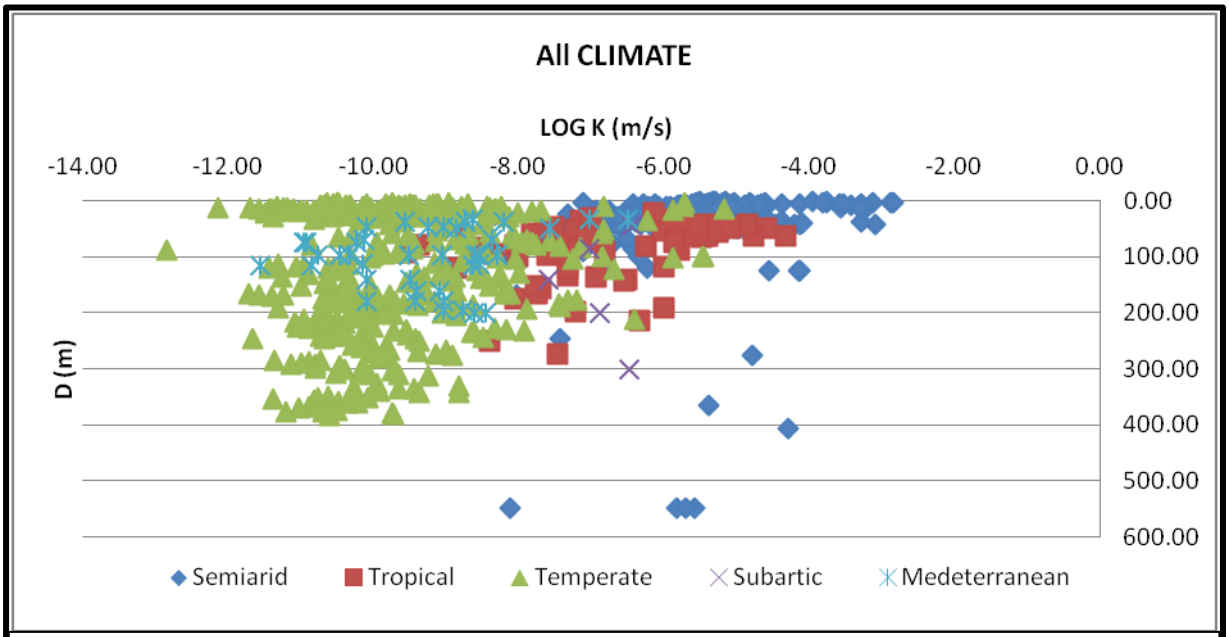

Figure 3.24a Variation of Log transformed hydraulic conductivity with depth for all climates yet in a section that is dealing with studies from sites with similar depths

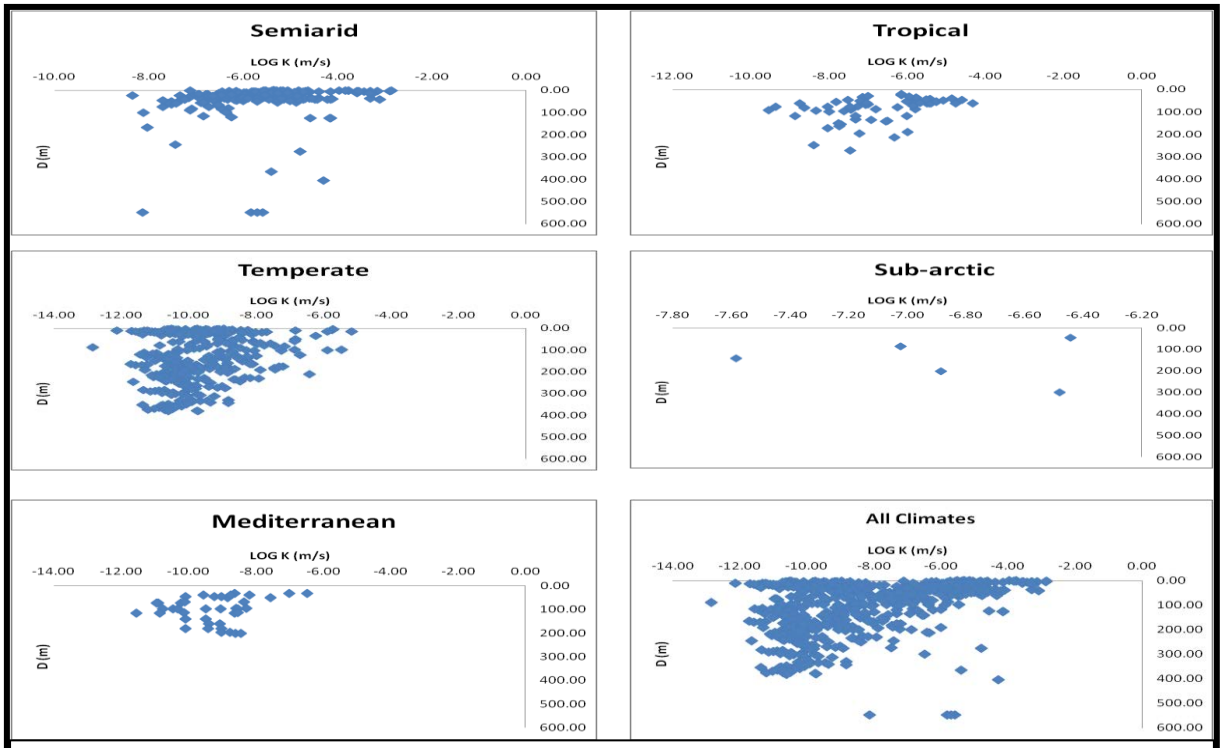

Figure 3.24b Variation of Log transformed hydraulic conductivity with depth for each climate

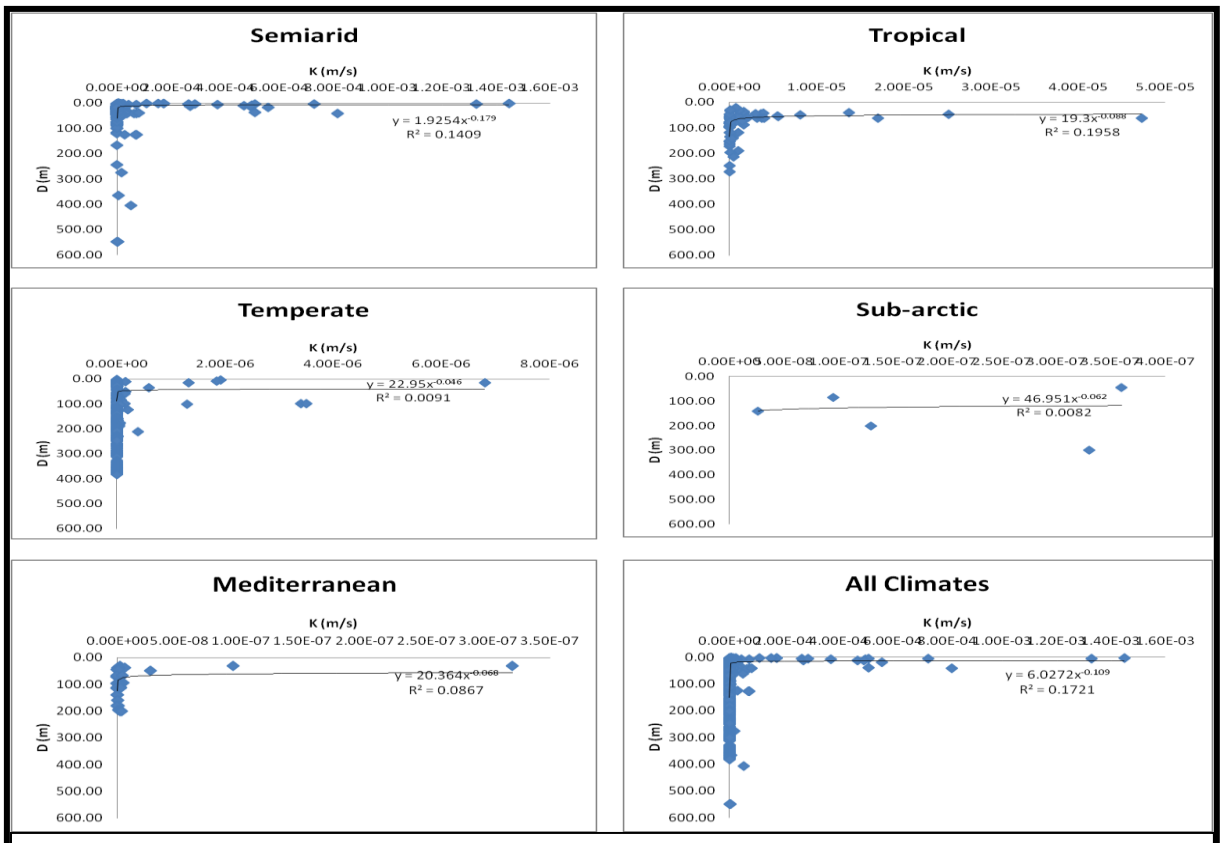

Figure 3.24c Variation of hydraulic conductivity with depth for each climate

3.8 Summary and discussion of findings

3.8.1 Introduction

In this summary, we focus on the characterisation of hydraulic conductivities estimated from more than 768 aquifer tests from 12 different studies conducted by various groups of researchers on hard rock aquifer worldwide, as has been presented so far in this study. The purpose for the estimates was to determine distributions of hydraulic conductivity of hard rock aquifers for use in the simulation of regional groundwater flow, as part of the investigation of potential impacts of open cast mine on the regional groundwater flow system. The summary presented for this chapter is based on the following themes:

1. Conceptual model for K distribution at a site :
   (a) K(z) relationship and (b) Fracture connectivity
2. K values based on whole dataset (global average).
3. Constraining universal K distribution and distribution parameters for site-specific purpose by the following factors: depth, rock type, rock class and climate.

3.8.2 Conceptual model for K distribution at a site: K(z) relationship and fracture connectivity

The spatial variability of all dataset and a couple of sites for which good depth data with similar geology and climate exist was characterised and analysed. As expected in a fractured aquifer system, K decreases with depth (Figure 3.11 and 3.12), though the scatter is often very large, even when data from an individual site is considered (Figure 3.17). An exponential relationship between K and depth appears to be as good as any.

Results from K-S tests on the whole data set (Table 3.10 and 3.11) show that at a 95% confidence level there is a significant difference in the mean value of K distribution with depth between the first and second 200m depth interval. Also, a plot of mean log K (m/s) values against depth interval (m) (Figure 3.14a) shows a decrease in K with depth to about 300m over a scale of three orders of magnitude after which there seems to be no significant difference in K distribution up to 400m depth. The decrease of permeability with depth may be used as indication measure of the extent of fracture variation and connection in hard rock aquifer systems. In the current study it is observed from the data analysis that fractures and connectivity are most abundant in the upper 300m. Hence, conclusions can be drawn

from the analysis that conceptually, K decreases exponentially with depth from the surface of the aquifer up to 300m. Beyond this depth, K remains approximately constant at this scale for at least the next 100m.

At the shallowest levels K is affected by weathering, with often greater K values being recorded (Table 3.2), at least in the moderately weathered, middle depth section of the weathered zone (e.g. Acworth, 1981). In Ghana, especially in the Tarkwaian rock system (Figure 3.2) the weathering zone depth is typically of around 20m (Kortatsi 2004), though it can vary from less than 1m to at least 100m (Singhal & Gupta, 1999). Typically at open pit mines, the least stable material at the top of the opening will be removed so that the slope in the weathered material is set back from the main face.

Section 3.5.2.3 discusses the effect on apparent borehole K measurements of fractures with limited regional connectivity, and suggested that measured K values may be greater than the regional K (patchy aquifer concept). This model of limited distance connectivity could also affect the flows around a mine, i.e. the borehole in Figure 3.5 could as easily represent a mine. In addition, the local permeability around a mine may be increased by blasting. Figure 3.25 illustrates an extreme version of this effect. The impact of this phenomenon is uncertain, but is unlikely to extend far beyond the pit and might be taken into account simply by considering an effective pit radius.

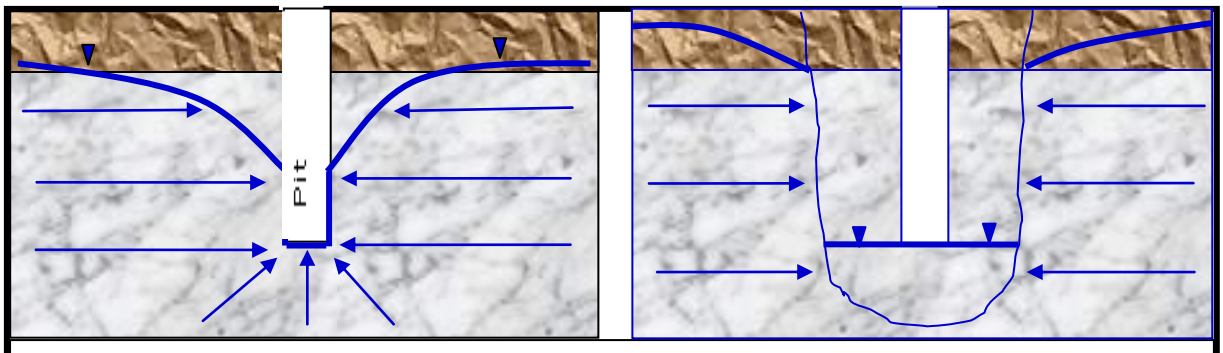

Figure 3.25 Two possible flow configurations of the dewatering effect in a regionally connected flow model (left) and a locally connected flow model (right) in a double layer (weathered zone over fractured bedrock) aquifer system. In this extreme case, K for the connected zone is much greater than K for the regional flow in the bedrock, and all flow from the weathered zone passes down through the bedrock to the pit.

Based on the considerations discussed above, Figure 3.26 summarises a conceptual model for the system and a number of possible flow systems.

The weathered zone is of limited thickness, and its most permeable levels have been removed and taken back from the main slope face. The pit induces a drawdown, typically with a base elevation at up to several 100 m. The water level in the bedrock is drawn down by the low elevation of the pit base. This induces leakage from the weathered zone, if present with the following flow characteristics:

- Greatest leakage will occur from the weathered zone.
- In some cases, as shown, the WZ will develop a perched water table. This may reach the pit slope, and in this case a seepage face will develop
- In other cases leakage will be enough so that the water table does not reach the slope face
- In yet other cases (not illustrated), the piezometric surface for the bedrock may lie within the WZ

Hydraulic conductivity varies with depth (see graph in figure) at the topmost levels, but below the soil, in the weathered zone complete weathering to clay may have resulted in moderate K with higher K in the deeper zone. In the bedrock, K decreases roughly exponentially, and has reached very low levels by the base of typical pits. This means that flow is greater in the upper part of the bedrock, and probably is very limited into the base of a typical pit. To this end it is reckoned that K anisotropy may be important, and could be at any angle.

In all cases (Figures 3.25 and 3.26), recharge will occur across the area, including directly into the pit. The amount of recharge entering the bedrock will depend on the head difference between the WZ and the bedrock, though the rate will reach a maximum if the bedrock piezometric surface falls below the base of the WZ.

Figure 3.27 includes a representation of a possible zone of connection of fractures around the pit. This may have the effect of slightly extending the effective diameter of the pit. In an

extreme case, water may be able to flow from the WZ down through the higher K connected zone and into the pit.

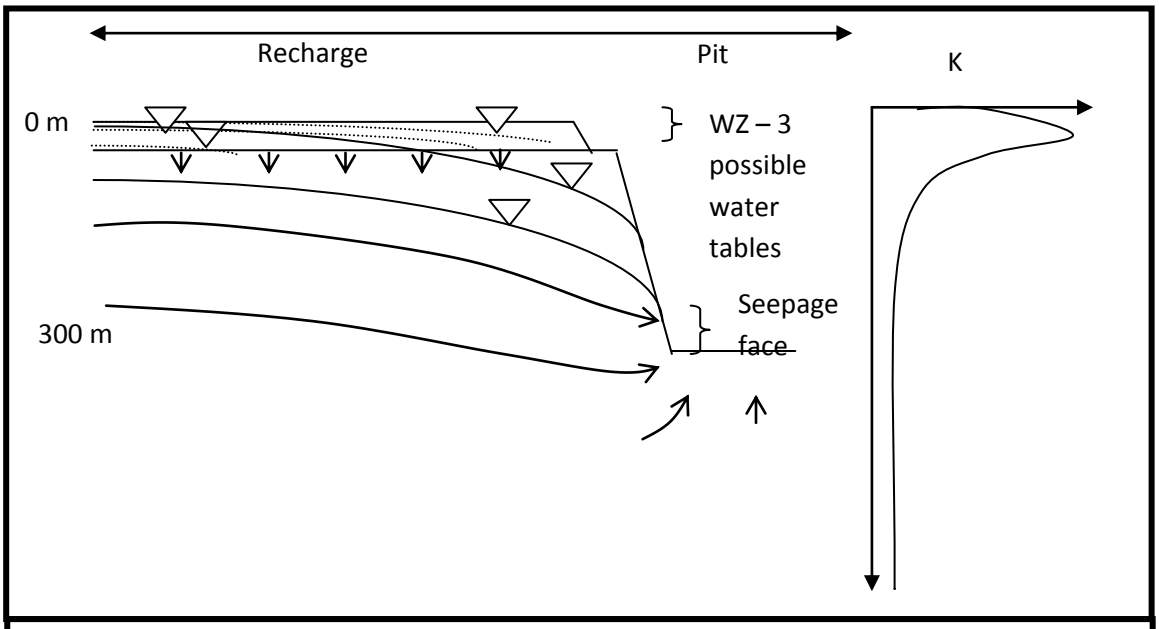

Figure 3.26 Vertical cross sectional profile of conceptual model showing the three possible water tables in the weathered zone (WZ) and two possible piezometric surfaces in the bedrock.

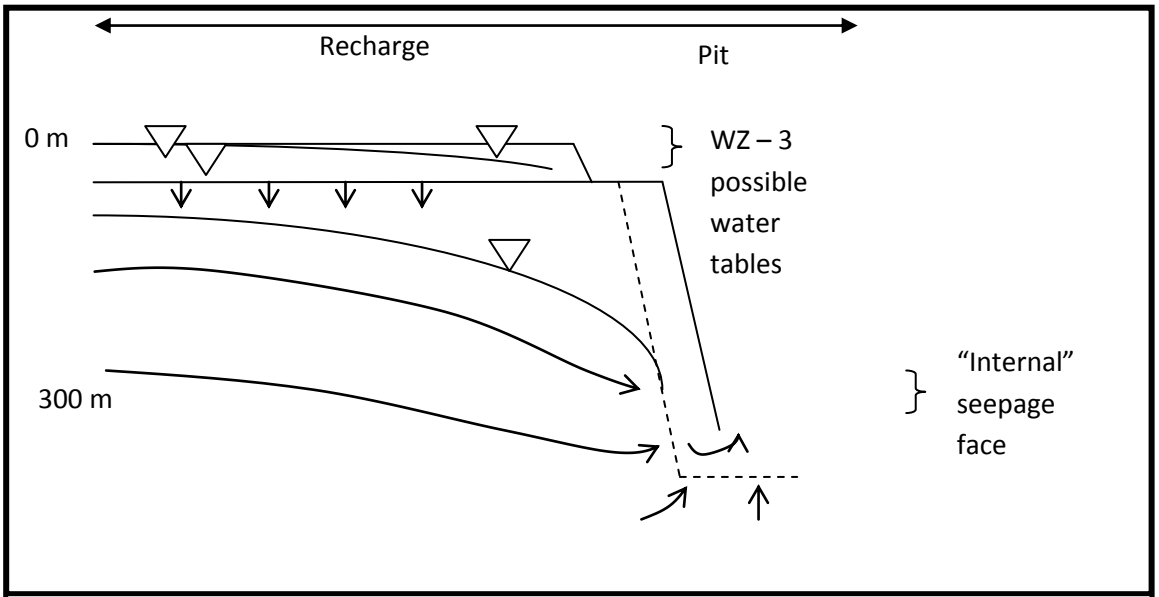

Figure 3.27 Vertical cross section of Figure 3.26, but with "connected zone" around pit included. WZ is weathered zone.

3.8.3 K values based on whole dataset

The main aim of this chapter has been to collate data from literature that would help in determining values for K for a given hard rock system. The first step in doing this has been to consider all the data available, irrespective of rock type, climate, tectonic regime, depth or purpose for which the K values have been obtained, or method of K measurement.

The K frequency distribution for the whole dataset has the following characteristics: asymmetric, spread and skewed to lower conductivity values, as shown in Figure 3.7b. Transformation to log K values makes the distributions much more normally distributed, but in the case of the whole dataset together, exhibits a bi-modal character consisting of two log-normal distributions (see Figure 3.7a). To this end, we conjecture that the bi-modality is probably due to differences in weathering degree of the rocks and the dominance of the two main types of studies from which data extracted may have contributed to such biasing (e.g., choice of very low conductivity sites for nuclear waste disposal and much high conductivity from dam and tunnel sites for grouting and water supply purposes).

Also, we reckon that estimates of universal hydraulic conductivities on the natural scale that could be used in generic calculations around mines, range from **1.40E-13m/s** to **1.45E-03m/s**. At 95% confidence interval for the actual mean, most of the data are estimated to lie within the range of **7.71×10^{-06}** to **2.18×10^{-05}** m/s. The representative geo-mean, median and the standard deviation are estimated to be **1.57×10^{-08}** m/s, **3.80×10^{-09}** m/s, and **9.74×10^{-05}** m/s respectively (Table 3.6). The geometric mean is three orders lower than the arithmetic mean. The difference between the mean and median reflects the non-normal nature of the distribution.

3.8.4 Constraining universal K distribution for site-specific purpose

However, by limiting the investigation to sites of similar geology and climate, the relationship with depth was found to be variable and characterized by a great deal of scatter. It was observed that depth variation is poorly developed at any specific site but with higher K at shallow depths. The high data scatter may be due to the fact that most of the data were obtained from small scale test measurements and also due to weathering differences of rock types. The main factors likely to affect K, including rock type, climate and

tectonic regime, were also investigated to see if they could be used to limit the range of possible K values at any given site. It was found that limiting data to similar rock type, similar climate, or similar tectonic regime did not constrain K ranges.. Hence the combined dataset was used to represent international dataset and also used for all the calculations.

CHAPTER 4

CHARACTERISATION OF POTENTIAL DIRECT RECHARGE

4.1 Introduction

Rushton and Ward (1979) define groundwater recharge as the amount of surface water that reaches the permanent water table. In order to determine the impact of surface mining on the regional groundwater flow systems, a value for recharge is required. This chapter therefore aims at determining the potential recharge rate for use in subsequent numerical modelling experiments. Potential recharge here is defined as the likely recharge in cases where the water table is deep enough that it no longer has an influence on the recharge rate. This is interpreted to mean that the recharge process can be estimated assuming that the flow in the unsaturated zone is freely draining (see Section 4.4). This rate is effectively a maximum rate, as in some cases the inability of groundwater to flow away fast enough will mean that recharge will be rejected. This is further discussed under groundwater flow modelling (Chapter 5). Recharge is a region-specific property, and thus work will concentrate on the Tarkwa mining district of South western Ghana, though the approach should also be applicable elsewhere. In addition, it is also aimed to establish an empirical relationship between potential groundwater recharge and precipitation that could be used for future predictions.

Since data for the study are limited, the HYDRUS-1D computer code has been used to analyze variability of precipitation recharge for the various soil types in the study area in response to rainfall and evapotranspiration. HYDRUS-1D computer code is chosen for this analysis because of its advantage of dealing with hydrological complexities, and the derivation and estimation of water budgets and fluxes. HYDRUS-1D is widely accepted to represent the soil water physics in both research and engineering communities and extensively verified by comparing model results with available field data, analytical solutions, and with other numerical models for water flow (e.g., Hernandez et al., 2003; Simunek and van Genuchten, 1999; Shah et al., 2007). In the following sections, the materials and methods used, the physical modelling process, the modelling results and discussion, and the summary and conclusion have been discussed in section 4.2, 4.3, 4.4, and 4.5 respectively.

4.2 Method and Approach

4.2.1 Introduction

Reviews of potential recharge assessment include (Rushton, 1988; Gee and Hillel, 1988; Allison et al., 1994; Scanlon et al., 2002; de Vries and Simmers, 2002). According to these researchers, recharge assessment can be based on a wide variety of models which are designed to represent the actual physical processes. The suitability of an approach or method depends on the scale and conceptualisation of the flow system as well as the level of accuracy required and crucially, on the available data. The various approaches that are usually used to estimate natural groundwater recharge include:

1. Inflow estimation (soil moisture budgets, unsaturated zone modelling, direct measurement; lysimeters).
2. Aquifer response analysis (analysis of groundwater level hydrographs; through-flow analysis).
3. Outflow estimation (baseflow analysis from suitable located gauging stations; concurrent flow gaugings).
4. Catchment water balance method (groundwater flow modelling)
5. Groundwater chemistry trends (isotope and solute profile techniques).

In the current study, considering approach 1, annual potential recharge has been forecasted through the modelling of the soil system. The basic approach is to perform numerical simulation with HYDRUS-1D computer software package (Šimunek et al., 2005) on a conceptual one-dimensional column from the surface to the watertable. The bottom flux is then used as a potential recharge for the regional groundwater flow modelling process with the MODFLOW Computer Code in Chapter 5.

4.2.2 The HYDRUS-1D Computer Code

HYDRUS is a software program for solving the Richards's equation for water flow and the advection-dispersion equation for heat and solute transport in variably saturated subsurface media (Simunek et al. 2005). HYDRUS comes with a graphical user interface that runs under the Microsoft Windows operating system and uses the finite-element method to simulate movement of water, heat, and multiple solutes in partially or fully saturated porous media.

In this study, a one dimensional version of the HYDRUS computer software program, HYDRUS-1D, has been used to simulate changes in soil water content under saturated/unsaturated one dimensional vertical groundwater flow.

HYDRUS-1D accommodates user-defined flow and head boundary conditions into a numerical solution of the Richard's equation for unsaturated and saturated flows. The model makes use of the Galerkin-type linear finite element method for space discretization (Simunek et al. 2005) and a finite-difference method for temporal discretization. The user interface includes pre-processing of data and graphical presentation of the output results in Microsoft Windows environment. The data pre-processing involves specification of all necessary parameters to run the FORTRAN source code successfully, discretization of the soil profile into finite elements, and the definition of the vertical distribution of hydraulic and other parameters characterizing the soil profile van Genuchten and Mualem (1980)

First of all, the processes to be simulated are selected (water flow, chemical transport, heat transport, root growth, and/or root water uptake). Length units, depth and inclination of the soil profile to be analyzed, as well as the number of materials to be used, are specified. After selecting the time and space scales, the boundary conditions are entered among many other operations. A catalogue of soil hydraulic parameters based on soil texture is part of the pre-processing unit. Parameter optimization can be carried out either by direct simulation or inverse solution.

The post-processing unit allows graphical presentation of the soil hydraulic properties, changes of a particular variable at selectable locations in the profile through time, and cumulative water fluxes across the upper and the lower boundaries. Moreover, water content and pressure head profiles can be obtained.

The profile module is matched by the discretization of the flow domain in a graphical mode and specification of domain properties. This is an external module which may be used to discretize a one-dimensional soil profile into finite difference cells. The module also allows a user to specify the initial conditions in the pressure head and the water content, as well as the spatial distribution of other parameters characterizing the soil profile (e.g., spatial distribution of soil materials and root water uptake parameter) and/or observation nodes.

4.2.2.1 Governing equations-Richards' equation

The vertical movement of water in the unsaturated zone is described by the Richards' equation. Depending on the selection of the dependent variable: the θ-based (moisture content-based), the h-based (head-based), and the mixed forms, the Richards' equation can be written in different forms (Celia et al., 1990; Miller et al., 1998). In a situation where the air phase of a homogeneous and isotropic soil does not affect the liquid flow processes and has negligible water flow resulting from thermal gradients, Celia et al., (1990) and Miller et al., (1998) formulated the one dimensional mixed form of Richards equation as follows:

$$\frac{\partial\theta(z,t)}{\partial t} = \frac{\partial}{\partial z}\left\{K(\theta)\left[\frac{\partial h(\theta)}{\partial z} + 1\right]\right\} - S \qquad (4\text{-}1)$$

This is subject to the initial and boundary conditions;

$$\frac{\partial h}{\partial z}(L,t) = 0 \qquad (4\text{-}2)$$

Or

$$h(L,t) = h_L(t) \qquad (4\text{-}3)$$

where the parameters are defined by van Genuchten and Mualem (1980) as; h[L]=soil water pressure head; θ[L^3L^{-3}]=volumetric water content; t[T]=time; z[L]=is the vertical distance; K[LT^{-1}]=unsaturated hydraulic conductivity, a function of saturated hydraulic conductivity Ks and water content; and S[$L^3L^{-3}T^{-1}$] represents the sink term to account for root water uptake. $h_0[z]$ is the initial condition, and $q_0(t)$ [LT^{-1}] is the fluid flux across the soil surface boundary.

It should be noted that the classical Richards-flow theory functions for only stable flow conditions, with the assumptions that the air phase does not play any significant role in the liquid flow process (Richards 1931). It is also assumed that water flow due to thermal gradients can be neglected. However, flow instability (which is non-Richard's) has been observed under a wide variety of circumstances such as sudden and gradual increases of hydraulic conductivity with depth, water repellence of the solid phase, compression of air ahead of the wetting front, and preferential flow through non-capillary macro pores.

4.2.2.2 Soil hydraulic properties

HYDRUS-1D solves the Richard's equation by establishing relationships between soil water retention θ(h) and hydraulic conductivity K(h) which are nonlinear functions of pressure head and water content respectively. However, HYDRUS-1D permits the use of four alternative analytical models for determining soil hydraulic properties (Brooks and Corey, 1964; van Genuchten, 1980; Vogel and Císlerová, 1988; Kosugi, 1996; and Durner, 1994). In modelling the unsaturated flow in the study area, the van Genuchten and Mualem (1980) analytical model (equation 4-4) was used to describe the soil water retention parameters. The equation is expressed as follows:

$$\theta(h) = \begin{cases} \theta_r + \frac{\theta_s - \theta_r}{[1+|\alpha h|^n]^m} for\ h \leq 0 \\ \theta_s \qquad\qquad\qquad for\ h \geq 0 \end{cases} \qquad (4\text{-}4)$$

The relationships between water retention and pressure head as expressed above have five parameters that define the shape of the function, $\boldsymbol{\theta_s}$ saturated porosity of the soil, $\boldsymbol{\theta_r}$ residual moisture content, $\boldsymbol{K_s}$ saturated hydraulic conductivity, **α** the inverse of the air entry value (or bubbling potential), and **n** pore size distribution index.

The hydraulic conductivity function in HYDRUS-1D is also described by the van Genuchten-Mualem (1980) pore size distribution model, with the relationship expressed as follows:

$$K(h) = \begin{cases} K_s S_e^{l/2}[1-(1-S_e^{1/m})^m]^2 & h < 0 \\ K_s & h \geq 0 \end{cases} \qquad (4\text{-}5)$$

where,

$$m = 1 - \frac{1}{n}; \qquad S_e = \frac{\theta(h) - \theta_r}{\theta_s - \theta_r} \qquad (4\text{-}6)$$

S_e is the effective saturation, and l is pore-connectivity parameter estimated to an average of 0.5 for most soils.

4.2.2.3 Initial and boundary condition determinations

4.2.2.3.1 Initial conditions

In order to model the transient soil water flow using the HYDRUS-1D, the initial soil moisture contents should be defined at each nodal point within the soil profile. The values of soil

water content (and hence the matric head) at each nodal point within the soil profile are required. However, when these data are not available, it is usual to define the water contents to be at field capacity or such that steady-state flow is occurring. Thus, the initial head distribution is defined

$$h(z,t) = h_i(z) \qquad t = t_0 \qquad (4\text{-}7)$$

where h_i [L] is a prescribed function of x, and t_o is the time when the simulation begins.
The above arbitrary starting condition has been dealt with in section 4.4 by running preparatory simulations to produce the same cyclic pattern.

4.2.2.3.2 Boundary conditions

The two main boundary conditions for the unsaturated zone are the upper (atmospheric) and lower boundary conditions. The upper boundary condition is the Neuman type (Neuman et al., 1974) which can change from a fixed flux to a fixed head when limiting pressure heads are exceeded and depends on precipitation and potential evaporation. The actual flux through the soil surface is limited by the ability of the soil to transmit water. And again, if the potential infiltration rate exceeds the infiltration capacity of the soil, part of the water will run off (van Genuchten, 1980).

Three different types of conditions can be defined at the lower boundary: (1) Dirichlet condition in which the pressure head is specified, (2) Neumann condition in which the flux is specified, and (3) the mixed boundary condition or Cauchy condition where flux normal to a boundary can be expressed in terms of the head along the boundary and a known constant. The phreatic surface is usually taken as the lower boundary in the situation where recorded watertable fluctuations are already known. In such a situation the flux through the bottom of the system can be calculated. A flux at lower boundary condition is usually applied in situations where one can identify a free drainage or no flow boundary (i.e., an impermeable layer). In regions with a very deep groundwater table, a Neumann type of boundary condition is often used as in the case of the current study.

4.2.2.4 Required input data

According to Šimunek et al. (2005), the required input data for the simulation of water dynamics in the unsaturated zones includes; model parameters, geometry of the system, boundary conditions and, initial conditions for transient flow simulation. The dimensions of the problem domain are defined via the geometry parameters. The physical properties of the system under consideration are described via the physical parameters. With respect to the unsaturated zone, these include the soil water characteristic, θ(h), and the hydraulic conductivity, K(h). For a proper description of the unsaturated flow, a proper description of the two hydraulic functions, K(h) and θ(h) is important. All these have been fully dealt with in the subsequent sections.

4.3 Development and representation of the conceptual model

4.3.1 Site and data description

As previously mentioned, recharge is a region-specific property and therefore work will concentrate on the Tarkwa mining district of South Western Ghana. The geographical characteristics of the area have already been discussed in Chapter 2 of the thesis. The study area is located in the Ankobra Basin bordered to the west by the Ankobra River which flows towards the south. Bordering the area to the north and south respectively are the Huni and Bonsa Rivers, major tributaries of the Ankobra (Kuma, 2007). The area is highly dissected and has moderate relief with a general decrease in elevation southwards (Kuma, 2007).

Stratigraphically, the Tarkwaian rock system in the direction of oldest to youngest, consists of the Kawere Group, the Banket-Series, the Tarkwa-Phyllite, and the Huni-Sandstone with weathered quartzites forming most of the surface rocks (Whitelaw, 1929). The landscape is defined by a series of parallel ridges and valleys orientated parallel to the NE/SW strike of the rocks (Kuma, 2007). Kuma (2007) further asserts that this geomorphology results from the inclined folds and dip-and-scarp slopes of the Banket Series and the Tarkwa Phyllites. Also, smaller tributary valleys cross the ridges being controlled by faulting and jointing.

Kuma and Younger (2000) and Kortatsi (2004) contend that vertical groundwater recharge from precipitation and evapotranspiration are the main components of the water cycle in

the study area, with the unsaturated zone playing an important role. Using the water budget method, Kuma (2007) estimated recharge rate of (299±72) mm/yr for the area. According to these workers, the humid climate of Tarkwa District is characterized by a surplus of precipitation over soil evaporation and plant transpiration, with no distinct monsoon. And therefore precipitation is the primary source of recharge, whereas seepage from other surface bodies, watercourses, terrain depressions, fractures, and diversion from denser soil contribute indirectly with a trivial volume, especially in the environments of new surface mine development. Once infiltrated and reduced by evapotranspiration, the rest of the moisture percolates down through the vadose zone to the watertable as a potential recharge to the groundwater. The shallow areas however, allow for some moisture to be driven back by a capillary rise in response to evapotranspiration demand.

4.3.2 Soil physical properties

The two main types of soil in the Tarkwa area are the forest oxysols in the south and the forest ochrosol-oxysol in the north (Asklund & Eldvall, 2005). The soil consists of mostly silty-sands with minor patches of laterite mainly on hilly areas and underlain by the Banket Series and the Tarkwa Phyllite rocks (Kuma & Younger, 2001; Kortatsi 2004). According to these researchers, soil thickness in the area is about 50m and varies from one place to the other with an average of 20m. A typical soil profile in the area consists of a relatively thin surficial unit of thickness 0-0.15m, enriched with organic matter. These researchers further argue that this unit form part of the A-horizon and normally has a dark brown colour. Below this unit is the B-horizon, the zone of infiltration which extends on average to 1.50m and exhibits a red to yellowish-brown colour. The unconsolidated parent rock is the C-horizon, located below the B-horizon which is much more variable in thickness compared to the A and B-horizons with much lighter colour (Kuma and Younger (2001).

Results of infiltration tests (Table 4.1) conducted by Kuma and Younger (2001) on the four main soil types; Huni, Tarkwa Phyllite, Banket and the Kawere at 56 sites in the study area show that the saturated hydraulic conductivity (Ks) of the soils falls within the range of 10^{-5} to 10^{-8} ms^{-1} with the majority in the 10^{-6} to 10^{-7} ms^{-1} bracket. Kuma and Younger (2001) further contended that in terms of both particle size distribution and saturated hydraulic

conductivity values the Banket soils were identified to display the best textural characteristics for groundwater percolation and are therefore the best medium for recharge.

Table 4.1 Soil textural properties in the mining district of Tarkwa in South Western Ghana (modified from Kuma and Younger, 2001)

Soil type	Soil Texture	Textural fractions				
		Gravel (%)	Sand (%)	Silt (%)	Clay (%)	Gs (Specific gravity)
Huni	Silty Sand	2	55	33	10	2.65
Tarkwa Phyllite	Laterite	69	9	13	16	2.74
Banket	Silty Sand Laterite	2 69	59 14	20 10	10 7	2.66 2.67
Kawere	Silty Sand	0	47	40	13	2.65

4.3.3 Meteorological data

Meteorological data for South Western Ghana used for this study were obtained from the Ghana Meteorological Service weather station at Tarkwa (Appendix B). The dataset span for almost a quarter of a century, from 1977 to 2001 and include: Average monthly summary of rainfall data with total rain days, Average monthly summary of potential evapotranspiration, solar radiation, maximum and minimum temperature (air and dew point) relative humidity at 06:00 and 15:00 hours and 2x per day wind speed. Data obtained was statistically processed and analysed, and appropriate graphs (Figure 4.1) generated using Microsoft Excel. Analysed data were used as input into the Hydrus Computer Code for modelling of bottom fluxes in the estimation of the potential recharge.

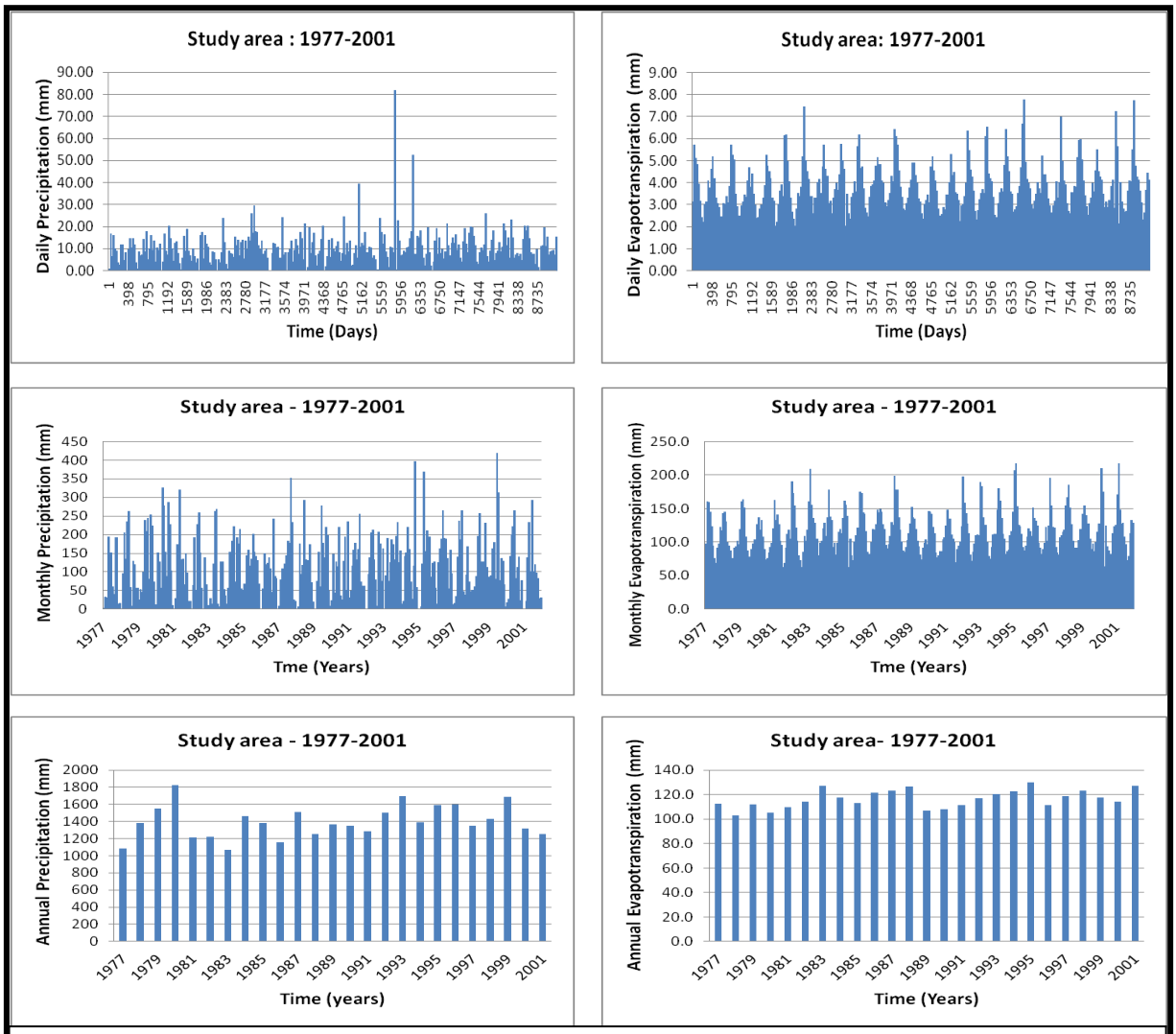

Figure 4.1 Daily (Top), monthly (middle) and annual (bottom) temporal variation of Precipitation and Potential Evapotranspiration of South Western Ghana averaged over 25yrs period

4.3.3.1 Spatial rainfall variation distribution pattern

The amount of groundwater recharge depends on rainfall intensity and temporal distribution, and calculations for recharge should be undertaken at least as frequently as daily (Howard and Lloyd, 1979). As only monthly data were available, monthly rainfall and evapotranspiration data were converted into daily time series in excel format by dividing the monthly totals by the number of rain days within each month. Four spatial rainfall variation distribution patterns D1, D2, D3, and D4 were defined based on rain day number data, with an intention to choose the suitable distribution pattern for the study area. On this basis, the relationship between distribution patterns and their corresponding recharge values were initially investigated to inform the choice of distribution for the groundwater modelling (Chapter 5).

4.3.3.2 Representative rainfall distribution

Due to variability of precipitation and evapotranspiration as well as soil and aquifer properties, recharge processes have a non-linear relationship with time and space. In view of this, the amount of rainfall over a period of time may result in no recharge due to high rate of evapotranspiration, but the same amount of rainfall spread over a shorter time period could be sufficient to saturate the soil and cause some recharge. In view of this, four different representative rainfall distributions were defined for the area and one of them chosen for the subsequent groundwater modelling (the reason for making a choice out of the four is explained below). The spatial daily variation within a month of each of the four models D1, D2, D3, and D4 are shown in Figure 4.2 and defined as follows:

1. D1: A lump distribution spread the full month rainfall for each of the number of days in the month i.e. the monthly total divided by the number of days in the month.
2. D2: A lumped distribution of the full month rainfall applied for only the first day of the month.
3. D3: A lumped distribution applied the full month rainfall in only two days at even intervals throughout the month, e.g. on the 1st and 15th day.
4. D4: A lumped distribution applied the full month rainfall in four days at even intervals throughout the month, e.g. 7th, 14th, 21st and 28th days.

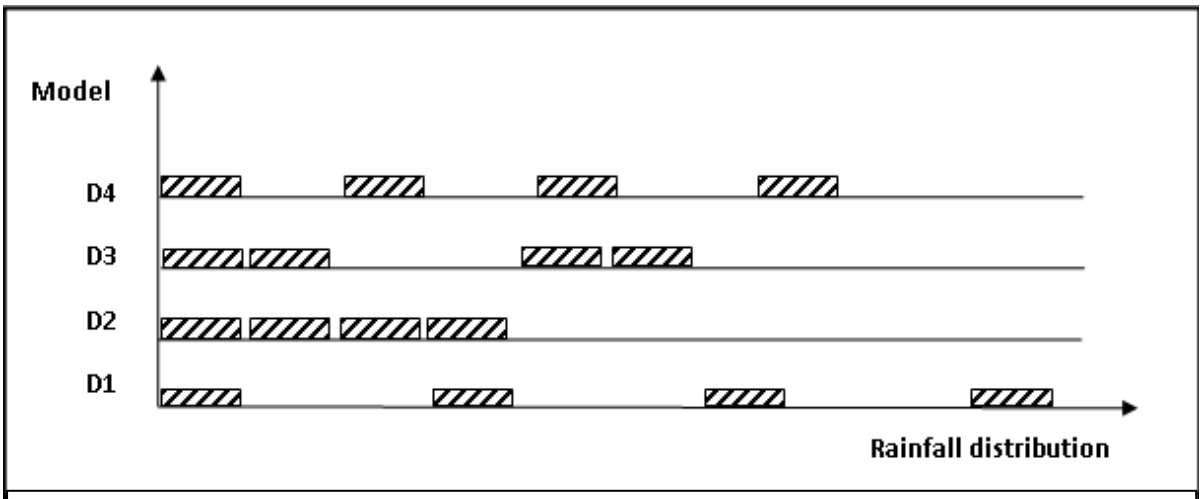

Figure 4.2 Representation of daily rainfall distribution models of monthly totals

Based on the above distribution pattern, a preliminary run of Hydrus-1D for the study area was carried out for a 5 year period (1997–2001) of rainfall and evapotranspiration to determine the appropriate rainfall distribution model for the area. The bottom water flux of the simulation was assumed to be equal to the potential recharge to the groundwater. For example in April 1997 the average monthly rainfall recorded for 12 rain days is 236mm/yr which is equivalent to 1.97cm/day and the corresponding distribution pattern for the four models is shown in Table 4.2. This is repeated for the rest of the time series.

Table 4.2 Different models showing daily rainfall distribution pattern of South Western Ghana for the month of April 1997

Time (Days)	Models			
	D2	D1	D3	D4
1	1.97	1.97	1.97	1.97
2	1.97	0	1.97	1.97
3	1.97	1.97	1.97	1.97
4	1.97	0	1.97	0
5	1.97	1.97	1.97	0
6	1.97	0	1.97	0
7	1.97	1.97	0	1.97
8	1.97	0	0	1.97
9	1.97	1.97	0	1.97
10	1.97	0	0	0
11	1.97	1.97	0	0
12	1.97	0	0	o

Continue in the next page

13	0	1.97	0	0
14	0	0	0	0
15	0	1.97	0	1.97
16	0	0	1.97	1.97
17	0	1.97	1.97	1.97
18	0	0	1.97	0
19	0	1.97	1.97	0
20	0	0	1.97	0
21	0	1.97	1.97	0
22	0	0	0	1.97
23	0	0	0	1.97
24	0	1.97	0	1.97
25	0	0	0	0
26	0	0	0	0
27	0	1.97	0	0
28	0	0	0	0
29	0	0	0	0
30	0	0	0	0

Given the potential evapotranspiration (PET) and precipitation (P) as input parameters the Hydrus computer code was run and got it to calculate recharge (R) and surface run-off (RO) for each distribution pattern based on equation 4.8, with the results shown in Table 4.3.

$$P = RO + R + PET \qquad (4\text{-}8)$$

It is observed that different rainfall distribution models resulted in variation in recharge and run-off. A plot of recharge against daily rainfall of the four distribution pattern is shown in Figure 4.3. A lump distribution of rainfall at the beginning of the month (D2) yielded the maximum recharge, whilst a lump distribution of rainfall spread equally for each day of the month (D1) resulted in a minimum recharge.

Thus, less recharge means that the radius of influence has to increase to capture the amount of water discharged from the mine. Hence, in order to obtain a maximum areal extent of mine impact in the study area, rainfall distribution pattern D1 with the smallest

recharge value was chosen for the numerical modelling of potential recharge using the HYDRUS computer code (section 4.4).

In the current study, Table 4.4 represents input values of daily precipitation and evapotranspiration rates, for the first month of the time series (1997 to 2001), for the implementation of the upper boundary condition for the Hydrus computer code using the distribution pattern of D1. The rest of the series follow the same trend.

Table 4.3 Water balance model for rainfall distribution pattern

Rainfall Distribution Model	PET (mm/5yr)	PET (mm/yr)	Recharge-R (mm/yr)	Rainfall-P (mm/yr)	PET + R (mm/yr)	Run-off (mm/yr)
D2	6280	897	500	1408	1397	11
D3	7000	1000	400	1408	1400	8
D4	7160	1022	376	1408	1398	10
D1	7230	1032	368	1408	1400	8

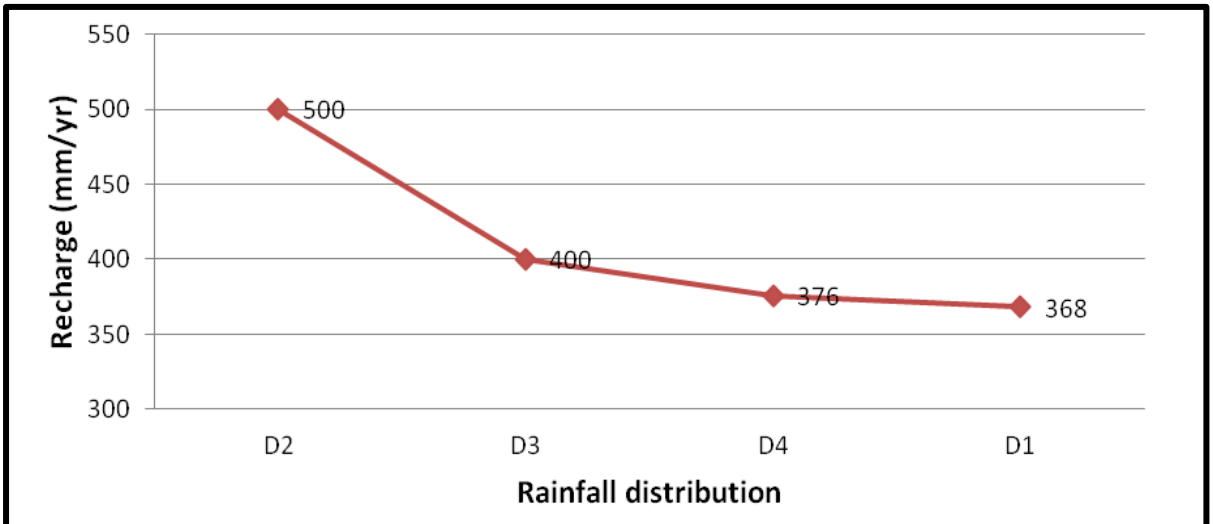

Figure 4.3 Relationship between recharge and rainfall distribution pattern

Table 4.4 Time variable atmospheric Boundary Conditions of precipitation (Precip) and evapotranspiration (EvapoT) for the period 1977-2001, using the distribution pattern of D1

Time Series	Time (days)	EvapT (mm/m)	No. of Days	Precip. (mm/m)	Rain days	Precip (mm/d)	Precip/sp (mm/d)	EvapT (mm/d)	hcritA
1	01/01/1977	97.9	31	3.6	5	0.72	0.00	3.16	100000
2	02/01/1977	97.9	31	3.6	5	0.72	0.00	3.16	100000
3	03/01/1977	97.9	31	3.6	5	0.72	0.00	3.16	100000
4	04/01/1977	97.9	31	3.6	5	0.72	0.00	3.16	100000
5	05/01/1977	97.9	31	3.6	5	0.72	0.00	3.16	100000
6	06/01/1977	97.9	31	3.6	5	0.72	0.72	3.16	100000
7	07/01/1977	97.9	31	3.6	5	0.72	0.00	3.16	100000
8	08/01/1977	97.9	31	3.6	5	0.72	0.00	3.16	100000
9	09/01/1977	97.9	31	3.6	5	0.72	0.00	3.16	100000
10	10/01/1977	97.9	31	3.6	5	0.72	0.00	3.16	100000
11	11/01/1977	97.9	31	3.6	5	0.72	0.00	3.16	100000
12	12/01/1977	97.9	31	3.6	5	0.72	0.72	3.16	100000
13	13/01/1977	97.9	31	3.6	5	0.72	0.00	3.16	100000
14	14/01/1977	97.9	31	3.6	5	0.72	0.00	3.16	100000
15	15/01/1977	97.9	31	3.6	5	0.72	0.00	3.16	100000
16	16/01/1977	97.9	31	3.6	5	0.72	0.00	3.16	100000
17	17/01/1977	97.9	31	3.6	5	0.72	0.00	3.16	100000
18	18/01/1977	97.9	31	3.6	5	0.72	0.72	3.16	100000
19	19/01/1977	97.9	31	3.6	5	0.72	0.00	3.16	100000
20	20/01/1977	97.9	31	3.6	5	0.72	0.00	3.16	100000
21	21/01/1977	97.9	31	3.6	5	0.72	0.00	3.16	100000
22	22/01/1977	97.9	31	3.6	5	0.72	0.00	3.16	100000
23	23/01/1977	97.9	31	3.6	5	0.72	0.00	3.16	100000
24	24/01/1977	97.9	31	3.6	5	0.72	0.72	3.16	100000
25	25/01/1977	97.9	31	3.6	5	0.72	0.00	3.16	100000
26	26/01/1977	97.9	31	3.6	5	0.72	0.00	3.16	100000
27	27/01/1977	97.9	31	3.6	5	0.72	0.00	3.16	100000
28	28/01/1977	97.9	31	3.6	5	0.72	0.00	3.16	100000
29	29/01/1977	97.9	31	3.6	5	0.72	0.00	3.16	100000
30	30/01/1977	97.9	31	3.6	5	0.72	0.72	3.16	100000
31	31/01/1977	97.9	31	3.6	5	0.72	0.00	3.16	100000

4.4 Numerical model design using Hydrus-1D Computer code

4.4.1 Conceptual infiltration model

A conceptual model for the flow processes following precipitation occurring on the soil surface is shown in Figure 4.4. A steady state finite element infiltration model is developed with Hydrus-1D computer code to deal with the flow process by taking into consideration the following processes; infiltration and surface ponding of precipitation at the surface of the soil profile, evapo(transpi)ration, and unsaturated flow in the unsaturated zone governed by the Richards' equation. The structure of vegetation reveals that the area under consideration has undergone and continues to undergo various degrees of degradation due to surface mining. The multi-storey structure representation of the South West rain forest and other similar forest types is lost. The resultant plant cover is a mixture of vegetation and open ground that reflects the various stages of land use. Precipitation was therefore assumed to reach the soil surface uninterrupted by any vegetation canopy. Time series data of precipitation and evaporation is introduced to the surface of the model grid system as a source term. As described by Simunek et al. (2005), when the top layer becomes saturated as a result of heavy downpour precipitation rate exceeds infiltration rate. Precipitation then begins to accumulate in the surface and the ponded water is assumed to be immediately removed by runoff whiles the model automatically converts the pressure head of the top layer to zero. The bottom water flux is assumed to be equal to the potential groundwater recharge.

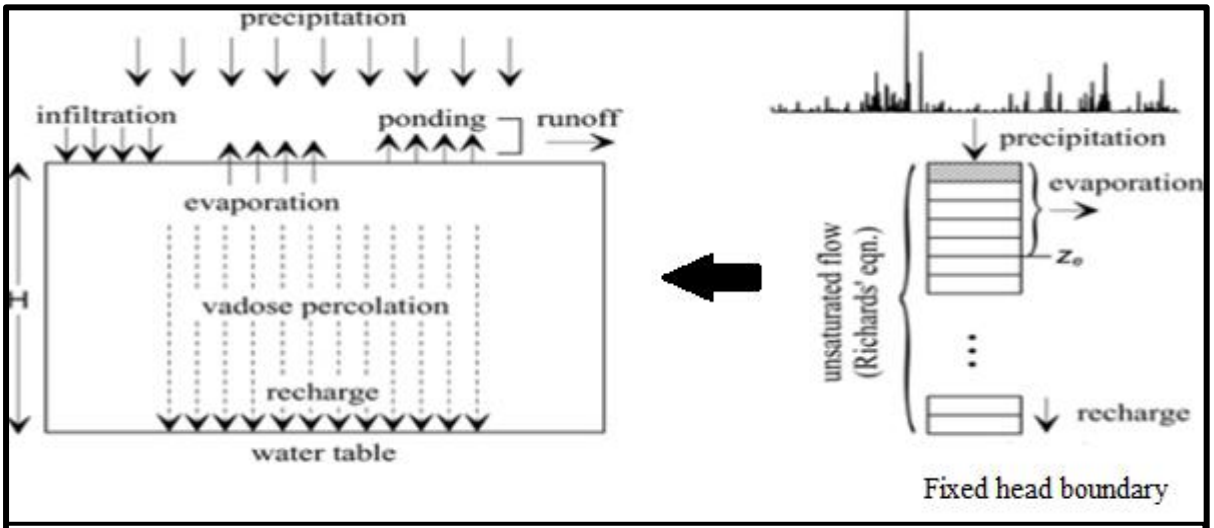

Figure 4.4 Schematic diagram of the implementation of the conceptual infiltration model on the left

4.4.2 Soil hydraulic properties

To run the hydrus computer numerical model requires specifying the number of layers in the soil profile, boundary conditions and the soil hydraulic parameters θr, θs, α, Ks and L. Homogeneous vertical conceptual soil column of average depth 600cm from ground surface was set up. The simulation was made with incorporation of the processes of precipitation and potential evapotranspiration as defined in previous sections.

Soil properties representing the four main soil types in the study area (Huni, Tarkwa Phyllite, Banket and the Kawere), were determined for each of the profile components in describing the soil profile, from results of infiltration tests conducted by Kuma and Younger (2001). The soil hydraulic parameters were estimated using a pedotransfer function model, Rosetta (Schaap et al., 2001) that predicts hydraulic parameters from soil texture and related data as implemented in HYDRUS-1D. The van Genuchten parameters were estimated using Rosetta, the latter based on the soils data collected by Carsel and Parrish (1988). Rosetta contains a hierarchy of pedotransfer functions that can be used depending on the available data. In this study, the hydraulic parameters were predicted and the results presented in Table 4.5) by using data for bulk density (Bd) and percentages of sand, silt, and clay of the four soil profiles from the results of infiltration tests conducted by Kuma and Younger (2001) on different soil types at 56 sites in the study area (Table 4.1).

Table 4.5 Estimated Van Genuchten hydraulic parameters by Rosetta (Schaap et al., 2001)

Soil Type	Soil Texture	Hydraulic parameters						
		Bd (gmm^{-3})	θr (m^3m^{-3})	θs (mm^{-3})	α (mm^{-1})	N (-)	Ks (mm/d)	L (-)
Huni	Silty Sand	26.5	0.0414	0.3889	0.00208	1.4186	336	0.5
Tarkwa Phyllite	Laterite	27.4	0.0537	0.3789	0.00313	1.394	320	0.5
Banket	Silty Sand Laterite	26.7	0.0404	0.3854	0.00372	1.4556	530	0.5
Kawere	Silty Sand	26.5	0.0485	0.3935	0.00114	1.4856	177	0.5

Where: Bd=bulk density; θr= residual soil water content; θs=saturated soil water content; α, N and L are empirical coefficients that determine the shape of the hydraulic functions

4.4.3 Setting the Boundary and initial conditions

4.4.3.1 Upper boundary conditions

The upper boundary condition is specified as an atmospheric boundary condition with surface runoff. And with this condition the potential flux across the boundary is controlled by precipitation and potential evapotranspiration. Implementation of the atmospheric boundary condition requires specifying daily precipitation and evapotranspiration rates and therefore a twenty five year daily time steps series (01/01/1977 to 31/12/2001) of precipitation and potential evapotranspiration (Figure 4.5) were defined in excel format (Table 4.4) and input into the Hydrus 1D computer code.

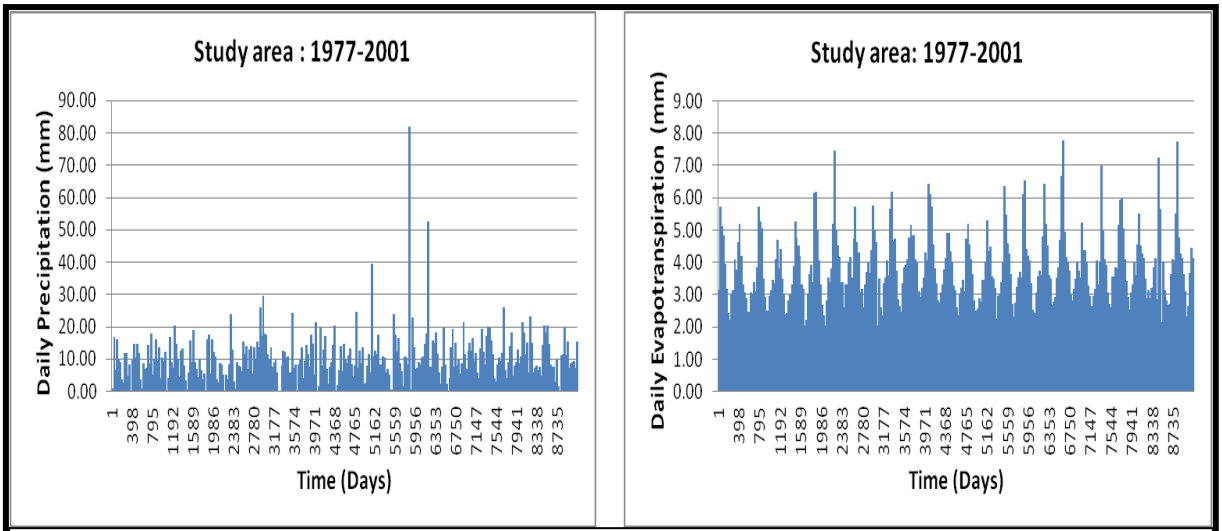

Figure 4.5 Input values of Precipitation and Potential Evapotranspiration rates of South Western Ghana averaged over the period of 1977-2001.

Simunek et al. (2005) observed that as long as the pressure head at the surface remains above a threshold value hcrit, evaporation of water from the soil surface continues at the potential rate E_p. These researchers further explain that if the soil surface dries out as a result of evaporation to the point that the surface pressure head reaches hcrit, the boundary switches to a constant pressure head condition (=hcrit). This generally leads to a computed actual evaporation rate that is well below the potential rate. In this study, hcrit value is assumed to be minus 1000000mm. However, because the surface soil remained relatively wet due to regular precipitation and remained above the hcrit threshold the simulation results obtained were insensitive to this parameter value when specified in the range minus 1500000mm to minus 1000000mm (Simunek et al. 2005).

4.4.3.2 Lower boundary conditions

Neuman et al. (1974) have observed that most studies that use unsaturated zone models to estimate groundwater recharge normally assume the unit gradient flow at the lower boundary (e.g. Nolan et al., 2003, 2007; Small, 2005; and Keese et al., 2005). However, because groundwater may return to the atmosphere through either capillary rise or groundwater evapotranspiration this boundary condition may not be valid for regions where water tables are shallow. (e.g. Gillham, 1984; Wu et al., 1996; Batelaan et al., 2003). Similarly, in regions with a 'deep' groundwater table, a Neumann type of boundary condition is used whereby the flux is specified to be fixed. In this study we decided to look at the maximum potential recharge hence the use of a deep water table and a fixed maximum boundary condition. The bottom water flux is taken to be equal to the potential groundwater recharge.

4.4.3.3 Initial conditions

Anderson and Woussner (1992) have observed that in order to get the resulting solutions to produce the same initial cyclic pattern, the initial conditions of the model have to be generated by running a certain period of preliminary cyclic simulation earlier to the time of interest. . Thus, in the current study three-year preliminary simulations were performed by a multiple-year precipitation and evapotranspiration sequence having a cyclic pattern of the first-year (Y1) meteo sequence such that Y2=Y3. Figure 4.6 shows the temporal changes of water fluxes at the lower boundary showing the cyclic pattern of the peaks representing Y1, Y1, Y1, Y2, Y3, Y4, Y5.

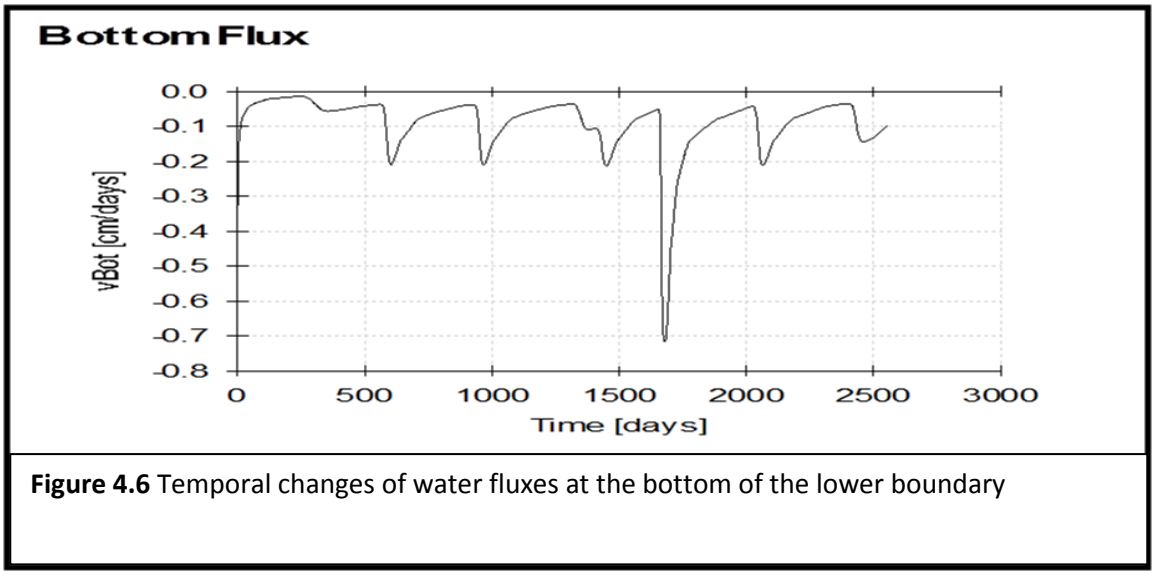

Figure 4.6 Temporal changes of water fluxes at the bottom of the lower boundary

4.5 Results and discussion

4.5.1 General comments on results

As already stated, the bottom water flux of the infiltration model was taken to be equal to the potential groundwater recharge. Figure 4.7 show breakthrough plots of the elevation, pressure and the total head in order to check whether the system was behaving properly, and in particular that the flow has reach the base of the model. The first 180 days was taken by the system's initial conditions to adjust to the temporal changes. The system became stable by 635 days, i.e. within the three year, year 1 cycling, with infiltration reaching the water table.

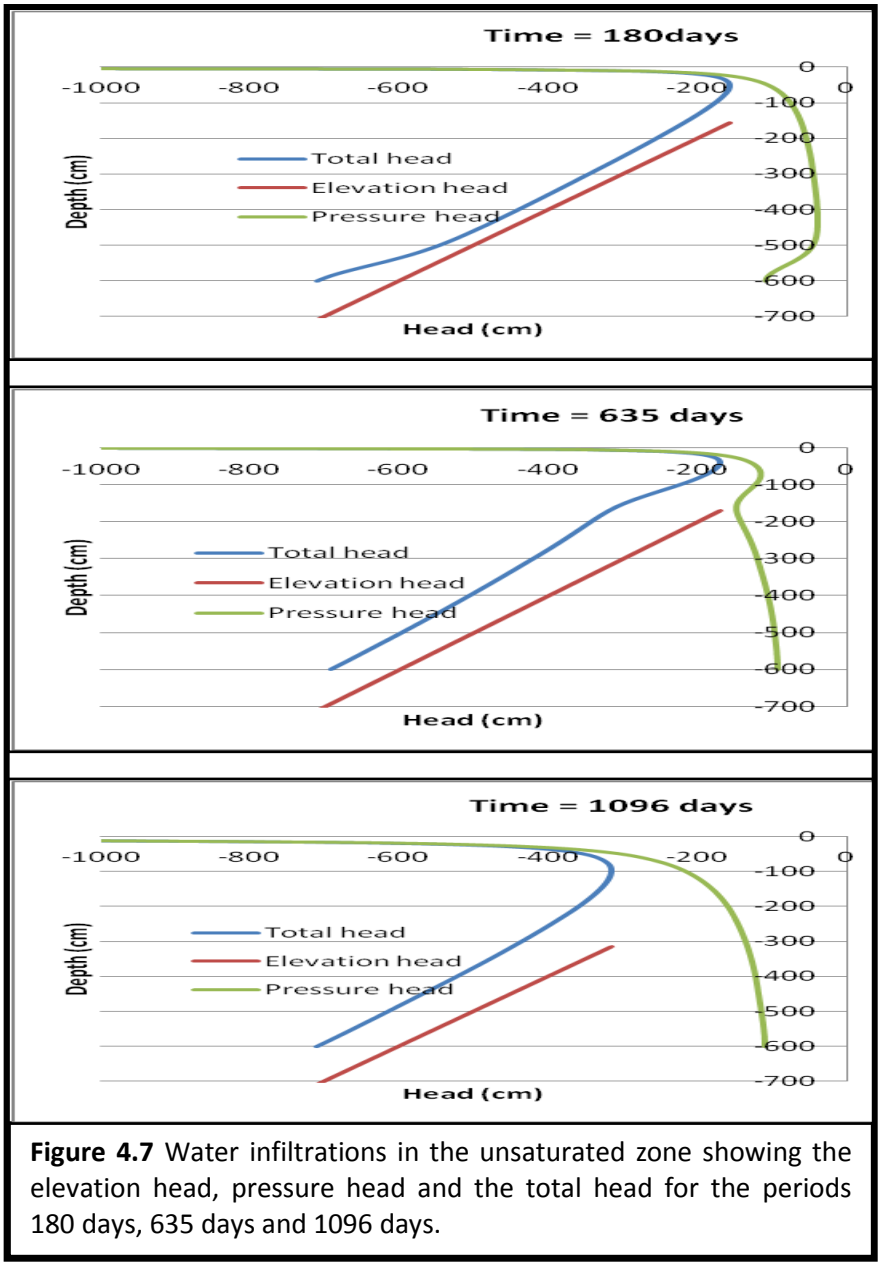

Figure 4.7 Water infiltrations in the unsaturated zone showing the elevation head, pressure head and the total head for the periods 180 days, 635 days and 1096 days.

Figure 4.8 show plots of temporal changes in actual and cumulative water fluxes and pressure heads across the upper and the lower boundaries of the infiltration model. The cumulative bottom flux was used in the calculations of the potential recharge estimates to the groundwater system for the period 1977 to 2001.

Data summary of the entire results of the various soil types in the study area are shown in Table 4.6. The annual percentage contribution of precipitation to recharge was also calculated. A preliminary investigation into the relationship between precipitation and recharge indicated that there is significant variation in the data and this might have resulted from a number of reasons, most notably different antecedent conditions. Depending on the soil types, the average potential annual recharge rates ranges from 355 mm/yr to 411 mm/yr and corresponds to 25.4% to 29.4% of the annual precipitation for the entire period (25yrs).

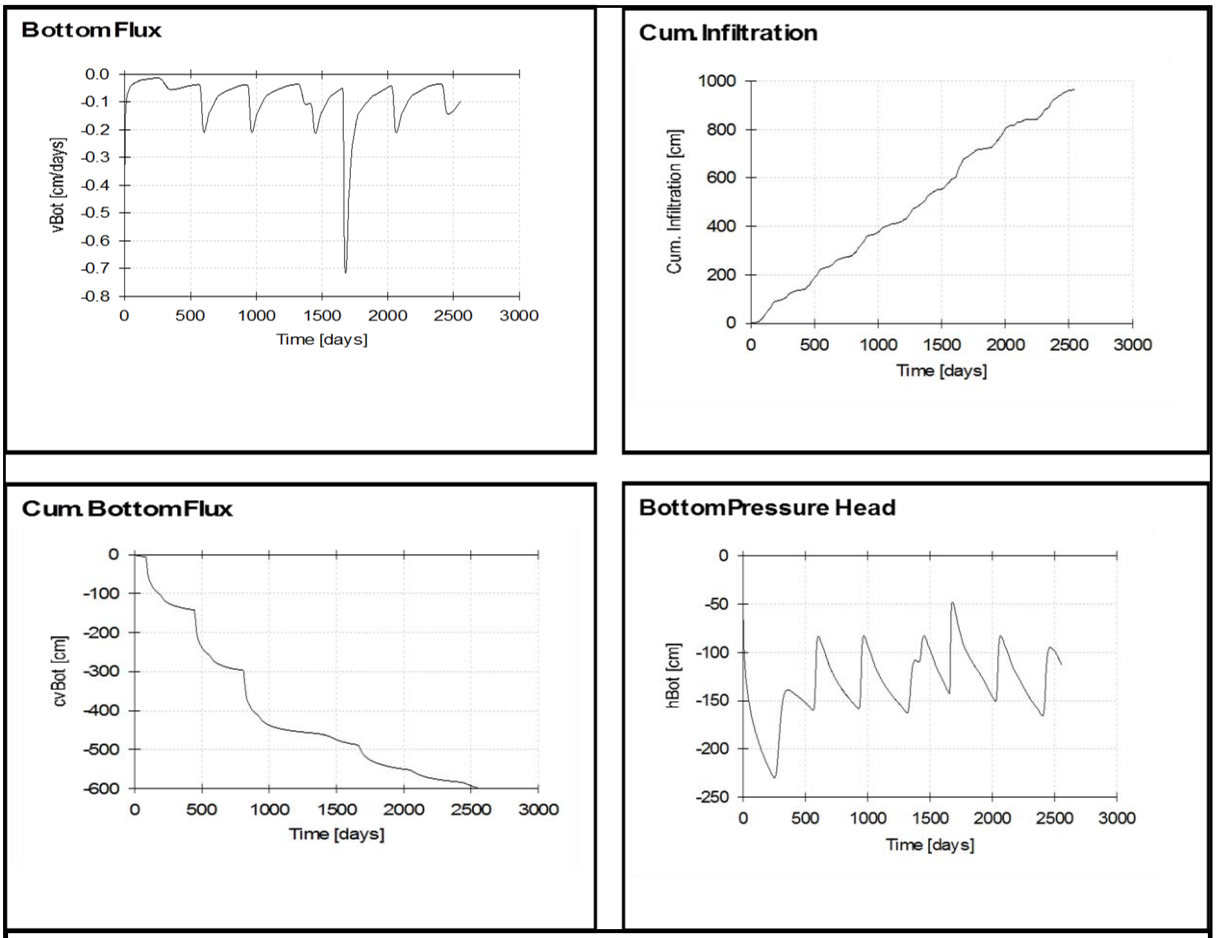

Figure 4.8 Graphs of temporal changes in actual and cumulative water fluxes and pressure heads across the upper and lower boundaries

Table 4.6 Predicted potential recharge values of Tarkwa District in South Western Ghana for a range of rainfall distribution spanning for the period 1977-2001

Time (Years)	Precip. (mm/yr)	Annual recharge (mm/yr)									
		Soil 1 Banket	% Precip	Soil 2 Huni	% Precip	Soil 3 Kawere	% Precip	Soil 4 Tarkwa	% Precip	Study Area	% of Ann. precip
1977	1085	223	21	192	18	165	15	217	20	199	18
1978	1383	516	37	459	33	403	29	511	37	472	34
1979	1554	530	34	506	33	480	31	558	36	519	33
1980	1827	796	44	763	42	821	45	730	40	778	43
1981	1216	450	37	434	36	341	28	471	39	424	35
1982	1225	405	33	375	31	350	29	398	33	382	31
1983	1071	269	25	242	23	221	21	265	25	249	23
1984	1459	246	17	215	15	185	13	249	17	224	15
1985	1385	380	27	364	26	338	24	375	27	364	26
1986	1158	232	20	216	19	215	19	218	19	220	19
1987	1507	379	25	423	28	381	25	479	32	416	28
1988	1255	351	28	231	18	204	16	231	18	254	20
1989	1368	440	32	415	30	375	27	466	34	424	31
1990	1351	290	21	265	20	273	20	261	19	272	20
1991	1284	426	33	367	29	302	24	419	33	379	29
1992	1502	279	19	260	17	257	17	281	19	269	18
1993	1692	489	29	435	26	380	22	486	29	448	26
1994	1389	447	32	426	31	411	30	470	34	439	32
1995	1594	594	37	555	35	527	33	559	35	559	35
1996	1598	453	28	436	27	422	26	448	28	440	28
1997	1352	428	32	394	29	372	28	417	31	403	30
1998	1429	181	13	172	12	171	12	191	13	179	13
1999	1686	721	43	680	40	640	38	403	24	611	36
2000	1320	469	36	440	33	414	31	460	35	446	34
2001	1253	270	22	235	19	222	18	263	21	247	20
Mean	**1398**	**411**		**380**		**355**		**393**		**385**	**27%**

4.5.2 Recharge- Precipitation relationships

Figure 4.9 and 4.10 shows the effect of rainfall pattern and distribution on the potential infiltration recharge over the period from 1977 to 2001 of the entire study area consisting of the four main soil types respectively. Although there is variation in precipitation recharge to the groundwater system in the study area, generally, the plots look similar which is an indication that there isn't much difference in precipitation recharge for the four main soil types. High recharge rates were observed from 1977 to 1984 and remain almost in dynamic equilibrium from 1984 to 2001 with the exception of 1998 where we had the minimum rate over the entire period. This is due to the corresponding variations in rainfall pattern and distribution in the area.

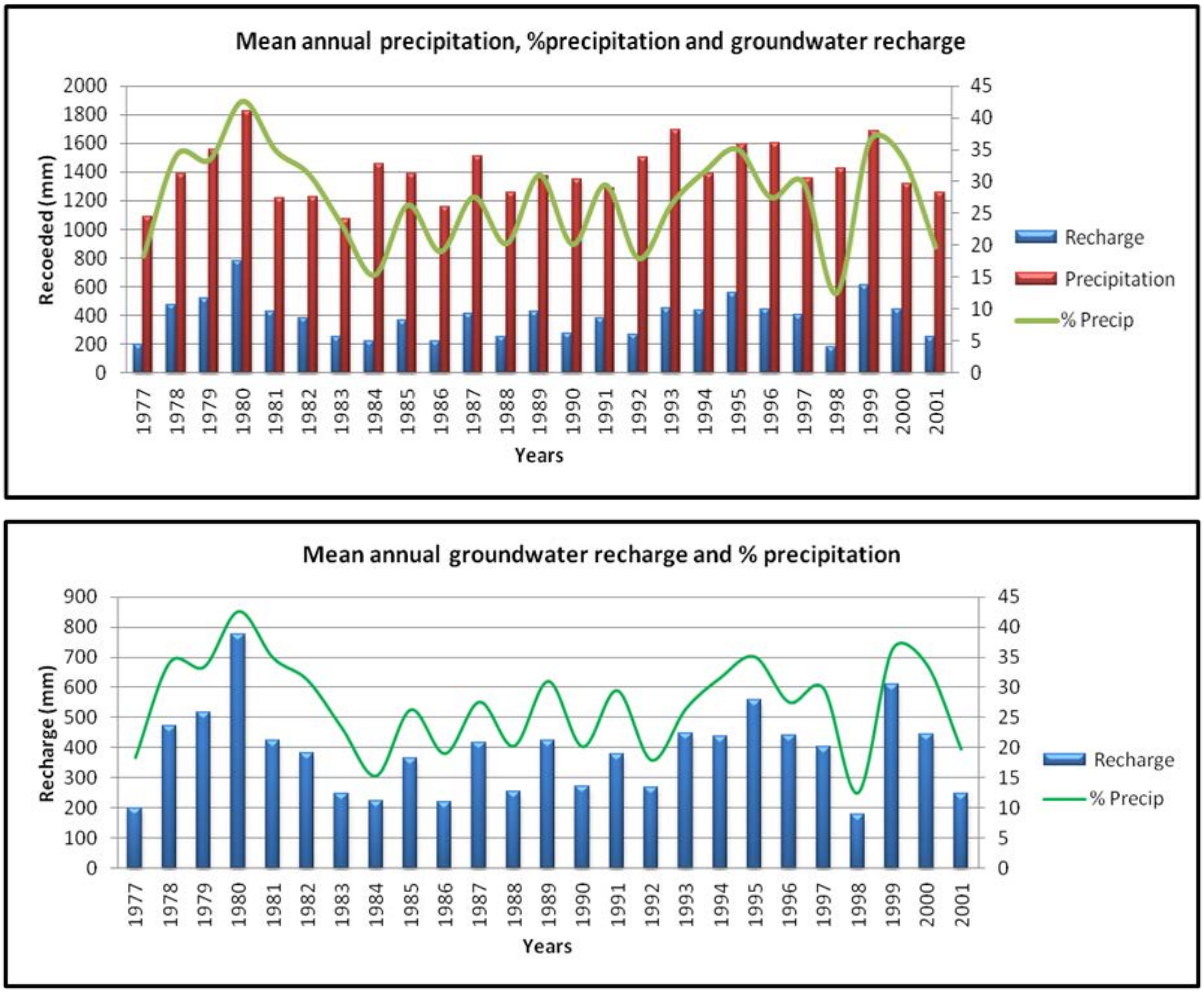

Figure 4.9 Data summary of mean annual precipitation, percentage of precipitation and groundwater recharge in Tarkwa District of South Western Ghana

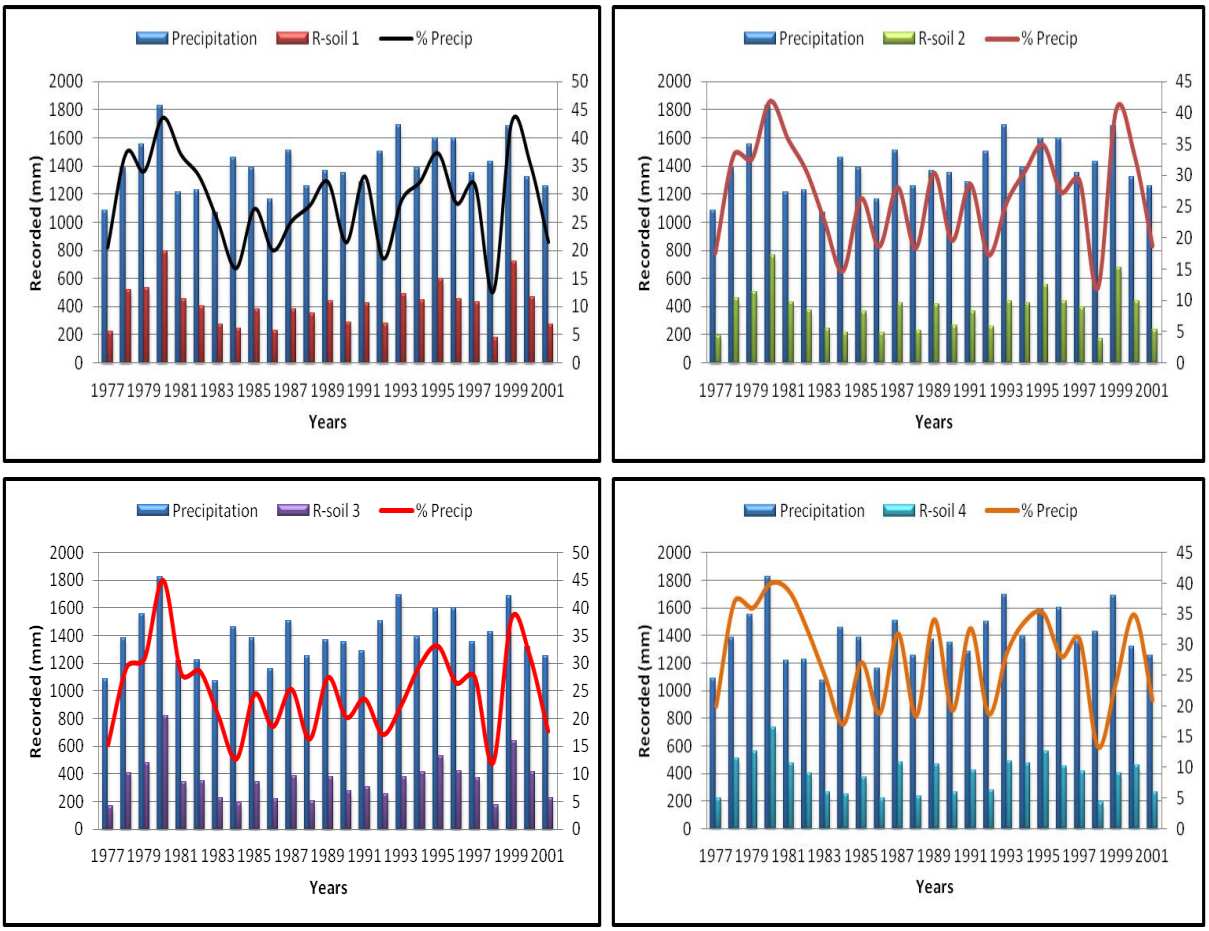

Figure 4.10 Mean annual precipitation, % of precipitation and groundwater recharge of soil type 1 (R-soil 1), (R-soil 2), (R-soil 3), and (R-soil 4) in Tarkwa District of S. W Ghana

The overall results presented so far clearly suggest that there is a strong dependence between annual rainfall and observed recharge. Therefore, to further investigate the relationship, an attempt was made to relate the dependent parameter (recharge) to the independent parameter (precipitation) by linear regression analysis of the form:

$$R = mP + C \qquad (4\text{-}9)$$

where R is the annual recharge rate (mm), P is the annual precipitation (mm), and m and C are calibration coefficients. Figure 4.11 and 4.12 show the linear variation between annual recharge and precipitation of the study area as well as the four main soil types in the area where (R^2), the standard coefficient of determination or correlation indicate the strength of the relationships.

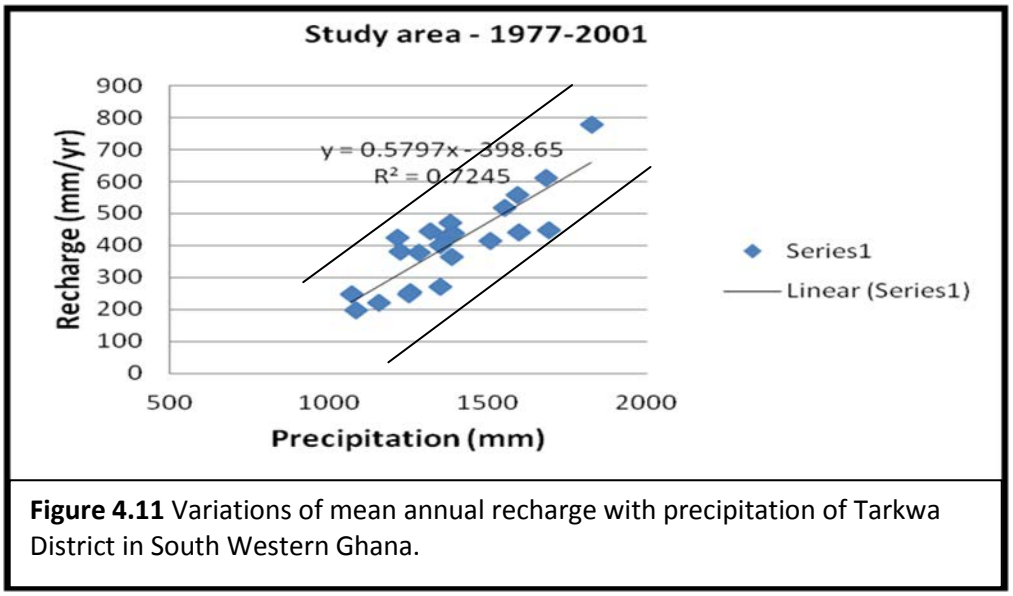

Figure 4.11 Variations of mean annual recharge with precipitation of Tarkwa District in South Western Ghana.

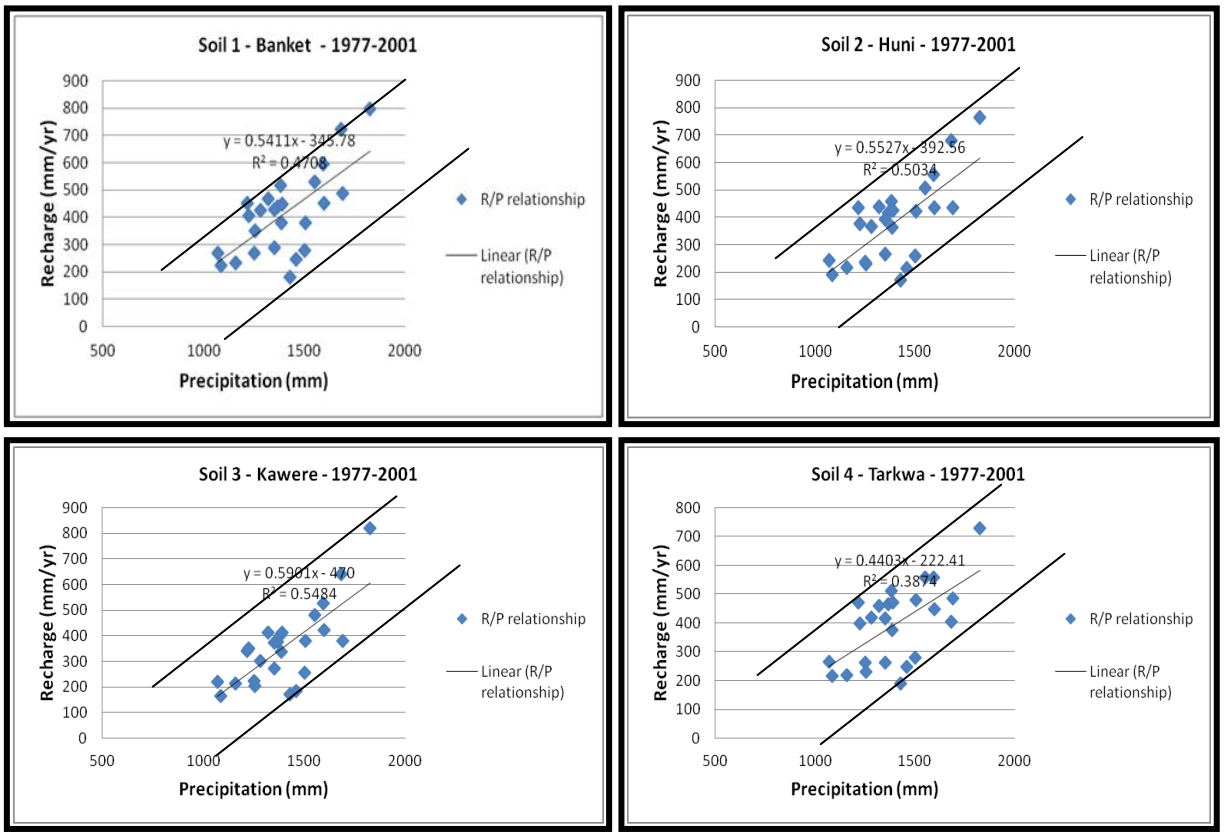

Figure 4.12 Variations of mean annual recharge with precipitation rate for soils 1 to 4 of Tarkwa District in South Western Ghana.

Results of the linear regression analysis of the above recharge-precipitation relationships are tabulated in Table 4.7 for the entire study area consisting of the four main soil types. Close observation of the results show that the coefficient of correlation of the linear relations is 0.72 for the study area and for the four main soil type the coefficient of correlation from the lowest, ranges from 0.39 to 0.55 with respect to soil 4, 1, 2 and 3.

It should be noted that negative c means that there is a threshold rainfall needed before recharge occurs, and that this threshold is quite large, from -222 to -470 making %P less meaningless when taken into consideration the low correlation between recharge and precipitation. Thus the high value of c may simply be that the relationship is not linear really, and therefore we should not extrapolate to P values below the lowest as seen in the data sets.

Table 4.7 linear regression analysis of recharge-precipitation relationships of study area for the period, 1977-2001

Soil Type	Mean annual recharge R	Mean annual precipitation P	% of Ann. Precip.	m	c	R^2
Soil 1- Banket	411	1398	29.40	0.54	-346	0.47
Soil 2 - Huni	380	1398	27.18	0.55	-393	0.50
Soil 3- Kawere	355	1398	25.39	0.59	-470	0.55
Soil 4 -Tarkwa	393	1398	28.11	0.44	-222	0.39
Study Area	406	1398	29.04	0.58	-399	0.72

R^2=regression coefficient m and c are calibration constants

4.6 Summary and conclusions

Using the Hydrus infiltration model, the mean potential annual recharge to the groundwater system in the Tarkwa District of South Western Ghana has been estimated for the period 1977 to 2001. The estimated recharge rate will be used as an input parameter to the MODFLOW computer code to design a conceptual model and simulate the impact of surface mining on the groundwater flow systems in Ghana (chapter 5).

The recharge estimation was conducted by analysing precipitation recharge for the four main soil types in response to rainfall pattern and distribution of the study area. Simulation results of infiltration recharge rates show linear relationship over the range of precipitation with pretty low correlation coefficient ranging from 0.39 to at least 0.72, with the selected soil type in this study. The variability of annual recharge in the study area may be caused by various reasons including variation in the weather pattern (rainfall, temperature, evapotranspiration etc), topography and hydraulic properties of the aquifer system.

In conclusion, the potential direct recharge rate was estimated to range from 269mm/yr to 611mm/yr (with an average value of 385mm/yr). This is as a result of infiltration of about 18% to 36% (average 27%) of the mean annual precipitation. This high value (385mm/yr) is reasonable on the basis that it represents the potential maximum value of the actual recharge value of 299±72 mm/yr as reported by Kuma et al., (2007).

CHAPTER 5

ASSESSMENT OF POTENTIAL DEROGATION IMPACTS OF MINE DEWATERING ON THE REGIONAL GROUNDWATER FLOW SYSTEM

5.1 Introduction

The main approach in this thesis is to use scoping calculations based on the poorly constrained data sets developed in the previous chapters to determine the likely importance of mines on derogating surrounding areas. As the data are so uncertain and even the detailed conceptual models will vary from site to site, the approach is scoping with the aim to see if generalisations can be made and general rules devised. Hence the emphasis will be on the development and use of the simplest reasonable representation. A previous model for this approach is that taken by Oakes and Wilkinson (1972) when investigating river augmentation (see also Downing et al., 1974).

The main aim of this chapter is to develop and evaluate the simple numerical model which will then be applied in chapter 6 to investigate the possible derogation impacts of open pit mines on regional groundwater flow systems.

The approach in this chapter is therefore to set up a basic model, and investigate the impacts of its various assumptions on its predictions. The basic model is based on the conceptualization shown in Figure 5.1. In this basic model, the pit is located in an infinite homogeneous and isotropic aquifer with uniform recharge and a steady state flow system. The importance of the following factors is then investigated; steady-state, flow below the mine base, seepage faces, variation of K with depth and K anisotropy.

The main variable is radius of impact and two measures of this have been considered (see Figure 5.1): (i) radius of influence (R_e) as estimated by the locus of a drawdown of variable X cm (see below), and (ii) radius of impact (R_i) as defined by the locus of a drawdown of 1m, this being an amount of drawdown likely to be noted by users of wells as well as the impact on surface water systems. The choice of 1m is rather arbitrary, but probably on the conservative side. Measurement of radius of impact is taken from the centre of mine in the horizontal direction at a metre drawdown unless otherwise indicated.

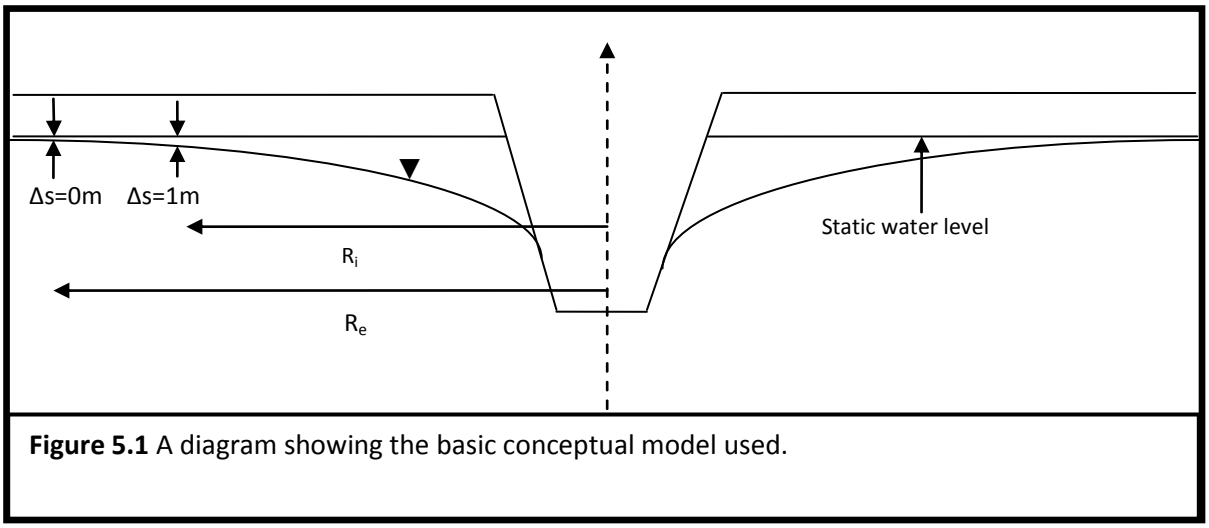

Figure 5.1 A diagram showing the basic conceptual model used.

The chapter has been scheduled as follows;

1. The numerical codes used are briefly discussed in section 5.2
2. Section 5.3 describes the base numerical MODFLOW model and sets the scene by presenting some preliminary results.
3. Section 5.4 investigates the main assumptions of the model of section 5.3:
4. Section 5.5 compares the numerical model with an analytical model
5. Section 5.6 summarises and concludes.

5.2 Computer Codes Used

5.2.1 Introduction

Two numerical codes have been used, the MODFLOW finite-difference and SEEP/W finite-element computer codes.

In the following subsections the description of the capabilities and weaknesses of the two numerical codes are discussed.

5.2.2 The MODFLOW 2000 Computer Code

The MODFLOW finite-difference numerical computer code is one of the most common simulation codes that have been widely used in simulating local and regional groundwater

flow phenomena. In recent times, the MODFLOW numerical modelling code has been shown to be reliable and versatile in simulating aquifer systems in which; (1) saturated flow conditions exist, (2) Darcy's Law applies, (3) the density and the viscosity of the groundwater does not vary, and (4) the principal directions of horizontal hydraulic conductivity or transmissivity do not vary significantly within the system (McDonald and Harbaugh, 2000).

The above conditions are appropriate for many aquifers for groundwater flow analysis is being undertaken, of which the current study is not an exemption. MODFLOW has the capability of simulating a wide range of hydrogeological processes and conditions (McDonald and Harbaugh, 2000). These features include drains, streams, lakes, springs, wells, and evapotranspiration, and recharge from precipitation and irrigation can also be simulated. MODFLOW has not less than four solution methods for solving the finite-difference equations that it constructs (McDonald and Harbaugh, 2000). The availability of different solution methods allows a user to select the most efficient for their particular problem. According to McDonald and Harbaugh (2000), the major limitations of MODFLOW are that the model cannot provide a water budget for the full hydrologic cycle because the unsaturated zone and overland flow are not simulated. Moreover, MODFLOW does not calculate evapotranspiration, infiltration, unsaturated zone flow or recharge (which is calculated separately). Also with certain model geometries and property values, including some which are relevant to the current project, modelling convergence issues arise especially with low K-values and three dimensional models.

With regards to the present study, Groundwater Vistas 6.20 Build 5, a model-independent graphical design system for MODFLOW and other models, has been used. A unique aspect of Groundwater Vistas is its use of grid independent boundary conditions which do not change position as the grid is modified. This allows for major changes to the meshing to be made without wasting time repairing the location of boundaries. In the current studies Groundwater Vistas has been used to display the model design in both plan and cross-sectional views using a split window. Model results are presented using contours, velocity vectors and detailed mass balance analyses.

5.2.3 The SEEP/W Computer Code 2007

The SEEP/W finite-element numerical computer code is part of a GEO-STUDIO package, a suite of commercial software used for geotechnical and geo-environmental engineering - SLOPE applications (GEO International Limited, 2007). According to the SEEP/W manual, this computer code can be applied to the analysis and design of geotechnical, civil, hydrogeological, and mining engineering projects by utilising the finite element method to solve the relevant boundary value problem. SEEP/W is used for analyzing groundwater seepage and pore-water pressures within soil and rock. It is capable of dealing with saturated-unsaturated time-dependent problems as well as saturated steady state problems.

Apart from conventional steady-state saturated flow analysis, the saturated/unsaturated formulation of SEEP/W makes possible the analysis of transient seepage and infiltration of precipitation (GEO International Limited, 2007). The transient feature allows the analysis of problems such as the migration of a wetting front and the dissipation of excess pore-water pressure (GEO International Limited, 2007). Furthermore, the SEEP/W can simulate heterogeneous hydraulic properties in anisotropic and heterogeneous flow systems, as observed by Ardejani and Singh (2004). SEEP/W allows the generation of finite element meshes by drawing regions on the screen and interactively applies boundary conditions and specifies material properties. SEEP/W offers various viewing options, once the task under investigation is solved. These include the plotting of contours of any computed parameter, e.g. pressure, head, velocity, gradient and permeability. SEEP/W shows transient conditions as the changing water table position over time (GEO International Limited, 2007) and the final can then be exported into other applications, such as Microsoft Excel or Word, for further analysis

Despite the preceding capabilities, the SEEP/W computer code has its own limitations, since it was developed to consider specific conditions. For instance, SEEP/W is formulated only for flow that is consistence with Darcy's Law and it is best suited for vertical cross-sectional models and lacks flexibility in recharge input. Also, vapour movement is not included (GEO International Limited, 2007).

5.3 Design of base numerical MODFLOW model

5.3.1 Introduction

This section describes the basic MODFLOW representation used to investigate the effect of a mine in a regional aquifer. Not all assumptions are discussed as some will be investigated in more detail in section 5.4. This section also presents a few example results.

5.3.2 Model and Model Assumptions

In the current study, some of the many assumptions made in the design process are due to the nature and limitations of the flow models themselves. Other assumptions regarding the geology and mining history have also been made due to data limitations. For instance, the deeper aquifer sequences in hard rock environments in Ghana are dominated by fracture flow (Kuma; 2007), but the modelling of fractures is beyond the scope of the present study because the geology of the Birimian and the Tarkwaian systems in Ghana are complex and detailed field data on fracture geometry and geo-hydrological characteristics is non-existent.

The model structure adopted is therefore based on a very simplified conceptualization of the groundwater flow system in the mining environments in Ghana. The weathered and fractured rock formations were modelled as equivalent porous media with any shallow weathered zone simply being represented as a more permeable part of the same system. Thus, it is assumed that groundwater flow can be described by use of a three-dimensional flow equation based on Darcy's Law. In this approach, the hydraulic conductivity used in the model represents the bulk property of the fractured rock formation. Flux of water through fractures of the rock mass is simulated as distributed throughout the formation. The model is approximated to represent regional flow controlled by a large density of fractures. This is because the model is not capable of simulating localized groundwater flow controlled by permeable fractures. More also, the aquifer is assumed to be unconfined in nature and groundwater occurs under water table conditions.

Potential recharge to the model is assumed to be spatially uniform because no detailed spatial information is available in the mining environments of Ghana. On the average, potential recharge to the water table was calculated as precipitation minus surface runoff and evapotranspiration in chapter 4. Surface run off was due only to rejection of rainfall due

to the permeability of the near surface soils, and any rejection of recharge due to filling up of the aquifer from below was not considered and needs to be considered in the numerical model. Areal recharge enters through the top model layer.

Unfortunately in this study, it has not been possible to develop a transient model due to general scarcity of hydrologic information, for example lack of historical water level data against which to calibrate any model developed. Moreover, no groundwater flow models are known to exist in the area as indicated by Kuma (2006) and Lutz et al. (2007) and for this reason, steady state groundwater flow conditions are assumed, but this assumption is investigated in section 5.4.

5.3.3 Model hydraulic and recharge parameters used

The model parameters used for the model design were estimates of mine geometry, hydraulic conductivity and potential groundwater recharge obtained from summary results of chapters 2, 3 and 4 of this thesis. The results of research conducted in Chapter 2 on the geometry of open-pit mines in Ghana indicated that on the average, depth of most open pits hovers around 300m. It was also realised that on the average, most open pits in Ghana and elsewhere in the mining environments assume a rectangular shape in plan-view of dimensions which range from 500 to 2000m.

Statistical characterisation of hydraulic conductivity values in chapter 3 table 3.6 gave distribution parameter values for the combined international dataset (e.g., central tendencies and spread) applicable for the calculations of groundwater flow near mines. Summary statistics of K-parameter values range from **$1.40\text{x}10^{-13}$** m/s to **$1.45\text{x}10^{-03}$** m/s with an overall mean, median, standard deviation and a geometrical mean of **$1.48\text{x}10^{-05}$** m/s, **$3.80\text{x}10^{-09}$** m/s, **$9.74\text{x}10^{-05}$** m/s, and **$1.57\text{x}10^{-08}$** m/s respectively. The K values used in the modelling process have been chosen bearing these figures in mind. In chapter 4, potential groundwater recharge is estimated to range between 18% and 36% (an average of 27%) of the mean annual precipitation in south western Ghana where there is greater concentration of open pit mines. This translates to an average annual potential recharge rates ranging from (269 - 611) mm/yr with an average rate of 385mm/yr. This high value is on the basis only of considering the soil system and the actual value of recharge may be much lower.

Recharge is input as an areally distributed value across the model. In general a value of 300 mm/y has been used. This is lower than the mean value obtained in chapter 4, but is close to the value suggested for actual recharge by Kuma et al. (2007). A lower value in general leads to a conservative estimate of radius of impact. However, the sensitivity to potential recharge rate is investigated in chapter 6 and it is shown that the difference between 300 and 385 mm/y is negligible in the present context.

5.3.4 Numerical model design using MODFLOW 2000 computer code

The numerical model has been set up using the Environmental Simulations International (ESI) modelling package, Groundwater Vistas 6.20 Build 5. MODFLOW-2000 was initialized and a grid system was developed. A model domain of size 25km by 25km area was discretized into 2500 cells with 50 cells in the x-direction (Δy=500m) and 50 cells in the y-direction (Δx=500m). Decreasing cell dimensions affects heads close to the mine as expected, but makes little practical difference to the estimate of radius of impact. The bottom and top elevations of the model domain were usually taken to be 0m and 500m, respectively. All horizontal grid boundaries were initially taken to be no-flow boundaries and located to be far enough from the main areas of interest in the middle of the domain to have no effect on drawdowns. The effects of boundaries has been investigated and discussed in chapter 6. Also, the bottom boundary was assumed to be a no-flow boundary because it is assumed that at such depth, hydraulic conductivity had decreased significantly, compared with the values in the upper aquifer. For the basic model, an open pit of dimensions measuring 2000 x 1000m in plan-view and 300m deep is placed at the centre of the model domain (see Figure 5.2).

An average annual potential recharge rate (R) of 300 mm/y was input as areally distributed values across the model. In order to keep the flow heads below the surface of the modelled domain, the evapotranspiration package was used. A notional value of evapotranspiration (0.009m/d (or sometimes 0.0009 m/d) with extinction depth at 498m and ET surface at groundlevel) was chosen to be more than the recharge value (0.000819m/d). The concept is that when all the recharge cannot enter the aquifer, the rest runs off, the ET package being used to remove the excess water. When recharge is in excess, as it is expected to be in this system, the water level remote from the mine will be held at the elevation of between the

extinction depth and the ET surface, the exact location depending on the 'evapotranspiration' rate / recharge rate ratio. The choice of extinction depth and ET rate affect the final water level and the recharge rate, and therefore potentially the radius of influence and accordingly this variable is investigated along with total recharge rate. MODFLOW was then simulated for steady state conditions to assess the area of impact (the radius of influence) in the presence of the mine. The various solvers (Preconditioned Conjugate Gradient Package (PCG2), Slice Successive Over-relaxation Package (SOR), and Strong Implicit Procedure Package (SIP)) available within the computer code were used in running the model; the default solver did not converged on several occasions, whereas PCG2 gave good results comparatively.

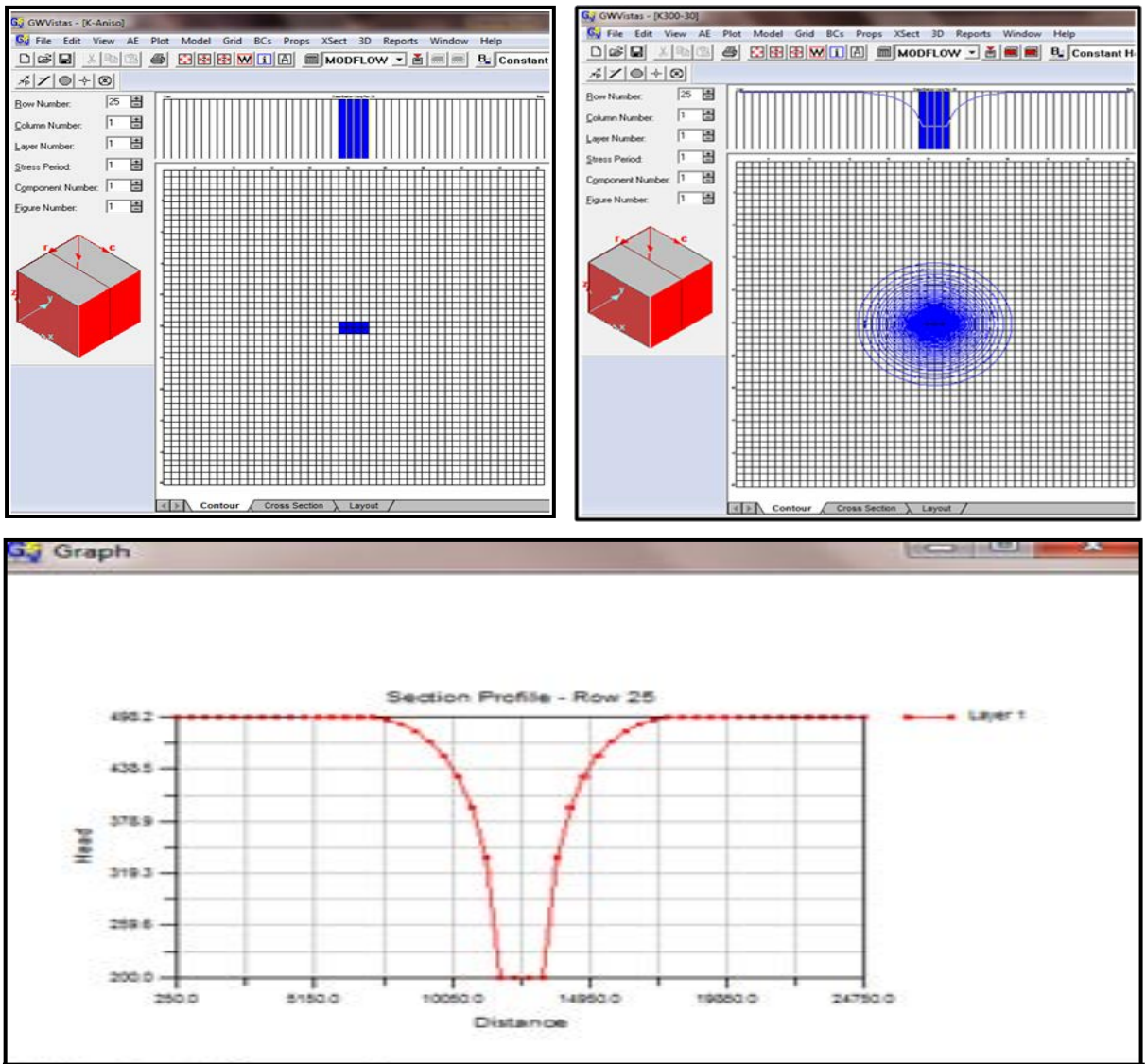

Figure 5.2 (Top): Plan and cross-sectional view of model domain and head contour profile, and (Bottom): Sectional profile of heads through the mine.

5.3.5 Example calculations of impact assessment with single-layer MODFLOW models

In this section a few example calculations are provided to illustrate the results from this simple model. The bottom and top elevations of the example model domain were taken to be 0m and 500m, respectively with head of water in mine fixed at 300m from the bottom. In order to keep the flow heads below the surface of modelled domain, the value of evapotranspiration (0.0009m/d with extinction depth at 498m) was chosen to be more than the recharge value of 0.000819m/d so that any excess water can be removed from the system as soon as there is surface ponding. A hydraulic conductivity value of $3.8x10^{-04}$m/d (4.4×10^{-9} m/s) was used. The results are given in table 5.1 (model 1).

Table 5.1 The effect of varying K by about a factor of 5 and 10, respectively on the radius of impact in a mining environment

	Model 1 (base model)	Model 2	Model 3
K (m/d)	$3.8x10^{-04}$	$1.9x10^{-03}$	$3.8x10^{-03}$
R (m/d)	$8.19x10^{-04}$	$8.19x10^{-04}$	$8.19x10^{-04}$
ET(m/d)	$9x10^{-04}$	$9x10^{-04}$	$9x10^{-04}$
R_i (m)	**1130**	**1412**	**1638**

To illustrate the system further, the hydraulic conductivity has been varied to see the general effect on the radius of influence. It was observed that in general, the radius of influence increases with increasing hydraulic conductivity values. As permeability increases, hydraulic heads drop and increase outwardly from mine and this indicates an increasing effect of radius of influence. For example in Table 5.1, an increase in the radius of impact of approximately 282m to about 508m is observed for an increment of 5 to 10 times the value of hydraulic conductivity. These runs of the model are illustrative only, as this chapter is concerned with setting up the models and looking at their assumptions. The results of applying the models will be mainly considered in chapter 6.

5.4 Assessment of the main assumptions of the basic numerical model

5.4.1 Introduction

Before using the models of section 5.3, the importance of the following assumptions of these models is investigated:

1. whether flows at all times can be considered as steady-state
2. whether a fully-penetrating constant head at the mine is appropriate
3. whether seepage faces affect the radius of influence significantly
4. how significant variation in hydraulic conductivity with depth is
5. how important hydraulic conductivity anisotropy is, in the vertical plane (the horizontal effect is examined as part of the examination of the model in chapter 6)

The aim of this section will be to determine whether these assumptions affect the results significantly and whether the base model is likely to over or under predict the radius of influence. The assumptions will be examined as listed above in sections 5.4.2 to 5.4.6.

5.4.2 Assumption of steady-state flow

In the present study, the assumption that whether flows at all times can be considered as steady-state in the mining environments in Ghana has been investigated by considering the time it may take for a system to adjust to a new mine base after dewatering. The steady-state assumption implies that uniform recharge to the water table and discharge to mine pits are in equilibrium and that hydraulic head is not changing in time. In the case of mine dewatering, the radius of impact R_i (cone of depression) does not expand under steady-state conditions since recharge rate equates discharge. Hydraulic conductivity and storage are the two main aquifer properties that allow quantitative time-variant prediction of the hydraulic response of the aquifer to recharge and discharge to be made. For example, storage coefficient is important for understanding hydraulic response to transient stresses on aquifers and indicates how fast a dewatered aquifer system recovers to steady state conditions. These parameters may vary spatially because of geologic heterogeneity, for instance decreasing with depth for a fractured aquifer system. For unconfined aquifers, specific yield is taken often to be 1-10% while the elastic storage coefficient ranges often from 10^{-5} to 10^{-4} (Lohman 1972). To determine reasonable inputs for the construction of models for the current investigation, aquifer parameters of hydraulic conductivity and storativity are considered. Storativity value of 10 percent (0.1) and one percent (0.01) for

the top weathered zone and the fractured zone respectively which according to Driscoll (1986) is a reasonable value for fractured bedrock aquifers are assumed. Based on the MODFLOW computer model described in section 5.3, four different models were constructed to simulate the time taken for a mine base to stabilise to steady state conditions when the mine is dewatered and the base is suddenly dropped to a new mine base. Modflow is initiated from a constant head everywhere and the changes in head with time simulated for monitoring wells placed at distances from the mine (Figures 5.3 and 5.4). In Table 5.2, aquifer parameters used and measurements of time taken for system to stabilise to steady state conditions are recorded. It is observed that generally, the time taken for the system to stabilise to a new mine base after dewatering increases with increasing distance from mine for both weathered and fractured zone but with longer duration for the weathered zone due to the higher storage coefficient, as expected. For instance, within a distance of 5km from mine, it took the top weathered zone of the aquifer system almost 10 years to recover to steady state conditions whereas it took just a year for the fractured zone. Following the above observation and taking into consideration the period of development of a typical mine in Ghana (at least 30yrs), it can be concluded that steady state flow conditions could be assumed for the mining environments in Ghana and therefore the current impact assessment. Errors will tend to be such to lead to overestimation of radius of impact.

Table 5.2 Measurements of time taken for a new mine base to stabilise to steady state conditions after mine dewatering for monitoring wells placed at various distances from mine

	Model 1	**Model 2**	**Model 3**	**Model 4**
Bulk layer hydraulic conductivity K (m/d)	$1.57x10^{-3}$	$1.57x10^{-3}$	$1.57x10^{-3}$	$1.57x10^{-3}$
Horizontal distance/m of monitoring well from mine	2000	3000	4000	5000
Time taken for system to stabilise for a weathered zone (StorageS=Sy=0.1)	2000 days (5.5 years)	2500 days (6.8years)	3000 days (8.2 years)	3500 days (9.6 years)
Time taken for system to stabilise for a fractured zone (storageS=Sy=0.01)	200 days (6.3 months)	250 days (8.3 months)	300 days (10 months)	350 days (12 months)

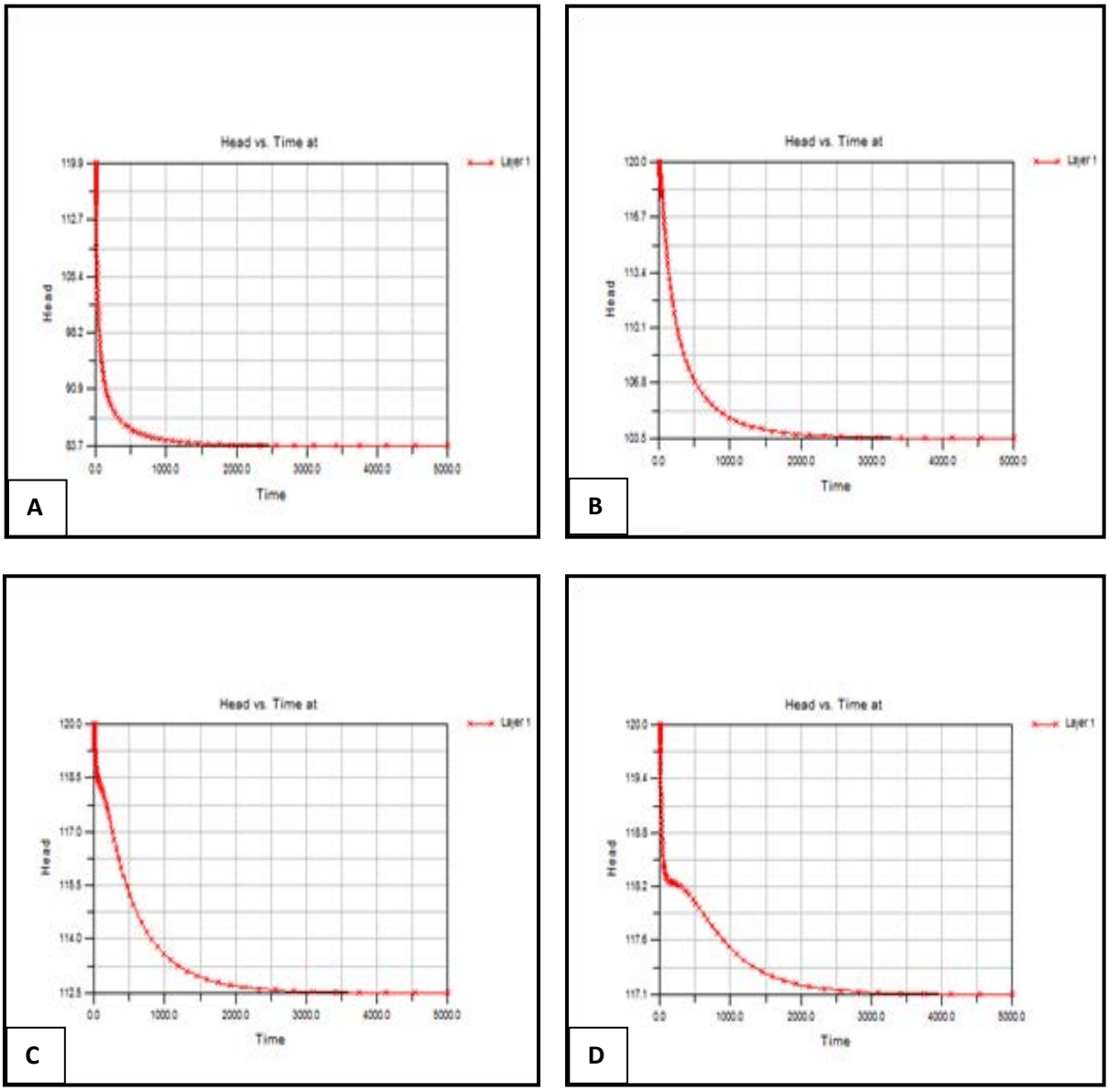

Figure 5.3 Time-drawdown plots (in days) assuming weathered zone properties (storage S=Sy=0.1) showing time (days) taken for heads to stabilise from an initial head of 120m to 30m (mine depth of 90m), measurements taken at various horizontal distances; A (400m), B (600m), C (800m) and D (1000m) from mine. The kink most clearly shown in C and D results from the ET extinction depth control

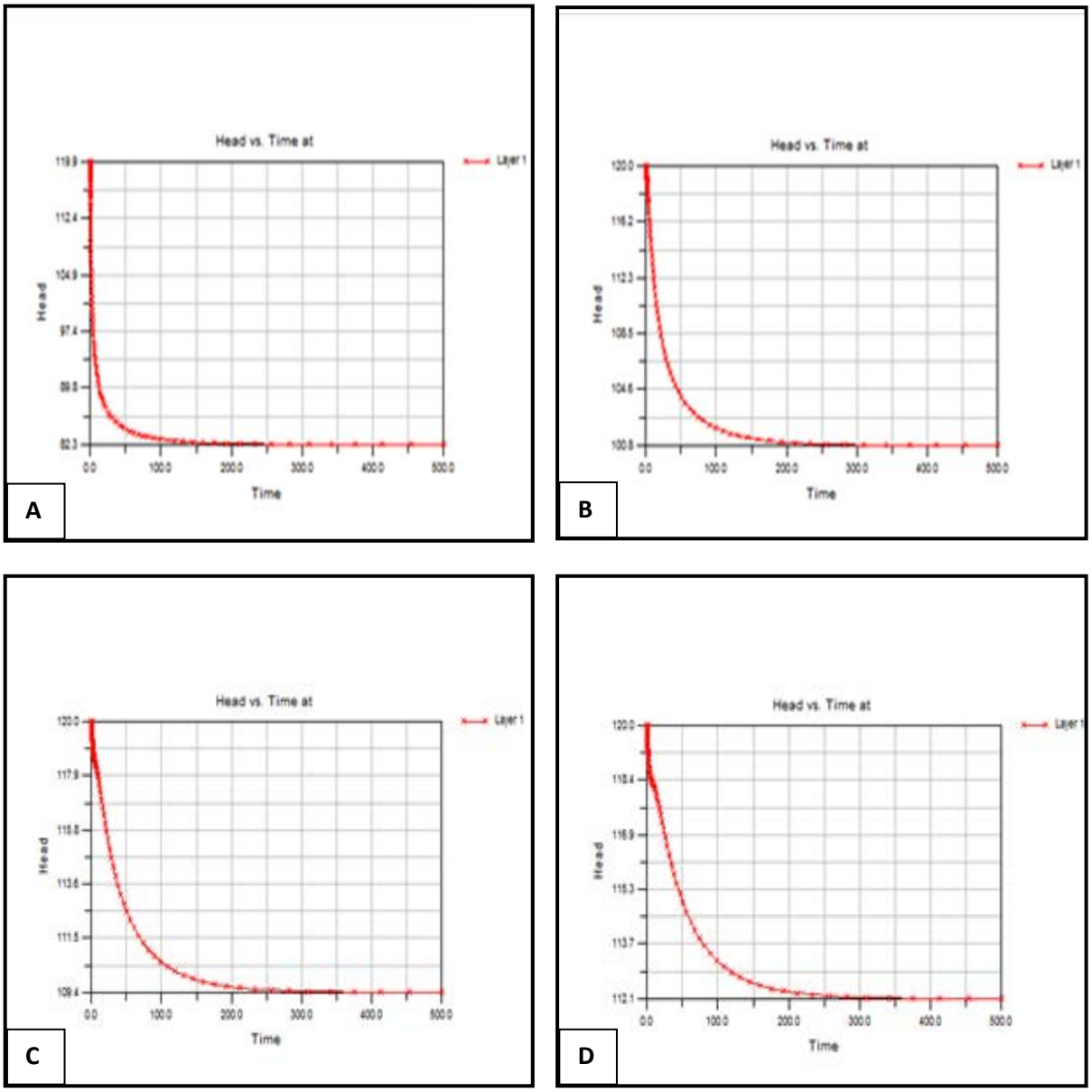

Figure 5.4 Time-drawdown plots (in days) assuming fractured zone properties (storage S=Sy=0.01) showing time (days) taken for heads to stabilise from an initial head of 120m to 30m (mine depth of 90m), measurements taken at various horizontal distances; A (400m), B (600m), C (800m) and D (1000m) from mine

5.4.3 Assumption of a fully-penetrating constant head to represent the mine

The MODFLOW model does not take into account the flow of the water below the constant head. One simple way of investigating if this may be of significance is to use a drain node in place of the constant head. This has been done for a few example models of an aquifer of thickness 500m, recharge 0.000819m/d and ET of 0.0009m/d and the results are shown in

table 5.3. The drain conductance were calculated with K = rock K, thickness =nominal, small distance of 1m. Table 5.3 indicates that representing the mine with the drain conductance affect the calculated radius of influence by reducing it. This reduction is significant at very high conductivity systems but not significant at low conductivity systems for the geometry investigated. This suggests that the basic model over-estimates the radius of influence. Though this means the basic model is probably less accurate, the estimates of radius of influence will include some degree of safety.

Table 5.3. Simulation results of the effect on the radius of influence of assumption of a fully penetrating constant head (drain) to represent the mine (partially penetrating constant head of 200m) by varying the hydraulic conductivity of base model by 20%.

Input parameters	Base Model 1		Base Model		Model 2	
	Drain	Fixed Head	Drain	Fixed Head	Drain	Fixed Head
Stage (m)	200		200		200	
Width (m)	500		500		500	
Length (m)	500		500		500	
Thickness (m)	1		1		1	
K (m/d) X 100, 10, 1	0.38	0.38	0.038	0.038	0.0038	0.0038
Radius of impact R_i (m)	5989	6959	3080	3137	1654	1825

5.4.4 Impact assessment of assumption of no seepage face

The occurrence of a seepage surface above the water level in a dewatered open-cast mine may have an impact on the groundwater flow regime and hence the radius of influence of the mining operations. Seepage surfaces frequently occur in dewatered mines in unconfined aquifers. In the report of Sakthivadivel & Rushton (1989) the presence of a seepage surface can be identified visually in the slope sides of large diameter wells or mine-pits with water entering slowly from the wet aquifer and moving down the mine surface to the dewatered water level. Seepage face is a less efficient means of drawing water into an open pit than when the water column extends over the full depth of the aquifer (Babbitt and Caldmine, 1948; Rushton, 2006).

The problem of seepage faces is connected to the Dupuit assumption for modelling groundwater flow (e.g. Raudkiwi and Callandar, 1976; Rushton, 2006). This assumption is that the velocity is constant throughout the flow depth with the flow horizontal. This assumption produces good estimates of flow rates to pumping wells but the heads are not well predicted close to the well. For larger systems such as open pit mines the errors for water table may be less pronounced unless water table gradients are particularly steep that may be the case near the pits. But at distance the heads obtained using the Dupuit assumptions (e.g. in one layer models such as used here) are close to those predicted by multi-layer models where vertical flow variations are taken into account (Rushton, 2006).

In the current study, the importance of seepage surface under steady state condition of flow in unconfined aquifers in the mining environments in Ghana has been investigated. The SEEP/W computer code which has the functionality to model seepage surfaces has been used to determine whether seepage surfaces could be developed at the side slope of open pits aquifer systems. The model shown in Figure 5.5 has been used to create the simulations. Important to this type of analysis, is the hydraulic boundary condition on the seepage surface. The boundary condition is set to be a no-flow boundary condition (Q=0) with a potential seepage surface. This means, the boundary condition does allow water out of the system if the pressures are positive or zero, but does not allow water to exit the aquifer if the rock has negative pressures. It is important to note that although flow around mine pits is approximately radial, linear flow geometry has been simulated and this is because the SEEP/W computer code is best suited for vertical 2-dimension cross-section models (GEO International Limited; 2007). Moreover, the adjacent boundary conditions do not allow quantitative measurements of the radius of influence to be made. The effects of the mine on the radius of influence have therefore been qualitatively assessed through changes in water level.

The model design represents a partially penetrated open-pit of vertical cross sectional area of dimensions L x H = 2000m x 300m in a single layer unconfined aquifer of thickness 600m. The model domain is discretized using predominantly quadrilateral and triangular mesh of 3229 nodes and 3055 elements with a global element size parameter (a numerically robust default discretization system that controls the meshing size) of 30. A uniform hydraulic conductivity within the upper permeability zone of 1.48×10^{-8}m/s is used for the unconfined

aquifer. The hydraulic conductivity is represented as a function of the pore water pressure in order that unsaturated conditions can be simulated. In fact, SEEP/W has an in-built predictive method that is used to estimate the hydraulic conductivity function by specifying the volumetric water content function and the K saturation value and for the current simulation the result is shown in figure 5.6. This representation is more likely to be correct in weathered material than fractured material, so more correct for shallow water tables.

The following boundary conditions have been assigned to the model: no-flow boundary condition at the outer ends and bottom boundaries to represent impermeable boundaries in the aquifer. A fixed-head boundary condition of value 300m is specified at the pit's bottom. A surface flux boundary condition of a steady-state infiltration rate of 300mm/yr ($9.5x10^{-9}$m/s) net infiltration is specified along the top of the aquifer. In fact, SEEP/W is formulated for saturated-unsaturated flow, making it possible to deal with infiltration, evaporation and runoff at the ground surface and hence recharge can be rejected. Along the side slope of the mine the boundary condition is set to be a no-flow boundary condition with a potential seepage face as described above. A two-dimensional vertical flow simulation was then performed under steady-state condition. The results obtained to analyse include; total head contours, velocity vectors, the location of the water table (the zero contour pressure head) and the total inflow rate to mine.

In Figure 5.7, simulation results of models constructed with and without seepage representation are shown. Model 1 and model 2 represent simulations with and without seepage surface respectively whiles models 1a and 2a are the magnified representation of model 1 (with seepage surface) and model 2 (without seepage surface). Comparison of simulated models revealed that seepage face has no significant effect on the flow and the extent of impact of the free water surface. The zero pressure contours meet the surface very close to the bottom of the mine for both representations and also there is no significant change in flux within the aquifer system and inflows (within 1%) into the mine between the two representations. Moreover, the head contours for both representations are at the same distance from the mine indicating that groundwater seepage has no significant effect on the flow regime, and hence the radius of mine impacted area.

This has not been a comprehensive investigation of seepage face effects as a wide range of properties have not been varied and the flow to the mine has been assumed to be linear. However, further models constructed using SEEP/W during the investigation of hydraulic conductivity anisotropy and change with depth have also not shown any significant effect when seepage faces have been used. Examination of the work on seepage faces in wells (Rushton, 2006), where the small surface area of inflow increases the chance of seepage faces, indicates that seepage faces would decrease drawdown close to the mines but make little effect on drawdown at distance. It is tentatively suggested that seepage faces will have limited effect on the predicted radius of influence.

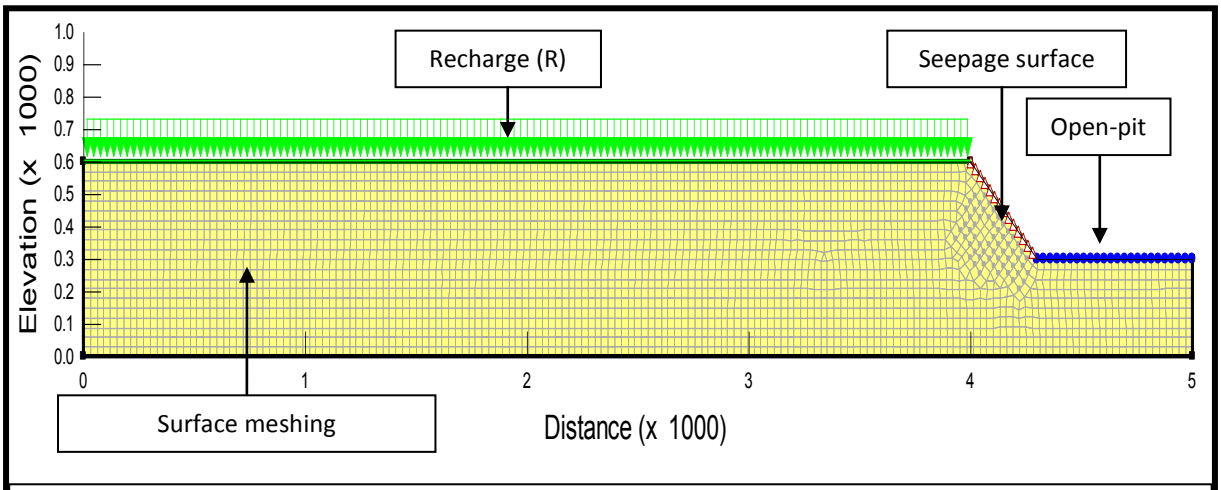

Figure 5.5 Configuration set up of model geometry, meshing, and boundary conditions for seepage analysis

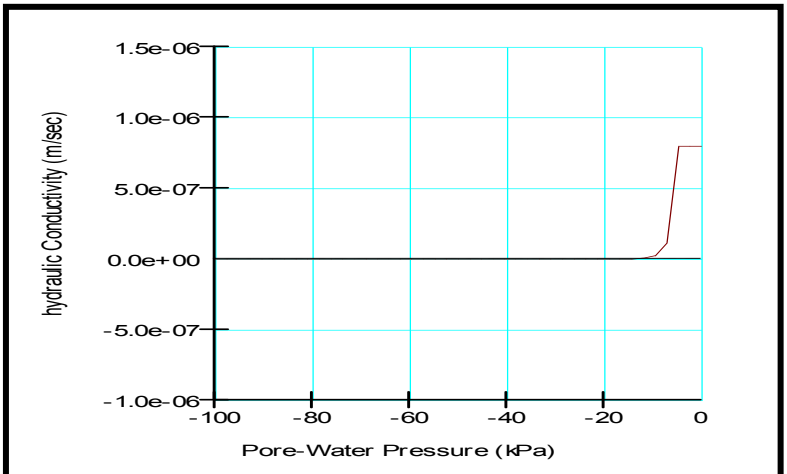

Figure 5.6 Hydraulic conductivity as a function of Pore-Water Pressure

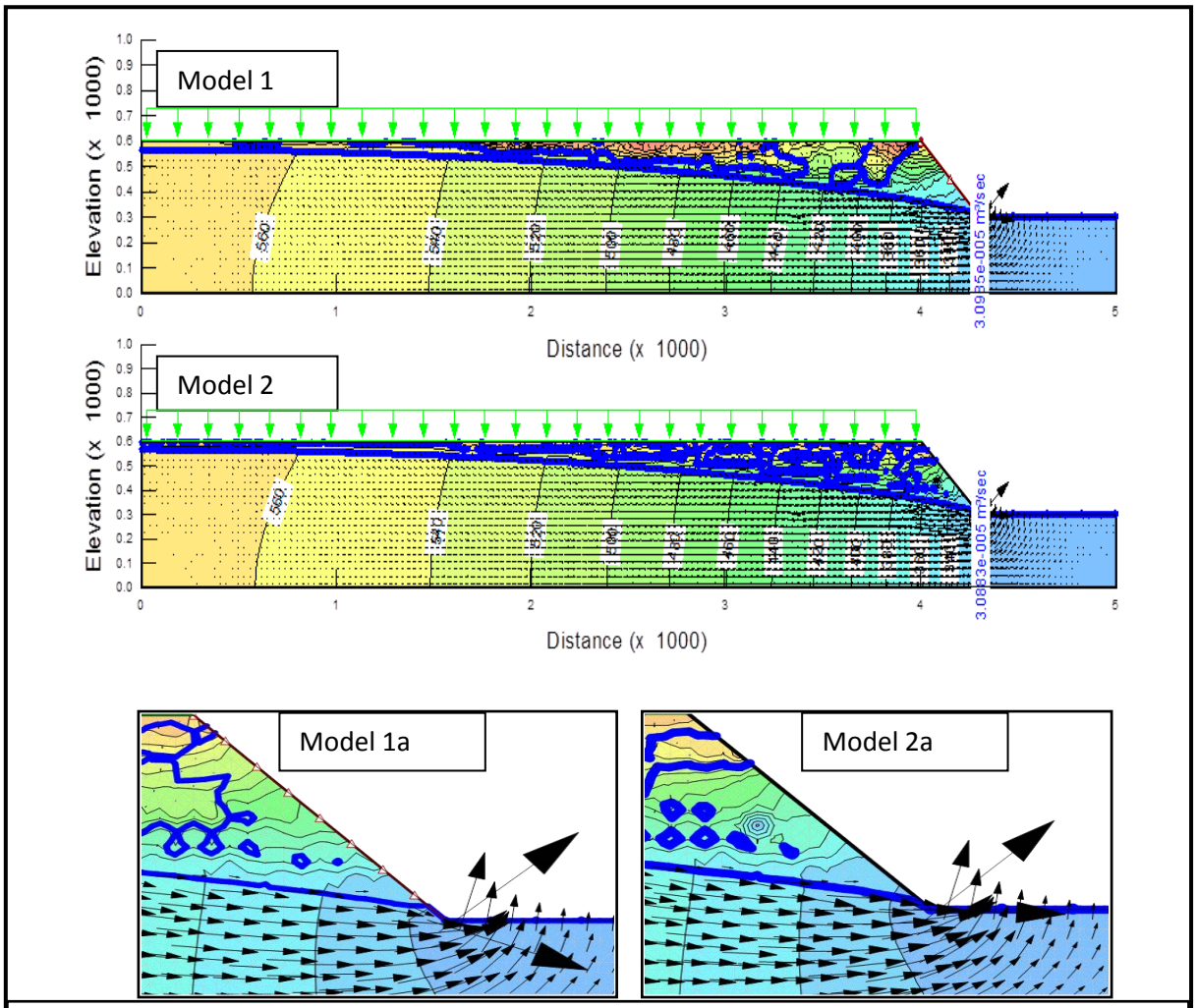

Figure 5.7 Simulation results of impact of assumption of seepage surface (Model 1 and 1a) and impact of assumption of no seepage surface (model 2,2a)

5.4.5 Impact assessment of variation of K with Depth

The characterisation of hydraulic conductivity of hard rock aquifer systems has been extensively dealt with in Chapter 3 of this study. Results show that hydraulic conductivity decreases approximately exponentially with depth from the surface to a depth of about 300m after which there seems to be no significant difference in K-distribution up to 400m depth and beyond (see Figure 5.8).

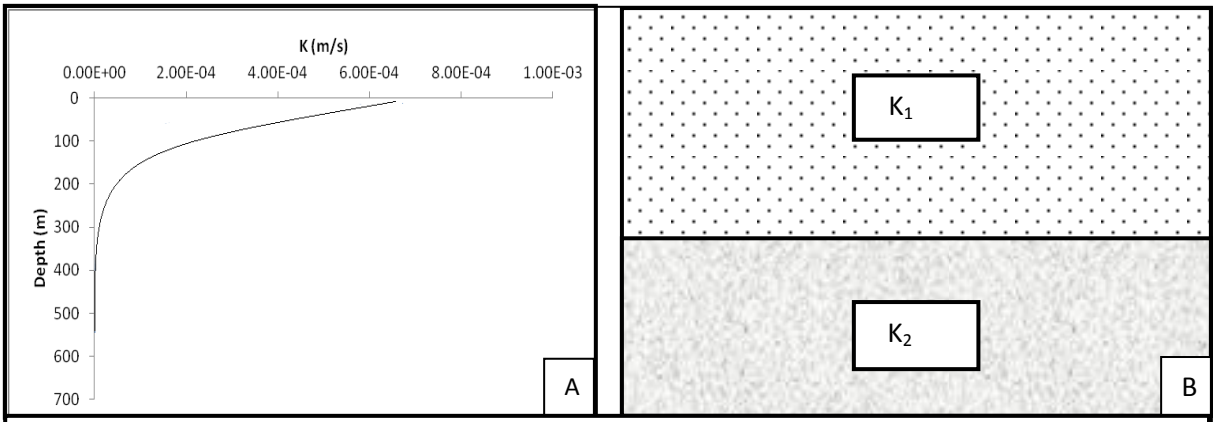

Figure 5.8 Representation of K distributions of hard rock aquifer in the mining environment. (a) general depth trend indicated by international dataset (see Chapter 3); (b) a very simple initial representation of (a).

Based on the above conceptual model of the aquifer system, the SEEP/W computer code has been used to develop four simple steady state models with varying hydraulic conductivity values in order to investigate the effect of K-distribution with depth on the flow rates, water level and the radius of influence (R_e). The models are developed based on the geometry and parameter values of the SEEP/W numerical model described in section 5.4.4. The configuration and set up of the model geometry, mesh, and boundary conditions are shown in Figure 5.9.

A surface flux boundary condition of a steady-state infiltration rate of $9.5x10^{-9}$m/s (300mm/yr net infiltration) is specified on top of each model. Input parameters of hydraulic conductivity and layer thickness used for the various regions are shown in Table 5.4. Steady state K(z) simulation results of total head contours, flow paths, location of the water table (the zero contour pressure head) are presented in Figure 5.10. Simulated mine inflow rates are per metre width of pit margin for each model is measured and recorded in table 5.4. In order to compare the various models run, the overall transmissivity (Kb) of each model is calculated to be approximately the same so as to observe the effect as K distribution changes assuming the whole system is saturated. However there will be possibly important changes in transmissivity in the region near the mine that mean that the models may not be precisely comparable as saturated depth changes. The flows in table 5.4 are specific to the locations indicated in figure 5.10. These locations have been chosen to allow approximate comparison from one model to another, but as the geometry changes this cannot be a

precise comparison. Flow in each layer varies along its length. In particular the flow at the toe of the mine side wall varies considerably with location (see figure 5.7) and the flows indicated at this location are the most uncertain to quantify. Finally, the flows are for the linear flow system modelled and do not take into account convergence in flow towards the mine. Consequently the following discussion relies mainly on the predicted heads.

It is observed that in all four models water infiltrates at the ground surface from precipitation recharge and travels vertically downward toward the water table. The water then travels laterally, primarily in the saturated zone, and discharges into the mine. Although, the total head contours (and consequently the pressure head contours) are very different between the four simulations, the effect on the flow system in the bottom layer (region 1 of each model) is minimal and gradually increases to the surface with increasing K. The water table level of model 1 is the lowest of the models as might be expected as it has high hydraulic conductivity throughout. The water table level of models 2, 3 and 4 is almost the same at the far left boundary suggesting little effect in these cases.

Table 5.4 Input parameter values of K-distribution, layer thickness and simulated flow rates

Model	Number of Layers	Layer conductivity (m/s)	Layer thickness (m)	Flow in each layer per metre width at location indicated in figure 5.10 ($m^3/s/m$)	Mine inflow rate per metre width at toe of mine slope ($m^3/s/m$)
1	1	$K_1=1.0x10^{-6}$	600	$2.32x10^{-5}$	$2.75x10^{-5}$
2	2	$K_2=1.3x10^{-6}$	450	$3.47x10^{-5}$	$2.17x10^{-5}$
		$K_1=1.0x10^{-12}$	150	$2.74x10^{-12}$	
3	3	$K_3=2.0x10^{-6}$	300	$2.75x10^{-5}$	$3.75x10^{-5}$
		$K_2=1.0x10^{-8}$	150	$1.07x10^{-7}$	
		$K_1=1.0x10^{-12}$	150	$3.00x10^{-12}$	
4	4	$K4=3.9x10^{-6}$	150	$2.84\ x10^{-5}$	$3.75x10^{-5}$
		$K_3=1.0x10^{-7}$	150	$2.94x10^{-6}$	
		$K_2=1.0x10^{-8}$	150	$3.42x10^{-7}$	
		$K_1=1.0x10^{-12}$	150	$2.18x10^{-12}$	

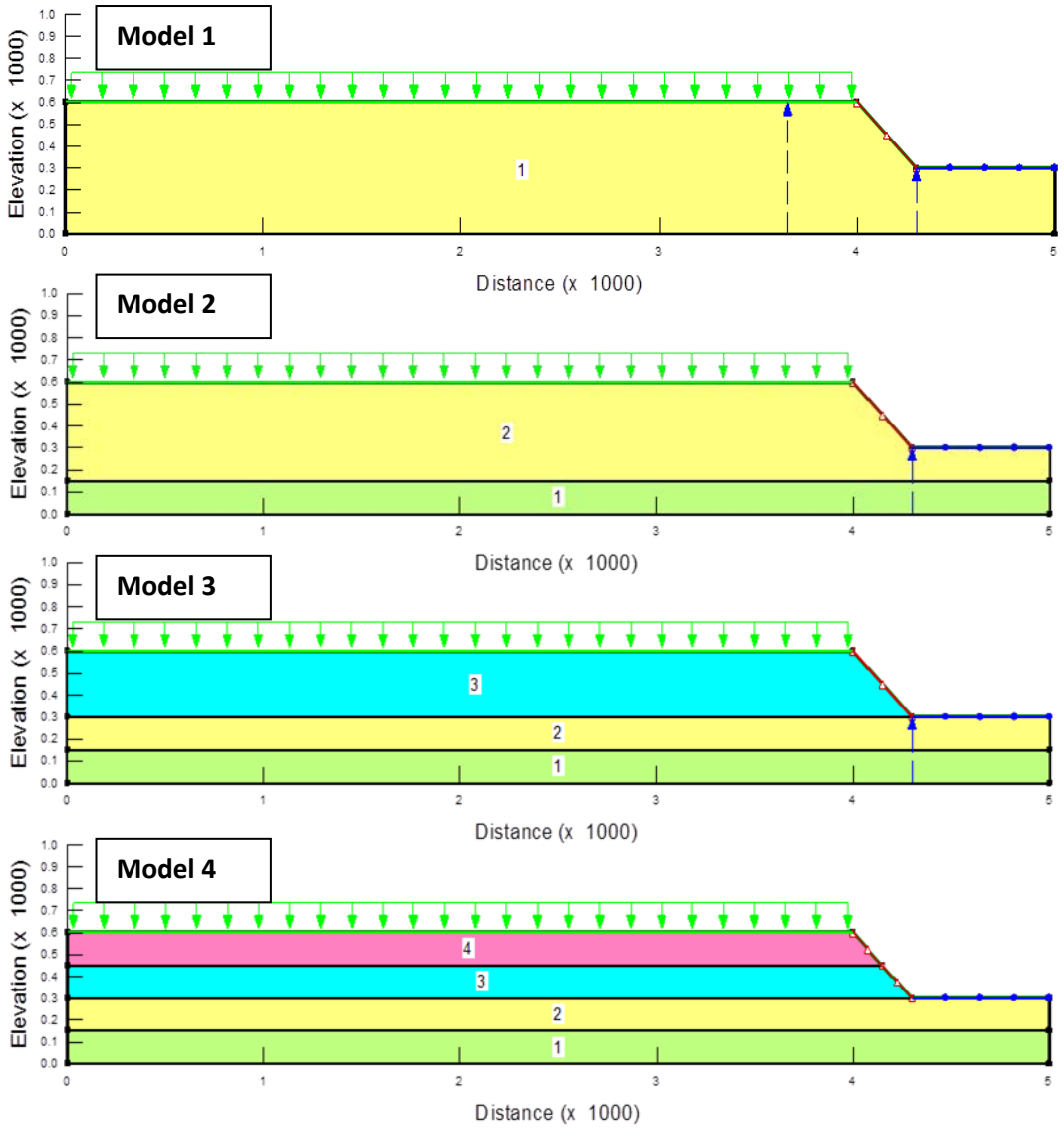

Figure 5.9 A vertical plane configuration and set up of model geometry showing model layers for the K (z) analysis. A fixed-head boundary condition of value 300m is specified at the pit's bottom with no flow boundary condition at the outer ends and bottom. No flow boundary condition with potential seepage face is specified at the side slope of the mine and a surface flux boundary condition of a steady-state infiltration rate of 300mm/yr ($9.5x10^{-9}$m/s) net infiltration specified along the top of the aquifer.

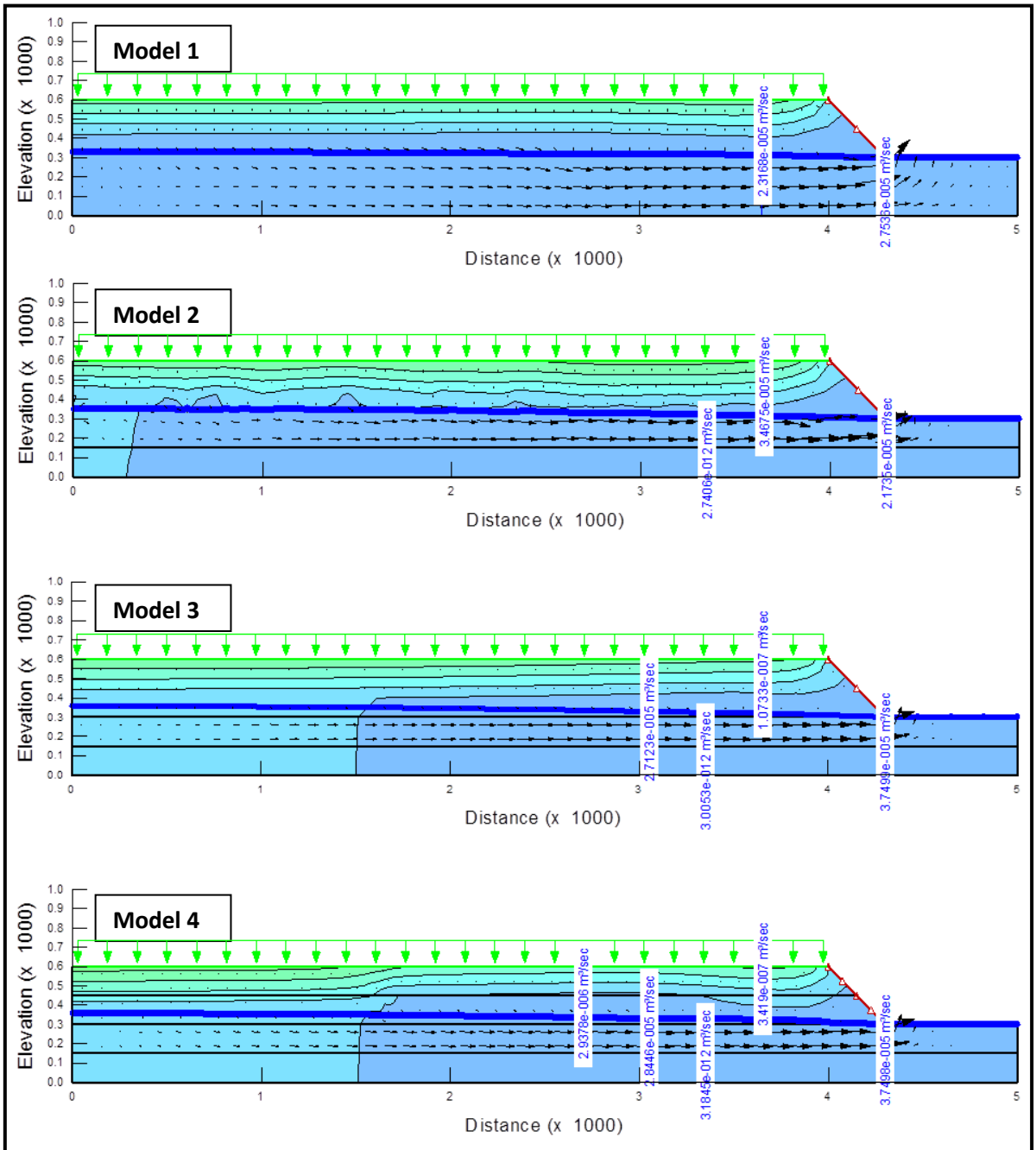

Figure 5.10 Steady-state simulation results showing total head contours, flow paths and flow rates for the K (z) impact analysis.

These results suggest that the distribution of hydraulic conductivity with depth can affect, as might be expected, the radius of influence in some cases for example model 1 compared with models 2 to 4. A constant hydraulic conductivity throughout to depths greater than the base of the mine appears to increase the radius of influence and this may be mostly because the change in K probably affects the zone immediately around the mine most. If this is a general result, then the base model used will tend to overestimate the radius of influence.

The decrease of K-values with depth as indicated in figure 5.10 is probably an indication of the extent of variation and interconnection of fractures in the first 300m of aquifer thickness. To this end, the simplest way that the aquifer system can be represented is as a two-layer model with the upper 300m layer having a higher average K (K_1) and the bottom layer having a lower average K ($K_{2,}$ which approaches zero). However, in further computations in this study 500m depth range has been considered as the average aquifer thickness.

The results of the research conducted in Chapter 2 on the geometry of open-pit mines in Ghana indicated that on the average most open pits do not go beyond a depth of 300m and therefore almost all open-pits in Ghana are assumed to lie within the first upper layer of the simple model of Figure 5.10. Although, the characterisation process in Chapter 3 indicated strong variations in K values within the upper layer, there was much scatter. Taking this into account with the results of the SEEP/W calculations above, it is suggested that the transmissivity will be over-estimated and that predicted radius of influences will also be overestimated. The predictions should therefore be on the safe side.

5.4.6 Assessment of vertical plane anisotropy of hydraulic conductivity

Aquifer anisotropy and heterogeneity, inherent in hard-rock aquifer systems, can affect both the direction and velocity of groundwater flow and hence the extent of impacted area in the mining environments. In this section the effects of K-anisotropy in the vertical plane on hydraulic heads have been investigated by use of SEEP/W. Conclusions are then drawn on the effects on the radius of influence impacted by the mine. An investigation of anisotropy in the horizontal plane will be undertaken in chapter 6 as part of the application of the MODFLOW model.

A model based on the geometry of the SEEP/W numerical model described in section 5.4.4 (figure 5.5) is used to create the simulations. Four scenarios of K-anisotropy ratios (K_y/K_x) = 0.1, 1.0, 10 and 100 are simulated, where K_x and K_y are K-values parallel and perpendicular to a plane dipping at an angle of either 160 degrees (clockwise) or 20 degrees (clockwise). K_y is varied by a factor of 10 keeping (K_x) constant and hence the overall permeability of the sequence changes in most but not all cases. Table 5.5 shows the input parameter values of K anisotropy ratios and input K values. Figures 5.11a and b, present the steady-state simulation results of the effects of anisotropy on the total head contours, flow paths, location of the water table (the zero contour pressure head) and the total flow and mine inflow rates of each of the four models.

Table 5.5 Input parameter values of K-anisotropy ratios and simulated mine inflow rates at 160 and 20 degrees dip in direction clockwise and counter clockwise to the horizontal.

Model	**Input K-function (m/s)**		**K-anisotropy ratio**
	K_x	**K_y**	**(K_x/K_y)**
1	$1x10^{-6}$	$1x10^{-5}$	0.1
2	$1x10^{-6}$	$1x10^{-6}$	1.0
3	$1x10^{-6}$	$1x10^{-7}$	10
4	$1x10^{-6}$	$1x10^{-8}$	100

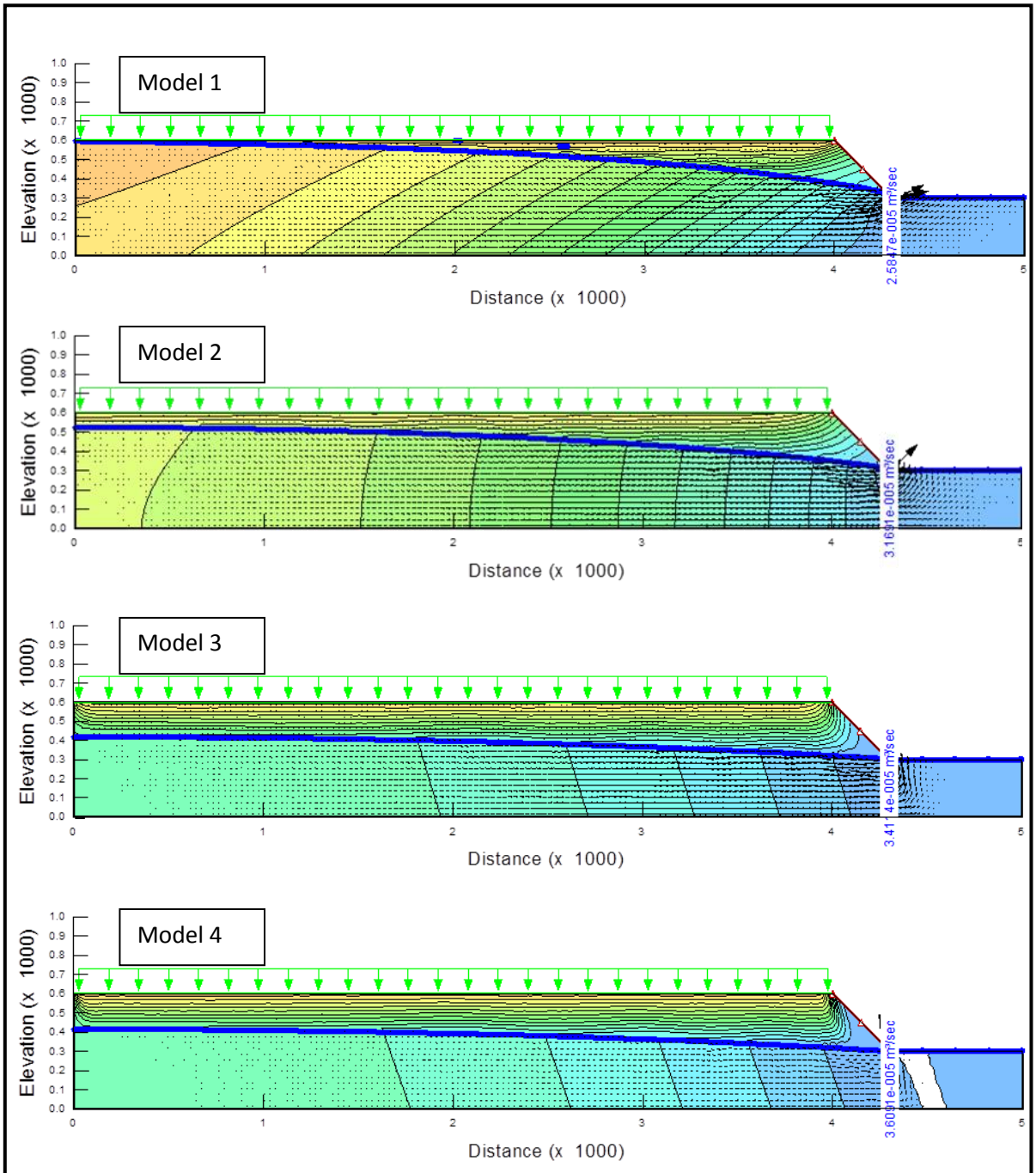

Figure 5.11a Models 1 to 4 represent simulation results of saturated flow through a vertical plane anisotropic system of K ratios (K_y/K_x); 0.1, 1, 10 and 100 respectively, at 160 degrees dip in direction clockwise to the horizontal.

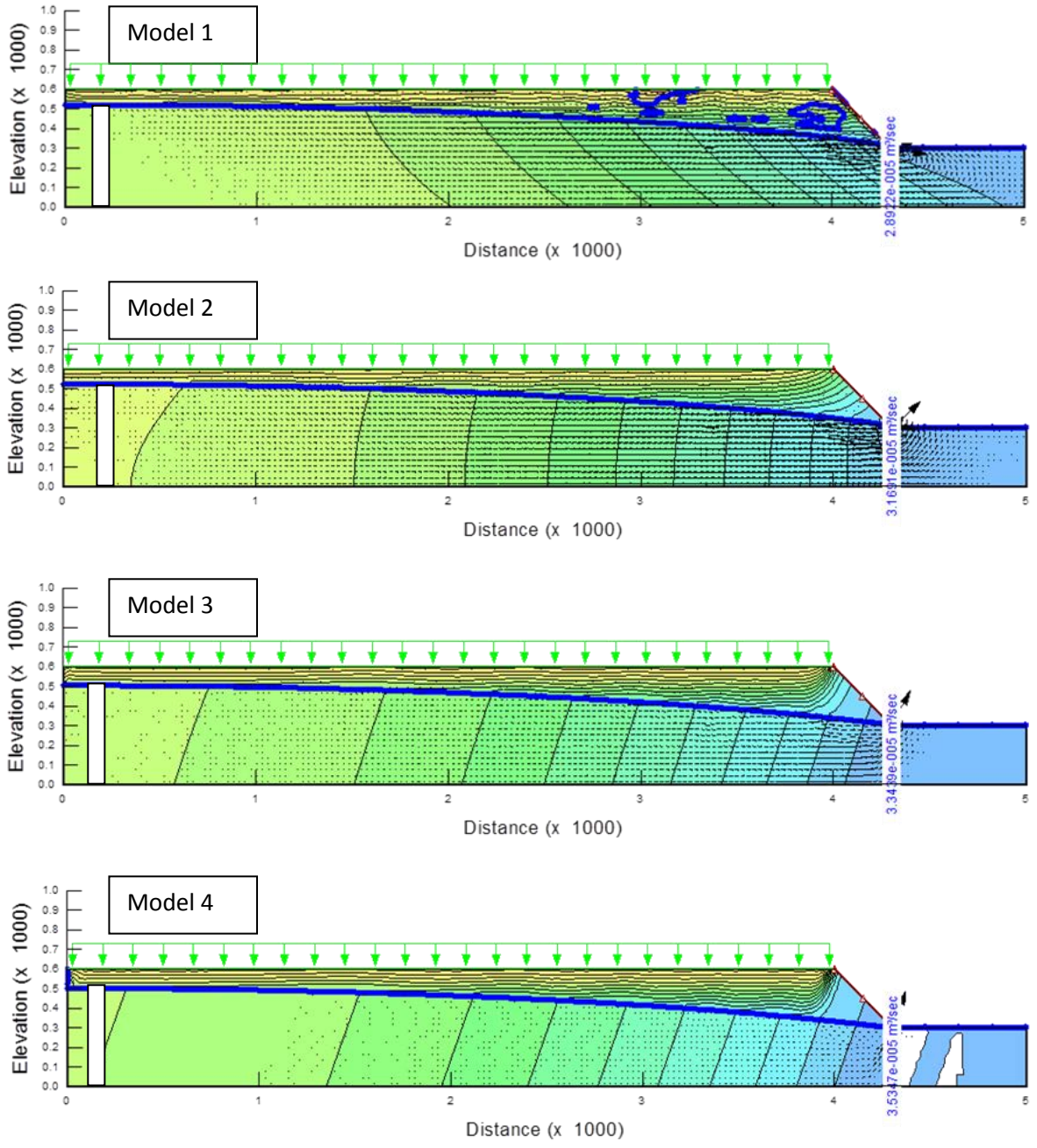

Figure 5.11b models 1 to 4 represents simulation results of saturated flow through a vertical plane anisotropic system of K ratios (K_y/K_x); 0.1, 1, 10 and 100 of models 1 to 4 respectively, at 20 degrees dip in direction clockwise to the horizontal.

The following have been designed to explain some general concept of anisotropy and the assessment of the vertical plane anisotropy of above results. The K in the direction of flow can be calculated using the following expression (e.g. Harr, 1962):

$$K = \frac{K_x K_y}{[K_x Sin^2(\alpha) + K_y Cos^2(\alpha)]} \qquad (5.1)$$

where α is the angle between the flow direction and the x axis (direction of K_x)(figure 5.12).

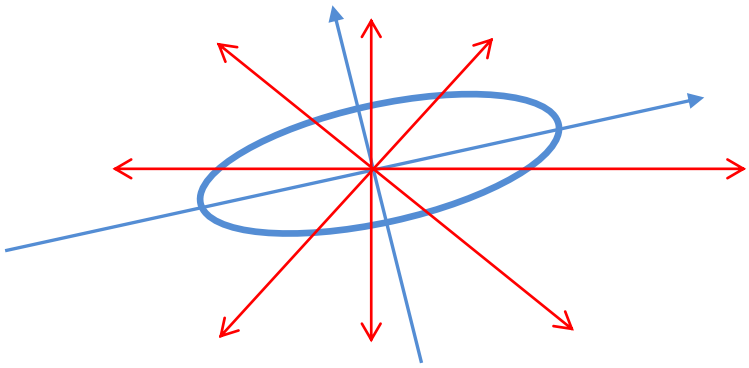

Figure 5.12 The hydraulic conductivity ellipse showing the x and y directions (blue) and example of flow directions (vertical, 45 degrees and horizontal).

Figure 5.13 shows this equation plotted out for the models M1 to M4 of Table 5.5. Figure 5.13 indicates that the regional K increases in these models in the order M4, M3, and M2. At first glance this would suggest that one might expect that there would be an increase in Ri in the same order, however, model results suggest lowest water levels, i.e. greatest impact at the far left boundary in the order M4~M3 (lowest water level), M2 (highest water level).

With the opposite order however, the largest differences in K occur for water flow in directions furthest from the Kx direction of anisotropy (figure 5.12) i.e. when is greatest; this is mainly when flow is close to vertical, including at recharge. This means that recharge rates are less, even though the horizontal K in all cases is very similar, the system cannot accept recharge at such a high rate when the vertical K is lower, but can transmit at almost

as high a rate in the saturated zone. The response of the system is to increase the area of recharge, thus extending the apparent radius of influence, with the greatest effect when the anisotropy is most restricted in the y direction. In the case of Model 1, vertical K is much increased, and a greater recharge rate is possible, hence Ro is reduced.

To explain why water levels in equivalent models for the 160^{o} and 20^{o} dip cases (Figure 5.11a and 5.11b) differ: It should be noted that an important zone is the discharge area where increase in K will not be partly countered by decrease in saturated thickness and for the case of figure 5.11a (160^{o} dip), K in this zone will be greater (flow is nearer to parallel with the x direction) than for figure 55.11b (20^{o})dip, thus allowing more flow and therefore a greater radius of influence.

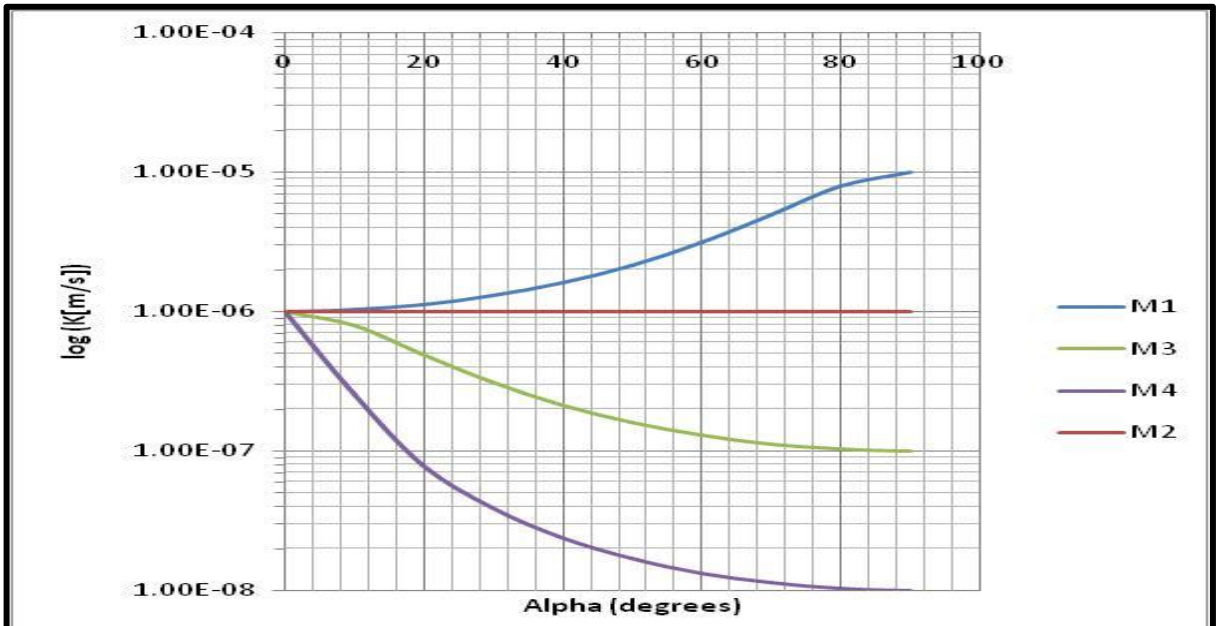

Figure 5.13 Plot of the K equation values for models 1, 2, 3 and 4 of figures 5.11a and 5.11b

The above concept is now used as Inferences for the MODFLOW model representation. Though, the SEEP/W results are not easy to interpret but they do highlight a couple of important points: K anisotropy in the vertical plane can make significant differences in water levels through (a) changing the K value for horizontal flow – decreases will lead to decreased R_i and (b) changing recharge acceptance rates – decreases will lead to increases in R_i. The relationship between K anisotropy and water levels is not straightforwardly predictable without explicit modelling. The orientation of the K anisotropy is significant as it determines the K values at different points in the flow system (e.g. the ~ horizontal flow over most of

the catchment or the mainly upward inclined flow at the end just before the mine) and also on recharge rates, thus prediction is not straightforward without explicit modelling.

With regard to the latter point, the flow towards a mine in an anisotropic system on different sides of the mine will affect the water levels in different ways; the plots of figure 5.11a and figure 11b could be interpreted as the flows on either side of a mine – just reverse 11b for example, and the anisotropy directions is now the same as for 11a and the flow is now directed right to left as it would be on the right of the mine. Therefore matching 11a and 11b indicates the effects on both sides of the mine.

Where anisotropy is caused by large well-separated fractures, the flows will not be represented by the anisotropy calculations here – in the extreme case permeable fractures may be parallel to the mine walls so flow is negligible and Ro is tiny. Finally, the effect of anisotropy, because of the competing effects of change in overall transmissivity and change in recharge, could result in either over or underestimation of R_i, and therefore vertical plane anisotropy must be borne in mind when considering the mine R_i estimates.

Similarly, the above inferences for the MODFLOW model representation can also be presented by highlighting a couple of important points as follows: K anisotropy in the vertical plane can make significant differences in water levels through increasing the Kx where x has a shallow dip. Firstly, this will increase the transmission of the water horizontally (though this will reduce head losses) thus tending to increase R_i. Secondly, this will reduce the vertical flow, especially recharge, thus decreasing the recharge rate and thus tend to increase R_i. Thirdly, depending on direction – upwards or downwards – may increase or decrease K in the discharge zone – a zone with limited space where there is little change in saturated thickness so the only way of changing flow is by change in K – so flow is directly related to K here

However, decreasing the Kx where x has a steep dip will cause the opposite effects (decrease horizontal flow rate, increase recharge rate, and decrease or increase K in the discharge zone). Accordingly, the relationship between K anisotropy and water levels is not straightforwardly predictable without explicit modeling

5.5 Analytical approach of estimating radius of influence by iteration method

The use of simple analytical tools can be of great importance to mine feasibility and environmental evaluations, for instance the use of analytical solutions for predicting the radius of influence of mine dewatering impacts on the natural static hydraulic conditions of the flow system. In this section an analytical solution by iteration method is looked at to see how it compares with the numerical results; the results are used in chapter 6 to develop an empirical relationship to estimate R_i. The analytical methods of Thiem-Dupuit (after Kruseman and de Ridder, 1994) and Marinelli & Nicolli (2000) for predicting groundwater inflows into wells have been adopted. Although the Thiem-Dupuit equation is usually used for abstraction boreholes in unconfined aquifers, it can also be applied to open excavations by equating the excavated void to a large diameter well. In the work of Marinelli & Nicolli (2000), inflows into surface mining excavations below the groundwater table may originate from local precipitation as well as from a deeper groundwater system that is treated as isolated. Thus the flow regime is divided into two zones with separate analytical equations applying to each (Figure 5.14). Inflows from the sides of the pit are calculated in Zone 1 which is located above the base. Zone 2 has an infinite depth below pit's base and represents inflow to pit's bottom. The total groundwater inflow to the excavated void (Q_T) therefore is the sum of the inflows calculated from Zones 1 and 2. Although in the current calculations of the radius of influence, only zone 1 has been used as this corresponds more closely with the numerical model.

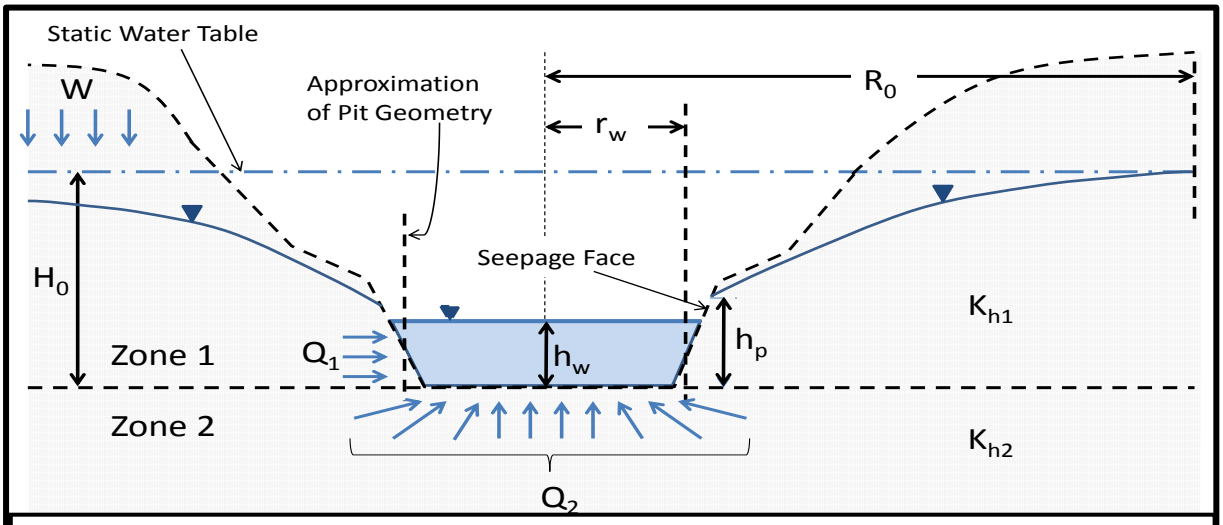

Figure 5.14 Analytical model of a steady-state flow towards an excavated mine in an unconfined aquifer (after Marinelli & Nicolli, 2000)

The symbols in figure 5.14 are as follows;

Q = groundwater inflow rate/mine discharge (m^3/s)

K = hydraulic conductivity (m/s)

H_0 = head of static water table above base of pit (m)

h_w = Head of water in the mine (m)

h_p = saturated aquifer thickness at the pit wall (m)

R_0 (R_e) = radius of influence of the mine (m)

r_w (r_p) = effective radius of the mine (m)

Q_1 = inflow from the pit walls (approximated as a right circular cylinder) (m^3/s)

W = distributed recharge flux (m/s)

Q_2 = inflow through base of pit (m^3/s)

K_{h1} = horizontal hydraulic conductivity of Zone 1 rock formation (m/s)

K_{h2} = horizontal hydraulic conductivity of Zone 2 rock formation (m/s)

5.5.1 Calculation of the radius of influence (R_e)

In the calculation of the radius of influence, the following assumptions (after Kruseman & de Ridder, 1994 and Marinelli & Niccoli, 2000) were made in the derivation of the equation for the solution of the above analytical model:

Zone 1

- the solution considers an infinite unconfined aquifer, homogeneous, isotropic, and of uniform thickness over the area influenced by the mine with equally distributed recharge at the water table;
- the pit is represented as a cylinder
- the initial water table is approximately horizontal, as the pre-mining water table;

- and the flow to the mine is in steady state and axially symmetric horizontal radial flow occurs at any vertical cross-section.
- the pit is fully penetrating and therefore pit receives water from the entire saturated thickness of the aquifer.
- there is no seepage face discharges and no groundwater flow occurs between Zones 1 and 2

Zone 2

- groundwater flows in a steady-state to one side of a circular disk sink of constant and homogeneous drawdown. Flow is axially symmetric and three dimensional.
- initial hydraulic heads are uniform throughout Zone 2
- the initial water table in Zone 1 equals the initial head in Zone 2
- the hydraulic head of the disk sink is constant and equals the head of the pit lake surface
- the aquifer materials are anisotropic with K being defined in the horizontal and vertical directions

Here only zone 1 will be considered.

The radius of influence is calculated from the analytical model of zone 1. Taking into consideration the assumptions made in zone 1, the flow rate across the pit's cylindrical surface of radius r is given by:

$$Q = 2\pi rhK\frac{dh}{dr} \qquad (5.2)$$

Assuming flow to be derived from recharge within the radius of influence (R_o) then the flow rate at radius r is

$$Q = W\pi({R_o}^2 - r^2) \qquad (5.3)$$

where W is the recharge rate. Elimination of Q from equations 5.2 and 5.3, separating the variables and integrating gives

$$\int_{r_p}^{r} \frac{W}{2K}\left(\frac{{R_o}^2}{r} - r\right) dr = \int_{h_p}^{h} hdh \qquad (5.4)$$

Completing the integration gives

$$h(r) = \sqrt{{h_p}^2 + \frac{W}{K}\left[{R_o}^2 Ln\left(\frac{r}{r_p}\right) - \frac{(r^2 - {r_p}^2)}{2}\right]} \qquad (5.5)$$

At r=R_o and the initial saturated thickness (H_o)

$$H_0 = \sqrt{{h_p}^2 + \frac{W}{K}\left[{R_o}^2 Ln\left(\frac{R_0}{r_p}\right) - \frac{({R_0}^2 - {r_p}^2)}{2}\right]} \qquad (5.6)$$

making the radius of influence (R_o) the subject of the equation gives

$$R_o = \sqrt{\frac{\frac{K}{W}({H_o}^2 - {h_p}^2) - \frac{{r_p}^2}{2}}{Ln\left(\frac{R_0}{r_p}\right) - \frac{1}{2}}} \qquad (5.7)$$

Equation 5.7 is a non-linear equation and has to be solved by iteration, and this has been done using Microsoft Excel. The convergence of the iteration is very sensitive to the choice of the initial guess when K is low and obtaining a correct answer can take quite a lot of experimentation with initial values.

Table 5.6 provides an example calculation. An initial static ground water level of 500m A.D and a sump of head 450m A.D are used to represent the heads for the flow system prior to dewatering. The pit has an approximate area of L x W = 2000m x 1000m = $2x10^6$ m^2 and an average depth of 300m. Because the pit area is not a perfect circle, the effective pit radius (r_p) was worked out from [$A = \pi(r_p)^2$] to be approximately 798m (equating perimeters gives slightly greater R_i values by < 100m for K = 0.1 m/d). The rest of the parameters used are shown in Table 5.6.

Table 5.6 Input parameter values for analytical models by iteration method	
Parameter	Value
Static initial ground water level H_o (m A.D)	500
Base of formation (m A.D)	0
Base of mine H (m A.D)	450
Radius of mine r_p (m)	798
hydraulic conductivity K (m/d)	1.49
Recharge rate W (m/d)	0.000819
Iteration	
Final value for Rmax (m)	5526

5.5.2 Correlation between radius of influence by numerical and analytical approaches

In Figure 5.15 values of radius of influence obtained by the MODFLOW numerical method are plotted against the Analytical method results. A perfect agreement between the two methods is not expected. There are several differences between the Modflow model and the analytical model, including a different mine size and shape, the purely radial geometry of the analytical model and the recharge for the analytical model is uniform whereas that for the Modflow model changes with amount of drawdown. For the latter point, the change in recharge only happens between a range of drawdown of about 0.1 m, but this is at the extreme edge of the cone of depression where areas are large. If the radius of influence had been measured in the y direction rather than the x-direction in the Modflow model, the radius of influence would have been around 15% less for the Modflow model.

From Figure 5.15, the Ri from the two methods correlate well overall, but the fit includes an intercept and a slope of < 1 that reflects that the agreement at small distances is less good. Now, forcing a fit through the mine centre results in a 1:1 fit, though at large distances Modflow values are slightly less than the analytical ones. The divergence for small distances might be expected as the way the mine geometries are represented is rather different in the two cases as discussed above. At small distances the numerical model would be the safes to use as it indicates greater R_i, but the converse is true for larger R_i values.

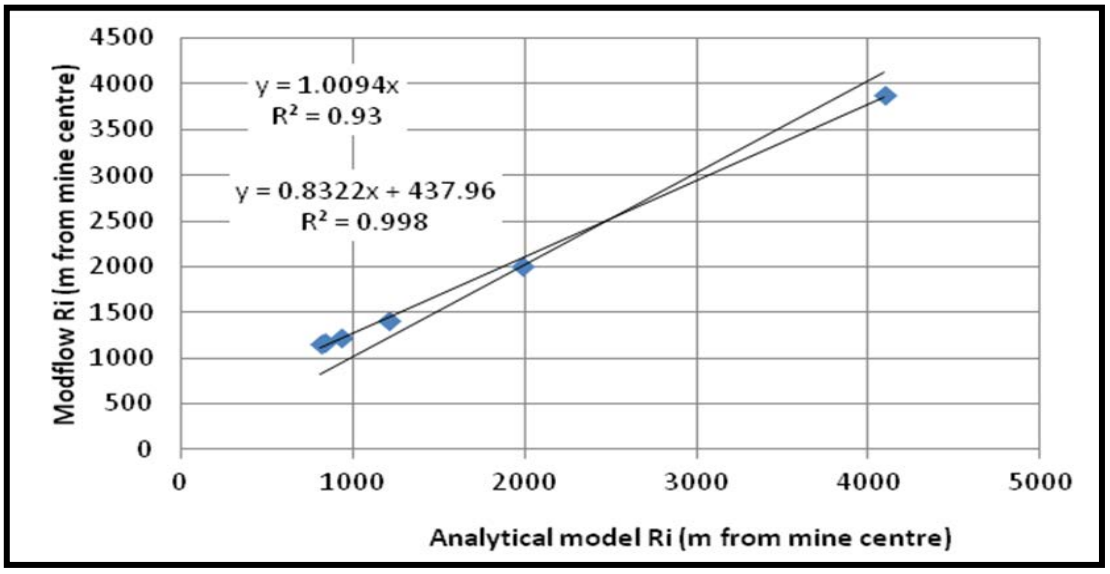

Figure 5.15 Relationship between R_i values of steady state analytical model and Modflow numerical model results showing a 1:1 fit and an intercept fit with the vertical axis (hp =300m; W = 300 mm/y; rp = 789m; Ho = 500m).

5.6 Summary and discussion of results

The main aim of this chapter was to develop and evaluate a simple numerical tool which will then be applied in chapter 6 to investigate the possible derogation impacts of open pit mines on regional groundwater flow systems. The model has been made as simple as possible as its application will depend on uncertain K and R data (chapters 3 and 4) and will be used only as a scoping tool.

The Modflow model was based on a very simple steady-state one layer set up with a constant head representing the mine. The main assumptions of this model were examined. It was found that

1. flows can reasonably be considered as steady-state
2. the fully-penetrating constant head at the mine probably results in a slight over estimation of the radius of influence, i.e. a safe inaccuracy
3. seepage faces appear to have limited effect on the radius of influence though will affect heads very close to the mines

4. it was found that not including reduction in hydraulic conductivity with depth in the model probably results in the predicted radius of influences being overestimated, again an inaccuracy on the safe side.
5. hydraulic conductivity anisotropy in the vertical plane and its orientation leads to some complicated results through both affecting flows and recharge acceptance rates. These effects require explicit modelling to predict. Flow to different sides of the same mine with constant anisotropy properties will be different. If the anisotropy is formed by discrete fractures and these are widely spaced then there could be further significant effects resulting from the relative orientation of the mine slopes and the fractures; for example there may be very little flow into one side of a mine if the fractures are oriented parallel to the slopes.

In addition an analytical model based on similar principles to the numerical model was examined and compared with the numerical model. It was found that the analytical model's radius of influences predictions were slightly larger than the numerical model's values. This was thought to be due mainly to the different ways in which the mine geometry was included in the models.

In conclusion it is concluded that provided that care is taken the Modflow model should provide a reasonable first pass means of investigating the size of the cones of depression formed by the mines. Errors will tend to be on the safe side with the model overestimating the radius of influence. If however the result from this first pass assessment (chapter 6) is uncertain, much more sophisticated models will need to be used and because of the lack of data to feed such models with many variables this would entail an extensive sensitivity exercise. These sophisticated models will need to include anisotropy, vertical variation in K and much more detailed investigation of the effects of drawdown on recharge.

CHAPTER 6

ASSESSMENT OF LIKELY RANGES OF MINE RADIUS OF INFLUENCE

6.1 Introduction

The radius of influence of an open pit mine is a function of the geometry of the mine (G), the hydraulic conductivity of the rock (K) and the recharge (R). It is also dependent on the conceptual model of the system including distributions of properties in time and space. Here K and R are very uncertain and so the approach is to take a very simple conceptual and mathematical model and test it to see what the main variables are and whether there is likely to be a problem with derogation. The mathematical model has been set up and investigated in chapter 5, and in this chapter the model is used. If it is found that the model provides a clear indication as to the importance of derogation then no more detailed work will be necessary. But if the conclusions from it are uncertain then it will be necessary to set up a much more sophisticated model. A more sophisticated model will have more variables to estimate values for and this will probably need more collection of data as the data available even for the simple model are not complete. In section 6.2 the basic relationships predicted by the mathematical model between G, K and R are presented and discussed for a fixed potential R of 300 mm/y. In section 6.3 the importance of R is assessed. In section 6.4 the effects of x-y K anisotropy and boundary conditions are looked at to see if they affect the conclusions from section 6.2 and 6.3. Section 6.5 discusses all the above results and section 6.6 describes the proposed method for applying findings

6.2 The importance of mine geometry and rock hydraulic conductivity on radius of influence

The MODFLOW computer model described in section 5.3 above has been used to investigate the sensitivity of the radius of influence to hydraulic conductivity (K) and elevation of mine depth (D). At a constant layer thickness of 500m and mine depths ranging from 50 to 450 metres above datum (base of aquifer)(m A.D.), in steps of 50 m A.D. for a range of hydraulic conductivity values, the radius of influence of simulation results were measured for 1m drawdown (radius of impact R_i) and recorded in Table 6.1. Following from these results, the general observation is that the radius of influence/impact of the mine

increases with increasing mine depth and increasing hydraulic conductivity as expected, but with a less pronounced effect as K values increase. This is shown graphically in Figure 6.1.

Table 6.1 Measurements of radii of impact (R_i) for range of mine depth (D) and hydraulic conductivity K(m/s) of a simulated numerical models with MODFLOW. The shaded area represents R_i corresponding to the inter quartile range (brown), and R_i corresponding approximately to the median K (black).

Layer thickness B (m A.D)	500	500	500	500	500	500	500	500	500
Mine depth D (m A.D)	50	100	150	200	250	300	350	400	450
Head in mine H (m A.D)	450	400	350	300	250	200	150	100	50
K (m/s)	Radius of impact (R_i)								
1.40E-13	1000	1020	1043	1065	1072	1089	1090	1095	1100
4.80E-12	1030	1045	1076	1100	1135	1150	1178	1194	1216
4.22E-11	1055	1100	1150	1173	1227	1258	1271	1298	1320
4.43E-10	1100	1145	1224	1285	1325	1350	1375	1390	1400
9.50E-09	1165	1225	1264	1340	1348	1448	1484	1516	1527
2.70E-08	1252	1390	1473	1515	1599	1641	1641	1641	1557
5.82E-08	1562	1557	1683	1809	1850	1891	1933	1933	1891
1.20E-07	1560	1808	1975	2100	2142	2226	2268	2268	2226
2.51E-07	1766	2100	2311	2476	2602	2685	2769	2810	2727
3.62E-07	1901	2309	2560	2727	2852	2978	3061	3104	3103
5.86E-07	2142	2602	2894	3145	3312	3437	3563	3605	3605
8.63E-07	2351	2894	3270	3521	3730	3897	4022	4064	4065
1.30E-06	2560	3270	3688	4022	4273	4482	4607	4681	4691
1.90E-06	2852	3646	4190	4566	4858	5109	5244	5337	5340
2.48E-06	3103	3981	4566	5025	5359	5610	5777	5871	5871
3.32E-06	3396	4398	5067	5568	5944	6237	6446	6529	6529
5.07E-06	3897	5067	5861	6488	6947	7281	7532	7616	7616
7.55E-06	4398	5819	6780	7156	8075	8460	8743	8827	8839
1.72E-05	5861	7825	9200	10500	11100	11900	12100	12500	12918

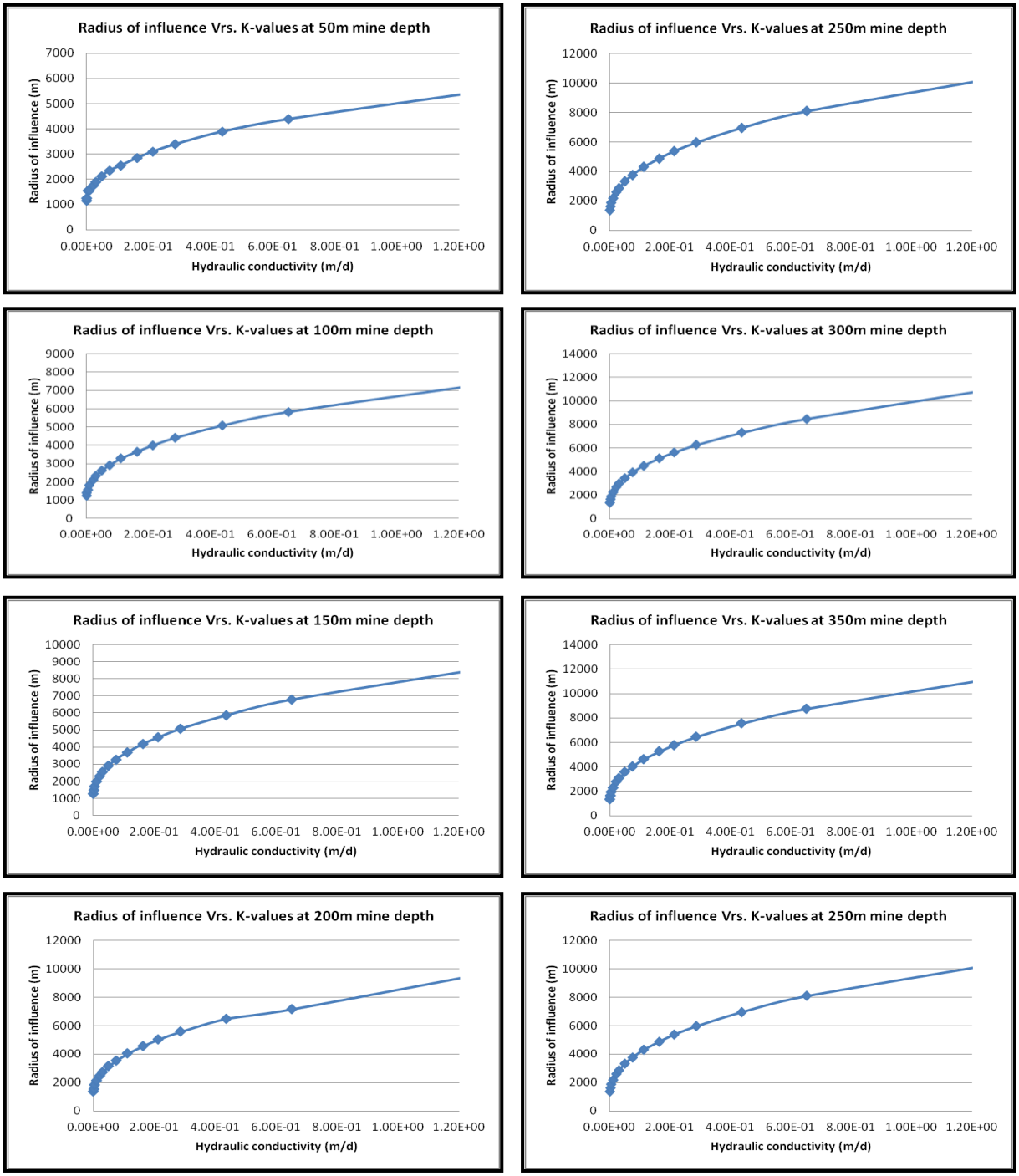

Figure 6.1 Plots showing variation of radius of impact with hydraulic conductivity at constant mine depths of 50, 100, 150, 200, 250, 300, 350 and 400m, respectively.

Though the focus is on derogation due to groundwater level drawdown, for first approximation, volume derogation due to groundwater abstraction and precipitation interception of a typical mine of radius 798m (see section 5.51) can be estimated from R_i values of Table 6.1 using the relation:

$$Q = W\pi\left({R_i}^2 - 798^2\right) + \pi(798)^2 P \qquad 6.1$$

where W is groundwater recharge (300 mm/yr=300x10^{-3}m/yr) and P is precipitation (1467mm/yr=1467x10^{-3}m/yr). Note that the total volume is greater than this, as the radius of influence is larger than the radius of impact (but the recharge rate in the model falls as the water level rise higher than the 'evapotranspiration' extinction level): however, sample calculations suggest that the error is less than a few percent. Table 6.2 shows the calculated annual volume of groundwater abstraction of a typical mine.

Table 6.2 Annual volume (Mm3/yr) of groundwater abstraction of a typical mine for a range of mine depth (D/ m), hydraulic conductivity K (m/s) for simulated R_i values of Table 6.1.

Mine Geometry									
Layer thickness B (m A.D)	500	500	500	500	500	500	500	500	500
Mine depth D (m A.D)	50	100	150	200	250	300	350	400	450
Head in mine H (m A.D)	450	400	350	300	250	200	150	100	50
K (m/s)	Volume (Mm3/yr)								
1.40E-13	3.28	3.32	3.36	3.41	3.42	3.46	3.46	3.47	3.48
4.80E-12	3.34	3.37	3.43	3.48	3.55	3.59	3.65	3.68	3.73
4.22E-11	3.39	3.48	3.59	3.64	3.76	3.83	3.86	3.93	3.98
4.43E-10	3.48	3.57	3.75	3.89	3.99	4.06	4.12	4.16	4.19
9.50E-09	3.62	3.75	3.84	4.03	4.05	4.31	4.41	4.50	4.54
2.70E-08	3.82	4.16	4.38	4.50	4.75	4.88	4.88	4.88	4.62
5.82E-08	4.64	4.62	5.01	5.42	5.56	5.71	5.86	5.86	5.71
1.20E-07	4.63	5.42	6.01	6.49	6.66	7.01	7.18	7.18	7.01
2.51E-07	5.28	6.49	7.37	8.11	8.72	9.13	9.56	9.78	9.34
3.62E-07	5.74	7.36	8.51	9.34	10.00	10.69	11.17	11.42	11.41
5.86E-07	6.66	8.72	10.23	11.66	12.67	13.47	14.30	14.58	14.58
8.63E-07	7.55	10.23	12.41	14.02	15.45	16.65	17.58	17.90	17.91
1.30E-06	8.51	12.41	15.15	17.58	19.54	21.26	22.33	22.98	23.07
1.90E-06	10.00	14.86	18.88	21.98	24.57	26.93	28.24	29.17	29.20
2.48E-06	11.41	17.27	21.98	26.13	29.39	31.99	33.78	34.81	34.81
3.32E-06	13.20	20.56	26.52	31.54	35.62	38.98	41.48	42.49	42.49
5.07E-06	16.65	26.52	34.70	41.99	47.80	52.28	55.78	56.98	56.98
7.55E-06	20.56	34.24	45.64	50.58	63.76	69.76	74.35	75.74	75.94
1.72E-05	34.70	60.02	82.07	106.19	118.40	135.74	140.26	149.53	159.54

The statistical analysis of hydraulic conductivity of the combined dataset and its dependence with depth (K(z)) has already been examined in chapter 3. And to put this in context table 6.3 and figure 6.2 repeats the summary statistical description of the data and K(z) distribution from chapter 3's literature survey respectively.

Table 6.3 Summary statistics of conductivity values (m/s) for the combined dataset (N means normal distribution)

Count		736
Min		1.20E-13
Max		1.25E-03
N Parameters	Mean	1.48E-05
	Stdev	9.74E-05
LogN Parameters	**Mean (Geom Mean)**	**-7.80 (1.57E-08)**
	Stdev	61.0
Undefined Distribution Parameters	**Median**	**3.80E-09**
	IQR (q3 to q1)	9.94E-07 & 1.10E-10

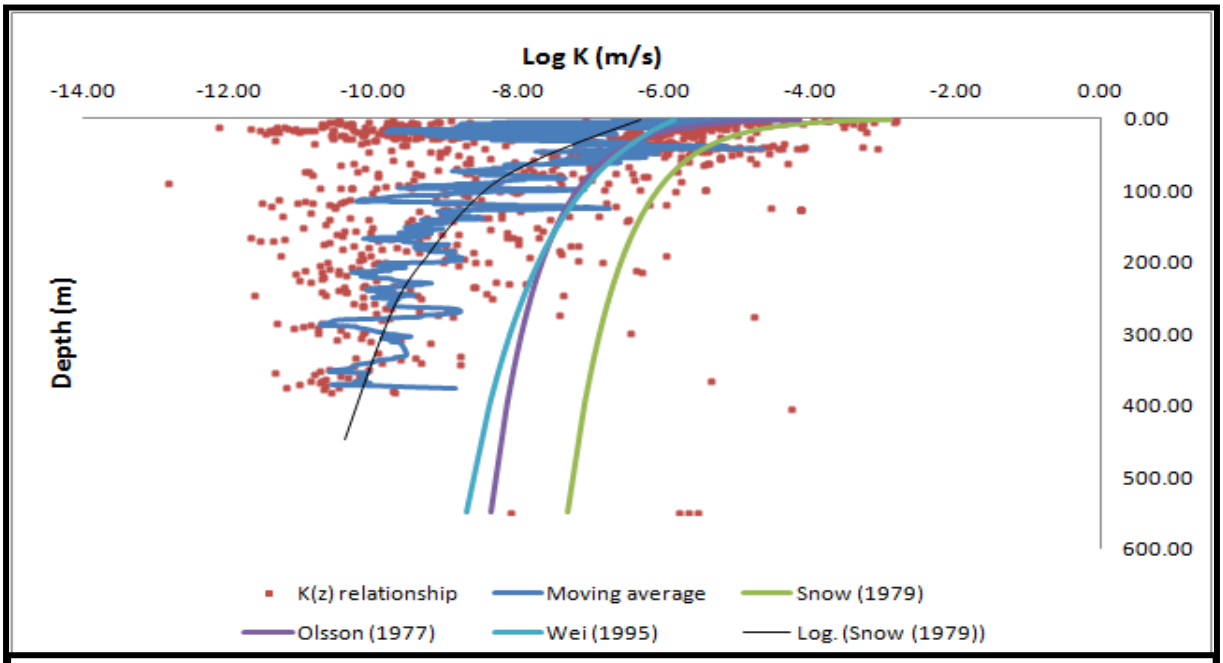

Figure 6.2 K variation with depth from literature survey of chapter 3

The dependence of the radius of impact on hydraulic conductivity and mine depth is shown for calculations of the whole dataset in Figure 6.3 on both the non transformed scale (Top) and the logarithm scale (Bottom).

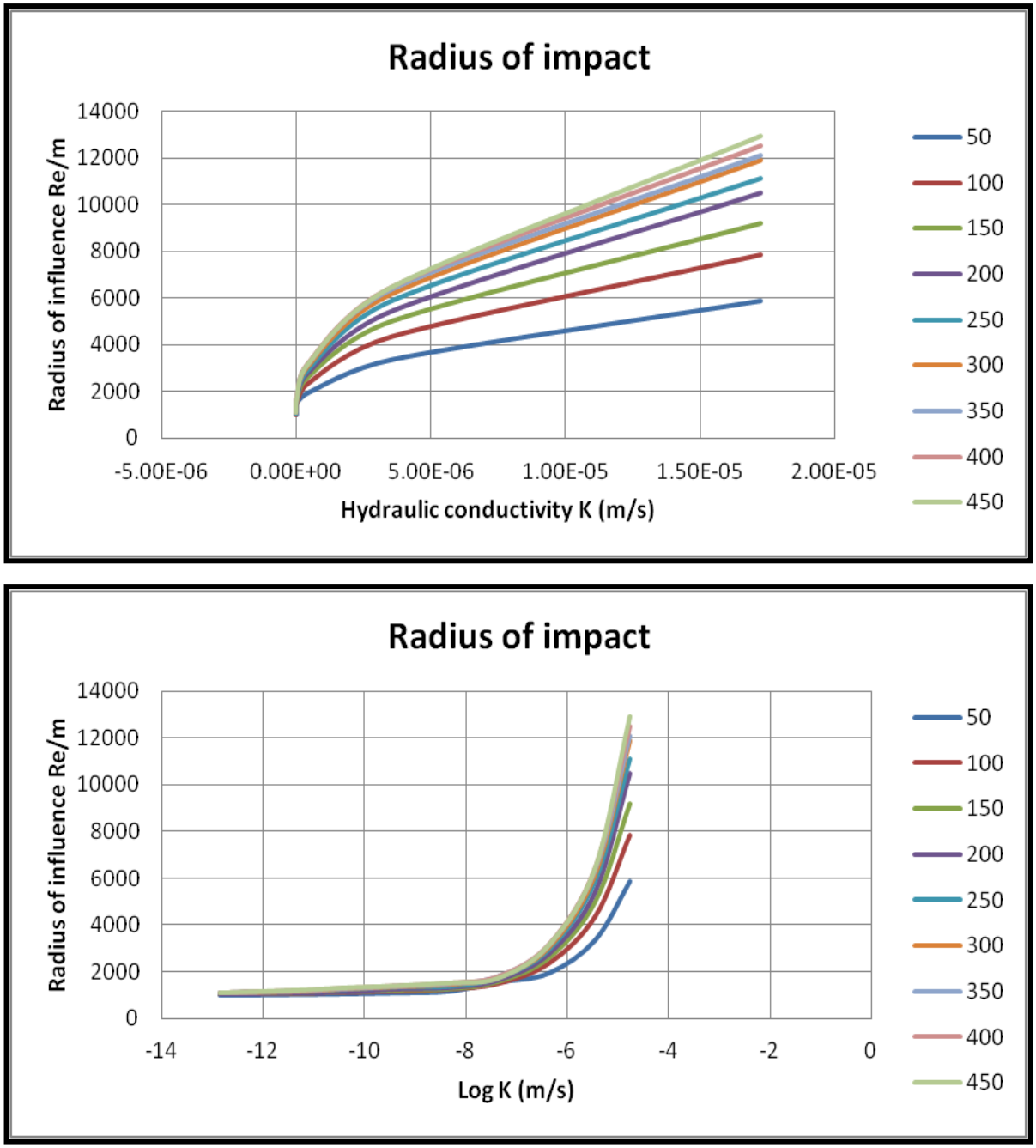

Figure 6.3 Relationship between estimated radius of impact and hydraulic conductivity at constant mine depths: (Top) on the natural scale (Bottom) on log scale. NB: 1m/d is approximately equal to $1x10^{-5}$ m/s

It is observed that, the radius of impact increases with increasing hydraulic conductivity and increasing mine depth with the relations trending to a constant radius of approximately 1km

from mine centre at a K value of 10^{-8}m/s. Thus at hydraulic conductivities below 10^{-8}m/s there will be a negligible derogation zone. The radius of impact is very close to the mine for K values less than 10^{-8}m/s and this value corresponds approximately to the geometric mean of the international data set and is higher than the median value. Hence if R is set at 300 mm/y then derogation is only expected at significant distances if the mine is in an aquifer with K value in the upper 25%.

To further investigate the potential for derogation due to groundwater level drawdown and volume of groundwater abstraction, descriptive statistics were used to describe the measured R_i values of Table 6.1. Table 6.4 shows the summary statistics obtained. It is accepted that the data set is not randomly chosen and includes a range of mine depths but the data do systematically cover the range of input parameter values. The range of the distribution is from 1km to 13km with an inter quartile range of 2km and a median value of 1.4km. Therefore, given that the mine size modelled is 1km in the direction measured to get R_i, in many of the conditions derogation will not be much of a problem except distances lower than the median and very close indeed to the mine as shown in the shaded portion of Table 1.6. At such close distances to the mine there may be other problems too from dust, stability, noise and especially loss of land. A range of major impacts on village life would also be expected. However, R_i could reach up to 3km in some circumstances.

Table 6.4 Summary statistics of measured radius of impact R_i (m) of simulation results and the corresponding volume of water abstraction.

Data Source	Count	Min	IQR (q_1)	Median	IQR (q_3)	Max	Mean	Standev
R_i (m) from MODFLOW Numerical Model	81	1,000	1158	1,400	3141	12,918	2,941	3,105
Volume of groundwater abstraction (m^3/yr)		**942,000**	**1,263,188**	**1,846,320**	**9,293,660**	**157,195,990**	**8,147,811**	**9,081,846**

It should be mentioned here that discussions made so far are based on the whole dataset (Group A). However, a significant concern is the dominant influence of the dataset obtained

by Gale and Witherspoon (1979) from Stripa mine site that was targeted for its low fracture occurrence in its original development work. Also of concern is the dataset obtained by Snow (1979) from grouting at dam and tunnel sites, as these sites are unusually permeable. The whole dataset has therefore been further analyzed and conclusions drawn to include the following groupings:

(i) Combined dataset, less dataset on radioactive waste of low fracture occurrence from Gale and Witherspoon (Group B).

(ii) Combined dataset, less dataset on radioactive waste of low fracture occurrence from Gale and Witherspoon and dataset of Snow from grouting at dam and tunnel sites of high fracture occurrence (Group C).

Table 6.5 and figure 6.4 below show summary statistics and box plot representation of K values for these groupings. It should be noted that the IQR (inter quartile range) ignores data below the 25th percentile or above the 75th, which may contain outliers that could inflate the measurement of variability of the entire dataset and hence the inter quartile range has been used here for the current analysis. However, there will be unusual cases where high K values may produce very large R_i values.

Table 6.5 Summary statistics of K values (m/s) for (Group A) (Group B) and (Group C) (N means normal distribution)

		A	B	C
Count		736	360	182
Min		1.40E-13	2.80E-12	2.80E-12
Max		1.45E-03	1.45E-03	5.60E-04
N Parameters	**Mean**	**1.48E-05**	**3.01E-05**	**2.25E-05**
	Stdev	9.74E-05	1.38E-04	9.12E-05
LogN Parameters	**Geom Mean**	**1.57E-08 (-7.80)**	**2.62E-07 (-6.58)**	**1.12E-07 (-6.95)**
	Multiplicative Stdev	61.0	51.10	65.8
Undefined Dist. Parameters	**Median**	**3.80E-09 (-8.42)**	**9.88E-07 (-6.01)**	**4.47E-07 (-6.35)**
	Interquartile range IQR (q3 to q1)	9.94E-07 To 1.10E-10	4.41E-06 To 9.61E-08	4.62E-06 To 8.69E-09

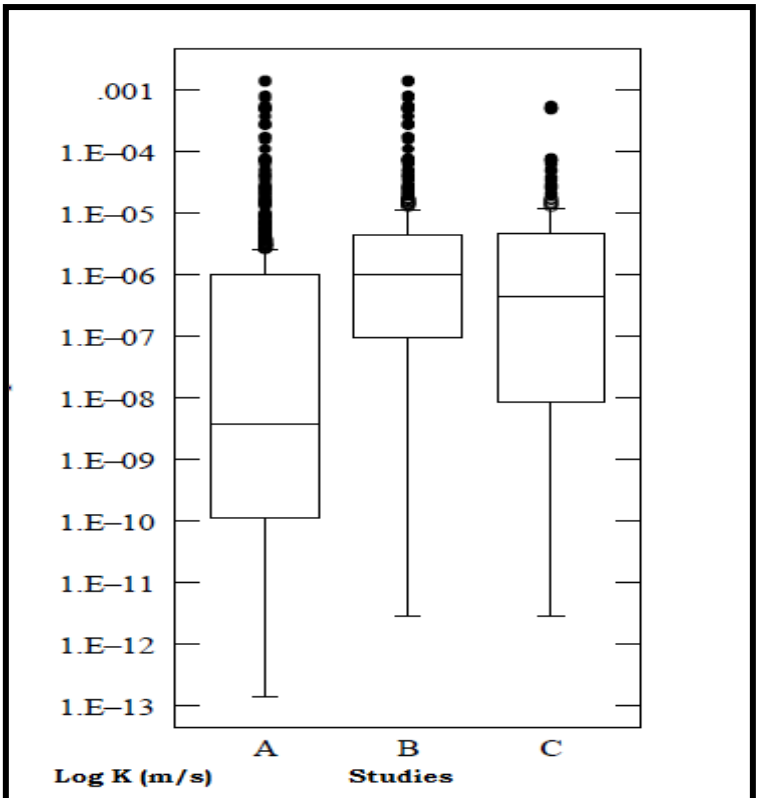

Figure 6.4 Box-and-whisker plot of K values for the various groupings (A, B and C) of the whole database

It is observed that the median values of groups A, B and C (3.80E-09, 9.88E-07 and 4.47E-07 m/s) are lower than the corresponding mean values (1.48E-05, 3.01E-05 and 2.25E-05 m/s), a function of the distribution for the three groups being skewed/spread to the right towards higher K. Variability in dataset (inter quartile range) is highest in group A (9.94E-07 to 1.10E-10 m/s) as expected, followed by group C (4.62E-06 to 8.69E-09 m/s) and then group B (4.41E-06 to 9.61E-08 m/s). The higher the values of K the higher the flow rate into mine and therefore the larger the radius of the impacted area R_i. By taking into consideration differences in inter quartile ranges and median values of various groups, the shaded portions of Tables 6.6 and 6.7 below represent the corresponding mine impacted area (R_i) for Groups B and C. The R_i values shaded in black represent approximately the values associated with the median K.

Table 6.6 Measurements of radius of impact (R_i) for range of mine depth (D) and Group B hydraulic conductivity K (m/s) of simulated numerical models with MODFLOW. The shaded area represents R_i corresponding to the inter quartile range (green), and R_i corresponding approximately to the median K (black)

Mine Geometry									
Layer thickness B (m A.D)	500	500	500	500	500	500	500	500	500
Mine depth D (m A.D)	50	100	150	200	250	300	350	400	450
Head in mine H (m A.D)	450	400	350	300	250	200	150	100	50
K (m/s)	Radius of impact (R_i)								
1.40E-13	1000	1020	1043	1065	1072	1089	1090	1095	1100
4.80E-12	1030	1045	1076	1100	1135	1150	1178	1194	1216
4.22E-11	1055	1100	1150	1173	1227	1258	1271	1298	1320
4.43E-10	1100	1145	1224	1285	1325	1350	1375	1390	1400
9.50E-09	1165	1225	1264	1340	1348	1448	1484	1516	1527
2.70E-08	1252	1390	1473	1515	1599	1641	1641	1641	1557
5.82E-08	1562	1557	1683	1809	1850	1891	1933	1933	1891
1.20E-07	1560	1808	1975	2100	2142	2226	2268	2268	2226
2.51E-07	1766	2100	2311	2476	2602	2685	2769	2810	2727
3.62E-07	1901	2309	2560	2727	2852	2978	3061	3104	3103
5.86E-07	1560	1808	1975	2100	2142	2226	2268	2268	2226
8.63E-07	1766	2100	2311	2476	2602	2685	2769	2810	2727
1.30E-06	1901	2309	2560	2727	2852	2978	3061	3104	3103
1.90E-06	2852	3646	4190	4566	4858	5109	5244	5337	5340
2.48E-06	3103	3981	4566	5025	5359	5610	5777	5871	5871
3.32E-06	3396	4398	5067	5568	5944	6237	6446	6529	6529
5.07E-06	3897	5067	5861	6488	6947	7281	7532	7616	7616
7.55E-06	4398	5819	6780	7156	8075	8460	8743	8827	8839
1.72E-05	5861	7825	9200	10500	11100	11900	12100	12500	12918

Table 6.7 Measurements of radius of impact (R_i) for range of mine depth (D) and Group C hydraulic conductivity K (m/s) of a simulated numerical models with MODFLOW. The shaded area represents R_i corresponding to the inter quartile range (blue), and R_i corresponding approximately to the median K (black)

Mine Geometry									
Layer thickness B (m A.D)	500	500	500	500	500	500	500	500	500
Mine depth D (m A.D)	50	100	150	200	250	300	350	400	450
Head in mine H (m A.D)	450	400	350	300	250	200	150	100	50
K (m/s)	Radius of impact (R_i)								
1.40E-13	1000	1020	1043	1065	1072	1089	1090	1095	1100
4.80E-12	1030	1045	1076	1100	1135	1150	1178	1194	1216
4.22E-11	1055	1100	1150	1173	1227	1258	1271	1298	1320
4.43E-10	1100	1145	1224	1285	1325	1350	1375	1390	1400
9.50E-09	1165	1225	1264	1340	1348	1448	1484	1516	1527
2.70E-08	1252	1390	1473	1515	1599	1641	1641	1641	1557
5.82E-08	1562	1557	1683	1809	1850	1891	1933	1933	1891
1.20E-07	1560	1808	1975	2100	2142	2226	2268	2268	2226
2.51E-07	1766	2100	2311	2476	2602	2685	2769	2810	2727
3.62E-07	1901	2309	2560	2727	2852	2978	3061	3104	3103
5.86E-07	2142	2602	2894	3145	3312	3437	3563	3605	3605
8.63E-07	2351	2894	3270	3521	3730	3897	4022	4064	4065
1.30E-06	2560	3270	3688	4022	4273	4482	4607	4681	4691
1.90E-06	2852	3646	4190	4566	4858	5109	5244	5337	5340
2.48E-06	3103	3981	4566	5025	5359	5610	5777	5871	5871
3.32E-06	3396	4398	5067	5568	5944	6237	6446	6529	6529
5.07E-06	3897	5067	5861	6488	6947	7281	7532	7616	7616
7.55E-06	4398	5819	6780	7156	8075	8460	8743	8827	8839
1.72E-05	5861	7825	9200	10500	11100	11900	12100	12500	12918

To further investigate the potential for derogation due to groundwater level drawdown and volume of groundwater abstraction for these groups of K datasets, descriptive statistics were used to describe the R_i values of Tables 6.6 and 6.7. Table 6.8 shows summary statistics of R_i values and corresponding water volumes for the three groups. Again it is accepted that the data set is not randomly chosen but the data do systematically cover the range of input parameter values.

Table 6.8 Summary statistics of measured radius of impact R_i (m) for the main groups (A, B and C) of K values and their corresponding volume of water of a typical mine in Ghana.

Data Source	Count	Min	Max	Median	IQR (q_3-q_1)	Mean
Radius of mine impacted area R_i (m)						
Group A	90	1100	4691	2184	3103 To 1550	2394.8
Group B	90	1560	7616	3626	5078 To 2717	3961.5
Group C	117	1165	7616	3061	4587 To 1917	3407.4
Corresponding volume of groundwater abstraction (Mm^3/yr)						
Group A		3.48	23.10	6.84	11.41 To 4.60	7.75
Group B		4.63	57.01	14.74	26.64 To 9.30	17.14
Group C		3.62	57.01	11.17	22.17 To 5.80	13.28

The range of R_i distribution for Group B is approximately from 1.5km to 7.6km with the most representative distance in the range of 3.6km from mine centre. 50% of cases would be

expected to have a radius of impact lying between 1 and 4.1km from the mine edge, but in extreme cases the radius of impact could reach at least 6.6 km from the mine, and further if the system was anisotropic.

Similarly for Group C, R_i values range from 1.2km to 7.6km with the most representative distance in the range of 3km from mine centre. 50% of cases would be expected to have radius of impact lying between 1 and 3.6km from the mine edge, but in extreme cases the radius of impact could reach at least 6.6 km from the mine, and further if the system was anisotropic.

Therefore, given that the mine size modelled is 1km in the direction measured to get R_i, in many of the conditions, unlike Group A where impact is limited, derogation of groundwater level drawdown and water volume will much more often be a problem for aquifer systems of Groups B and C.

Annual volumes of about 15 Mm^3 and 11 Mm^3 of water is likely to be abstracted from aquifer systems of Groups B and C respectively. And this is about 3 times and 2 times the volume of water likely to be extracted from Group A aquifer systems. This would have much more impact on the water system.

Thus for systems like Groups B and C, villages within a distance of a few km from mine edge, as represented in the shaded portions of Table 6.1, 6.6 and 6.7, are most likely to be affected. For a system characterized by Group A, the impact radii are rather less, with in many cases the impact being only within a few hundred metres, a zone where other mining-related impacts would be severe too. With regard to Ghana, it is uncertain what hydraulic conductivity group is most appropriate, and therefore what the impact would be. However, there are some annual mine abstraction volumes available, and these can be used to indicate the likely Group to which the Ghana mines belong.

Table 6.9 shows some data on annual rates of freshwater usage from 2005 to 2008 for the two major mining districts in Ghana, Tarkwa and Obuasi. It is not known whether these abstraction volumes include surface inflow as well as groundwater inflow. It is therefore not easy to compare the field measured volumes with the statistically estimated volumes of groundwater abstractions of Groups A, B and C (Table 6.8) but because as a first

approximation we tentatively want to establish which rock group is appropriate for Ghana, a comparison has been made. On the average the annual total volume of freshwater usage by mines in Ghana is about 17Mm^3/y and this falls within the annual range of 15Mm^3/y to 19Mm^3/y (Table 6.9). This would suggest that the appropriate K Group for Ghana mines is B, having a range of R_i values of about 2.7km to 5.1km from mine centre and reaching a radius of about 7.6km in extreme cases, a potentially significant problem for nearby villages in Ghana.

Table 6.9 Annual volume of freshwater usage for gold mining operations in Ghana by the Tarkwa Goldfields Limited (Tarkwa) and Ashanti Goldfields Limited (Oboasi) (Source: Anglogold Ashanti Obuasi, Tarkwa goldfields and Iduaprem Country report 2008)

Gold mining company	Volume of water (m^3/Year)			
	2005	2006	2007	2008
Goldfields Limited (TGL) Tarkwa	5,200,000	3,529,537	5,596,000	7,941,690
Goldfields Limited (TGL) Tarkwa Damang	800,000	673,439	594,376	547,910
Ghana Australia gold-fields Limited (GAG); Iduaprem Tarkwa	977,466	98,000	1,000,000	1,000,000
Ashanti Goldfields Limited (AGC) Obuasi district	9,005,564	10, 356,870	10,621,257	9,419,952
Total annual volume of water (m^3/y)	15983030	14657846	17811633	18909552

6.3 The importance of recharge on radius of influence

The results of section 6.2 indicate that derogation may not be a problem in most mines for Group A aquifer system mines but could be more of a problem for Groups B and C assuming a potential R of 300 mm/y. However, it is possible that recharge may be less or possibly more and this will change the estimated radius of influence. For example Table 6.10 shows simulation results of the effect of recharge on radius of impact by decreasing recharge from 360mm/yr down to 30mm/yr for a mine of depth 200m. As recharge decreases, hydraulic heads drop and increase outwardly from mine and this indicates an increasing effect of radius of impact of about 500m for a change in recharge from 300mm/yr to 30mm/yr. Thus, in arid regions where recharge is very minimal as compared to humid climatic regions of the current research, mine derogation is expected to affect a larger area.

It is noted that increasing recharge from 300mm/yr to 360mm/yr did not result in much difference in the radius of impact, about 30m as indicated in Table 6.10 Model 5. Though the choice of a potential recharge value of 300mm/yr close to the actual recharge value of Kuma (2007) has erred on the safe side since lower recharge means greater radius of impact, it is clear that the difference between Kuma's (2007) estimate and that obtained in chapter 4 (385mm/y) makes no significant difference to the estimated radius of impact.

In the MODFLOW models recharge will be 300 mm/yr over most of the cone of depression, but if the water level rises enough it will drop rapidly over the interval from the 'evapotranspiration' ('ET') extinction depth to ground surface. Applying 'ET' is just a means of setting a maximum water level. If 'ET' is ten times the recharge rate then the maximum water level will be held at a tenth of the distance between the extinction depth and ground surface. This means that water levels will be at most about 1.9m below ground level and then above this there is no recharge. This assumption is investigated here by changing the 'ET' rate and then investigating the sensitivity of radius of impact. Simulation results of Table 6.11 indicate that an increase in evapotranspiration by a factor of 5, and 10 results in reduction in recharge and hence an increment of up to about 10% of the radius of impact, about 100m. This change is not very significant in comparison with the sensitivity of the radius of impact to the value of potential Recharge.

Thus recharge rate affects radius of impact, but unless the potential recharge rate is much less than estimated in chapter 4 the effect is very much less important than the effect of having changes in hydraulic conductivity. Very low potential recharge may occur in Ghana if there is a low permeability layer at shallow depths. In this case drawdowns would be larger but the shallow subsurface would be supplied by recharge at a much greater rate than the deeper aquifer uses and a perched system would happen. This perched system would then potentially support shallow wells.

Table 6.10 The effect of varying recharge from 360mm/yr down to 30mm/yr on the radius of impact in a mining environment for a mine depth of 200m, base of aquifer at 500m depth.

	Model 5	Model 1 (base model)	Model 2	Model 3	Model 4
K (m/s)	$3.8x10^{-09}$	$3.8x10^{-09}$	$3.8x10^{-09}$	$3.8x10^{-09}$	$3.8x10^{-09}$
ET (m/s)	$9x10^{-09}$	$9x10^{-09}$	$9x10^{-09}$	$9x10^{-09}$	$9x10^{-09}$
R (m/s)	9.86 x10-9	$8.19x10^{-09}$	$5.48x10^{-09}$	$2.73x10^{-09}$	$8.22x10^{-10}$
R (mm/y)	360	300	200	100	30
R_i (m)	**1162**	**1130**	**1184**	**1408**	**1685**

Table 6.11 The effect of varying evapotranspiration by about a factor of 5, 10 and 15 respectively on the radius of impact in a mining environment for a mine depth of 200m

	Model 1 (base model)	Model 2	Model 3
K (m/s)	$3.8x10^{-09}$	$3.8x10^{-09}$	$3.8x10^{-09}$
R (m/s)	$8.19x10^{-09}$	$8.19x10^{-09}$	$8.19x10^{-09}$
ET (m/s)	$9x10^{-09}$	$4.5x10^{-08}$	$9x10^{-08}$
R_i (m)	**1130**	**1186**	**1243**

6.4 Effect of x-y K anisotropy and boundary conditions

6.4.1 Introduction

The previous sections have indicated that the radius of influence under many though not all circumstances will be very limited when there is an isotropic infinite aquifer. Here in section 6.4.2 the effect of K anisotropy in the horizontal direction will be investigated. In section 6.4.3 the effect of boundaries will be investigated.

6.4.2 Impact assessment of K-anisotropy

The MODFLOW computer model has been used to simulate the impact of horizontal K-anisotropy on the groundwater flow regime and the radius of impact (R_i) measured along both the x and y axis. It should be noted that MODFLOW can only consider horizontal anisotropy with the principal axes of the conductivity tensor parallel to the x- and y-axis of the model grid.

A model domain of size 25km by 25km area was discretized into 2500 cells with 50 cells in the x-direction (Δy=500m) and 50 cells in the y-direction (Δx=500m), a coarse discretization. The bottom and top elevations of the model domain were taken to be 0m and 500m, respectively. All the horizontal grid boundaries of the model were initially taken to be no-flow boundaries because they were assumed to be far enough from the main areas of interest in the middle of the domain. An open pit of dimensions 2000m by 1000m in plan-view and a depth of 300m with a lake/sump of 200m constant head is placed at the centre of the model domain. The condition [R<ET] was maintained in order to keep hydraulic heads below the surface of the aquifer. A range of horizontal K-anisotropy ratio values (K_x/K_y) were used as inputs into MODFLOW whilst keeping recharge (R) and 'evapotranspiration' ('ET') constant.

Table 6.7 shows the input parameters used and the estimated radius of impacts as measured from the MODFLOW simulation results of Figure 6.5. The term radius will be used here for convenience even though the affected area is not circular. Measurement of radius of impact is taken in the direction of the axes of the ellipsoidal impacted area, with the biggest change in R_i occurring along the direction of high K (x-direction).

Table 6.12 Effect of horizontal anisotropy on the radius of impact (R_i) by varying K_x of the base model by a factor of 10, 50 and 100.

	Base model	Model 1	Model 2	Model 3
K_x (m/s)	$6.8x10^{-8}$	$6.8x10^{-7}$	$3.4x10^{-6}$	$6.8x10^{-6}$
K_y (m/s)	$6.8x10^{-8}$	$6.8x10^{-8}$	$6.8x10^{-8}$	$6.8x10^{-8}$
K-anisotropy ratio **(K_x/K_y)**	1.0	2.0	3.0	4.0
R (m/s)	$8.2x10^{-9}$	$8.2x10^{-9}$	$8.2x10^{-9}$	$8.2x10^{-9}$
ET (m/s)	$9x10^{-9}$	$9x10^{-9}$	$9x10^{-9}$	$9x10^{-9}$
R_{ix} (X-axis)	**1768**	**4278**	**8442**	**11750**
R_{iy} (Y-axis)	**1483**	**1312**	**1198**	**1147**
Ratio, R_{ix}/R_{iy}	1.2	3.3	7.1	10.2

Simulation results of Figure 6.5 show the effect of changing horizontal anisotropy ratio on the flow pattern and subsequently the radius of impact. Note that the regional K of the aquifer is increased at the same time as the change in anisotropy ratio. Simulation results of the first model show an isotropic and homogeneous flow with values of hydraulic conductivity the same in all directions. With increments in anisotropy ratio the models show a corresponding increase in radius of impact in the direction of increasing K. The radius increases from about 2 km in isotropic conditions to about 11.75 km in the direction of enhanced K for an increase in K in that direction of 100 times. If the aquifer had been isotropic with the higher value of K the radius of impact would have been about 8.5 km. The values used here include some very high K values for this environment but do show that anisotropy can be important. Thus within the constraint of the parameter values within the mining environments in Ghana hard rock anisotropy, in general, has an effect on the impacted area of surface mining with increasing horizontal anisotropy of the aquifer system. Hence greater drawdowns even than expected from isotropic aquifers with K values the same as the K in the maximum K direction should be expected in the direction of greatest K

direction in the aquifer. This direction may be indicated by the main fracture or bedding orientations observed in the field or by remote sensing. Analytically, the values in table 6.12 can be approximated by considering the following: The contours of equal drawdown around a pumping well lie on an ellipse described by the following parametric equation

$$r' = \left[\left(\frac{K'}{K_x}\right)x^2 + \left(\frac{K'}{K_y}\right)y^2\right]^{0.5} \qquad (6.2)$$

$$= \left[\left(\frac{K_y}{K_x}\right)^{0.5}x^2 + \left(\frac{K_x}{K_y}\right)^{0.5}y^2\right]^{0.5} \qquad (6.3)$$

where $K' = (K_xK_y)^{0.5}$ is the geometrical mean of permeability and x and y are the Cartesian coordinates (e.g. Huisman, 1972). It is observed that the radius of impact lies on one of these ellipses with the axis of the ellipse in the x direction equal to $(K_x/K_y)^{0.25}$ times the value for the isotropic case where K = K'. Similarly, in the y-direction R_i lies on one of these ellipses with the axis of the ellipse equal to $(K_y/K_x)^{0.25}$ times the value for the isotropic case. Thus the effect of anisotropy can be estimated by taking the following few steps:

1. take the isotropic case ($K = K' = (K_xK_y)^{0.5}$) and calculate the radius of impact $R_{ik'}$ (look up in Table 6.1, or use the equation developed later in Chapter 6)
2. calculate the R_i in the x direction from $(K_x/K_y)^{0.25}$ x $R_{ik'}$
3. calculate the R_i in the y direction from $(K_y/K_x)^{0.25}$ x $R_{ik'}$

Taking Model 3 in Table 6.12 as an example;

1. $K=K'=(K_xK_y)^{0.5}=(0.684\text{x}0.00684)^{0.5}=0.0684$m/d and from Table 6.1 above this value corresponds to an $R_{ik'}$ value approximately equal 3500m for a mine depth of 300m.
2. Therefore radius of impact in the X-direction due to anisotropy:
   $R_i = (K_x/K_y)^{0.25}$ x $R_{ik'}) = (0.684/0.00684)^{0.25}$ x 3500 =11067m
3. Similarly in the Y-direction the radius of impact die to anisotropy:
   $R_i = (K_y/K_x)^{0.25}$ x $R_{ik'}) = (0.00684/0.0684)^{0.25}$ x 3500 =1107m

Thus by comparing these results with those in Table 6.12, the radius of impact R_i in the X-direction is given by 11067m and 11750m whilst in the Y-direction gave 1107 and 1147m respectively. This is an error of about 6% in the X-direction and 3.5% in the Y-direction in estimation of the radius of impact.

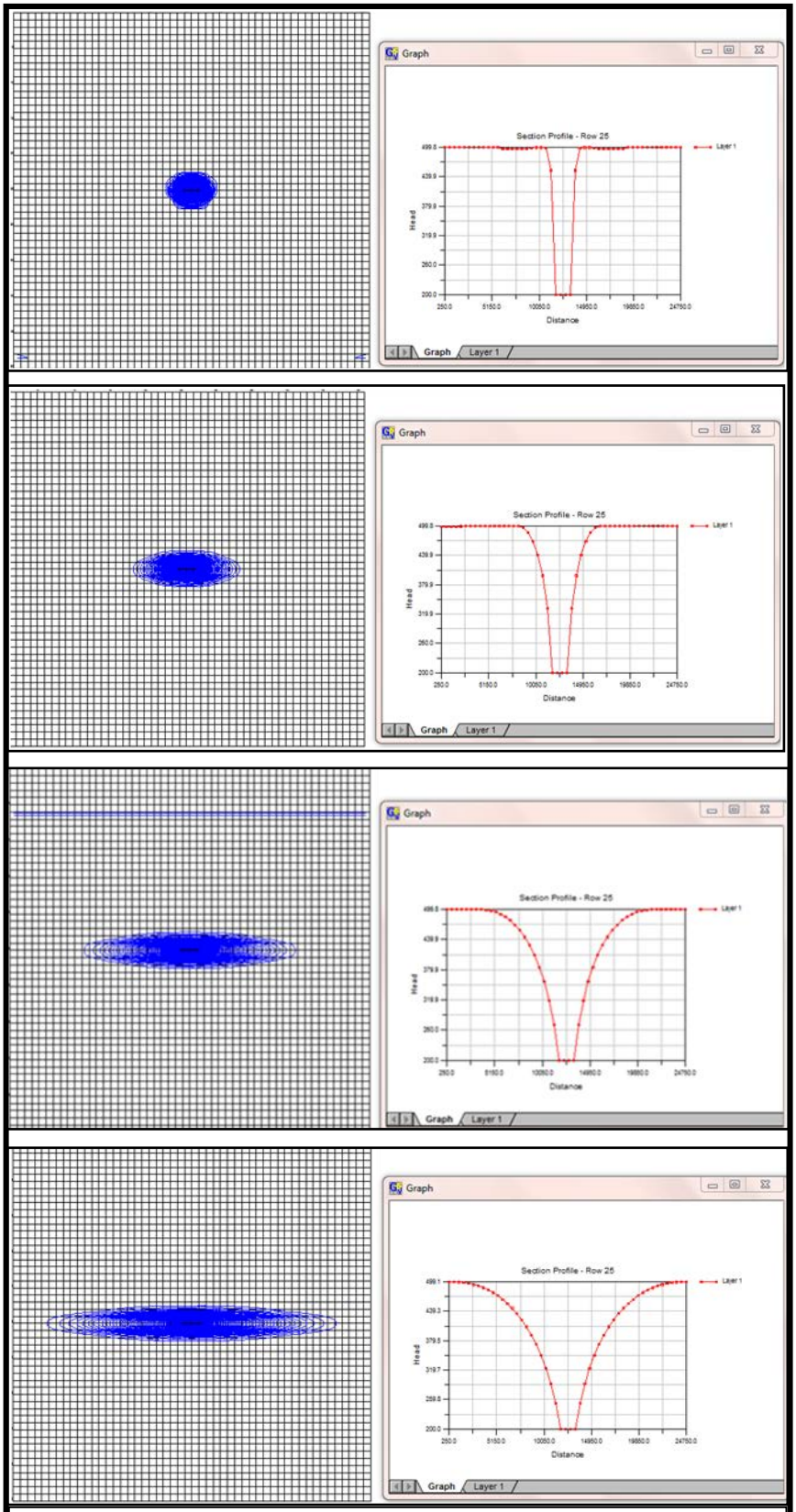

Figure 6.5 Simulation results showing the effect of horizontal anisotropy on R_i by varying K_x of base model (1 from top) by a factor of 10, 50 and 100 to obtained models 2, 3 and 4

6.4.3 Impact assessment of aquifer boundaries

The effect of boundaries is an issue in the mining environment of Ghana, taking into consideration the topography and drainage systems. The mining environments are characterised by gentle topography of low hills with rivers and streams meandering through them. The rivers and streams serve as recharge and discharge centres and the hills acting as groundwater divide. In addition there are often faults some of which may have low permeability or bring lower permeability rocks into contact with the aquifer.

This assessment demonstrates the effects of different lateral constant heads and no flow boundary conditions on the radius of influence of a steady state aquifer system. In the current study, the boundaries were placed in the model domain within the radius of influence. Simulations of five different combinations of boundary geometries were developed to illustrate this effect (Figure 6.6, Models 2 to 5). The head values and their separations were chosen to be consistent with major boundaries, for instance, the separation between major rivers and lakes within the mining environments in Ghana.

Comparison of results of models 2 to 5 with the base reference model (model 1) shows the effect of respective boundary conditions on the response of these systems. Model 1 is the base reference model of the mine in an effectively infinite aquifer system. In the presence of an impermeable boundary, water can no more be drawn from recharge beyond the boundary. The mine therefore exhibits more drawdown (model 4 and 5). Depending on head difference, constant head boundaries however, serve as either recharge or discharge points competing with the mine centre for groundwater flow and thereby can reduce or augment groundwater flow to the mine (model 3, 4 and 5).

If a village is between the mine and impermeable boundary (village B) then, by image theory drawdown will be increased at a proportion that increases as the village approaches the boundary, reaching a maximum of twice that is expected in the absence of the boundary when the village is at the boundary.

Similarly, if a village (village A) is between the mine and a constant head boundary, drawdown will be decreased at a proportion that increases as the village approaches the

boundary and reaching a maximum of zero drawdown at the boundary itself. If either boundary is partial, then the effect is diminished. However, if the village is on the opposite side of the mine from an impermeable or constant head boundary then drawdowns is unlikely to be affected much by that boundary as they are so far away.

Furthermore, the results obtained show that by placing constant heads as boundary conditions, groundwater flow divides can be formed. The constant heads serve as discharge points competing with the mine centre for groundwater flow and thereby reducing groundwater flow to the mine and rivers. However, the mine may increase total recharge by lowering water level and increasing the vertical head gradients, thereby maximizing recharge (possibly to values that may exceed soil infiltration rates).

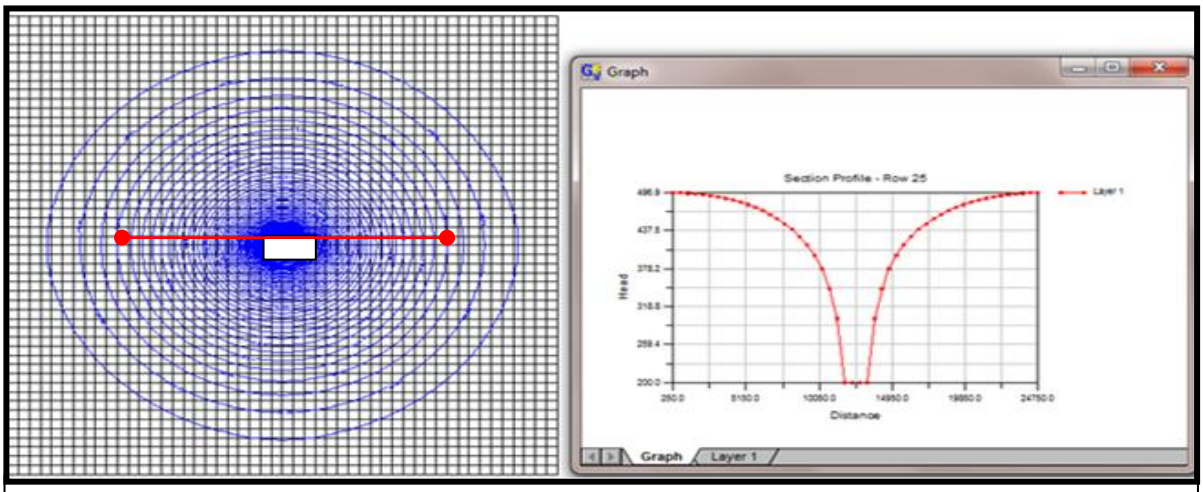

Model 1 The base reference model of aquifer thickness 500m and mine depth of 300m

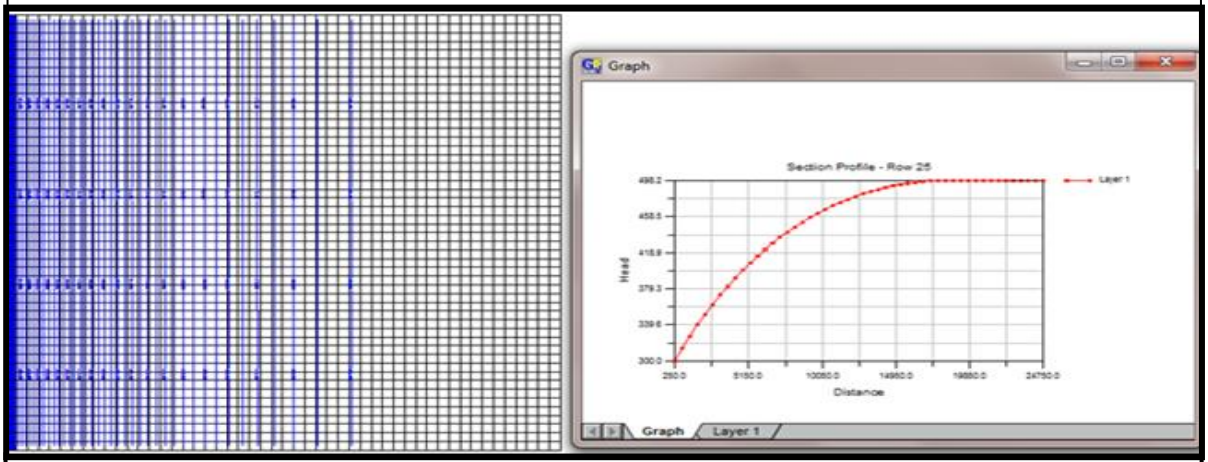

Model 2 Reference model with constant head of 300m placed in the western boundary

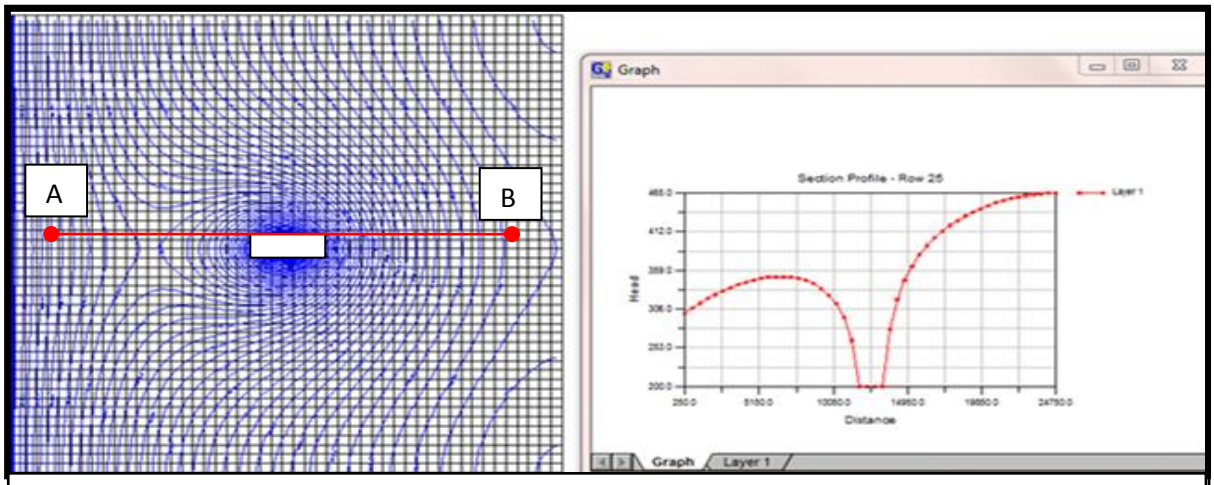

Model 3 Constant head of 300m in the western boundary with mine at the centre

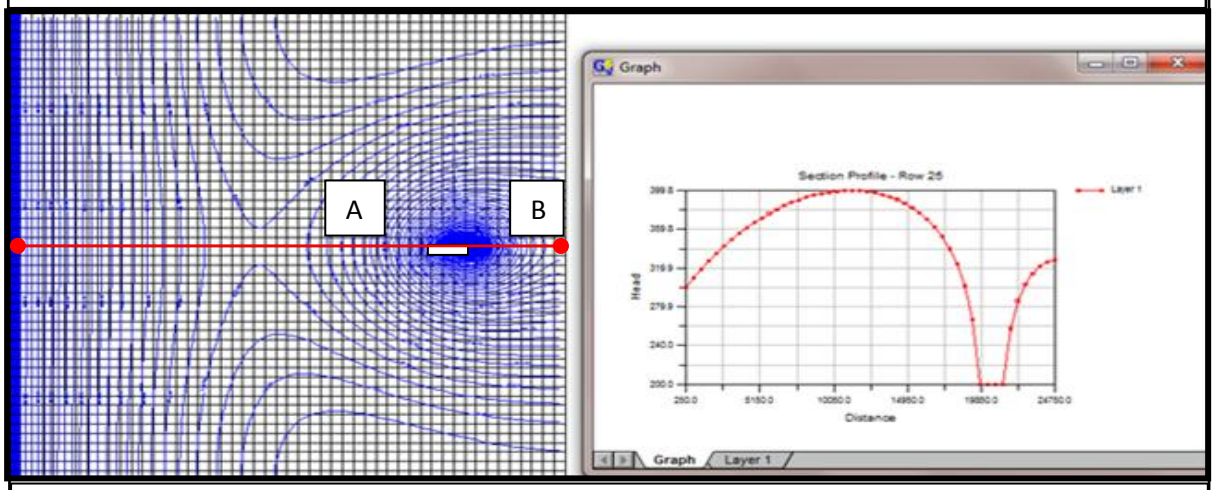

Model 4 Constant head of 100m in the west, and 50m in the east boundaries

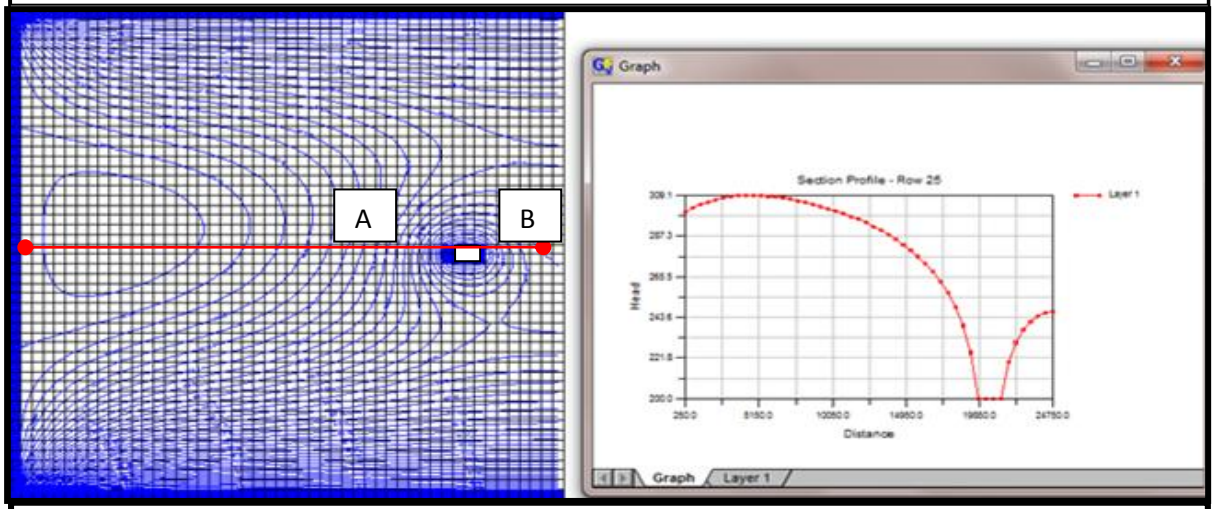

Model 5 Constant head of 300m, 200m, and 100m in the west, north and south boundaries respectively and no flow boundary in the eastern boundary.

Figure 6.6 The sensitivity of hydraulic heads and the radius of influence to different boundary conditions in the presence of a typical mine and settlements (village A and B) in the mining environment

6.5 Discussion

For most of the G, R and K and range of relevance, the simple models used here indicate that for Group A aquifer systems, the radius of impact will be so close (less than few 100m) to the mine that inhabitants may decide to move as a result of other issues. Table 6.1 has conditions where the radius of impact is predicted to be within 300m of the mine and shows that even at values of K equal to the median (3.8×10^{-9} m/s) found in the international literature survey, only the deepest mines will have any effect beyond 400m from mine's edge although in some cases the radius of impact is expected to reach 2km at the upper quartile K value. Uncertainties in estimates of radius of impact at such close distances are probably significant, but this has little practical importance as within a few 100 m various adverse impacts unrelated to derogation would be expected and really there is no practical need to know the precise radius of impact. For instance there may be other problems too from dust, stability, noise and especially loss of land. At such distances a range of major impacts on village life would also be expected.

Unlike Group A with its low K influence and hence less impact, derogation of groundwater level drawdown and water volume will be more of a problem for aquifer systems of Groups B and C of higher K values. The R_i corresponding to the median K is 3.6km for Group B and 3km for Group C from mine centre with 50% of cases occurring in the range of 2.7km to 5.1km and 2km to 4.6km, respectively. However, in extreme cases the radius of impact could reach at least 7.6 km from the mine for both Groups and further if the system was anisotropic.

Calculation shows that median annual volumes of water likely to be abstracted from Group A, B and C aquifer systems are about 7 Mm^3, 15 Mm^3 and 11 Mm^3, respectively. Thus the volume of water that could be extracted from Group B and Group C aquifer systems is about thrice and twice that of Group A respectively. Because there are very few data in Ghana, it is uncertain what hydraulic conductivity group is most appropriate, and therefore what the impact would be. However, the few available annual mine abstraction volumes were used to indicate the likely Group to which the Ghana mines belong. Preliminary calculations of the average annual field volume of water discharge by mines in Ghana (see Table 6.9) is about 17Mm^3/y, i.e. in the range of 15Mm^3/y to 19Mm^3/y, indicating that the most appropriate

Group of K data for Ghana is that of Group B of interquartile range of 2.7km to 5.1km and a median value of 3.6km. The radius of influence might also extend to significant distances if R is limited by some process (section 6.3). One possibility might be low vertical hydraulic conductivity in a weathered sequence. However if this were to happen then the shallow aquifer would be effectively perched and hence protected from derogation.

Aquifer anisotropy and heterogeneity, inherent in hard-rock aquifer systems, can affect both the flow direction and velocity of groundwater and hence the extent of impacted area in the mining environments. For instance, investigations on the effect of anisotropy (section 6.4.2) show that K anisotropy in the vertical plane and its orientation both affect flows and recharge acceptance rates, though such systems require explicit modelling to predict. The orientation of K anisotropy is significant as it determines the K values at different points in the flow system. In particular, flow to different sides of the same mine in an anisotropic K aquifer are not the same. In the extreme case, if the anisotropy is formed by widely spaced discrete fractures with little interconnection then there may be very little flow into one side of a mine if the fractures are oriented parallel to the slopes. More also, villages lying along the strike of fractures from the mine will be most vulnerable. It is noted that radius of impact in the direction of fracture strike can be much greater than expected from an isotropic case with the same K as the maximum K in the anisotropic case. Hence greater drawdowns even than expected from isotropic aquifers with K values the same as the K in the maximum K direction should be expected in the direction of greatest K direction in the aquifer.

Hydraulic boundaries within the region near the mine will also affect water levels especially in the case where the village lies between an impermeable boundary and the mine. Drawdown will be increased at a proportion that increases as the village approaches the boundary, reaching a maximum of twice that is expected in the absence of the boundary when the village is at the boundary. In other cases the effects are expected to be limited.

For any mine that is located in an unusually permeable aquifer where R_i values are greatest, there will be higher inflow rates and hence more possibilities for supplying surplus water to any villages affected. However, more data on K and volume from Ghana are needed to confirm.

6.6 Proposed method for applying findings

Returning to the analytical model discussed in chapter 5, and in particular equation 5.7, the relationship between radius of impact and $(K/W)^{0.5}$ has been investigated to see if this could be used as a rough indication of radius of impact. Using R_i data from MODFLOW and the analytical model, plots of R_i' against $(K/W)^{0.5}$ have found to be approximately linear (figure 6.7) where R_i' is the distance to 1 m drawdown measured from the edge of the mine; i.e. $R_i' = A(K/W)^{0.5}$ where A is a constant of proportionality. The constant of proportionality calculated for each mine depth is recorded in Table 6.8 and figure 6.8 shows the relationship between A and mine depth D. From figure 6.8 the relationship between mine base level (D) and the constant of proportionality (A) is given by the relation:

$$A = 25.83D^{0.44} \qquad (6.4)$$

The predictions are not accurate at small radius of impacts but are within about 15% at high radiuses. Thus, it is proposed that for assessing possible derogation of a village the following scoping calculations and heuristic rules could be followed:

1. estimate the radius of impact as measured from the mine edge using $R_i' = A(K/W)^{0.5}$ where A is given by equation 6.3 for mines of typical radius in Ghana, K is the hydraulic conductivity and W is the recharge rate
    a. K values can be based on the results from chapter 3, for instance for group A, with a median value of 3.28×10^{-04}m/d and interquartile range from 8.59E-02 to 9.50E-06 m/d
    b. W values can be based on proportions of recharge or on estimates using Hydrus or equivalent methods (chapter 4)
2. if the village lies along the strike of the fractures impacts may be expected to possibly twice the R_i' distance; alternatively the effects can be estimated by the method outlined in section 6.4.2
3. if the village lies between the mine and a possible impermeable boundary then the drawdowns may be up to twice that expected from the calculation in point
4. if the village lies between the mine and a permanent water body then the drawdown will be less than predicted from the calculation in point 1.

If no calculations are possible then in general in Ghana derogation distances are expected to be within a few hundred metres for Group A aquifer system but much greater for Groups B and C aquifer systems. In other regions of the world where there is much less recharge there may be greater effects.

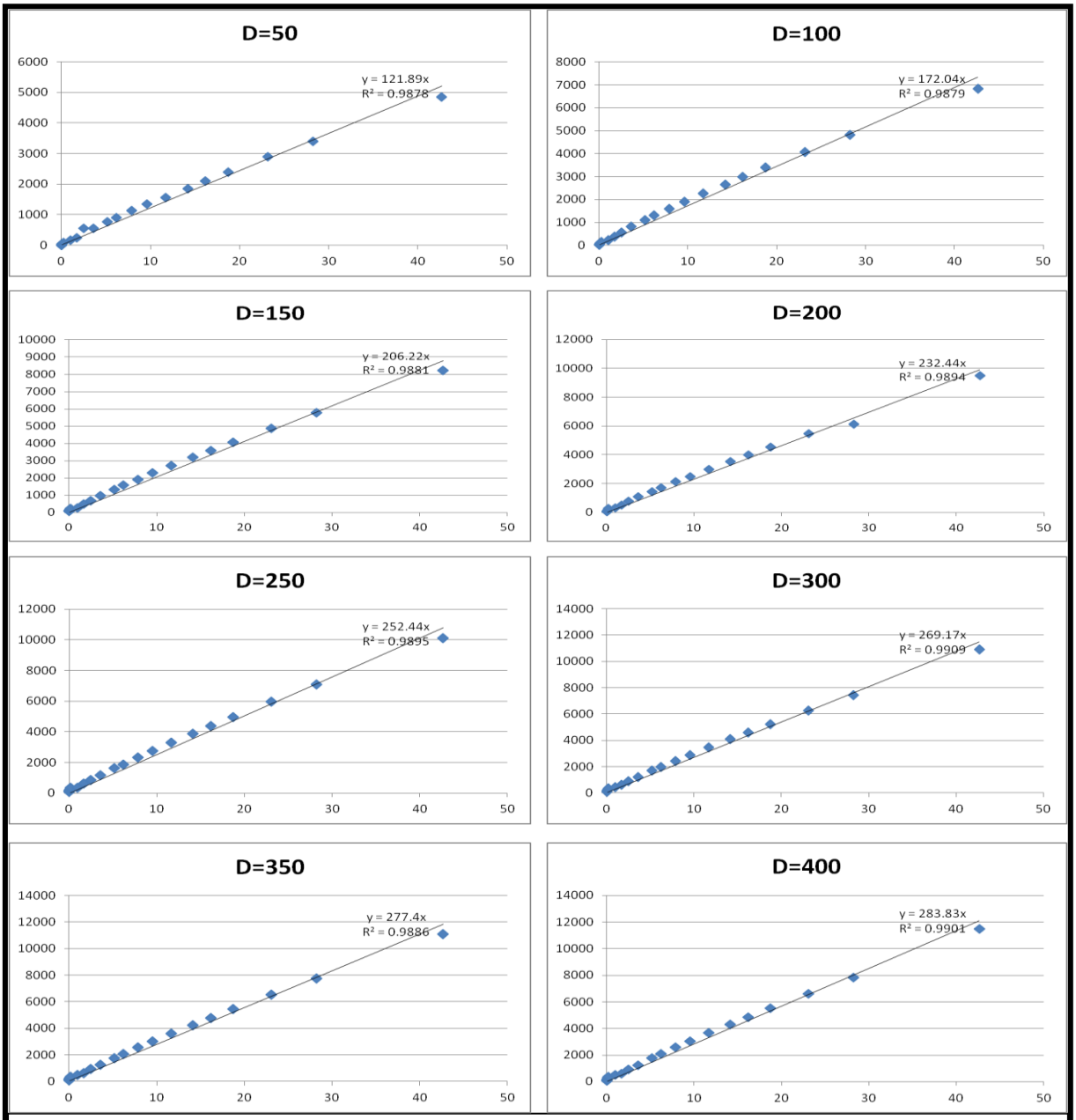

Figure 6.7 Plots of radius of impact (R_i') as measured from mine edge against $(K/W)^{0.5}$ for different mine depths D (m).

Table 6.13 Constant of proportionality (A) of plots from Figure 6.7 for various mine depths (D)								
Mine Depth D(m)	50	100	150	200	250	300	350	400
Constant of proportionality A (m)	122	172	206	232	252	269	277	284

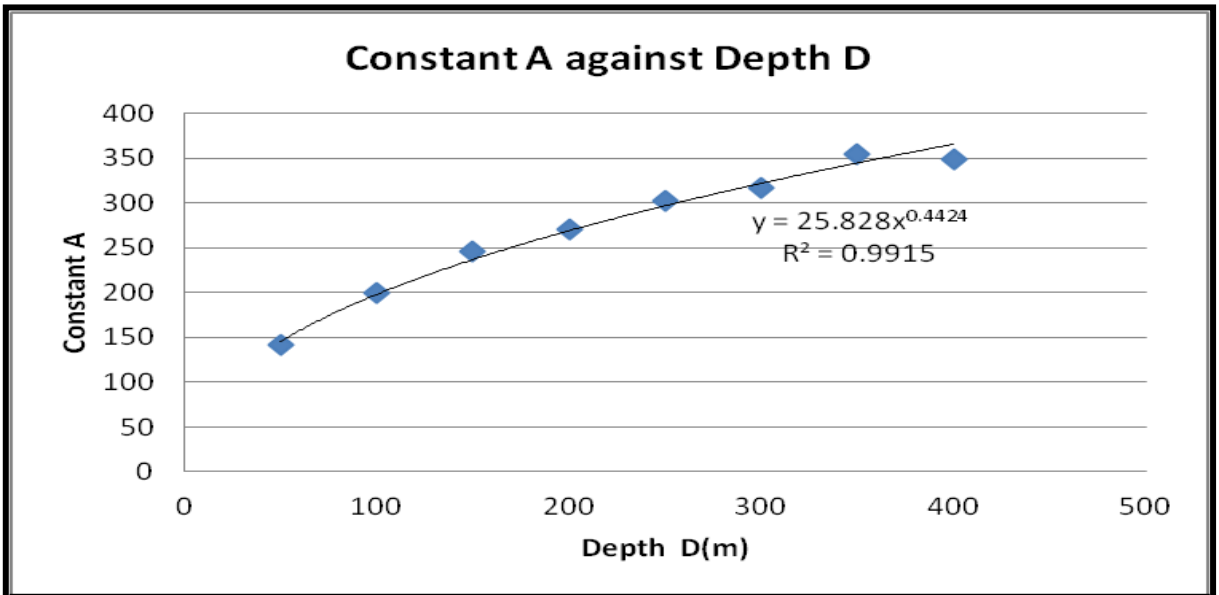

Figure 6.8 Relationship between constant of proportionality (A) and mine depth (D)

CHAPTER 7

CONCLUSIONS AND RECOMMENDATIONS

The aim of this research has been to determine under what circumstances gold mines in Ghana are likely to have an adverse effect on water levels in surrounding villages/farms and in particular to try and come up with heuristic rules that would indicate under what circumstances there may be derogation problems in the regional groundwater flow system.

Because adequate data were not available to this study to investigate particular mines, this study has adopted a scoping approach involving;

1. assessment of mine geometries in Ghana (G)
2. collation and examination of hydraulic conductivity (K) data on hard rock aquifers from around the world
3. assessment of recharge (R) using an unsaturated zone flow model to account for infiltration rejection
4. use of simple mathematical models with G, K and R data from the previous sub studies to undertake scoping calculations
5. use of the results from 4 to determine what conditions would result in significant derogation issues.

7.1 Mine geometry

Mine geometry is needed to build simple conceptual and numerical models of open pit mines to undertake simple scoping calculations on the effects of mine derogation on the regional groundwater flow system. Assessment of mine geometries shows that generally, the layout of surface mines depends on the geometry (shape, size and depth) of the mineral deposit. In most cases, the shape and size of the pit is designed to fit the geometry of the deposit as well as the characteristics of the host rock, especially when the ore-body is typically of vein-type, pipe-shaped, steeply dipping stratified or irregular and closer to the surface. Considering the geometry properties of ore reserves in Ghana, the layout of most open pits mines are characterised by rectangular and oval shape with benches and spiral

roads. In plan-view, the dimensions of the pits on the average range between 500m to 2000m and reach a maximum economic depth of approximately 300m.

7.2 Hydraulic conductivity

The entire database includes about 768 hydraulic property estimates (hydraulic conductivity (K), transmissivity (T) and specific capacity (Sc)) collected from 17 different studies and about 20 published reports worldwide. Of the total number of estimates, 27 were compiled from pumping tests, 13 from specific capacity tests, 90 from slug/pulse tests, and 645 from packer/injection and drill stem tests. Due to variation of K in space the following two main difficulties were encountered in the estimation of appropriate K for modelling at the regional scale level: (1) the process of transforming or linking the apparent conductivity (K_{app}) values obtained from field testing to the representative conductivity (K_{reg}) values appropriate for modelling at regional scale, and (2) the possible bias in field data resulting from the purpose for which the field measurements were made.

In view of the above difficulties, a simple statistical method was used to characterize the range of K values required for the construction of the numerical models of the groundwater flow system in the mining environments. And because the distribution of quantities of hydraulic parameters in fractured and heterogeneous crystalline rocks is often strongly skewed to the right, the median in combination with the inter-quartile range (IQR) of the data provided a much better representation of hydraulic conductivity for the combined dataset. Summary statistics of K-parameter values ranges from $1.40x10^{-13}$ m/s to $1.45x10^{-03}$ m/s with an overall mean, median, standard deviation and a geometrical mean of $1.48x10^{-05}$ m/s, $3.80x10^{-09}$ m/s, $9.74x10^{-05}$ m/s, and $1.57x10^{-08}$ m/s respectively.

The overall distribution exhibited a bi-modality which was thought to be due to the influence of dataset obtained by Gale and Witherspoon (1979) from Stripa mine site that was targeted for its low fracture occurrence in its original development work. And more also the dataset obtained by Snow (1979) from grouting at dam and tunnel sites with its high fracture occurrence. Therefore, in order to have a fair K distribution in the assessment process the whole dataset has been further analyzed to include the following groupings:

(i) The whole dataset, less dataset on radioactive waste of low fracture occurrence from Gale and Witherspoon (Group B).

(ii) The whole dataset, less dataset on radioactive waste of low fracture occurrence from Gale and Witherspoon and dataset of Snow from grouting at dam and tunnel sites of high fracture occurrence (Group C).

Variability in dataset (inter quartile range) is highest in group A (9.94E-07 to 1.10E-10 m/s) followed by group C (4.62E-06 to 8.69E-09 m/s) and then group B (4.41E-06 to 9.61E-08 m/s) with corresponding median values of 3.80E-09, 9.88E-07 and 4.47E-07 m/s respectively.

Generally, taking all the data together, K decreases approximately exponentially with depth in hard rock aquifer systems with permeable fractures present at shallow depths but reduce in frequency with depth as expected. K was found to decrease with depth from the surface of the aquifer up to 300m, beyond which K remains approximately constant at this scale for at least the next 100m. At the shallowest levels K is affected by weathering, with often greater K values being recorded, at least in the moderately weathered, middle depth section of the weathered zone. In Ghana, especially in the Tarkwaian rock system the weathering zone depth is typically of around 20m (Kortatsi 2004), though it can vary from less than 1m to at least 100m (Singhal & Gupta, 1999).

However, by limiting the investigation to sites of similar geology and climate, the relationship with depth was found to be variable and characterized by a great deal of scatter. It was observed that depth variation is poorly developed at any specific site but with higher K at shallow depths. The high data scatter may be due to the fact that most of the data were obtained from small scale test measurements and also due to weathering differences of rock types. The main factors likely to affect K, including rock type, climate and tectonic regime, were also investigated to see if they could be used to limit the range of possible K values at any given site. It was found that limiting data to similar rock type, similar climate, or similar tectonic regime did not constrain K ranges. Hence the combined dataset was used to represent international dataset and also used for all the calculations but took into consideration the influence of the dataset obtained by Gale and Witherspoon (1979) from Stripa mine site that was targeted for its low fracture occurrence in its original

development work and also the dataset obtained by Snow (1979) from grouting at dam and tunnel sites with its high fracture occurrence. Thus three groups of hardrock systems were identified: Group A including all the data obtained in the study; Group B including all the data except those from the Stripa site; Group C including all the data except those from Stripa and those from grouting at dam sites. Group A data are biased to low K; Group B to high K, and Group C are possibly the least biased. Which group is most relevant to Ghana is uncertain, but is discussed below.

7.3 Potential direct recharge

A study was conducted to estimate the potential direct recharge rate to be used in the assessment of likely impacts of mine derogation on the regional groundwater flow system in South Western Ghana, where the greatest concentration of open pit mines are found. The basic approach was to perform numerical simulation of direct infiltration of the unsaturated zone, of the top soil of hard rock areas using HYDRUS-1D computer software package (Šimunek et al., 1999). The bottom flux was then used as a potential recharge for the regional groundwater flow modelling process with the MODFLOW Computer Code (Chapter 5). Recharge was input as an areally distributed value across the model.

The potential direct recharge rate was estimated to range between 18% and 36% (an average of 27%) of the mean annual precipitation rates. This translates to an average annual potential recharge rate ranging from 269 to 611 mm/yr with an average annual rate of 385mm/y. This high value (385mm/yr) is reasonable on the basis that it represents the potential maximum value of the actual recharge and compares with an estimate of 299±72 mm/yr for actual recharge as reported by Kuma et al. (2007). Regression analysis between the calculated recharge rate and the measured precipitation rate showed that annual predicted recharge rate is proportional to annual precipitation rate but with a low correlation coefficient, ranging from 0.39 to at least 0.72, for the selected soil types. The limited correlation suggests that estimating recharge as a proportion of precipitation may not be a good method for Ghana.

7.4 Assessment of radius of impact

7.4.1 Approach

The radius of influence/impact is the main variable of this assessment process and by definition two measures of this were considered when using numerical models: (i) radius of influence (R_e) as estimated by the locus of a drawdown of an amount X cm, and (ii) radius of impact (R_i) as defined by the locus of a drawdown of 1m, this being an amount of drawdown likely to be noted by users of wells as well as the impact on surface water systems. Measurement of radius of impact was taken from the centre of mine in the x direction, the direction of the long axis of the mines modelled.

Because the data available were so uncertain and of limited types, the approach taken was to use very simple numerical models with few parameters and to determine the sensitivity to assumptions and the likely direction in which errors would change R_i. More sophisticated models would be needed if greater accuracy is required for a particular mine but this would require much greater data availability that would only come as the mine investigation proceeded.

7.4.2 Results of model calculations

Using the Group A (entire) K data set, most of the simple models used in conjunction with mine geometries, recharge rates, conductivity and range of relevance predicted very close radius of impacts to the mine, less than few 100m with a median distance of 400m from mine's edge although, though it is expected that 25% of cases could reach up to 2km and further if the system was anisotropic. For distances from the mines of only a few 100m as Group A predicts for many conditions, there may be other problems too from dust, stability, noise and especially loss of land. At such close distances a range of major impacts on village life would also be expected.

Unlike Group A with low K influence and hence less mining impact, derogation of groundwater level drawdown and water volume is more of a problem for Group B and C aquifer systems of higher K values. For these systems, model results show that 50% of cases could reach up to 3.6km for Group B and 3km for Group C from the mine centre respectively and occurring within the range of 2.7km to 5.1km and 2km to 4.6km for the two groups.

However, in extreme cases the radius of impact could reach at least 7.6 km from the mine centre, and further if the system was anisotropic.

Corresponding calculations of mine derogation (Table 6.8) of water volumes for the three Groups (A, B and C) show that annual volume of about 7 Mm^3, 15 Mm^3 and 11 Mm^3 respectively are likely to be abstracted. Preliminary estimates of average annual field volume of water discharge by mines in Ghana, about 17Mm^3/y with a range of 15Mm^3/y to 19Mm^3/y, suggest that the appropriate K dataset for the Ghana mines is that of Group B implying that derogation of water volume and water level are likely to occur to significant distances from mines in Ghana. It should however, be noted that the results are very sensitive to K, and therefore there is the need in Ghana to publish K and/or volume data that will enable suggestions from this work to be confirmed.

The radius of influence might also extend to greater distances if R is limited by some process, e.g. low vertical hydraulic conductivity in a weathered sequence. However if this were to happen in Ghana then the shallow aquifer would be protected from derogation as the relatively high potential recharge rate would be able to maintain shallow and deep aquifers.

Anisotropy can affect the radius of impact significantly (section 6.4.2) and hence villages lying along the fracture strike from the mine will be more vulnerable than those lying in the dip direction. However, the hydraulic conductivity still needs to be high to affect at distance. The orientation of K anisotropy is significant as it determines the K values and hence flows in different directions away from the mine. It is established that flow to different sides of the same mine with constant anisotropy properties are different. For the extreme case where the anisotropy is formed by widely spaced largely unconnected fractures then there could be very little flow into the sides of a mine oriented parallel to the fractures but much from the sides intercepting the fractures.

Hydraulic boundaries will also affect water levels and hence the impacted area significantly especially in the case where the village lies between an impermeable boundary and the mine. In other cases the effects are expected to be limited. Model results show that, by

image theory, if a village is between a mine and impermeable boundary then, drawdown will be increased by an amount that increases as the village approaches the boundary, reaching a maximum of twice that is expected in the absence of the boundary when the village is at the boundary.

Similarly, if a village is between the mine and a constant head boundary, drawdown will be decreased at a proportion that increases as the village approaches the boundary and reaching a maximum of approximately zero drawdown at the boundary itself. If either boundary is partial, then the effect is diminished. However, if the village is on the opposite side of the mine from an impermeable or constant head boundary then drawdowns are unlikely to be affected much by that boundary. For any mine that is located in an unusually permeable aquifer there will be higher inflow rates and hence more possibilities for supplying surplus water to any villages affected.

In conclusion, simple models have allowed estimates of R_i but are very sensitive to K. By constraining K using water volumes produced by mines in Ghana, and comparing with the model output, it is tentatively suggested that for Ghana the most likely R_i values are the Group B dataset in the range of 2.7km and 5.1km from mine centre. To confirm this there is a need for more K or volume data for Ghana.

7.5 Applications of findings

7.5.1 Overview of implications for Ghana

As indicated by Kuma (2006) and Lutz et al. (2007), no groundwater flow model is known to exist in the study area. The research findings therefore have the implication of first and foremost providing first-pass qualitative information for hydrogeologists and engineers for gold mining design purposes.

It will also serve as guidelines for the most important data to collect for early assessment of derogation impacts. And finally, it will provide a means of informing decision-making and regulatory bodies on environmental implications when allocating mining concessions or giving out permits for mining operations in Ghana.

7.5.2 Specific application in Ghana

Specifically, the semi-quantitative approach discussed in the last section of chapter six could be used to assess possible derogation of domestic wells and surface water systems in nearby villages and settlements in the mining environments.

In instances whereby villages and settlements lie along the strike from the mine, horizontal anisotropy is expected to be significant and therefore radius of impact of derogation effects could be estimated by the use of the analytical formulation of anisotropic systems developed in section 6.4.2.

7.5.3 Application elsewhere

The research effort could be applied elsewhere apart from Ghana.

1. Local assessment of mine geometry (G) which is a function of the geometry of ore reserves in the location of interest.
2. Because recharge is region specific it should be locally assessed, but could take the same approach as the current use of Hydrus.
3. The K dataset, if none locally, could be used elsewhere due to its international characteristics.
4. The model calculations and correlation approach could be adapted simply to other systems, e.g. other mine geometries.

7.6 Recommendations

This thesis has attempted to assess the likely distances to which open pit hard rock mining operations of the type common in Ghana are likely to derogate village wells and surface water bodies. As indicated by Kuma (2006) and Lutz et al. (2007), no groundwater flow model is known to exist in the study area. Therefore, arising from the detailed findings presented and the conclusions drawn, the following recommendations can be made:

1. despite clear results in general, no substitute for representing local conditions, therefore suggest testing out the validity of the empirical results against mine data though getting such data, even if it existed, proved impossible in the present investigation

2. conduct much fuller investigation of the weathered zone, and how it interacts with the deeper system
3. investigate into details the issue of seepage face
4. more data collection should be undertake especially on K
5. use mine discharges to further calibrate models
6. more work to confirm high potential recharge rates
7. investigate the importance of non-Darcian flows
8. collate more international data on hard rock K
9. look at how measured K values using small scale testing relates to regional flow systems
10. confirm that equivalent porous media are an appropriate way to represent flow near mines
11. Put together a tool including the proposed methods in the thesis and the K data base (and a similar one for R)
12. To release, publish and collate K and volume data for Ghana and other countries.

List of Reference

Acquah, P. C., (1992). Emerging trends in gold processing and some related environmental issues in Ghana. *Regional Trends in African Geology, Proceedings of the 9th International Geological Conference Accra, 2-7 November 1992.* Geological Society of Africa

Acworth, R. I., (1981). The evaluation of groundwater resources in the crystalline basement of northern Nigeria, *Unpublished PhD Thesis*, University of Birmingham

Acworth, R., (1987). The development of crystalline basement aquifers in a tropical environment, *Quarterly Journal of Engineering Geology*, Vol. 20: 265-272

Agyapong, W. A., Amanor, J. A., and Acheampong, E. O., (1992); Selective open pit gold mining at Ashanti Goldfields, Obuasi, Ghana. *Regional Trends in African Geology; Proceedings of the 9th International Geological Conferenc Accra, 2-7th November 1992.* Geological Society of Africa

Akabzaa, A., and Darimani, M., (2001). Impact of Mining Sector Investment in Ghana: A study of the Tarkwa Mining Region. *A report prepared for SAPRI*, January 2001.

Akabzaa, T., and Darimani, A., (2001). Impact of Mining Sector Investment in Ghana: A case study of the Tarkwa Mining Region*, a Draft Report,* www.saprin.org/ghana/research/gha_mining.pdf. Accessed on 27/03/13

Akosa, A.B., Adimado, A.A., Amegbey, N.A., Nignpense, B.E., Carboo, D., and Gyasi, S., (2002). Report submitted by Cyanide investigation committee, *Ministry of Environment and Science.* June 2002.

Allibone, A.H., Hayden, P., Cameron, G., and Duku, F., (2004). Paleoproterozoic gold deposits hosted by albite and carbonate altered tonalite in the Chirano district, Ghana, West Africa. *Economic Geology,* vol. 99, p, 479-497.

Allison, G.B., Gee, G.W., and Tyler, S.W., (1994). Vadose-zone techniques for estimating groundwater recharge in arid and semiarid regions. *Soil Sci. Soc. Am. J.* 58, 6–14.

Amonoo-Neizer, E. H., and Busari, G. L., (1980). Arsenic status of Ghana soils-contamination of soils near gold smelters; *Ghana J. Sci*. 20 (1&2): 57–62

Anderson, M.P., and Woussner, W.W., (1992). Applied groundwater modeling: Simulation of flow and advective transport; *Academic Press*, San Diego, 381 p

Appiah, H., Norman, D. I., Kuma, J. S., Nartey, R. S., and Dankwa, J. B. K., (1993). Sources of diamond in the Bonsa field. *Regional Trends in African Geology. Proceedings of the 9th International Geological Conference (Accra, 2-7November 1992.* Geological Society of Africa.

Asklund, R., and Eldvall, Björn, (2005). Contamination of water resources in Tarkwa mining area of Ghana, Department of Engineering Geology, Lund University, 2005

Avotri, T.S.M., Amegbey, N.A., Sandow, M.A., and Forson, S.A.K., (2002). The health impact of cyanide spillage at gold fields Ghana Ltd., Tarkwa. May (funded by Goldfields Ghana limited, GFGL)

Babbitt, H.E., and Caldwel, D.H., (1948). The free surface around, and interference between, gravity wells; *Engineering Experimental Station Bulletin*, 374 University of Illinois, USA

Bandis, S., Lumsden, A.C., and Barton, N.R., (1983). Fundamentals of rock joint deformation. *Int J Rock Mech Min Sci Geomech* Abstr 20:249–268.

Barfield, B.J., Warner, R.C., and Haan, C.T., (1981). Applied Hydrology and Sedimentology for Disturbed Lands*,* Oklahoma *Technical Press*, Stillwater, OK, 603 pp.

Barker, J.A., (1988). A generalized radial-flow model for pumping tests in fractured rock, *Water Resour*: Res., 24 (10), 1796-1804.

Barker, R. D. (2001). Imaging fractures in hardrock terrain. University of Birmingham, UK. http://www.bham.ac.uk/EarthSciences/research/hydro/envgeo/. Accessed on 23/03/13.

Batelaan, O.F., De Smedt, and L., Triest, (2003). Regional groundwater discharge: Phreatophyte mapping, groundwater modelling and impact analysis of land-use change, *J. Hydrol*., 275, 86 – 108, doi:10.1016/ S0022-1694(03)00018-0.

Belcher, W.R., Elliot, P.E., and Geldon, A.L., (2001). Hydraulic Properties for Use With a Transient Ground-water Flow Model of the Death Valley Regional Ground-water Flow System, Nevada and California: *U.S. Geological Survey Water Resources Investigation Report* 01-4120: Carson City, NV.

Belcher, W.R., Sweetkind, D.S., and Elliot, P.E., (2002). Probability Distributions of Hydraulic Conductivity for the Hydrogeologic Units of the Death Valley Regional Ground-Water Flow System, Nevada and California: *U.S. Geological Survey Water Resources Investigation Report* 02-4212: Carson City, NV.

Benneh, G., Agyepong, G.T., and Allotey, J.A., (1990). Land degradation in Ghana. Food Production and Rural Development Division. Commonwealth Secretariat, Marlborough House. Pall Mall. London.

Bjerg, P.L., Hinsby, K., Christense, T.H., and Gravesen, P., (1992). Spatial variability of hydraulic conductivity of an unconfined aquifer determined by a mini slug test. *J Hydrol* 136:107–122.

Black, J.H., (1987). Flow and flow mechanisms in crystalline rock, in Fluid Flow in Sedimentary Basins and Aquifers, *Geol. Soc. Special Publication* No. 34, pp. 186-200.

Bliss, J., and Rushton, K., (1984). The reliability of packer tests for estimating the hydraulic conductivity of aquifers. *Q. J. Eng. Geol*. Vol. 17, pp. 81-91.

Bower, H., and Rice, R.C., (1976). A Slug Test For Determining Hydraulic Conductivity Of Unconfined Aquifer with Completely Or Partially Penetrating Wells. *Water Resources Research*. vol. 12, no. 3, pp. 423- 428 June.

Brace, W.F., (1980). Permeability of crystalline and argillaceous rocks. *Int. J. Rock Mech. Min. Sci. and Geomech*. Abstr. 17:241.

Brace, W.F., (1984). Permeability of crystalline rocks: New in-situ measurements. *J. Geophys. Res.* 89(B6):4327.

Braester, C., and Thunvik, R., (1984). Determination of formation permeability by double packer tests. *J. of Hydrology*.vol.72, pp. 375-389.

Brammer, H., (1956). C. F. Charter's interim scheme for the classification of tropical soils, Kumasi Division of Agriculture, Soil and Land-use Survey Branch, Occasional paper 2, Accra, Ghana.

Bredehoeft, J.D., and Papadopulos, S.S., (1980). A method for determining the hydraulic properties of tight formations; *Water Resources Research* (16):1,233-238

Bredehoeft, J.D., (1965). The drill-stem test, the petroleum industry's deep-well pumping test: *Groundwater*, vol. 3, no. 3, p. 31–36.

Brooks, R.H., and Corey, A.T., (1964). Hydraulic properties of porous media. *Hydrol Pap.* 3. Colorado State Univ., Fort Collins

Brown, S. G., (1963). Problems of utilizing ground water in the west-side business district of Portland, Oregon: *U.S. Geological Survey Water-Supply Paper* 1619-O, 42 p.

Burgess, A., (1977). Groundwater Movements Around a Repository. Regional Groundwater Analysis, Kaernbraenslesaekerhet, Stockholm, Sweden.

Canter, L.W., (1996). Environmental Impact Assessment *McGraw Hill International Editions*, pp 660

Carboo, D., and Sarfo-Armah, Y., (1997). Arsenic pollution in stream sediments in the Obuasi area. *Proceedings of the Symposium on the Mining Industry and the Environment; KNUST/IDRC 1997*, 114–119.

Carlsson, H., Carlsson, L., Jamtlid, A., Nordlander, H., Olsson, O., and Olsson, T. (1983). Cross-hole techniques in a deep seated rock mass. *Bull Int Assoc Eng Geol* 26–27:377–384.

Carlsson, A., and Olsson, T., (1977). Hydraulic properties of Swedish crystalline rocks-hydraulic conductivity and its relation to depth, *Bulletin of the Geological Institute,* University of Uppsala, 71–84.

Celia, M.A., Bouloutas, E.T., and Zarba, R.L., (1990). A general massconservative numerical solution for the unsaturated flow equation. *Water Resources Research*, 26(7), 1483−1496.

Cheng-Yu Ku, S. M., Hsu, L.B., Chiou, G. F. and Lin, (2009). An empirical model for estimating hydraulic conductivity of highly disturbed clastic sedimentary rocks in Taiwan, *Engineering Geology*, Vol. 109.

Chilton, P. J., and Foster, S. S. D., (1993). Hydrogeological characterisation and water-supply potential of basement aquifers in tropical Africa. *IAH XXIV Congress Mémoires* (in press).

Chilton, P. J., and Foster, S. S. D., (1995). Hydrogeological characterisation and water supply.

Chilton, P.J., and Foster, S.S.D., (1984). Hydrogeological characterization and water-supply potential of basement aquifers in tropical Africa, *Hydrogeology J.,* 3(1), 36-49

Chirano Gold Mine Limited Project (CGMLP), Environmental Impact Statement (2004 and 2010).

Chirlin, G.R., (1990). The slug test: The first four decades, in: *Ground Water Management, No. 1, Proceedings 1990 Cluster of Conferences, Kansas City, MO, 20-21 February 1990, National Water Well Assoc*., p. 365-381.

Clauser, C., (1992). Permeability of crystalline rocks. EOS, Trans. *Amer. Geophys. Union,* 73(21):233–240.

Clement, C., Asmah, R., Addy, M. E., Bosompem, K. M., and Akanmori, B. D., (1997). Local sulphooxidizing bacteria for environmentally friendly gold mining. *Proceedings of the Symposium on the mining industry and the environment, .KNUST/IDRC 1997*. pp. 120–122.

Coakley, G.J., (1999). The mineral industry of Ghana. *Minerals Yearbook*, Vol. III, United States of the Interior, Geological Survey.

Cook, P. G, (2003). A guide to regional groundwater flow in fractured rock aquifers, csiro Land and Water, Glen Osmond, SA, Australia.

Cook, F.J., and Cresswell, H.P., (2008). 'Estimation of soil hydraulic properties [Chapter 84]', in Carter, M.R., and Gregorich, E.G, eds, *Soil Sampling and Methods of Analysis,* Canadian Society of Soil Science, Taylor and Francis, LLC, Boca Raton, FL pp. 1139-1161.

Cooper, H.H., Jr., Bredehoeft, J.D., and Papadopulos, S.S., (1967). Response of a finite diameter well to an instantaneous charge of water: *American Geophysical Union, Water Resources Research,* vol. 3, no. 1, p. 263–269.

Curtis, W.R., (1971). Strip mining erosion and sedimentation. In: Wood, P.A, (1981), *Trans, American Soc Ag Eng* 14(3): p 434 – 436

Cyanide Investigative Committee, (2002): Ministry of Environment and Science cyanide investigative report.

Dagan, G., (1978). A note on packer, slug, and recovery tests in unconfined aquifers. *Water Research*, 14(5): 929-934.

Dagan, G., (1986). Statistical theory of groundwater flow and transport: Pore to laboratory, laboratory to formation, and formation to regional scale: *Water Resources Research*, vol. 22, no. 9, p. 120S–135S.

Damang Gold Mine Technical Short Form Report 31st December 2010

Davis, S.N., and Turk, L.J., (1964). Optimum depth of wells in crystalline rocks. *Groundwater*, 22, pp. 6-11

Dawson, KJ, Istok J.D., (1991). Aquifer testing—design and analysis of pumping and slug tests. Lewis, Chelsea, 344 pp.

De Vries, J.J., Simmers, I., (2002). Groundwater recharge: an overview of processes and challenges. *Hydrogeology Journal*. 10, 5-17.

Dershowitz, W., Wallmann, P., and Kindred, S., (1991). Discrete fracture modelling for the Stripa site characterisation and validation drift inflow predictions. *SKB Stripa Project Technical Report* 91-16, Swedish Nuclear Fuel and Waste Management Co. Stolkholm.

Dickson, K. B. and Benneh, G. 1988. *A new geography of Ghana*. Longman Group UK Limited. Longman House Burnt Mill, Harlow, Essex, England.

Doulati Ardejani, F., Singh, R.N., (2004). Assessment of ground water rebound in backfilled open cut mines using the finite element method. J. Rock Mech. Tunnelling Tech., 10 (1), 1-16 (16 pages).

Downing R.A., Oaks D.B., Wilkinson W.B., and Wright C.E. (1974). Regional development of groundwater resources in combination with surface water. Journal of Hydrology 22, 174-177.

Driscoll, Fletcher G., (1986). Groundwater and Wells, Second Edition, Johnson Filtration Systems, Inc., St. Paul, Minnesota.

Durner, W., (1994). Hydraulic conductivity estimation for soils with heterogeneous pore structure, *Water Resour. Res*., *32*(9), 211-223, 1994.

Dzigbodi-Adzimah, K., (1996). Environmental concerns of Ghana's gold booms: past, present and future. Ghana Min J ;2(1):21– 6.

Eisenlohr, B.N., (1989). The Structural Geology of Birimian and Tarkwaian Rocks of Southwest Ghana, BGR Report 80.2040.6.

El-Naqa, A., (1994). Estimation of transmissivity from specific capacity data in fractured carbonate rock aquifer, central Jordan: *Environmental Geology*, v. 23, no. 1, p. 73-80.

Faust, Charles R., and Mercer, J.W., (1984). Evaluation of slug tests in wells containing finite-thickness skin, *Water Resources Research*, Vol. 20, No. 4, pp. 504-506.

Ferris, J. G., and Knowles, D. B., (1963). The slug-injection test for Estimating the coefficient of transmissivity of an aquifer. U.S. Geol. Survey Water Supply Paper1536-1

Foyo, A., Sa'nchez, M. A., and Tomillo, C., (2005). A proposal for secondary permeability index obtained from water pressure test in dam foundations, J. *Geo. Eng.*, Vol. 77, 69-82.

Freeze, R.A., (1975). A stochastic-conceptual analysis of one-dimensional groundwater flow in a nonuniform homogeneous media. *Water Resour Res* 11(5):725–742.

Freeze, R. A., and Cherry, J. A., (1979). Groundwater. Prentice-Hall, Englewood Cliffs.

Gale, J. E., and Witherspoon, P. A., (1979). An Approach to the Fracture Hydrology at Stripa: *Preliminary Results, Lawrence Berkely Laboratory Report* LBL-7079, SAC-15.

Gale J. E., Rouleau A., and Witherspoon, P.A., (1982). Fundamental hydraulic characteristics of fractures from field and laboratory investigations. Papers of the Groundwater in Fractured Rock Conference; Canberra, Australia. *Australian Government Publishing Service, Canberra,* 95–108.

Gale JE, MacLeod R, Welhan JE, Cole C, and Vail, L., (1987). Hydrogeological characterization of the Stripa site. *Stripa Project Technical Report* 87–15, SKB, Stockholm.

Gee, G.W., and Hillel, D., (1988). Groundwater recharge in arid regions: review and critique of estimation methods. *Hydrol. Proc*. 2, 255-266.

Ghana Chamber of Mines (2008)- Factoid, www.ghanachamberofmines.org. Accessed on 25/01/12.

Gillham, R. W., (1984). The capillary fringe and its effect on water-table response, J. Hydrol., 67, 307– 324, doi:10.1016/0022-1694(84)90248-8.

Gold Fields Ltd. (2007)- Annual Report- 2007, www.goldfields.co.za. Accessed on 25/01/12.

Griffis, R.J., Barning, K., Agezo, F.L., and Akosah, F.K., (2002). Gold Deposits of Ghana. Minerals Commission of Ghana.

Grubaugh, K. "Profile of Mining Industry Ghana's," 2002.

Gupta, A.S., and Rao, K.S., (2001). Weathering indices and their applicability for crystalline rocks. *Bulletin of Engineering Geology and the Environment*.,60, 201-221.

Gustafson et al., (1989). Groundwater flow calculations on a regional scale at the Swedish Hard rock Laboratory. SKB SHRL Progress Report 25-88-17, Swedish Nuclear Fuel and Waste Management Co. Stolkholm

Hamm, S.; Kim, M.; Cheong, J.; Kim, J.; Son, M. and Kim, T. (2007). Relationship between hydraulic conductivity and fracture properties estimated from packer tests and borehole data in a fractured granite, *Engineering Geology*, 92, 73-87.

Harbaugh, A., Banta, E., Hill, M., and McDonald, M., (2000). User Guide for MODFLOW 2000, an Update to the US Geological Survey Modular Finite – Difference Ground-Water Flow Model, US. *Geological Survey Open-File Report* 00-92.

Harr, M.E., (1962). Groundwater and seepage. McGraw-Hill, New York.

Hart, D.J., and Hammon III, W.S., (2002). Measurement of hydraulic conductivity and specific storage using the shipboard Manheim squeezer. In: Salisbury MH, Shinohara M, Richter C, et al (eds) Proceedings of the Ocean Drilling Program, 2002, Initial Reports vol 195, chap 6, Ocean Drilling Program, College Station, TX

Hartman, H.L., (1 987). Introductory Mining Engineering. New York: *Wiley and Sons*. 633 Pg.

Heath, et al., (1993). Environmental impact of mining in tropical forest. Mining Environmental Management.

Heath, R.C., (1983). Basic ground-water hydrology: U.S. Geological Survey Water-Supply Paper 2220, 84 p.

Helsel, Dennis R., and Hirsch, Robert M., (1992). Statistical Methods in Water Resources, *Elsevier*, 522 p.

Hernandez, T., Nachabe, M., Ross, M., and Obeysekera, J. (2003). Runoff from variable source areas in humid shallow water table environments. *J. Am. Water Resour. Assoc.*, 39_1_, 75–85.

Hess, K.M., Wolf, S.H., and Celia, M.A., (1992). Large-scale natural gradient tracer test in sand and gravel, Cape Cod, Massachusetts 3. Hydraulic conductivity variability and calculated macrodispersitivities. *Water Resour Res* 28(8):2011–2027.

Hirdes, W., and Nunoo, B., (1994). The Proterozoic paleoplacers at Tarkwa gold mine, SW Ghana: sedimentology, mineralogy and precise age dating of the main reef and west reef, and bearing of the investigations on source area aspects. *Geol Jahrb* D 100:247– 311.

Hirst, T., (1938). The geology of the Tarkwa Goldfield and adjacent country. Gold *Coast Geological Survey, Bulletin* 1 O, 28p.

Hoek, E., and Brown, E.T., (1980). Undersound Excavations in Rock London: Institute of Mining and Metallurgy, 527 pages.

Hoek, E., and Bray, J. (1974). Rock Slope Engineering. Institute of Mining and Metallurgy, London. UK.

Howard, K.W.F., and Lloyd, J.W., (1979). The sensitivity of parameters in the Penman evaporation equations and direct recharge balance. *Journal of Hydrology*, 41, 329-344.

Hsieh, P.A., (2000). A brief survey of hydraulic tests in fractured rocks. In: Faybishenko B., Witherspoon P.A. and Benson S.M. (ed.) Dynamics of Fluids in Fractured Rock. *Geophysical Monograph 122, American Geophysical Union*, 59–66.

Huisman, L., (1972). Groundwater recovery. Macmillan Press Ltd., London

Huntley, David, Nommensen, Roger, and Steffey, Duane, (1992). The use of specific capacity to assess transmissivity in fractured-rock aquifers: *Ground Water*, v. 30, no. 3, p. 396-402

Hurst et al., (2000) as quoted in: http://www.mhnederlof.nl/lognormal.html)

Hvorslev, M.J., (1951). Time Lag and Soil Permeability in Groundwater Observations. U.S. Army Corps of Engineers Waterways Experiment Station. Bull. 36, pp 1-50.

Jetuah, F., (1997). Production of sulphuric acid from flue gases of Prestea and Obuasi gold mines. In *Proceedings of the Symposium on the Mining Industry and the Environment. KNUST/IDRC 1997*. pp. 139–144.

Jiang XW, Wan L, Wang XS, Liang SH, and Bill, H., (2009a). Estimation of fracture normal stiffness using a transmissivity-depth correlation. *Int J Rock Mech Min Sci* 46:51–58.

Jones, M.J., (1985). The Weathered Zone Aquifers of the Basement Complex Areas of Africa. *QuarterlyJournal of Engineering Geology* 18, pp 35-46.

Keese, K. E., Scanlon, B. R., and Reedy, R. C., (2005). Assessing controls on diffuse groundwater recharge using unsaturated flow modeling, *Water Resour. Res.*, 41, W06010, doi:10.1029/2004WR003841.

Kesse, G.O., (1985). The Mineral and Rock Resources in Ghana. Balkema, Rotterdam-Boston, pp. 610.

Kortatsi, B.K., (2004). Hydrochemistry of groundwater in the mining area of Tarwa-Prestea, Ghana, PhD thesis, University of Ghana, Legon-Accra, Ghana.

Kosugi, K., (1996). Lognormal distribution model for unsaturated soil hydraulic properties, *Water Resour. Res*., *32*(9), 2697-2703.

Kruseman, G.P., De Ridder, N.A. (1991). Analysis and evaluation of pumping test data. International Institute for Land Reclamation and Improvement, The Netherlands, 377 pp

Kruseman, G., and de Ridder, N., (1994). Analysis and Evaluation of Pumping Test Data. *ILRI publication*, Second Edi.

Kruseman, G. P., and de Ridder, N. A., (1990). Analysis and evaluation of pumping test data, 2nd edition: Wageningen, The Netherlands, International Institute for Land Reclamation and Improvement, 377 p.

Kuma, J. S., (2006). Water Resources Management Study (WARM). (1998). Ghana's Water Resources, Management Challenges and Oppurtunities, Prepared for the Ministry of Works and Housing, Accra, Ghana.

Kuma, J. S., (2007). Hydrogeological studies in the Tarkwa Gold Mining District, Ghana, *Bulletin of Engineering Geology and the Environment* 66, , , pp 89-9

Kuma, J. S., and Ewusi, A., (2009). Water Resources Issues in Tarkwa Municipality, Southwest Ghana, *Ghana Mining Journal*, Vol. 11, , pp. 37-46.

Kuma, J. S., and Younger, P. L., (2000). Conceptual ground water model and related environmental concerns in the Tarkwa area, Ghana, *Ghana Mining Journal*, , , Vol. 6, pp 42-52.

Kuma, J. S., Younger, P. L., and Bowell, R. J., (2002). Expanding the hydrogeological base in mining EIA studies A focus on Ghana, *Environmental Impact Assessment Review, 22*, , , pp 273-286.

Kuma, J.S., and Younger, P.L., (2001). Pedological characteristics related to groundwater occurrence in the Tarkwa area, Ghana, *Journal of African Earth Sciences*, vol. 33(2), pp. 363-376.

Kuma, J.S., and Younger, P.L., (2004). Water quality trends in the Tarkwa gold-mining district, Ghana, *Bull. Eng. Geol. Env,* vol. 63, pp. 119-132.

Kusimi, J., (2007). master thesis on ''groundwater hydrogeochemistry and landcover change in the Wassa West District of ghana''

Kwesi, A. T., and Kwesi, D. B., (2011). The Mining Industry in Ghana: A blessing or curs, *International Journal of Business and Science* vol. 2, No 12.

Lee, C. H., and Farmer, I., (1993). Fluid flow in discontinuous rocks, Chapman &Hall, London, UK.

Lerner, D.N., and Harris, R.C., (2009). The relationship between land use and groundwater resources and quality. *Land Use Policy*, 26, December, pp S265-S273. ISSN 0264-8377

Leube, A., and Hirdes, W., (1986). The Birimian Supergroup of Ghana- Depositional Environment, Structural Development and Conceptual Model of an Early Proterozoic Suite. Ghana- German Mineral Prospective Project. Federal Institution for Geosciences and Natural Resources (BGR), Hanover (unpublished).

Leube, A., Hirdes, W., Mauer, R., and Kess, G.O. (1990). The Early Proterozoic Birimian Supergroup of Ghana and some aspects of its associated gold mineralization. *Precambrian Research* 46, 139-165.

Logan, J., (1964). Estimating transmissivities from routine tests of waterwells. *Groundwater* 2: 35-37.

Lohman, S.W., (1979). Ground-water hydraulics: U.S. Geological Survey Professional Paper 708, 70 p.

Lohman, S.W., (1972). Ground-Water Hydraulics. U.S. Geol. Survey Prof. Paper 708 70 pp.

Louis, C., (1974). Rock hydraulics. In: Muller L (ed) Rock mechanics. Springer, Vienna, pp 299–387.

Lutz, A., Thomas, J.M., Pohll, G., and McKay, W.A., (2007). Groundwater resource sustainability in the Nabogo Basin of Ghana. *Journal of Hydrology* 49, 61–70.

Lyon, J.S., Hilliard, T.J, and Bethell, T.N., (1993). Burden of gilt. Washington, DC: Mineral Policy Center. 68 p.

Mace, R. E., (1997). Determination of transmissivity from specific capacity data in a karst aquifer, *Ground Water*, v. 35 no. 5, p. 738-742.

Marinelli, F.. and Niccoli, W. L., (2000). Simple Analytical Equations for Estimating Ground Water Inflow to a Mine Pit. *Ground Water*, 38(2), 311–314.

McDonald, M.C., and Harbaugh, A.W., (2000). A modular three-dimensional finite difference ground-water flow model: U.S. Geological Survey Techniques of Water- Resources Investigations, book 6, chap. A1, 586 p.

Melville, J. G., Molz, F. J., Guven, O., and Widdowson, M. A., (1991). Multilevel slug tests with comparisons to tracer data. *Ground Water*. V. 29, 6, pp. 897-907.

Miller, C.T., Williams, G.A., Kelly, C.T. and Tocci, M.D., (1998). Robust solution of Richards' equation for non-uniform porous media. *Water Resources Research*, 34, 2599−2610.

Miller, J.C., and Miller, J.N., (1995). Statistics for Analytical Chemistry. Ellis Horwood.

Mining Watch, (2000). Statement by WACAM on the cyanide spillage by Bogoso Gold Ltd by Daniel Owusu-Koranteng, Executive Director on 23rd October 2004.

Morris, BL., Lawrence, A.R., Chilton, P.J., Adams, B., Calow, R., and Klinck, B.A., (2003). Groundwater and its susceptibility to degradation: A global assessment of the problems and options for management. Early Warning and Assessment Report Series, RS, 03-3. United Nations Environment Programme, Nairobi, Kenya.

Nastev, M., Morin, R. H., Godin, R., and Rouleau, A., (2008). Developing hydrogeological models for Potsdam sandstones in southwestern Quebec, Canada. *Hydrogeology Journal* 16: 373-388.

National Research Council (NRC) (1996). Rock Fractures and Fluid Flow: Contemporary Understanding and Applications. *National Academy Press, Washington DC*. 551pp.

Neuman, (1982). Statistical characterization of aquifer heterogeneities: an overview, in Narasimhan, T.N., ed., Recent trends in hydrogeology: Boulder, Colo., Geological Society of America Special Paper 189, p. 81–102.

Neuman, (1990). Universal scaling of hydraulic conductivities and dispersivities in geologic media: *American Geophysical Union, Water Resources Research*, v. 26, no. 8, p. 1749–1758.

NEUMAN, S. P., (1994). Generalized Scaling of Permeabilities: Validation and Effect of Support Scale, *Geophys. Res*. Lett., 21, 5, 349–352.

Neuman, S. P., Fogg, G. E., and Jacobson, E. A., (1980). A Statistical Approach to the Inverse Problem of Aquifer Hydrology, 2. Case study. *Water Resour. Res.* 16(1): 32-58.

Neuman, S. P., Feddes, R. A., and Bresler E., (1974). Finite element simulation of flow in saturated-unsaturated soils considering water uptake by plants, third annual report, Proj. A10-SWC-77, Hydraul. Eng. Lab., Technion, Haifa, Israel.

Neuzil, C.E., (1986). Groundwater flow in low-permeability environments. *Water Resour Res* 22:1163–1195.

Nguyen, S. P., and Pinder, G. F., (1984). Direct Calculation of Aquifer Parameters in Slug Test Analysis, *Water Resource Monograph Series* 9, pp. 222-239.

Nolan, B. T., Baehr, A. L., and Kauffman L. J., (2003). Spatial variability of groundwater recharge and its effect on shallow groundwater quality in southern New Jersey, *Vadose Zone J*, 2, 677–691.

Nolan, B. T., Healy, R. W., Taber, P. E., Perkins, K., Hitt, K. J., and Wolock D. M., (2007). Factors influencing ground-water recharge in the eastern United States, J. Hydrol., 332, 187 –205, doi:10.1016/j.jhydrol.2006. 06.029.

Ntibery, B.K., Atorkui, E., and Aryee, B.N.A., (2003). Trends in small-scale mining of precious minerals in Ghana: a perspective on its environmental impact, *Journal of Cleaner production*, vol. 11, pp. 131-140.

Oaks, D.B., and Wilkinson, W.B., (1972). Modelling of groundwater and surface water systems. I-Theoretical base flow. Water Resource Board, Reading, UK.

Oda, M., Saitoo, T., and Kamemura, K., (1989). Permeability of rock masses at great depth. In: Maury and Fourmaintraux (eds), rock at great depths, 449-445, Balkema.

Ollier, C. D., (1975). Weathering. London: Longman Group Limited.

Peprah, and Pappoe, (2008). Environmental Statistics of Ghana, An environmental Statistics Workshop in Abuja, Nigeria (19-23 May, 2008).

Raudkiwi, A.J., and Callander, R. A., (1976). Analysis of groundwater flow. Edward Arnold, London, 214pp.

Raven K.G., Gale, J.E., (1985). Water flow in a natural rock fracture as a function of stress and sample size*. Int J Rock Mech Min Sci Geomech* 22:251–261.

Razack, M., and Huntley, David, (1991). Assessing transmissivity from specific capacity in a large and heterogeneous alluvial aquifer: *Ground Water*, v. 29, no. 6, p. 856-861.

Rehfeldt, K.R., Boggs, J.M., Gelhar, L.W., (1992). Field study of dispersion in a heterogeneous aquifer 3. Rep. 10080, Lawrence Berkeley Natl. Lab., Berkeley, Calif.

Richards, L.A., (1931). Capillary conduction of liquids through porous mediums. *Physics* 1:318–333.

Rushton, K. R., (2006). Significance of a seepage face on flows to wells in unconfined aquifers. *Quarterly Journal of Engineering Geology and Hydrogeology* v. 39; p. 323-331.

Rushton, K.R., Ward, C., (1979). The estimation of groundwater recharge. *J Hydrol* 41:345–361.

Rushton, K. R., (1988). Numerical and conceptual models for recharge estimation in arid and semi-arid zones. In: Simmers, I. (Ed.).

Sahimi, M., (1995). Flow and transport in porous media and fractured rock, Wiley-VCH.

Sakthivadivel, R., and Rushton, K.R., (1989). Numerical analysis of large diameter wells with a seepage face. *Journal of Hydrology,* 107, 43–55.

Scanlon, B.R., Healy, R.W., and Cook, P.G., (2002). Choosing appropriate techniques for quantifying groundwater recharge. *Hydrogeol. J*. 10, 18–39.

Schaap, M.G., Leij, F.J., and van Genuchten, M.Th., (2001). ROSETTA: a computer program for estimating soil hydraulic parameters with hierarchical pedotransfer functions. *J. Hydrol*. 251, 163–176.

Shah, N., and Ross, M., (2009). Variability in Specific Yield under Shallow Water Table Conditions. *J. Hydrol. Eng.*, 14(12), 1290–1298.

Shah, N., Nachabe, M., and Ross, M., (2007). Extinction depth and evapotranspiration from ground water under selected land covers. *Ground Water*, 45,3, 329–338.

Shapiro, A.M., and Hsieh, P.A., (1998). How good are estimates of transmissivity from slug tests in fractured rock?, *Groundwater*, v. 36, p. 37–48.

Siddiqui, S. H., and Parizek, R. R., (1971). Hydrgeologic factors influencing well yields in folded and faulted carbonate rocks in central Pennsylvania. *Water Resource Research.* V. 7, no. 5, pp. 1295-1312.

Sidle, W.C., and Lee, P.Y., (1995). Estimating local ground-water flow conditions in a granitoid: preliminary assessments in the Waldoboro Pluton Complex, Maine. *Ground Water*, 33(2):291–303.

Siegel, J., (1997). Ground Water Quantity. *In:* Marcus, J.J., ed., *Mining Environmental Handbook, Effects of Mining on the Environment and American Controls on Mining,* Imperial College Press, London, pp. 164-168.

Simunek, J., and van Genuchten, M. Th., (1999). Manual of HYDRUS-2D computer program for simulation of water flow head and solute transport in variably saturated porous media, USDA, Calif.

Simunek, J., van Genuchten, M. Th., and Sejna, M., (2005). The Hydrus-1D software package for simulating the one-dimensional movement of water, heat, and multiple solutes in variably-saturated media, Version 3.0. Manual of HYDRUS Software Series 1, Department of Environmental Sciences, Univ. California Riverside, Riverside, Calif.

Singh, G., (2006). Water pollution in mining areas – issues related to its protection and control. In: Shringarputale SB, Muthreja IL, Yerpude R (Eds), Proc, International Symp on Environmental Issues of Mineral Industry, Visveswaraya National Institute of Technology (VNIT), Nagpur, India, p 95 –108.

Singhal, B.B.S., and Gupta, R.P., (1999). Applied Hydrogeology of Fractured Rocks. Kluwer, Dordrecht, 400pp.

Small, E. E., (2005). Climatic controls on diffuse groundwater recharge in semiarid environments of the southwestern United States, *Water Resour. Res*., 41, W04012, doi:10.1029/2004WR003193.

Smedley, P.L., Edmunds, W.M., Pelig-Ba, K.B., (1996). Mobility of arsenic in groundwater in the Obuasi gold mining area of Ghana: implications for human health. In: Appleton JD, Fuge R, McCall GJH, editors. *Environmental Geochemistry and Health, Geological Society Special Bulletin* No. 113, 163– 81.

Snow, D.T., (1968a). Rock fracture spacings, openings, and porosities. *J Soil Mech Found Div ASCE* 96:73–91.

Snow, D. T., (1979). Packer injection test data from sites on fractured rock.

Soni, A.K., (2006). Effect of deepening of surface mine workings on hydro-geological regime of area – a case study of limestone mining in India. In: Bose LK, Bhattacharya BC (Eds), Proc, 1st Asian Mining Congress, Mining Geological and Metallurgical Institute of India, Kolkata, India, p 273 –280

Statement by WACAM on the cyanide spillage by Bogoso Gold Ltd by Daniel Owusu-Koranteng, Executive Director on 23rd October 2004 (Mining Watch, 2000)

Sudicky, E.A., (1986). A natural gradient experiment on solute transport in a sand aquifer: spatial variability of hydraulic conductivity and its role in the dispersion process. *Water Resour Res* 22(13):2069–2082.

Summary Report; On The Mpatasie and Asafo Projects, Ghana July15, 2010 Tarkwa Gold Mine Technical Short Form Report 31st December 2010.

Technical Short Form Report on Damang Gold Mine, Ghana, December 2010.

The United Nations Economic Commission for Africa (ECA) in 1999

Theis, C. V., (1935). The relation between the lowering of the piezometric surface and the rate and duration of discharge of a well using groundwater storage: *American Geophysical Union Transactions*, v. 16, p. 519–524.

Theis, C. V., (1963). Estimating the transmissivity of a water-table aquifer from the specific capacity of a well: U.S. Geological Survey Water Supply Paper 1536-I, p. 332-336.

Theis, C. V., Brown, R. H., and Myers, R. R., (1963). Estimating the transmissibility of aquifers from the specific capacity of wells. Methods of determining permeability, transmissivity, and drawdown: U.S. Geological Survey Water Supply Paper, 1536-I.

Thomasson, H. J., Olmstead, F. H., and LeRoux, E. R., (1960). Geology, water resources, and usable ground water storage capacity of part of Solano County, CA: U.S. Geological Survey Water Supply Paper 1464, 693 p.

Ugorets, V., and Howell, R., (2008). 3-D Characterisation of Groundwater Flow in Hard-rock Uranium Deposits – in publications of 2nd International Symposium "Uranium: Resources and Production", Moscow.

van Genuchten, M.Th., (1980). A closed-form equation for predicting the hydraulic conductivity of unsaturated soils. *Soil Sci. Soc. Am. J.* 44:892–898.

Veiga, M.M., and Beinhoff, C., (1997). UNECA centers: a solution to reduce mercury pollution from artisanal gold mining activities. UNEP Industry and Environment 20, 49–52.

Vogel, T., and Císlerová, M., (1988). On the reliability of unsaturated hydraulic conductivity calculated from the moisture retention curve, *Transport in Porous Media, 3*, 1-15.

Voss, C. I., and Andersson, J., (1993). Regional flow in the Baltic shield during Holocene coastal regression. *Groundwater,* vol 31, No 6, 989-100.

WACAM (2008). Baseline Survey of Mining Community Rivers/Streams and Their Conditions. (www.wacamghana.com).

Walker, D., Rhén, I., Gurban, I., (1997). Summary of hydrogeological conditions at Aberg, Beberg and Ceberg. SKB Technical Report, TR 97–23, SKB, Stockholm, Sweden.

Walton, W.C., (1970). Groundwater Resource Evaluation. McGraw-Hill, New York. 664 pp.

Wang, X.S., Jiang, X.W., Wan, L., Song, G., Xia, Q., (2009). Evaluation of depth-dependent porosity and bulk modulus of a shear using permeability–depth trends. *Int J Rock Mech Mining Sci* 46 (7):1175−1181. doi:10.1016/j.ijrmms.2009.02.002.

Warhurst, A., (Ed.), (1999). Mining and the Environment: Case-Studies from the Americas. Stylus Publishing, VA.

Warhurst, A., (1994). Environmental Degradation from Mining and Mineral Processing in Developing Countries: Corporate Responses and National Policies. Development Centre, OECD, Paris.

Wassa Communities Affected by Mining (WACAM), (2011). Public Eye awards ceremony in Davos, Switzerland.

Wassa West District Assembly Medium Term Development Plan 2002-2004.

Wei, Z.Q., Egger, P., Descoeudres, F., (1995). Permeability predictions for jointed rock masses. *Int J Rock Mech Min Sci Geomech Abstr* 32:251–261.

Whitelaw, O.A.L., (1929). Geological and mining features of the Tarkwa-Aboso Goldfield. Gold Coast Geol Surv Mem 1:12–17.

Whitelaw, O.A.L., (1929). Geological and mining features of the Tarkwa-Aboso Goldfield. Gold Coast Geological Survey, Memoir 1, 46p.

Whittemore, D.O., Macfarlane, P.A., Doveton, J.H., Butler, J.A.J., Chu, T.M., Bassler, R., Smith, M., Mitchell, J., and Wade, A. (1993). The Dakota aquifer Program annual report, FY92, KGS Open-File Rep 93–1, Kansas Geological Survey, Lawrence, KS.

Widdowson, M. A., Molz, F. J., and Melville, J. G., (1990). An analysis technique for multilevel and partially penetrating slug test data. *Ground Water*. V. 28, no. 6, pp. 937-945.

Woodbury, A.D., Sudicky, E.A., (1991). The geostatistical characteristics of the Borden aquifer. *Water Resour Res* 27(4):533–546.

Wu, J., Zhang, R., and Yang J., (1996). Analysis of rainfall-recharge relationships, J. Hydrol., 177, 143– 160, doi:10.1016/0022-1694(95)02935-4.

Yin, Z. Y., and Brook, G. A., (1992). The topographic approach to locating high-yield wells in crystalline rocks: Does it work? *Ground Water*. V. 30, no. 1, pp. 96-102.

Zhao, J., (1998). Rock mass hydraulic conductivity of the Bukit Timah granite, Singapore. Eng Geol 50:211–216

Appendix A – Summary statistics of hydraulic conductivity values

Appendix A-1

Table 3.6 Summary statistics of conductivity values (m/s) for combined dataset

	Data Source (Study)	Count	Min	Max	N Parameters		LogN Parameters		Median	IQR (q3-q1)	MAD	qs	Swanson's Mean
					Mean	Stdev	Mean (Geom Mean)	Stdev (Geom Stdev)	Undefined Distribution Parameters				
M	**All dataset**	**736**	**1.40E-13**	**1.45E-03**	**1.48E-05**	**9.74E-05**	**-7.80** **1.57E-08**	**1.79** **61.0E+00**	**3.80E-09**	**9.94E-07** **1.10E-10**	**1.48E-05**	**7.25E-01**	**7.18E-06**

Appendix A-2

Table 3.7 Summary statistics of conductivity values (m/s) for individual studies

	Data Source (Study)	Count	Min	Max	N Parameters		LogN Parameters		Median	IQR (q3-q1)	MAD	qs	Swanson's Mean
					Mean	Stdev	Mean (Geom mean)	Stdev (Geom Stdev)	Undefined Distribution Parameters				
A	Snow, (1979)	178	4.65E-09	1.45E-03	3.79E-05	1.73E-04	-5.82 1.52E-06	0.98 9.43E+00	1.43E-06	4.26E-06 3.72E-07	1.21E-06	7.25E-01	7.18E-06
B	Merecel et al., (2004)	31	2.00E-08	5.10E-04	3.15E-05	9.14E-05	-5.34 4.58E-06	1.02 1.04E+01	6.50E-06	2.60E-05 1.10E-06	6.06E-06	7.74E-01	2.13E-05
C	Akaha et al., (2008)	12	5.65E-07	2.51E-05	3.89E-06	6.76E-06	-5.67 2.12E-06	0.41 2.60E+00	1.62E-06	3.48E-06 1.20E-06	6.07E-07	9.10E-01	2.08E-06
D	Ali-El Naqa, (1994)	23	2.86E-07	5.60E-04	1.14E-04	2.12E-04	-5.02 9.58E-06	1.01 1.02E+01	5.30E-06	1.44E-05 2.60E-06	4.20E-06	7.62E-01	1.52E-04
E	Larry Cook & Associates (2008)	7	2.31E-07	9.49E-06	2.91E-06	4.30E-06	-6.03 9.37E-07	0.69 4.88E+00	4.63E-07	8.91E-06 3.47E-07	1.16E-07	9.74E-01	3.02E-06
F	Cheng-Yu Ku et al, (2009)	27	2.86E-10	1.64E-06	2.50E-07	4.38E-07	-7.44 3.67E-08	1.04 1.09E+01	4.68E-08	1.56E-07 9.08E-09	4.45E-08	7.04E-01	3.16E-07
G	Plume (1996)	12	7.51E-09	7.25E-05	2.66E-05	3.09E-05	-5.34 4.54E-06	1.31 2.03E+01	1.02E-05	6.50E-05 1.63E-06	1.02E-05	8.45E-01	2.58E-05
H	Ken Kuchling et al, (2009)	5	2.60E-08	3.60E-07	1.88E-07	1.48E-07	-6.88 1.31E-07	0.47 2.92E+00	1.30E-07	3.45E-07 6.05E-08	1.04E-07	8.51E-01	1.72E-07
I	Miguel M et al, (2009)	40	2.80E-12	3.20E-07	1.22E-08	5.22E-08	-9.27 5.33E-10	1.08 1.21E+01	8.55E-10	2.48E-09 7.55E-11	8.30E-10	6.69E-01	1.88E-09
J	Witherspoon and Gale (1979)	376	1.40E-13	6.80E-06	4.50E-08	4.36E-07	-9.69 2.05E-10	1.13 1.34E+01	1.65E-10	8.38E-10 3.30E-11	1.59E-10	8.35E-01	1.70E-09
K	Anglogold Obuasi Ghana (AGC)	9	1.74E-09	4.73E-05	1.16E-05	1.44E-05	-5.46 3.45E-06	1.29 1.93E+01	5.54E-06	1.54E-05 3.84E-06	2.56E-06	8.39E-01	1.00E-05
L	Ghana Australia Goldfields (GAG)	16	1.70E-08	3.00E-06	3.91E-07	7.84E-07	-6.98 1.05E-07	0.68 4.74E+00	7.40E-08	3.03E-07 3.43E-08	4.20E-08	8.45E-01	3.53E-07

Appendix A-3

Table 3.15 Summary statistics of conductivity values (m/s) for all rock types.

	Data Source (Study)	Count	Min	Max	N Parameters		LogN Parameters		Median	IQR (q3-q1)	MAD	qs	Swanson's Mean
					Mean	Stdev.	Mean (Geo mean)	Stdev. (Geom Stdev)	Undefined Distribution Parameters				
A	*Granite*	489	1.40E-13	8.16E-04	4.79E-06	4.71E-05	-8.41 3.92E-09	1.69 4.92E+01	3.00E-10	4.15E-09 4.70E-11	4.79E-06		7.18E-06
B	*Mica -schist/Phyllite*	23	1.74E-09	1.33E-03	6.39E-05	2.76E-04	-5.67 2.16E-06	1.52 3.30E+01	1.91E-06	8.10E-06 3.44E-07	6.33E-05		2.13E-05
C	*Quartzite*	35	1.70E-08	6.73E-06	9.16E-07	1.70E-06	-6.60 2.53E-07	0.75 5.63E+00	1.67E-07	8.55E-07 4.80E-08	8.56E-07		2.08E-06
D	*Sandstone/meta sandstone*	56	2.86E-10	5.60E-04	5.25E-05	1.48E-04	-6.23 5.91E-07	1.63 4.24E+01	9.93E-07	5.56E-06 4.84E-08	5.23E-05		1.52E-04
E	*Bindook Porphyry*	8	1.16E-07	9.49E-06	2.56E-06	4.10E-06	-5.46 3.50E-06	0.87 7.39E+00	4.05E-07	6.83E-06 2.60E-07	2.30E-06		3.02E-06
F	*Tuff-Breccia, Tuff-Siltstone*	7	8.18E-07	5.07E-06	2.29E-06	1.95E-06	-5.74 1.82E-06	0.42 2.64E+00	1.09E-06	5.07E-06 8.64E-07	1.33E-06		3.16E-07
G	*Curtain diabase*	11	7.58E-08	8.55E-06	2.89E-06	2.81E-06	-5.85 1.40E-06	0.80 6.36E+00	2.43E-06	4.58E-06 5.20E-07	2.07E-06		2.58E-05
H	*Greenstone*	24	3.07E-08	1.45E-03	8.83E-05	2.97E-04	-5.21 6.21E-06	1.23 1.68E+01	2.26E-06	2.27E-05 1.01E-06	8.72E-05		1.72E-07
I	*Meta-andesite/rhyollite*	9	4.69E-08	2.42E-05	3.31E-06	7.85E-06	-6.06 8.63E-07	0.97 9.28E+00	7.34E-07	1.41E-06 3.72E-07	2.94E-06		1.88E-09
J	*Metavolcanics Amphibolite*	7	1.49E-07	7.71E-07	4.38E-07	2.26E-07	-6.42 3.76E-07	0.33 2.15E+00	3.72E-07	6.22E-07 2.32E-07	1.80E-07		1.70E-09
K	*Sandstone and Shale*	14	1.67E-07	2.88E-04	3.57E-05	8.28E-05	-5.38 4.14E-06	1.12 1.31E+01	1.86E-06	1.66E-05 7.38E-07	3.49E-05		1.00E-05
L	*Sandstone/ Tuff & Conglomerate*	9	4.37E-07	7.25E-05	3.33E-05	3.31E-05	-5.00 9.89E-06	1.08 1.20E+01	2.75E-05	7.11E-05 1.75E-06	2.88E-05		3.53E-07
M	*Quartz, Porphry granodiorite*	4	N/A	N/A	N/A	N/A	N/A	N/A	N/A	N/A	N/A		
N	*Slate/talc schist/Serpentine*	8	5.68E-08	7.29E-04	9.34E-05	2.57E-04	-5.32 4.82E-06	1.61 4.08E+01	2.99E-06	4.17E-06 2.16E-06	9.15E-05		
O	*Gneiss*	32	4.65E-09	1.74E-04	9.05E-06	3.10E-05	-5.90 1.26E-06	1.12 1.33E+01	1.70E-06	4.03E-06 4.18E-07	8.52E-06		
	All rock type	**736**	**1.40E-13**	**1.45E-03**	**1.48E-05**	**9.74E-05**	**-7.80 1.57E-08**	**1.79 6.10E+01**	**3.80E-09**	**9.94E-07 1.10E-10**	**1.47E-05**		

Appendix A-4

Table 3.18 Summary statistics of conductivity values (m/s) for rock class

	Data Source (Study)	Count	Min	Max	N Parameters		Log N Parameters		Median	IQR (q3-q1)	MAD	qs	Swanson's Mean
					Mean	Stdev.	Mean (Geom mean)	Stdev (Geom Stdev)	Undefined Distribution Parameters				
A	*IGNEOUS*	**512**	1.40E-13	8.16E-04	4.72E-06	4.60E-05	-8.34 4.55E-09	1.7 49.7	3.65E-10	8.20E-09 5.03E-11	4.72E-06		
B	*METAMORPHIC*	**145**	1.74E-09	1.45E-03	3.45E-05	1.76E-04	-5.83 1.49E-06	1.14 13.9	1.00E-06	4.07E-06 2.60E-07	3.42E-05		
C	*Meta-SEDIMENTARY*	**79**	2.86E-10	5.60E-04	4.36E-05	1.27E-04	-6.06 8.69E-07	1.54 34.3	1.30E-06	6.79E-06 1.56E-07	4.32E-05		
D	**All rock classes**	**736**	**1.40E-13**	**1.45E-03**	**1.48E-05**	**9.74E-05**	**-7.80 1.57E-08**	**1.79 6.1**	**3.80E-09**	**9.94E-07 1.10E-10**	**1.47E-05**		

Appendix A-5

Table 3.20 Summary statistics of conductivity values (m/s) for specific regional climate

	Climate	Count	Min	Max	N Parameters		Log N Parameters		Median	IQR (q3-q1)	MAD	qs	Swanson's Mean
					Mean	Stdev	Mean (Geom Mean)	Stdev (Geom Stdev)	Undefined Distribution Parameters				
A	*Semi-Arid*	**248**	4.65E-09	1.45E-03	4.30E-05	1.64E-04	-5.59 2.56E-06	1.07 11.7	2.00E-06	7.07E-06 4.50E-07	4.24E-05		7.18E-06
B	*Tropical*	**63**	2.86E-10	4.73E-05	2.61E-06	7.12E-06	-6.78 1.66E-07	1.27 18.7	1.56E-07	1.62E-06 3.00E-08	2.57E-06		2.13E-05
C	*Temperate*	**380**	1.40E-13	6.80E-06	5.94E-08	4.59E-07	-9.26 5.54E-10	1.29 19.4	1.70E-10	8.93E-10 3.30E-11	5.94E-08		2.08E-06
D	*Sub-Arctic*	**4**	2.60E-08	3.60E-07	1.88E-07	1.48E-07	-6.90 1.27E-07	0.66 4.60	1.30E-07	3.45E-07 6.05E-08	1.14E-07		1.52E-04
E	*Mediterranean*	**40**	2.80E-12	3.20E-07	1.22E-08	5.22E-08	-9.21 6.12E-10	1.21 16.1	8.55E-10	2.48E-09 7.55E-11	1.20E-08		3.02E-06
F	**All rock classes**	**736**	**1.40E-13**	**1.45E-03**	**1.48E-05**	**9.74E-05**	**-7.80 1.57E-08**	**1.79 6.1**	**3.80E-09**	**9.94E-07 1.10E-10**	**1.47E-05**	**All rock classes**	3.16E-07

Appendix B-Meteorological data of South Western Ghana (SWGH) from 1964 to 2001

Appendix B-1

Monthly rainfall chart (mm) of SWGH from 1964 to 2001													
YEAR	**JAN**	**FEB**	**MAR**	**APR**	**MAY**	**JUN**	**JUL**	**AUG**	**SEP**	**OCT**	**NOV**	**DEC**	**Annual**
1964	71.1	69.9	111.3	142.7	143.3	294.4	111.3	66.8	44.5	138.2	75.2	17.5	1286
1965	3.6	92.5	96.8	73.7	170.9	346.5	214.9	115.6	201.7	163.8	81	14.5	1576
1966	35.3	41.4	178.8	172	149.4	170.2	229.4	114.8	162.1	231.4	85.3	36.1	1606
1967	6.3	43.9	94.7	204	318.5	381.8	98.3	35.8	188.7	172.7	108.7	9.7	1663
1968	47	106.4	169.4	314.7	242.6	479.5	179.8	563.1	392.7	248.1	91.2	16.5	2851
1969	26.2	93.7	34	277.4	140.2	198.4	165.9	29.7	29	135.6	202.9	46	1379
1970	5.1	51.3	105.7	306.3	239	150.9	45.2	95.5	189.5	229.6	115.1	0	1533
1971	7.9	102.4	200.4	185.9	181.1	268	73.7	62.5	197.6	173.7	81.5	1.5	1536
1972	28.7	33.8	148.1	183.4	139.4	241.8	100.3	18.5	99.3	153.2	42.4	71.4	1260
1973	0	148.8	117.9	129.5	75.4	249.7	17	224.5	204.7	132.1	65.3	12.5	1377
1974	47	39.4	214.9	241.5	107.7	271	129.8	127	348.5	82.3	61.7	31.7	1703
1975	0.0	188.2	125.7	143.3	186.9	166.6	243.8	71.9	114.5	160	117.6	59.9	1578
1976	10.2	52.1	165	142.2	237.7	271.7	73.2	81.3	35.8	159.1	227.8	2.8	1459
1977	3.6	33.8	32.2	195.3	149.9	152.6	61.6	40.1	192.5	192.5	13.9	17	1085
1978	0.0	96.5	206	136.1	235.6	264.3	60	9.8	130.3	130.4	56.8	57.6	1383
1979	26.3	53.5	45.4	99.7	239.4	209.2	245.5	81.3	254.7	224.8	73.7	0	1554
1980	12	151.6	128.2	57.9	326.8	278.2	153.6	89.2	286.6	227.6	104.4	10.4	1827
1981	0.5	28.7	173.6	64.4	321.4	133	134.6	66.2	150.3	98.6	22.8	21.9	1216
1982	0.0	64.8	192.3	50.8	227.6	259.9	152.9	57.6	2.5	138.9	67.1	10.2	1225
1983	0.0	30.1	14.8	123.2	262.7	269.8	15.1	7.9	128.5	128.0	54.3	36.6	1071
1984	15.5	58.2	154.1	60.7	182.7	223.1	74.5	193.3	175.2	214.5	55.1	52.3	1459
1985	69.3	58.9	144.4	159.2	116.6	136.1	202.8	154.1	142.9	131.8	69.0	0.3	1385
1986	0.0	54.9	150.0	120.5	125	138.7	108.4	45.5	243.8	88.7	82.9	0.0	1158
1987	8.4	79.3	110.0	46.2	122.5	144.3	184.1	178.2	353.3	233.4	25.7	21.3	1507
1988	0.0	6.8	176.5	93.6	117.8	292.5	132.6	37.1	131.7	173.8	72.2	20.4	1255
1989	0.0	1.8	76.7	154.6	61.1	278.3	178.4	138.5	221.4	198.5	49.3	9.1	1368
1990	24.1	148.1	44.2	127.0	114.9	220.7	37.0	25.1	128.8	193.8	51.5	236	1351
1991	32.2	50.3	116.0	158.5	177.1	133.0	160.9	255.1	74.0	63.3	63.3	0.7	1284
1992	0.6	95.3	138.9	206.5	212.7	132.9	80.1	9.2	208.5	177.0	76.2	164.0	1502
1993	0.7	91.4	191.4	75.5	126.1	187.3	174.2	133.6	196.0	233.1	125.1	158.0	1692
1994	15.4	22.5	142.0	151.1	220.5	161.3	74.4	28.5	116.5	396.5	58.5	2.2	1389
1995	0.0	7.9	122.6	369.9	154.9	211.9	135.8	195.6	86.9	123.3	128.6	56.7	1594
1996	13.7	125.8	163.7	188.2	264.7	191.0	189.9	137.5	54.8	159.7	96.9	12.2	1598
1997	16.8	34.5	140.1	236.6	188.1	265.7	48.1	39.5	92.0	169.1	74.3	47.5	1352
1998	52.0	26.7	61.1	88.9	196.4	257.3	61.3	127.1	127.1	231.3	112.4	86.9	1429
1999	21.3	91.5	162.7	179.7	82.0	418.5	312.8	77.0	136.8	130.1	65.7	7.6	1686
2000	19.2	28.5	141.8	200.5	222.6	265.7	83.7	112.3	141.5	24.4	78.1	1.7	1320
2001	0.0	22.5	138.2	234.6	102.0	293.1	101.0	120.8	97.7	83.1	29.2	30.7	1253
Mean	16.3	66.52	129.73	160.42	181.14	237.08	127.52	104.40	160.08	167.00	80.60	36.35	1467.14

Appendix B-2

Total number of rain days of SWGH from 1964 -2001												
Year	**Jan**	**Feb**	**March**	**April**	**May**	**June**	**July**	**Aug**	**Sept**	**Oct**	**Nov**	**Dec**
1964	3	6	9	15	17	21	13	17	12	12	13	7
1965	1	9	10	10	17	21	23	16	18	16	10	2
1966	2	4	12	10	15	17	23	22	21	25	12	6
1967	1	4	6	15	15	20	16	18	16	17	8	4
1968	2	7	8	12	14	24	21	24	23	20	13	4
1969	3	7	6	16	15	21	19	17	13	16	12	2
1970	2	6	13	9	16	16	12	16	23	15	10	0
1971	2	7	13	15	11	20	15	17	18	13	12	1
1972	3	7	11	13	17	22	16	10	15	16	11	4
1973	0	6	7	11	9	19	7	19	23	13	7	2
1974	2	2	15	14	14	23	17	14	21	12	7	3
1975	0	10	6	12	16	15	15	15	15	15	11	6
1976	1	6	14	8	15	29	16	12	11	14	17	1
1977	5	2	5	12	15	17	16	15	16	16	3	2
1978	0	10	14	13	16	22	16	12	15	17	8	4
1979	3	3	9	10	15	22	18	20	24	24	6	0
1980	3	9	14	8	16	19	15	20	23	17	13	3
1981	1	5	11	7	17	15	19	15	15	15	6	4
1982	0	4	11	9	14	21	14	15	1	16	8	2
1983	0	6	4	15	11	21	5	9	14	16	7	6
1984	1	5	11	9	14	16	14	14	18	14	4	2
1985	4	2	8	9	10	14	15	20	16	13	12	1
1986	0	7	12	10	12	13	18	8	10	12	10	0
1987	1	8	8	11	13	10	16	23	20	16	5	1
1988	0	4	9	12	9	17	19	17	17	19	5	1
1989	0	1	12	11	10	19	18	16	20	15	6	2
1990	3	6	6	10	13	16	15	9	16	17	9	6
1991	3	4	10	9	21	16	15	24	13	9	12	1
1992	1	4	8	17	13	15	13	6	19	17	9	2
1993	1	4	14	11	17	21	21	13	18	16	7	3
1994	2	3	9	10	12	14	13	12	15	20	7	1
1995	0	2	9	19	20	14	17	20	16	14	6	5
1996	2	10	11	15	16	20	16	23	14	12	5	1
1997	2	2	7	12	12	23	12	13	11	16	8	4
1998	2	4	15	10	14	14	13	16	14	18	13	8
1999	1	5	14	12	14	18	21	13	19	16	10	1
2000	4	2	7	11	11	18	10	15	19	8	8	1
2001	0	2	12	12	9	19	14	14	11	9	4	2

Appendix B-3

Mean Daily Temperature (o^C) of SWGH from 1964 - 2001												
Year	**Jan**	**Feb**	**March**	**April**	**May**	**June**	**July**	**Aug**	**Sept**	**Oct**	**Nov**	**Dec**
1964	25.4	27.6	28.1	27.5	26.5	25.9	24.6	24.4	25.1	25.4	26.1	25.4
1965	25.9	26.9	27.5	27.4	26.9	25.8	25.2	24.9	25.4	26.6	26.9	25.3
1966	26.2	27.6	28.2	27.6	27.5	26.3	26.1	25.2	25.7	26.7	26.9	26.6
1967	24.9	27.5	27.8	27.8	27.2	26.1	25.2	24.7	25.4	26.3	26.9	26.6
1968	25.7	27.5	27.4	27.1	27.3	26.4	25.8	25.6	25.8	26.6	26.5	26.8
1969	26.6	27.9	28.6	28.2	27.9	26.6	24.2	25.3	25.7	26.6	26.6	27.2
1970	21.7	28.4	28.2	27.9	27.1	26.6	25.3	25	25.7	26.6	26.6	26.3
1971	26.3	26.8	27.4	27.1	25.9	25.6	24.8	25.4	26.3	26.5	26.5	25.5
1972	26.7	28.1	27.4	27.2	27.3	26.1	25.7	24.9	26.1	26.7	27.1	26.5
1973	26.8	28.6	28.5	28.1	28.0	26.9	26.6	25.9	26.2	26.9	26.9	26.5
1974	25.7	28.2	27.9	27.7	26.9	26.5	25.4	25.7	25.7	26.8	26.9	26.3
1975	25.4	27.8	28.1	27.7	27.0	26.5	25.7	24.9	25.7	26.5	27.1	26.4
1976	26.2	27.9	28.2	27.7	27.5	26.3	25.4	25.1	25.7	26.2	26.5	26.4
1977	27.5	28.9	29.0	28.8	28.1	26.8	25.7	24.8	26.7	27.1	27.8	26.1
1978	28.6	28.8	28.1	27.9	27.9	26.5	25.1	25.3	26.1	26.9	27.5	27.2
1979	28.4	29.2	29.2	29.1	27.6	26.9	26.3	26.3	26.9	27.5	27.5	26.4
1980	28.3	28.2	28.0	28.9	27.7	27.3	25.9	25.9	26.5	27.1	27.1	25.5
1981	26.5	29.1	28.7	28.5	27.4	27.1	25.5	25.5	26.7	27.5	27.3	27.4
1982	27.3	29.4	28.9	28.3	27.3	26.5	25.7	24.8	26.1	27.3	27.3	26.9
1983	25.9	29.3	30.7	29.5	28.9	26.7	26.3	25.7	26.3.	27.1	26.6	27.0
1984	27.9	28.8	28.4	28.5	27.8	27.1	26.7	26.7	26.7	26.9	27.7	25.7
1985	26.9	28.2	28.3	28.2	27.8	27.0	25.9	26.3	26.3	.27.0	27.4	25.8
1986	26.8	29.1	27.8	28.5	27.6	26.8	25.7	25.7	26.5	26.4	27.5	26.5
1987	28.7	29.0	28.7	29.3	28.5	27.7	27.4	26.9	27.3	27.5	28.5	27.1
1988	27.2	30.3	29.1	29.1	28.9	27.2	26.4	25.9	26.7	27.3	27.7	26.5
1989	26.9	29.5	29.1	28.5	28.2	27.0	26.7	26.3	26.4	26.9	28.1	27.5
1990	27.7	28.1	30.1	28.9	28.3	28.6	26.1	25.5	26.7	27.3	27.7	26.7
1991	27.3	29.1	28.9	28.6	28.1	28.1	27.1	25.9	27.1	26.6	27.2	27.3
1992	27.5	29.7	29.0	28.7	28.2	26.6	25.7	25.7	26.7	27.5	27.1	27.5
1993	27.1	29.9	27.8	28.3	28.9	27.4	26.3	25.9	26.9	27.4	27.1	26.4
1994	26.8	29.1	28.7	28.6	27.9	27.4	26.3	26.3	26.9	27.5	27.7	27.1
1995	27.1	30.4	29.1	28.6	28.3	27.3	26.5	26.5	26.7	27.0	27.5	26.6
1996	26.6	28.3	28.3	28.3	28.4	26.8	26.3	25.9	26.2	26.5	27.6	27.1
1997	27.5	28.9	28.9	28.0	28.2	27.0	25.8	25.5	27.0	27.5	27.3	27.1
1998	26.5	29.3	30.5	29.7	28.7	27.3	26.5	25.5	26.5	27.0	27.5	27.1
1999	27.9	27.4	27.8	27.8	27.8	27.2	26.3	26.2	26.7	26.9	27.7	27.6
2000	27.9	27.8	29.6	29.2	28.7	27.5	26.3	26.1	26.5	27.7	28.1	27.3
2001	28.2	29.8	28.8	28.5	29.0	27.6	26.6	25.7	26.0	28.1	28.8	28.9

Appendix B-4

Mean Daily Potential Evapotranspiration (mm)													
Year	Jan	Feb	March	April	May	June	July	Aug	Sept	Oct	Nov	Dec	Ave
1964	104.1	129.5	116.8	114.3	96.5	88.9	76.2	68.6	78.7	91.4	94.0	96.5	96.3
1965	121.9	104.1	114.3	109.2	109.2	81.3	83.8	73.7	76.2	94.0	94.0	101.6	96.9
1966	104.1	129.5	116.8	114.3	96.5	88.9	81.3	68.6	83.8	96.5	101.6	96.5	98.2
1967	124.5	134.6	132.1	121.9	104.1	81.3	76.2	66.0	76.2	76.2	99.1	104.1	99.7
1968	111.8	116.8	114.3	109.2	109.2	86.4	73.7	66.0	83.8	99.1	91.4	96.5	96.5
1969	104.1	129.5	137.2	127.0	111.8	88.9	68.6	71.1	81.3	96.5	96.5	94.0	100.5
1970	104.1	129.5	116.8	114.3	96.5	88.9	76.2	68.6	78.7	91.4	94.0	96.5	96.3
1971	121.9	104.1	114.3	109.2	109.2	81.3	83.8	73.7	76.2	94.0	94.0	101.6	96.9
1972	109.2	137.2	121.9	106.7	101.6	83.8	73.7	73.7	86.4	94.0	83.8	101.6	97.8
1973	129.5	129.5	137.2	119.4	127.0	94.0	96.5	76.2	81.3	96.5	104.1	109.2	108.4
1974	139.7	134.6	129.5	116.8	99.1	88.9	81.3	83.8	83.8	101.6	104.1	111.8	106.3
1975	152.4	137.2	134.6	119.4	101.6	94.0	81.3	73.7	91.4	99.1	104.1	96.5	107.1
1976	146.3	145.7	141.8	122.6	113.1	84.4	77.1	79.9	86.6	86.1	104.1	107.4	107.9
1977	97.9	160.3	159.2	145.1	123.1	95.0	75.9	68.6	91.1	97.3	122.6	117.0	112.8
1978	143.4	145.7	130.5	99.5	95.0	87.1	76.5	76.2	91.6	93.9	101.6	96.5	103.1
1979	119.8	160.3	163.7	151.3	108.5	87.7	78.1	78.1	89.4	97.9	104.0	103.5	111.9
1980	126.6	136.7	118.7	132.7	108.0	90.0	74.3	75.9	84.4	92.8	99.0	120.9	105.0
1981	163.1	133.3	140.6	126.6	102.4	95.6	63.0	69.2	91.1	112.5	118.1	104.6	110.0
1982	190.7	173.3	154.7	121.5	102.4	80.4	73.1	63.0	84.9	109.1	101.8	118.7	114.5
1983	160.9	208.7	155.3	135.6	128.8	101.8	104.6	80.4	99.0	102.4	120.9	128.8	127.3
1984	109.2	137.2	177.8	138.4	133.3	92.3	98.4	81.0	99.0	115.3	119.3	113.6	117.9
1985	135.6	161.4	155.3	138.9	63.0	104.6	80.4	73.1	100.7	109.7	121.5	111.4	113.0
1986	175.5	173.3	144.6	142.3	116.4	85.5	82.1	76.5	100.1	119.3	118.1	127.1	121.7
1987	147.9	144.0	149.7	145.1	127.1	119.8	96.2	90.6	96.8	109.1	129.4	125.4	123.4
1988	199.1	177.8	177.8	136.7	118.7	100.7	87.8	85.5	92.3	102.9	113.1	127.7	126.7
1989	152.4	137.2	134.6	119.4	101.6	94.0	81.3	73.7	91.4	99.1	104.1	96.5	107.1
1990	146.3	145.7	141.8	122.6	113.1	84.4	77.1	79.9	86.6	86.1	104.1	107.4	107.9
1991	124.9	148.5	135.0	134.4	110.8	104.6	99.6	70.3	89.4	94.5	101.3	123.2	111.4
1992	197.4	158.6	142.9	127.7	113.1	81.6	72.0	85.5	97.3	109.7	110.8	109.7	117.2
1993	189.6	183.4	136.7	126.0	126.0	100.1	78.8	75.4	92.3	110.8	112.5	111.9	120.3
1994	148.5	180.6	161.4	135.6	111.9	105.2	82.7	86.6	88.3	109.7	115.9	145.1	122.6
1995	207.0	217.7	153.6	125.4	123.2	112.5	92.8	87.2	95.1	108.0	120.9	116.4	130.0
1996	109.1	151.9	135.6	131.6	124.9	98.4	91.7	82.1	89.4	99.0	122.1	102.4	111.5
1997	124.3	195.8	154.1	122.6	121.5	92.3	84.4	81.0	107.4	110.3	115.3	118.1	118.9
1998	154.7	166.5	185.1	151.3	126.6	102.4	91.1	78.2	91.7	102.9	119.8	111.9	123.5
1999	141.8	154.1	140.1	127.7	127.7	105.2	90.0	97.3	86.6	99.8	115.0	128.0	117.8
2000	88.4	210.4	174.9	64.2	124.9	93.9	87.2	82.7	81.6	112.8	123.2	126.0	114.2
2001	171.0	217.1	147.9	128.2	128.3	108.6	96.8	72.6	79.3	113.6	133.3	128.3	127.1